UNIVERSITÀ
DEGLI STUDI
DI PADOVA

Effects of Environmental Pollutants in Plants: Sulfadiazine and Perfluoroalkyl Substances

THESIS

Submitted by

NISHA SHARMA

In partial fulfillment for the award of the degree

of

DOCTOR OF PHILOSPHY

PhD Course in Animal and Food Science 32° Cycle

Department of Agronomy, Food, Natural resources, Animals and Environment (DAFNAE)

University of Padova

Director of the School: Prof. Stefano Schiavon

Supervisor: Prof. Antonio Masi

September 2019

Declaration

I hereby declare that this submission, to the best of my knowledge, contains no material previously published or written by other people. The experimental works described in this thesis are part of scientific manuscripts published, submitted or to be submitted to international peer reviewed journals. People involved within the research work are specially marked in the text.

Nisha Sharma, 29.09.2019

TABLE OF CONTENTS

ACKNOWLEDGEMENTS

I am grateful for the fully funded grant by University of Padova through Fondazione Cassa di Risparmio di Padova e Rovigo (CARIPARO), Padova Italy. As well I would like to thank the University of Padova for supporting the acquisition of the TSQ Quantitative Mass Spectrometer by 2015/CPDB 15489 funding.

I consider a privilege to work under the guidance of Prof. Antonio Masi, who gave me an opportunity to work at Department of Agronomy, Food, Natural Resources, Animals and Environment with a challenging and interesting topic on environmental pollutants including Sulfadiazine (SDZ) and perfluoroalkyl substances (PFASs). His continued encouragement and fatherly attitude have always helped me to keep going and to overcome the critical situations during my research work. I express my gratitude to him for his commitment and help which has greatly helped me in pursuing this work. I am extremely grateful to Prof. Rossella Ghisi, her guidance and stimulating remarks were of great help through the whole project.

I particularly wish to acknowledge the help rendered by Prof. Andre Simpson and his group for helping in NMR part of my research at Department of Physical & Environmental Sciences, in University of Toronto.

I offer my cordial & profound thanks to all my lab fellow and lab technician Dr. Anna Rita Trentin for her help, cooperation, encouragement, support and scientific discussions. I would like to acknowledge Dr. Leonard Barnabas Ebinezer, Post doctorate Student for his help and support throughout my work. He helped me realise what I am capable of and made sure I never forget it.

I would like to express my sincere thanks to Prof. Stefano Dall'Acqua, from pharmacy department, UNIPD for helping me in analysing the NMR data and directing me in a manuscript for which I am deeply indebted. I am also thankful to Stefania, PhD student of Prof. Dall'Acqua, for her invaluable help throughout the tenure of my work related to NMR

I am exceedingly lucky to have wonderful friends Aynur, Susen, Victor, Lina and Nalayeni, who shared all the good and bad times of my Ph.D. research tenure and have always boosted my morale especially in times of difficulty.

Last but not the least I offer my sincere thanks and profound admiration to my affectionate parents; Mr. Dhundi Raj Sharma, Mrs. Shanti Sharma and my sister Anisha Sharma, who are the source of encouragement for me, infact this work became possible only because of their love, moral support and prayers for my success.

LIST OF ABBREVIATIONS

AFFF, aqueous film-forming foams
CDNB, 1-chloro-2, 4-dinitrobenzene
CMP-NMR, Comprehensive Multiphase Nuclear Magnetic Resonance spectroscopy
CNR, Consiglio Nazionale delle Ricerche
ECF, Electrochemical fluorination
EU, European Union
iTRAQ, Isobaric Tags for Relative and Absolute Quantification
LC-MS/MS, Liquid chromatography–Tandem mass spectrometry
NMR, Nuclear Magnetic Resonance spectroscopy
PAHs, polycyclic aromatic hydrocarbons
PBSF, perfluorobutane sulfonyl fluoride
PFAAs, perfluoroalkyl acids
PFAI, perfluoroalkyl iodide
PFASs, perfluoroalkyl and polyfluoroalkyl substances
PFBA, perfluorobutanoic acid
PFBS, perfluorobutane sulfonate
PFCAs, Perfluoroalkyl carboxylic acids
PFCs, perfluorinated compounds
PFDA, perfluorodecanoic acid
PFDoA, Perfluoro dodecanoic acid
PFHpA, perfluoroheptanoic acid
PFHxA, perfluorohexadecanoic acid
PFNA, perfluorononanoic acid
PFOA, perfluorooctanoic acid
PFOS, perfluorooctanesulfonate
PFPeA, perfluoro-n-pentanoic acid
PFSAs, Perfluoroalkyl sulfonic acids
PFUnA, perfluoroundecanoic acid
POPs, persistent organic pollutants
POSF, perfluorooctane sulfonyl fluoride
PPCPs, pharmaceutical and personal care products
SDZ, Sulfadiazine
TFE, tetrafluoroethyl
TFHQ, tetrafluoro-1,4-hydroquinone

AIMS OF THE WORK

The main aim of this PhD study was to analyze the effects of contaminants, here SDZ and PFASs, on plants (*Arabidopsis thaliana, Zea mays* and *L Salix* species), taken as model plants for the purpose of knowing plant responses to chemicals. The general purpose of this work was to check the adaptive responses of PFASs toxicity. Furthermore, the ability of three willow species to accumulate PFASs was also assessed to the purpose of application of phytoremediation techniques.

To achieve this aim,

1. The effect of SDZ on growth, antioxidant metabolite content and enzyme activities related to oxidative stress in *Arabidopsis thaliana* plants grown in Petri dishes for three weeks, were studied. Furthermore, proteome alterations were investigated by means of a combined iTRAQ-LC-MS/MS quantitative proteomics approach.

2. A protocol to investigate the phytotoxic effects of PFASs on S*alix* and maize grown in a hydroponic system, through photosynthetic measurements was applied. The analysis was done by Licor Li-6800.

3. A protocol to measure PFAAs content in plants, through Mass Spectrometry (MS) was applied

4. A novel NMR approach named Comprehensive Multiphase-Nuclear Magnetic Resonance (CMP-NMR) was applied to assess the metabolites which are influenced by PFASs exposure, namely PFOA and PFOS on *A. thaliana* seedlings.

SUMMARY

The main aim of this PhD project was to study the effects of emerging contaminants in different plant species, in order to assess their responses and eventually their accumulating ability. Under this context, the effects of sulfadiazine (SDZ) and perfluoroalkyl substances (PFASs) and particularly the perfluoroalkyl Acids (PFAAs) were analysed on three different plant species: *Arabidopsis thaliana*, *Zea mays* and *Salix*. To this purpose, morphological observations, photosynthetic measurements, biochemical and proteomic analysis as well as the study of the abundance of metabolites through NMR process were conducted. *Arabidopsis* seeds were grown in Petri plates whereas Maize seeds and *Salix* cuttings were grown hydroponically in the laboratories at Agripolis, Legnaro.

Among the antibiotics, sulfadiazine (SDZ) belongs to sulfonamides, a group of synthetic antibacterial agents, that are used in human medicine and are one of the most sold classes of veterinary antimicrobial compounds. The content of sulfadiazine can remain high in contaminated soil for months and years so contributing to the spreading of the antibiotic resistance and can further enter the food chain. However, not much is known about the effects of antibiotics on the proteome of plants. Hitherto, to the best of our knowledge, there is no information pertaining to the changes in root proteome of Arabidopsis and its correlation with the physiological and biochemical effects in response to SDZ. Hence, **chapter 2** describes the alterations on the level of anti-oxidant metabolites and enzyme activities, and on the proteome occurring in Arabidopsis thaliana roots in response to SDZ. The manuscript of which was published in Ecotoxicology and Environmental Safety.

Per- and polyfluoroalkyl substances (PFASs), man made chemical pollutants, are widely used as surfactants, especially for the consumer products. They are ubiquitously found in the entire globe due to their extensive use and high persistence. Studies and different evidences suggest that PFAS exposure is directly or indirectly linked to potential risks to human, wildlife and the whole environment. For the concerns about the potential environmental and toxicological impact, PFOS has been added to the persistent organic pollutants (POPs) list of the Stockholm Convention in May 2009 resulting in global restriction of its production UNEP, (2009), whereas PFOA is expected to be added to this banned list. Therefore, it is important to identify appropriate technologies to remove PFAS from the environment. Since, physicochemical

techniques are expensive, and the application of microbial biodegradation is still unfeasible, the only practical method would be bioremediation techniques involving plants. Thus, **Chapter 3** describes the evaluation of the ability of three different *Salix* species, i.e. *S. eleagnos L., S. purpurea L.* and *S. triandra L.* grown in hydroponics to carry out the PFAS phytoremediation process. To this purpose, the effects of these substances on willow plant growth and photosynthesis and the amounts of PFAAs accumulated by these species were evaluated. The manuscript of which was submitted to Ecotoxicology and Environmental Safety on September 12, 2019 and now it is under minor revision.

As PFAAs predominantly exist as a mixture, our study gains significance as it addresses their combined effects on growth rate, fresh and dry weights at environmentally relevant concentration. The general trend in uptake and accumulation of PFAAs based on the carbon chain length and the functional group, differences in the effects of PFAAs on the growth rate and photosynthesis were observed. But still, effects of PFAAs on photosynthesis still needs further research to understand thoroughly. Considering that PFASs are taken up by the transpiration stream it would be interesting to examine its effects of plant-water relations, which could have a larger impact when plants are grown on soil. While the hydroponic-based study provided novel insights and indicated the potential of willow plants to uptake and accumulate PFAAs, their applicability under field condition needs to be demonstrated, which together with the results would have direct implications for phytoremediation of PFAAs by willow plants.

Chapter 4 illustrates the significant effects of PFAAs on the growth of maize plants, affecting the uptake of the nutrient solution for their own development. Moreover, the data presented here show that the most frequently detected PFAS in the environment, i.e. PFOA and PFOS, can enter the plants and, consequently, into the human food chain. I could conclude that PFASs are potentially phytotoxic and can be accumulated by higher plants. Because of these results, maize may contribute to increase human PFAAs exposure when grown in hot-spot regions, with possible toxic effects on population. For this reason, it would be considerably important to continue the studies regarding the effects of these substances on the environment, plants and humans and it may well be worthwhile to consider the alternatives to substitute longer-chain PFASs in industrial processes.

Chapter 5 concerns the application of the novel spectroscopy called CMP-NMR to highlight significant metabolic changes *Arabidopsis thaliana* upon exposure to PFOA, PFOS and to a mixture of PFASs (11 PFAAs). This chapter deals with one published manuscript in which there is a section describing the growth of ^{13}C glucose labelled *Arabidopsis thaliana* seedlings. The protocol mentioned in this paper was optimized and further used for my PhD project. The *A. thaliana* seedlings were spiked with PFAAs and grown in the dark in the presence of ^{13}C glucose as the unique carbon source, and the metabolite changes due to the PFASs treatment were easily detected by CMP-NMR. Two metabolites (Alanine and Glutamine) were identified as significantly altered in seedlings treated with the 11 mixture PFASs as compared to control.

Publications

The following cumulative doctoral thesis "Effects of Environmental Pollutants in Plants: Sulfadiazine (SDZ) and Per fluoroalkyl Substances (PFASs)" is based on the scientific publications listed below. Two of them are published and one has been submitted for publication.

Publication I.

Nisha Sharma, Giorgio Arrigoni, Leonard Barnabas Ebinezer, Anna Rita Trentin, Cinzia Franchin, Sabrina Giaretta, Paolo Carletti, Sören Thiele-Bruhn, Rossella Ghisi, Antonio Masi. (2019). A proteomic and biochemical investigation on the effects of sulfadiazine in Arabidopsis thaliana. Ecotoxicology and environmental safety, 178, 146-158.

Publication II.

Amy Jenne, Ronald Soong, Wolfgang Bermel, **Nisha Sharma**, Antonio Masi, Maryam Tabatabaei Anaraki and Andre Simpson, 2018. Focusing on "the important" through targeted NMR experiments: an example of selective 13C–12C bond detection in complex mixtures. Faraday discussions.

Publication III.

Nisha Sharma, Giuseppe Barion, Inisha Shrestha, Leonard Barnabas Ebinezer, Anna Rita Trentin, Teofilo Vamerali, Giustino Mezzalira, Antonio Masi, Rossella Ghisi. Accumulation and effects of perfluoroalkyl substances in three *Salix* L. species. Submitted the manuscript in Ecotoxicology and environmental safety on 12 September 2019 and now it is under minor revison.

Publication IV.

Nisha Sharma, Sara De Vecchi, Leonard Barnabas Ebinezer, Anna Rita Trentin, Rossella Ghisi, Antonio Masi. Accumulation, Physiological and morphological alterations induced by perfluoroalkyl substances in Maize (*Zea mays*) plant.

This manuscript is under review for submission.

Publication V.

Nisha Sharma, Stefano Dall'Acqua, Stefania Sut, Leonard Barnabas Ebinezera, Antonio Masi, Andrea Simpson. The study on Perfluoroalkyl acids contaminated *Arabidopsis thaliana* seedlings with a powerful approach: Comprehensive Multiphase NMR Spectroscopy.

This manuscript is under review for submission.

CONFERENCES AND PROCEEDINGS

Poster Presentation

Nisha Sharma, Stefano Dall'Acqua, Stefania Sut, Antonio Masi, (2019). Comprehensive multiphase NMR: a powerful technology to study the effects of PFASs on the model plant Arabidopsis thaliana. First Joint Meeting on Soil and Plant System Sciences (SPSS 2019), Bari (Italy), September 2019.

Nisha Sharma, Giuseppe Barion, Inisha Shrestha, Leonard Barnabas Ebinezer, Anna Rita Trentin, Teofilo Vamerali, Rossella Ghisi, Antonio Masi, (2019). Accumulation and effects of Perfluoroalkyl Substances (PFASs) in three Salix species. Electronic poster presentation at American Society of Plant Biology (ASPB), San Jose, (United State of America), August 2019.

Nisha Sharma, Giorgio Arrigoni Anna Rita Trentin, Cinzia Franchin, Sabrina Giaretta, Antonio Masi, Rossella Ghisi. Biochemical and proteomic analyses in Arabidopsis thaliana plants treated with sulfadiazine. XXXV Convegno Nazionale SICA, Udine 11- 13 September 2017.

Shilpi Misra, **Nisha Sharma**, Pietro Magnabosco, Sara De Vecchi, Silvia Millan, Anna Rita Trentin, Teofilo Vamerali, Rossella Ghisi, Antonio Masi. Plants treatment with Perfluoroalkyl Substances (PFASs): Uptake and effects on growth and morphology. XXXV Convegno Nazionale SICA, Udine 11-13 September 2017.

Oral presentation

Nisha Sharma, Giorgio Arrigoni, Anna Rita Trentin, Cinzia Franchin, Sabrina Giaretta, Antonio Masi and Rossella Ghisi. Protein Composition Readjustment in Arabidopsis Thaliana following Sulfadiazine Treatment. Poster Presentation at INPPO 2016: Nisha Sharma 2 International Plant Proteomics Organization, September 4 to September 8, 2016.

Nisha Sharma* NMR-Based Metabolomics for Arabidopsis thaliana treated with PFASs. NMR 4 NMR, University of Padova, 24 February, 2019.

Nisha Sharma*, Shilpi Misra, Anna Rita Trentin, Rossella Ghisi, Antonio Masi. Plants treatment with perfluoroalkyl substances (PFASs): uptake and effects on growth and morphology. Oral Presentation at CleanUp Conference 2017, Melbourne, Australia. September 10-14, 2017.

Nisha Sharma*, Shilpi Mishra, Silvia Millan, Anna Rita Trentin, Rossella Ghisi, Antonio Masi. Plant's adaptation to the environment: abiotic stress, antioxidant metabolism, "omics" tools. Oral Presentation at Plant Fascination Day, Botanical Garden, PD. May 16, 2017.

CHAPTER 1

GENERAL INTRODUCTION

1.1 Chemical Pollution

Chemical pollution is due to the presence of chemical substances (organic or inorganic compounds) in our environment that are not naturally present or are found in amounts higher than their natural background values. There are many potentially toxic compounds which are contaminating water, soils, plants, animals and also food. They include inorganic and organic substances such as metals/metalloids, polycyclic aromatic hydrocarbons (PAHs), perfluorinated compounds (PFCs), pharmaceutical and personal care products (PPCPs), radioactive elements and nanoparticles. Some of these occur naturally in the environment, but most of them have anthropogenic sources. These contaminants may cause direct or indirect and acute, chronic or latent effects to the human beings, animals and plants and can cause different effects according to the species, depending on their sensitivity or resistance.

1.2 Antibiotics in the Environment

Antibiotics are defined as chemotherapeutic agents who restrain or prevent the growth of micro-organisms (Gothal et al. 2015) and that are used for the treatment of infectious diseases in animals and humans being (Mirzaei et al. 2018). They are usually used in human medicine and stockbreeding operations to treat infectious diseases. (Cabello, 2006; Lu et al. 2015). However, in some countries, they are also used in animals like cattle, swine, poultry and fish as a growth promoter (Cowieson and Kluenter, 2018). After the discovery of Penicillin in 1928 by Fleming, antibiotics have been widely synthesized and used for humans, animals and also plants health. However, the excessive use of the substances in the daily use is leading to unwanted release into the environment and natural ecosystem (Kumar et al. 2018). Similarly, Marti et al. (2014) mentioned the probability of antibiotics entering the environment through treated and untreated sewage, hospital wastewater and agricultural wastewater, ranging from nanograms to micrograms per liter (Sharma et al. 2016; Gothwal and Shashidhar, 2015; Verlicchi et al. 2015). Thus, the contamination in the environment due to antibiotics can promote the emergence and dissemination of antibiotics resistance (Wei et al. 2011) and further it could lead to a direct or indirect transfer of these compounds into human and animals so posing a risk to public health (Xu et al. 2015).

1.3 Sulfadiazine (SDZ) in the Environment and Plants

Sulfadiazine (SDZ) is a synthetic antibacterial agent belonging to the class of sulfonamides, that contain the sulfonamide group (R1-SO2NH-R2) (Huschek et al. 2008). They are used in human medicine and are one of the most sold classes of veterinary antimicrobial compounds in EU countries for their low cost and broad-spectrum antibacterial and anti-coccidian activity (De Liguoro et al. 2007). Because of the field application of contaminated manure and slurry, extractable concentrations of sulfonamides up to 0.4 mg kg−1 in soil have been measured (Karcı and Balcıoğlu, 2009). The extractability of these compounds from soil decreases with time owing to immobilizing processes, which can involve physical-chemical interactions with soil components (Förster et al. 2009; Wegst-Uhrich et al. 2014; Wehrhan et al. 2010) as well as reactions mediated by oxidoreductase enzymes, such as peroxidases and laccases (Bialk et al. 2005; Schwarz et al. 2010, 2015). However, the total contents of sulfadiazine remain high in contaminated soil for months and years (Rosendahl et al. 2011; Schmidt et al. 2008).

It has been proved that plants can incorporate various drugs (Boxall et al. 2006; Carter et al. 2014; Carvalho et al. 2014), thus contributing to the entry of these compounds into the food chain and the spread of antibiotic resistance (Jechalke et al. 2013). Hence, information on the distribution of antibiotics in manure-applied and wastewater-irrigated soils and their uptake and accumulation by plants/crops has been accumulating over the recent years (Kang et al. 2013; Pan et al. 2014; Rosendahl et al. 2011; Schmidt et al. 2008). Antibiotics can directly affect plant physiological processes such as photosynthesis, respiration and root functionality (Carvalho et al. 2014; Li et al. 2011; Michelini et al. 2012, 2013). Regarding plant growth, sulfonamides have been shown as either promoting or inhibitory substances (hormesis) depending on the plant and the concentrations used (Migliore et al. 2010; Michelini et al. 2012; Pan and Chu, 2016).

1.4 Per fluorinated Substances – Background, Structure, Production and Use

Per- and polyfluorinated chemicals (PFCs), specifically Per- and polyfluoroalkyl substances (PFASs), are a large group of chemicals including oligomers and polymers (The EFSA Journal, 2008), that have been used since the 1950s. In these years, the production of PFCs was started

and they were used in industrial and consumer products like surfactants and surface protectors (OECD, 2013). Because of their peculiar properties like water and oil repellent and their stability, they have been widely used in many industries and commercial products, such as coatings for textiles and papers or firefighting foams. However, some of these properties are the reason that contributes to making PFASs dangerous to the environment (Felizeter et al. 2014).

PFASs are resistant to hydrolysis, photolysis, biodegradation and metabolism having an environmental persistence and bio-accumulative potential which are causing a big problem for the whole environment (Valsecchi et al. 2017). During the last decade, PFAS has attracted much attention to their persistent, accumulative, and toxic nature (Blaine et al. 2014; Nzeribe et al. 2019). Initially, most attention was given to perfluorooctane sulfonic acid (PFOS) and perfluorooctanoic acid (PFOA) because they are found commonly in the environment, biota and human, and are mostly studied for their toxicity and ecotoxicity (Lindim et al. 2016; Yang et al. 2019, Liu et al. 2019). Lately, more attention was also given to other PFAAs, which include both PFCA and PFSA (OECD, 2013).

From the studies about PFASs of the last years, their presence is very common in all environmental and biological matrices (air, surface, drinking and ground water, sediments, arctic ice, soils, birds, polar bears, marine organisms and individuals) (Muir et al. 2019), even in remote regions, such as the Arctic. Open ocean water is the largest global reservoir of PFAAs such as PFOA, PFNA, transported by the water currents (OECD, 2013).

1.4.1 Production and uses of PFASs

PFASs is a manmade organic chemicals group which have been extensively produced and applied in various industries worldwide starting from the 50s. The manufacturing of PFAS is done by two different processes:

- Electrochemical fluorination (ECF)
- Telomerisation.

The products from the first process contain a sulfonyl group (ECF-products) and there is the replacement of all the hydrogen atoms by fluorine atoms. In the ECF process, organic feed stocks are dispersed in liquid anhydrous hydrogen fluoride, and an electric current is passed

through the solution. ECF yields even and odd numbered, branched and straight perfluoroalkyl chains and it is different from the telomerisation that only yields even, linear chains and

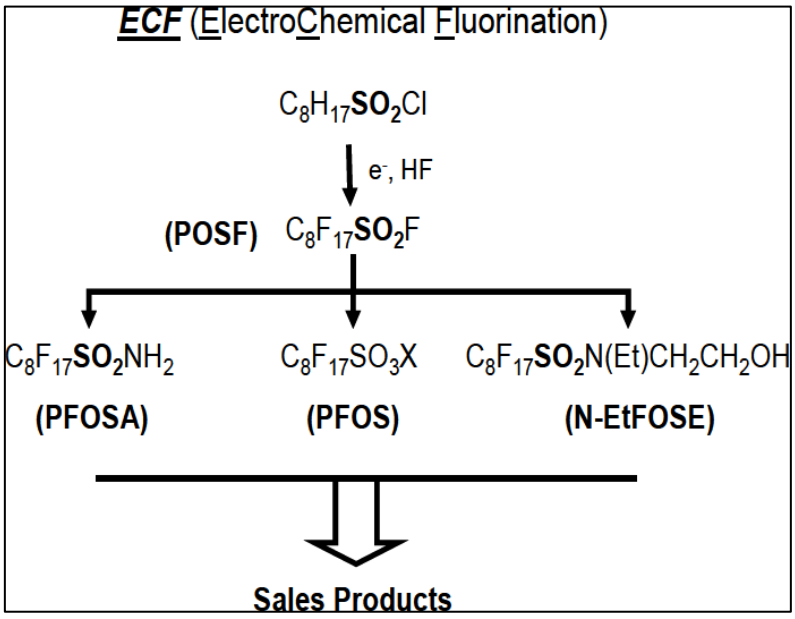

products that contain an ethylene group (telomers).

Figure 1.1 Electrochemical fluorination (ECF) process schematic (The EFSA Journal, 2008).

Telomerisation is a technology in which there is a reaction between a perfluoroalkyl iodide (PFAI) and tetrafluoroethylene (TFE) to produce a mixture of perfluoroalkyl iodides with longer per fluorinated chains. Then, there are other steps to create a family of surfactant and polymer products based on fluorotelomer. Among them, Perfluorooctanesulfonyl fluoride (POSF) ($C_8F_{17}SO_2F$) is the most important production intermediate for electrochemical fluorination and 8:2 FTOH ($C_8F_{17}C_2H_4OH$) for telomer production (Fig 1.1) (The EFSA Journal, 2008; Danish EPA, 2015; Hekster et al. 2002).

The global annual production volume of perfluorooctanoic acid (PFOA) was 1200 metric tons in 2004, and perflurooctane sulfonate (PFOS) reached 3500 metric tons just in two years. But, due to their extensive production and long-term use, PFASs have been globally detected in a variety of biotic and abiotic matrices (Zhao et al. 2016; Byrne et al. 2018; Zafeiraki et al. 2019; Ghisi et al. 2018; Bao et al. 2019). The past and recent widespread use of this compounds are due to their properties: dielectric properties, low surface energy, low friction properties and resistance to heat and chemical agents. The carbon-fluorine bonds present in the PFASs, has

a high strength, is extremely stable and nonreactive; for this reason, these substances are present in many products because of their high versatility, strength, resilience and durability (OECD, 2013). They are used extensively by the textile industry as surfactants and surface protectors for the treatment of all-weather and waterproof clothing, with the brand name Gore-Tex® (Walter et al. 2006), umbrellas, bags, (Supreeyasunthorn et al. 2016) sails, tents, parasols, sunshades, upholstery, fabrics (Janousek et al. 2019), leather, footwear, mats, carpets (Zille and Raous 2019) and the like to repel water, oil and dirt. Other area in which fluorinated chemicals are used is the paper industry (Clara et al. 2008; Trier et al. 2011) to produce waterproof and greaseproof paper. The perfluoroalkyl substances have an important application also for the Teflon production (Olsen et al. 2015), largely used in the pots for its non-stick properties (Sajid et al. 2017). PFAS have been used both in food contact applications such as plates, food containers, popcorn bags, pizza boxes and wraps and in non-food contact applications such as folding cartons, containers, carbonless forms and masking papers. PFASs have historically been used as surfactants to lower surface tension and improve wetting in a variety of industrial and household cleaning products such as automobile waxes, alkaline cleaners, denture cleaners and shampoos, cosmetics, floor polish, dishwashing liquids and car wash products (Lorenzo et al. 2015). Furthermore, PFASs derivatives have several uses in coating, paint and varnishes to reduce surface tension and they can be used as surfactants in the oil and mining industry. In the photographic industry PFASs related substances have been used in manufacturing film, paper and plates to reduce surface tension and static electricity because imaging materials that are very sensitive to light benefit particularly from the properties of these materials. PFOS was used in X-ray film for photo imaging for medical and used in film for other industries, such as the movie industry but now PFOS is not longer in use by the industries. Other applications are common in electrical and electronic equipment: digital cameras, cell phones, printers, scanners, satellite communication systems and radar systems. A large use of PFASs is spread in aviation hydraulic fluids: hydraulic oils have been used in civil and military airplanes since the 1970s to prevent evaporation, fires and corrosion. The PFASs based fire-fighting foams is effective for extinguishing liquid fuel fires at airports and oil refineries and storage facilities (aqueous film-forming foams – AFFF - developed in the 1960s and used for aviation, marine and shallow spill fires), which are no longer in use but still

PFOS, PFOA and their precursors are still present at significant levels in the environment due to their past usage. Again, PFASs have been applied as ingredients in some plant growth regulators, herbicides and ant baits to control leaf cutting ants, red imported fire ants and termites and as inert ingredients in pesticide formulations (OECD, 2013; UNEP, 2011).

1.4.2 PFAAs: structure and types

The perfluoroalkyl acids (PFAAs) are chemicals consisting of a hydrophobic alkyl chain, with all carbons bound to fluorine, of varying length (typically C4 to C16) and a hydrophilic end group, X. Their general structure is given in Figure 1.2 (The EFSA Journal, 2008).

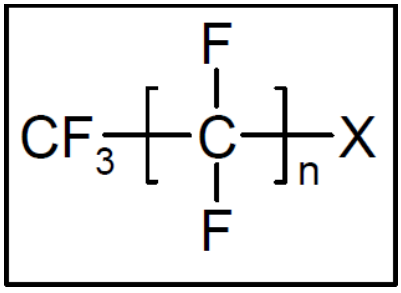

Figure 1.2 General structure of perfluorinated alkyl substances (The EFSA Journal, 2008).

They include many compounds, some of them showed in Table 1.1, and they consist in linear or branched carbon chains with fluorine atoms, belonging to the category of organo-halogenated group (Buck et al. 2011). These chains are linked, to a functional group, most frequently: carboxylic and sulfonic groups (these are ionizable groups, able to bring an electric charge and to solubilize in the water). For this reason, they have an amphiphilic character and they show at the same time lipophilic and hydrophilic characteristics (Farinola, 2016).

Table 1.1 List of PFAAs (Russo et al. 2016).

Number of carbon atoms	**Number of fluorine atoms**	**Chemical name of perfluoroalkyl substance**	**Acronym of the name**
4	7	Heptafluorobutyric acid	**PFBA**
4	9	Nonafluorobutane sulfonic acid	**PFBS**
5	9	Perfluoropentanoic acid	**PFPeA**
6	11	Perfluorohexanoic acid	**PFHxA**
6	13	PerfluoroHexane Sulfonate	**PFHxS**

7	13	Perfluoroheptanoic acid	**PFHpA**
8	15	Pentadecafluorooctanoic acid	**PFOA**
8	17	Perfluorooctanesulfonic acid	**PFOS**
9	17	Perfluorononanoic acid	**PFNA**
10	19	Perfluorodecanoic acid	**PFDeA**
11	21	Perfluoroundecanoic acid	**PFUnA**
12	23	Tricosafluorododecanoic acid	**PFDoA**

In the past, PFASs were often referred to as “PFCs” (per- and polyfluorinated chemicals), but this term can also be understood as perfluorocarbons, containing only carbon and fluorine and with properties and functionalities different from those of PFASs. PFASs are divided into two sub-groups: non-polymeric and polymeric PFASs (see Figure 1.3).

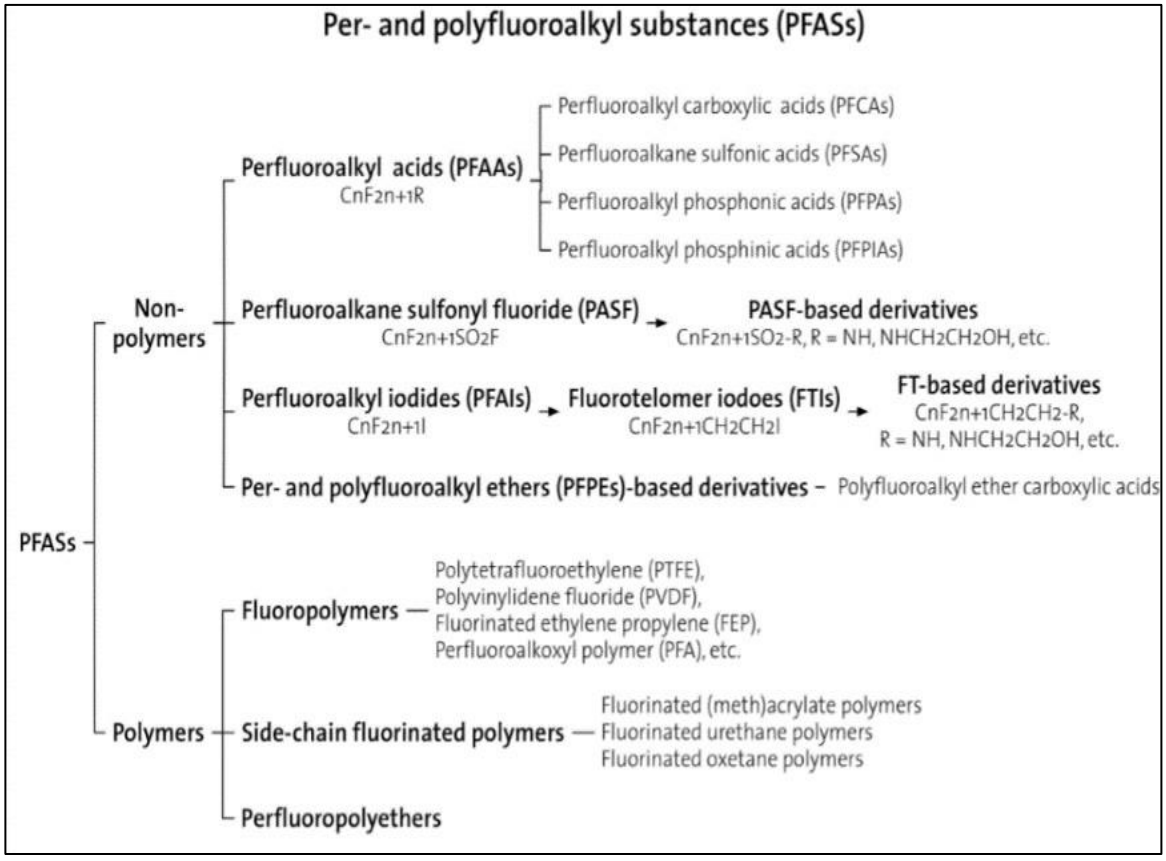

Figure 1.3 Non-polymeric and polymeric PFASs (OECD, 2013).

Non-polymeric PFASs contain the “long-chain PFAS”, referred to:

- Perfluoroalkyl carboxylic acids (PFCAs) with 7 and more perfluoroalkyl carbons, such as PFOA (with 8 carbons or C8 PFCA) and PFNA (with 9 carbons or C9 PFCA);

- Perfluoroalkane sulfonic acids (PFSAs) with 6 and more perfluoroalkyl carbons, such as PFHxS (with 6 perfluoroalkyl carbons, or C6 PFSA) and PFOS (with 8 perfluoroalkyl carbons or C8 PFSA);

- Substances that have the potential to degrade to long-chain PFCAs or PFSAs, i.e. precursors such as perfluoroalkane sulfonyl fluoride (PASF) and fluorotelomer based compounds (OECD, 2013; Ateia et al. 2019; Land et al. 2018).

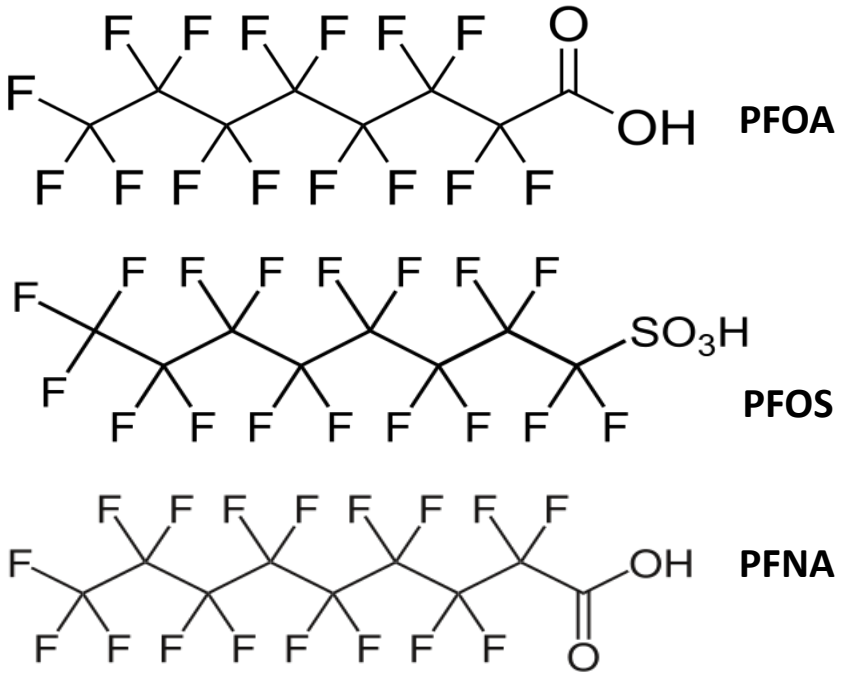

Figure 1.4 PFOS, PFOA, and PFNA: molecular structures. PFOS has an eight-carbon chain with a sulfonate end group, PFOA has an eight-carbon chain with a carboxyl end group, and PFNA has a nine-carbon chain backbone with a carboxyl end group (Jantzen et al. 2016).

Within the polymeric, PFAS are differentiated between:

(i) Fluoropolymers: fluorinated polymers consisting of carbononly backbone with fluorines directly attached to this backbone, which are not made from perfluoroalkyl carboxylic acids (PFCAs) or their potential precursors. They are used for processing aids in the polymerization of some fluoropolymers.

(ii) Side-chain fluorinated polymers: fluorinated polymers consisting of variable compositions of non-fluorinated carbon backbones with polyfluoroalkyl side chains, including PASF- and fluorotelomer-based derivatives, are potential precursors of PFCAs.

(iii) Perfluoropolyethers: fluorinated polymers consisting of backbones containing carbon and oxygen with fluorines, which are not made from PFCAs or their potential precursors and are not involved in the manufacturing of perfluoropolyethers (OECD 2013).

1.4.3 PFASs diffusion in the environment

During the production processes or after usage, PFASs are released into the environment and (especially PFOA and PFOS) are often detected in significant concentrations in environmental samples. They are then distributed globally, because of their high chemical stability, persistence, long range transportation and bioaccumulation given (Fujii et al. 2007) (Taniyasu et al. 2013). For this reason, they are highly resistance to the environment.

They further can propagate through water exchanges for many years even after the input source has been removed. It can be assumed that predominant mode of distribution of PFAAs occurs via the aqueous pathway (Schaefer et al. 2018). PFAAs can be detected almost ubiquitously, for example, in water, sediments, air, soil, sludge from waste water treatment plants, biosolid for agricultural application, house dust and organisms such as fishes, birds and mammals as well as in human breast milk and blood (Ahrens et al. 2009; DeWitt, 2015; Stahl

et al. 2009). PFOA and PFOS are the most frequently detected species and they have long residence times in human blood of more than 1000 days (OECD, 2013).

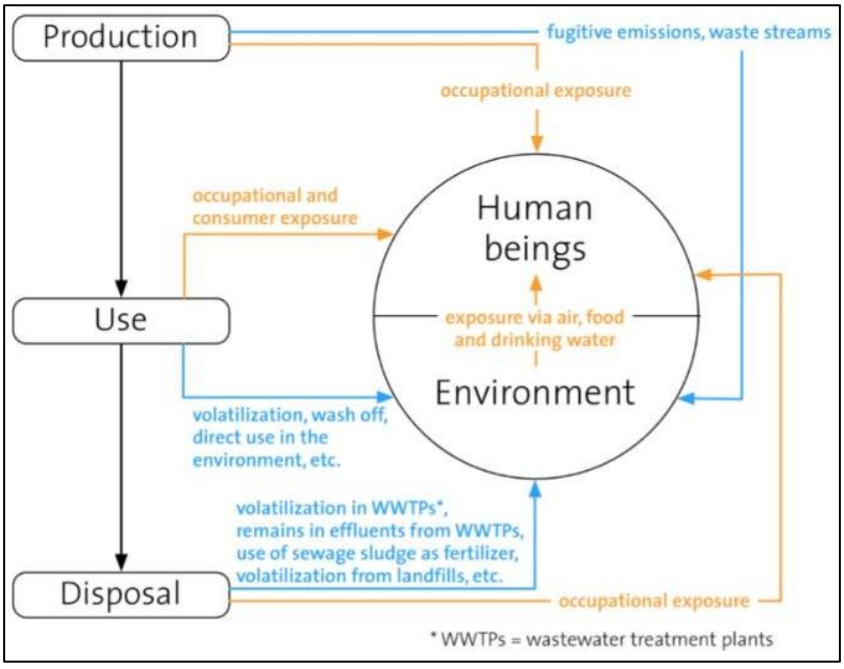

Figure 1.5 PFASs exposure in the environment and human beings during the life cycle of PFASs contaminated products (OECD, 2013).

The historical PFSAs pollution occurred in five locations around the world where chemical companies manufacture PFASs (see Figure 1.6): in the mid of Ohio valley, USA (Defenbaugh, 2014; Herrick et al. 2017); in Dordrecht, the Netherlands (Möller et al. 2010; Noorlander et al. 2011; Zafeiraki et al. 2015), in North Rhine-Westphalia, Germany (Fromme et al. 2009) and in Veneto region, Italy in Europe (Mastrantonio et al. 2017); in Shandong Province, China (Zhu et al. 2014).

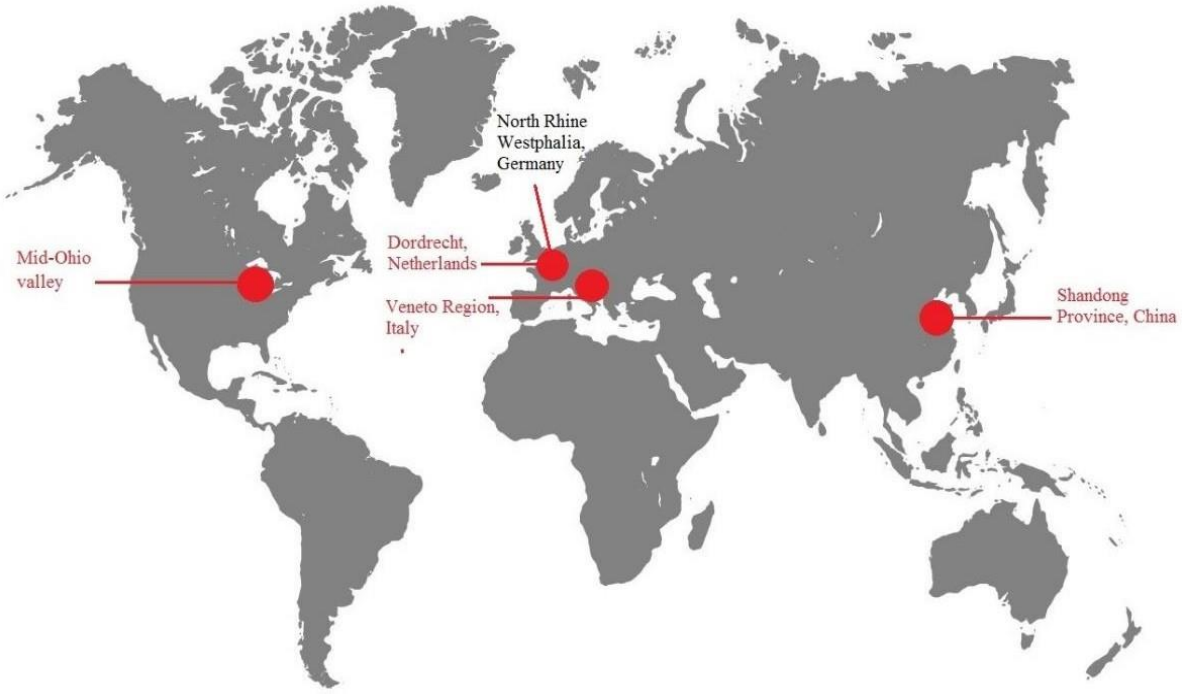

Figure 1.6 Five PFAS pollution hotspots in the world (Greenpeace 2016).

The situation in Veneto region, North East of Italy, was discovered in 2013. The Italian Ministry of Environment reported the presence of the persistent and hazardous chemicals PFASs in the ground, surface and drinking water in some areas of Italy (Vicenza, Padova and Verona) which was attributed to the drains of a factory producing fluorinated intermediates for different applications including water repellent treatments for textiles and leather. Since then, the studies in river, vegetables, human blood (Ingelido et al. 2018; WHO 2017) and human semen (Sharon, 2018) have been widely carried out. The maximum concentrations of PFASs, other than PFOA and PFOS, in the Veneto region, were very high: up to 2000 ng/L for all PFASs, up to 1400 ng/L for PFOA and up to 120 ng/L for PFOS in 2013 (WHO 2017) in the human blood.

One of the main sources of PFAS contamination in Veneto region of Italy was wastewater treatment plant which was receiving waste discharges from many industries. Miteni, a chemical company in Trissino, near Vicenza, was the one who was discharging the waste effluents into the river since long time. They were producing fluorinated intermediates for different applications including water repellent treatments for textiles and leather (ARPAV, 2017). The waste containing PFASs discharging into the sewage system became high risk to

human health and the environment. Due to this reason a safety measures were carried out in July 2013, based on Article 245 of Legislative Decree 152/06. It consisted of three barrier wells for water extraction, positioned on the southernmost side of the Miteni factory, downstream from the source, and in purification system consisting of two groups of activated carbon filters. For this purpose, the Basin Authorities, the regions and autonomous provinces expanded an additional monitoring program related to some PFAAs (PFOS, PFOA, PFBA, PFPeA, PFHxA, PFBS) by 22 December 2018.

1.4.4 PFASs in plants

High levels of PFASs have been found in biosolids, landfill leachates, effluents from wastewater treatment plants (Ahrens et al. 2011; Sepulvado et al. 2011).). Thus, their migration from soil or contaminated water to plants, can induce phytotoxicity but also pose a risk to animal and human health through the food chain (Qu et al. 2010; Rankin et al. 2016). The plant foods are the basic diet for humans and animals, which might be substantial source of high level of PFASs exposure, particularly when grown in contaminated sites (Gobelius et al. 2017; Zhao et al. 2016; Krippner et al. (2014)). The study conducted by Stahl et al. (2009) was the first systematic research showing the transfer of PFOA and PFOS from soil to wheat, oats, maize, rye grass and potatoes plants. Likewise, Lechner et al. (2011) reported that PFOS and PFOA were taken up from contaminated soils by plants like potatoes, carrots and cucumbers, entering the food chain. Indeed, the ways for the plant to be exposed to PFASs may be mainly through the roots from the contaminated soils but also through the above-ground parts from the atmosphere could be considered (Zhao et al. 2016).

Another way of PFASs migration to plants could be biosolids. They are widely used in agricultural soil as ideal agricultural conditioner and fertilizer (Frank 1998). Blaine et al. (2013) used urban biosolids to grow the maize plants. And found out that maize stover contained PFAAs, indicating that biosolids could be one of the sources of PFAAs. Not only biosolids, the contaminated water could be source of PFAAs too. The study by Müller et al. (2016), used a contaminated irrigation water in (hydroponic) model plant *Arabidopsis thaliana* which might be exposure route for humans. There are several studies on plants like lettuce, tomato, cabbage and zucchini which was grown in a nutrient solution spiked with 14 PFAAs (Feli

zeter et al. (2012); Felizeter et al. (2014)). These vegetable plants might enter directly or indirectly into food chain which could pose potential risks to species consuming plant parts. (Zhao et al. 2013; Krippner et al. 2014).

It is possible that PFAAs are accumulated from contaminated soil or water irrigation system to plants. PFAAs are efficiently transported and accumulated in shoots for the continuous increase in concentrations in the tissues. The accumulation of PFAAs has been studied on vegetables comprising the C4 to C14 PFCAs, and the C4, C6 and C8 PFSAs (Felizeter et al. 2012; 2014). Plants tended to accumulate the lighter C4 - C7 chemicals in the leaf and higher chain lengths tended to accumulate in the roots (Blaine et al. 2014). Krippner et al. (2014) also confirmed that the accumulation was depended on chain length; longer the chain compounds lower the accumulation rate. And among the functional groups, PFSAs have generally lower accumulation rates than PFCAs. In this way, the accumulation of PFAAs by plant has giving a real picture of the potential exposure to humans through food, as many kinds of PFAAs are present in soil, waters, and consequently in plants.

The uptake and storage occurred much less in storage organs (e.g., tubers, ears) of the plants than in vegetative compartments (e.g., straw, leaves) (Stahl et al. 2009; Lechner et al. 2011). Similarly, Yoo et al. (2011) also observed linear relationships between log grass/soil accumulation factors for C6–C14 PFCAs and carbon chain length in their uptake study on grass species. However, it is necessary to understand that PFAAs distribution across roots, stem, leaf, fruit and head varied among species, as seen in Blaine et al.'s (2013; 2013 a) experiments in cereals. Zhao et al. (2013) mentioned that the plant uptake PFOS with the strong influence of the environmental factors such as temperature, contaminant concentrations, salinity and pH value. Moreover, there is a strong correlation between root concentration factors and the octanol water partition coefficient (KOW), with the observed fact that roots uptake more contaminants with a higher log KOW, for the affinity to the lipophilic portion of the roots (Müller et al. 2016).

Some adverse effects on plants by PFAAs has been continuously reported. Qu et al. (2010) reported the inhibition of wheat seedlings roots and leaves biomass and lower chlorophyll accumulation at 10 mg/L PFOS treatment. The significant difference was observed on the

growth of wheat between the control (0 mg/kg) and a PFOA/PFOS soil concentration at 10 mg/kg, regarding to a significant reduction in the yield. Also, the root elongation of lettuce, pakchoi and cucumber was affected by PFOS and PFOA at the concentration ranged from 99 200 mg/L (Li et al. 2009).

1.4.5 Toxic effects on animals and humans

Toxicological studies on PFAAs, particularly PFOA and PFOS, has been widely studied, with clear results on animals with less statistical evidence as compare to humans (DeWitt, 2015). With increasing recognition of toxicity in animals, research on the short- and long-term impact of PFAAs on human health has increased. These chemicals, in particular PFOA and PFOS, have a high affinity for proteins. Once ingested these compounds are distributed among tissues and stored in liver, in kidney, in blood compartments and, with lower concentrations, also in other organs such as spleen, heart and blood serum, human milk (Eriksen et al. 2009; Sundström et al. 2011). The half life of PFOS and PFOA changes in relation to the animals and tend to increase from rodents (hours to days) to monkey (days to months) and for the humans it is longer (months to years) (DeWitt, 2015). PFASs are not metabolized and they are excreted primarily in urine and then in feces, to a lesser extent. In addition, during pregnancy, both PFOS and PFOA can cross the placental barrier (in both laboratory animals and humans), with the result that newborns are exposed to these substances contained in the maternal blood (DeWitt, 2015; Mamsen et al. 2017).

PFASs has several toxic effects on human beings and animals. Profound developmental toxicity has been described with gestional and lactational exposure to PFOS, PFOA and PFNA in the reproduction and development of the rodents (DeWitt, 2015; OECD, 2013). But among the PFAAs, PFOA was classified as a possible carcinogen for human beings reported by the International Agency of Research on Cancer (IARC). Even studies done by Grandjean et al. (2012) mentioned that the elevated exposures to PFCs were associated with reduced humoral immune response to routine childhood immunizations in children aged 5 and 7 years. Furthermore, a relationship between elevated PFOA blood levels and the following diseases: high cholesterol (hypercholesteremia), ulcerative colitis, thyroid diseases, preeclampsia, testicular cancer, kidney cancer was described (OECD, 2013). Thus, European Community

included PFOS and PFOA, which are PBT (Persistent, Bioaccumulation and Toxic, Wang et al. 2015), among the priority substances to be monitored for their risks. Owing to the reported effects of PFOA and PFOS, the production of these two compounds was almost banned in several countries (Rodea-Palomares et al. 2012).

However, we still can expect some exposure to these PFAAs and to other fluorinated alternatives in the upcoming years. That's why It is very necessary to study the effects of mixture of PFAAs to living organisms. Therefore, I decided to address my studies towards the effect of eleven different PFAAs on three different model plants.

1.4.6 International and national limits

The European law explicates perfluorooctane sulfonic acid (PFOS) in the directive 2006/122/CE as a dangerous compound. It is persistent, bio-accumulative, toxic for mammals and has long range propagation potential in the environment. The two PFAAs, PFOA and PFOS, as well as their precursors, were recommended monitoring of the presence in food by EU in 2010. In order to protect health and the environment, Delegates at the Stockholm Convention meeting in 2018 agreed to tighten a restriction on the uses of PFOS, the semi-finished products and articles containing PFOS (Stockholm Convention 2018, Rome). Stockholm convention has not set any limitation but still there are few limits in drinking water proposed by European and non-European states. The limits are listed in a tabular form (Table 1.2). The definitions and meanings of the reference values may vary depending on the national body control who has proposed them.

Table 1.2: Reference values in drinking water - Potable water values for perfluorooctanoic acid (PFOA), Perfluorooctanesulfonic acid (PFOS) and the sum of other PFASs, as proposed by various European and non-European control bodies.

National control bodies	Definition of drinking water reference values	PFOA	PFOS	Sum of other PFASs
Germany Trinkwasserkommission - Drinking water agency, 2006	Strictly health-based guide value	Sum FOA+PFO S ≤0,3 µg/L (300 ng/L)	Sum PFOA+PFO S ≤0,3 µg/L (300 ng/L)	-
United Kingdom Drinking Water	Guidance value	5 µg/L (5000 ng/L)	1 µg/L (1000 ng/L)	-

Inspectorate, 2009				
Netherlands National Institute of Public Health and Environment, 2011	Maximum Tolerable Level	-	0,53 µg/L(530 ng/L)	-
Italy Ministry of Health, 2014	Performance levels (objective)	0,5 µg/L (500 ng/L)	0,03 µg/L(30 ng/L)	0,5µg/L (500 ng/L)
Italy Veneto regional council, 2017	Performance levels (objective)	Sum PFOA+PFOS ≤0,09 µg/L (≤ 90 ng/L)	≤ 0,03 µg/L(≤ 30 ng/L)	≤0,3 µg/L (≤ 300 ng/L)
Denmark Danish Environmental Protection Agency, 2015	Health-based quality criteria	0,3 µg/L (300 ng/L)	0,1 µg/L (100 ng/L)	-
Sweden National Food Agency, 2016	Action limit	Sum 11 PFASs <0,09 µg/L (90 ng/L)	Sum 11 PFASs <0,09 µg/L (90 ng/L)	Sum 11 PFASs <0,09 µg/L (90 ng/L)
USA U.S. EPA - American Environmental Protection Agency, 2016	Health Advisory	Sum PFOA+PFOS ≤0,07 µg/L (70 ng/L)	Sum PFOA+PFOS ≤0,07 µg/L (70 ng/L)	-
New Jersey New Jersey Drinking Water Quality Institute, 2016	Health-based maximum contaminant level	0,014 µg/L (14 ng/L)	-	-
Canada Health Canada, government of Canada, Committee of drinking water, 2016	Maximum acceptable concentration	0.2 µg/L (200 ng/L)	0,6 µg/L (600 ng/L)	-
Australia enHealth- Environmental Health Standing Committee of the Australian Health Protection Principal Committee, **2016**	Recommended interim values	5 µg/L(5000 ng/L)	0,5 µg/L(500 ng/L)	-

About the limits of the PFASs presence in the human body, there are not any international guidelines and unique detection methods. But there are the limits for the main international rating institutions:

Table 1.3: PFASs limits in the human body for PFOA and PFOS.

International institution	PFOA	PFOS
EFSA (Environmental and Food Safety Agency)	1,5 µg/KgBW (1500 ng/ Kg BW)	0,15 µg/ Kg BW (150 ng/Kg BW)
UK COT (UK Commettee on Toxicity)	3 µg/KgBW (3000 ng/ Kg BW)	0,3 µg/ Kg BW (300 ng/Kg BW)
Trinkwasserkommission (German drinking water agency)	0,1 µg/KgBW (100 ng/ Kg BW)	0,1 µg/ Kg BW (100 ng/Kg BW)
US-EPA (American Environmental Protection Agency)	0,2 µg/KgBW (200 ng/ Kg BW)	0,08 µg/ Kg BW (80 ng/Kg BW)

Some Quality standards (SQA) have been developed from the workgroup in which Veneto region was admitted in August 2016. They selected five most prominent substances found in the environment and in humans: PFBA and PFBS (both with 4 carbon atoms), PFPeA (5 carbon atoms), PFHxA (6 carbon atoms) and PFOA and PFOS (8 carbon atoms). Table 1.4 summarizes the values proposed by the workgroup.

Table 1.4: Quality Standards for some PFASs.

Pollutant	**SQUA-MA** (Environmental Quality Standard) indoor surface water (ng/l)	**Groundwater threshold** (ng/l)	**Groundwater threshold in interaction with surface water** (ng/l)
PFBA	7000	-	-
PFBS	3000	3000	3000
PFPeA	3000	3000	3000
PFHxA	1000	1000	1000
PFOA	100	500	100
PFOS (priority substance)	0,65		

1.4.7 PFASs pollution in Italy

After the discovery of PFAS pollution in Veneto region in 2013, the engineers from Consiglio Nazionale delle Ricerche (CNR) started doing many investigations, focused especially on human exposure. The biomonitoring was carried out between July 2015 and April 2016 on people from contaminated Veneto territory. Blood sampling was carried out to determine the levels of PFASs (12 compounds), and a questionnaire was distributed to get some information about lifestyles and dietary habits (Ingelido et al. 2018). The study found significantly higher PFOA concentrations in the blood of people living in contaminated areas (median 13.8 ng/ml,

up to 70 ng/ml in the most exposed municipalities) compared to control group (median 1.64 ng/ml).

Since the national news were speaking a lot about these situations in the current time, people are aware of PFASs contamination and its effects on human beings. Thus, people are making slogans like “Zero PFAS” in the Veneto contaminated areas to bring the awareness about this problem. Even the families are very concerned about their child and asking to use clean water to cook in the school canteens.

That's why it's important to continue doing research on this topic and it would be more important to equip the aqueducts connected to the polluted site. The main objective is not only the investigation which was carried out by the Vicenza Public Prosecutor, but it is also for the purpose of an effective environmental remediation which explains the occurrence of PFASs contamination.

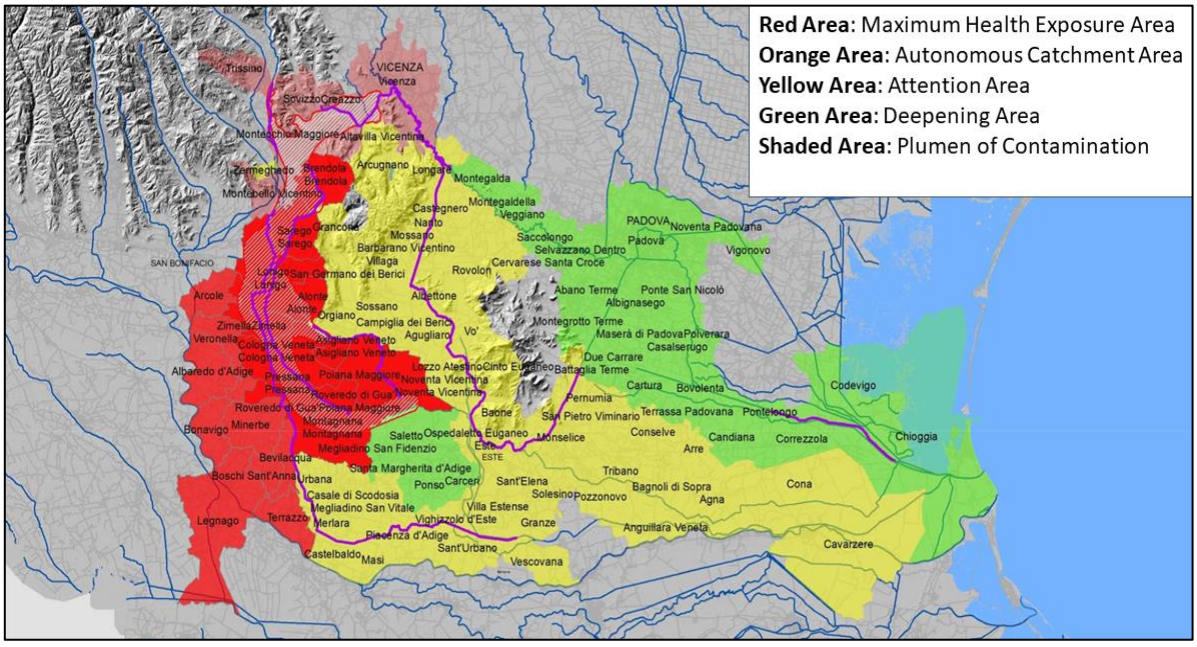

Figure 1.7: Veneto contaminated areas between Vicenza, Padua and Verona provinces. **(https://www.aulss9.veneto.it/)**

1.4.8 Future alternatives of PFAS

As already mentioned, the long chain PFAAs are highly persistent, bio-accumulative, and toxic to the environment (Birnbaum et al. 2015; Blum et al. 2015). Due to this reason,

Perfluorooctane sulfonic acid (PFOS), perfluorooctanoic acid (PFOA), and PFCAs with 11–14 perfluorinated carbons are now regulated in the EU and Canada. For the same reasons there have been several voluntary actions by the manufacturing industries to phase out these substances or to reduce their emissions. Long chain PFAAs including perfluoroalkyl carboxylic acids (PFCAs) with 7 or more perfluorinated carbons, perfluoroalkyl sulfonic acids (PFSAs) with 6 or more perfluorinated carbons, and their precursors, are being replaced by a wide range of fluorinated alternatives (Scheringer et al. 2014). Since 2002, the use of alternative chemicals or non-chemical techniques has been studied to replace the long chain PFAAs, particularly PFOS and PFOA.

The commercially available alternatives to long-chain PFAs have the following possibilities:

- substances with shorter per- or polyfluorinated carbon chains;
- non-fluorine containing substances;
- non-chemical techniques (OECD, 2013).

Firstly, the most common replacements are short-chain PFASs with similar structures, or compounds with fluorinated segments joined by ether linkages (Blum et al. 2015). The fluorinated alternatives are various substances with shorter carbon chain developed for the replacement of many uses of long-chain PFASs, that include homologues of long-chain PFASs, typically with six or fewer perfluoroalkyl carbons. Other groups are the perfluorobutane sulfonyl fluoride (PBSF)-based derivatives as replacements of perfluorooctane sulfonyl fluoride (POSF)-based chemicals in surface treatment and coatings of the mono and polyfluorinated-ether-functionality compounds (e.g., polyfluoroalkyl ether carboxylic acids). Finally, we can take a note on the possible other alternatives like fluorinated oxetanes and other fluorinated polymers (OECD, 2013).

The disadvantage of using short chain PFASs is that they are bioaccumulated by plants (Scheringer et al. 2014). From several studies we already know that shorter-chain PFASs are transferred predominantly at higher concentrations to the shoots as compared to long-chain PFASs (Felizeter et al. 2012; 2014; Krippner et al. 2014). The short-chain PFCA and PFSA homologues (PFHxA and PFBS) are persistent in the environment as the long-chain homologues (Wang et al. 2013). Although some short-chain PFAAs, i.e. C < 7 for PFCAs and C < 6 for PFSAs (Buck et al. 2011), are not considered to be bio-accumulative, owing to their low

half-life. But they are as recalcitrant to degradation as long-chained PFAAs and are highly soluble. They have lower sorption to solids, which lead to greater mobility in the environment (Vierke et al. 2012, Wang et al. 2015). But on the other hand, we need to understand the potential adverse health effects of short-chain PFAAs exposure, especially regarding low dose endocrine disruption and immunotoxicity (Birnbaum & Grandjean 2015). The goal should be to introduce non-persistent alternatives to long-chain PFAAs that can be fully degraded and mineralized. This may imply on nonfluorinated products because the switch to short-chain and other fluorinated alternatives may not reduce the amounts of PFAAs in the environment. Therefore, development of non-persistent alternatives should be strongly encouraged and PFASs should only be used in applications where they are truly needed and proven indispensable (Blum et al. 2015; Scheringer et al. 2014).

Some non-chemical techniques, such as biological, physical or natural control methods, can be used to replace the long-chain PFAAs. For example, foam blankets and other barrier materials are used for mist suppression in electrochemical metal plating (OECD, 2013). The other technique could be phytoremediation techniques which may counter the spread of PFAAs in the environment, as it has been shown that tree plants and constructed wetlands are able to accumulate these pollutants (Gobelius et al. 2017; Yin et al. 2017). But still extensive studies are needed on uptake capacity of PFAAs by different plant species.

The function and performance level of PFAAs are difficult to substitute due to their chemical and thermal stability as well as their hydrophobic and oleophobic properties that provide unique material benefits (Birnbaum, 2015). But the other big problem is the lack of information required to assess the safety of alternatives, due to concerns of business confidentiality. For the future, it would be necessary to provide the following steps, with a transparent knowledge exchange among the stakeholders (manufacturers of fluorinated materials, industrial users, regulators, farmers, scientists and the public):

- developing accurate analytical techniques for alternatives;
- developing data analysis for environmental fate, toxicity and bioaccumulation studies;
- developing a new industrial ecology using the latest scientific findings to implement materials with similar function (Wang et al. 2013).

- Adaptation of phytoremediation techniques (Gobelius et al. 2017; Yin et al. (2017)
- Growing vegetables in hydroponics in contaminated areas should be avoided
- Addition of unpolluted manure to the contaminated soil for the agricultural purpose
- the use of plant residues, like maize stover, in animal feeds should be avoided (Ghisi et al. 2018).

1.5 Nuclear Magnetic Resonance (NMR) spectroscopy

Metabolomics is the comprehensive analysis of different metabolites involved in the biological specimen, which has been used to study the toxicological mechanisms. The current metabolomics technologies used are going beyond the scope of standard techniques and are capable to analyze thousands of metabolites without destroying the tissue sample. Among them, Nuclear Magnetic Resonance (NMR) is the one, the most powerful analytical tool in this modern era (Simpson et al. 2015). Nearly all the matrices including organic and inorganic can be studied by some sort of NMR spectroscopy (Simpson et al. 2012). NMR is especially useful for organic structures for common nuclei like hydrogen, carbon, nitrogen, phosphorus. When a molecule is placed in a magnetic field, the nuclei resonate at certain frequencies, characteristic to their chemical environment (Lin et al. 2006). The specific frequency is referred to as the “chemical shift” and identifies the different types of chemical groups within a molecule and their bonding environment. Also, the peak area, in a properly acquired spectrum, is fully quantitative. Thus, in its most basic form one-dimensional (^{1}D) NMR identifies the types of nuclei present (via chemical shift) which is the most commonly used nuclei for metabolomics studies (De Graaf 2019) and how many of each type is present (via peak intensity). Multidimensional NMR on the other hand can be used to identify correlations that depict how nuclei are connected to form a complete structure. A series of multidimensional spectra are analogous to a “molecular jigsaw puzzle”, and assuming no spectral overlap, can be pieced together in one way to produce a single unambiguous chemical structure (Simpson et al. 2012).

NMR however, is not restricted to simple chemical structures but could be used to solve the primary structure of proteins as well as their folding, dynamics, 3D solvated shape, and inter/intramolecular interactions. This has made the technique attractive for many

metabolomics studies. Similarly, NMR is excellent for kinetic studies to measure the chemical reaction rates and biological processes (Kaufman et al. 1982). Due to its numerous advantages, NMR has been widely used in environmental research (Viant et al. 2003). Unlikely, it represents an effective and reproducible method of determining which contaminants in the environment have deleterious effects on organisms. Thus, NMR is serving as a powerful tool in providing in-depth information on the metabolic responses of plants (Kim et al. 2011; Fernie et al. 2003; ward et al. 2007) and animals (Zhang et al. 2008), and information on the toxic mode of action of contaminants in the environment.

1.5.1 Types of NMR Spectroscopy as an Environmental tool

The NMR has considerable capability to resolve overlapping signals of a complex structure like protein or complex environmental matrices such as soil, sediment, water, or air particles. Thus, combined modern NMR approaches provide a powerful framework to better understand sustainable agriculture, contaminant fate, bioavailability, toxicity, sequestration, and remediation.

There are different types of available NMR which has been used to unravel the molecular complexities found in many environmental samples.

1. Solution-State NMR Spectroscopy, is the spectroscopy providing the highest resolution data and comprehensive molecular information for soluble components. The NMR probes used range from 1 mm (~5 µL sample) to 10 mm (~5 mL sample) diameter with the sample size being 5 mm (~600 µL sample). This technique can be performed in all the natural water samples without preconcentrating (lam et al. 2008) and the samples can be completely unperturbed. The disadvantages of this instrument is, the analysis takes at least 24 h, the water suppression involved is challenging, and only 1D NMR can be collected routinely (Simpson et al. 2012). *2. Solid-State NMR Spectroscopy,* is the type of NMR which is normally performed on dried samples packed in the rotor. The rotor sizes are 7 mm (~500 mg sample) and 4 mm (~100 mg sample), where the samples are spun between 5 and 13 kHz at the magic angle to reduce any unwanted nuclear spin interactions. $^{1}H–^{1}H$ dipole interactions are very strong in solid state which results in ^{1}H NMR with a very wide spectral profile. ^{13}C is the one

most commonly detected nucleus in the solid state for environmental samples. Samples such as plant samples which are rich in organic matter are dried and benefited more with little pre-treatment. Whereas, soils sediments or air particles that have high inorganic contents can benefit from hydrofluoric acid treatment (Gelians et al. 2001) which dissolves paramagnetic minerals and concentrates organic matter resulting in high-quality NMR data. In the solid-state Multidimensional NMR is possible which is useful for the analysis of environmental samples. *3. Gel-Phase NMR Spectroscopy,* used swellable or gel like samples. The probes used have low power circuitry and are optimized for ^{1}H detection and can observe the signals from structures that are not in the true solid state. One major advantage of this NMR is that the information from the liquid or gel-like components can be obtained from intact samples. Many environmental studies have used gel-phase NMR for monitoring the sorption kinetics of contaminants across the soil−water interface, (Shirzadi et al. 2008) and provide a structural information on a range of environmental matrices like plants, microbes, and in vivo organisms. *4. Comprehensive Multiphase (CMP) NMR Spectroscopy*, a new approach for performing the NMR on environmental and biological intact samples in natural state, which includes all the above-mentioned methods into one single approach (Courtier-Murias et al. 2012). Not only the individual phases; solid, gel, solution also can be studied and fully differentiated in situ, but interactions and kinetics at interfaces can also be monitored. This technique provides a detailed insight of contaminants in a soil matrix and as such represents a powerful tool to assess the efficiency and effectiveness of existing and novel remediation approaches. Due to its unique abilities to study the samples in their native state CMP-NMR will have a significant impact on environmental research field.

1.5.2 CMP-NMR in environmental samples

NMR spectroscopy being a powerful tool has been widely used for elucidating the molecular interactions between biological components in solution, gel and solid phases (Zheng et al. 2012). However, these techniques focus only on analysis in a single physical state (Pautler et al. 2012). But, to understands the process of chemical sequestration fully, it is important to investigate and differentiate the molecular interactions from all phases. Thus, CMP-NMR was

introduced, for the study of kinetic transfer and molecular interactions during contaminant sequestration for each phase (solid, liquid and gel).

The study done by Masoom et al. (2015) obtained multiple phase kinetics in a whole PFP and PFOA contaminated soil through CMP-NMR and CPMG-SS techniques. PFP showed more general partitioning behavior, but its ability to act as a solvent and the properties of the soil−water interface was changed which was hard to predict without NMR data. Conversely, PFOA which was found to be selectively bind to soil microbial protein was significance. To illustrate the capability of ^{19}F NMR soil samples, Courtier-Murias et al. (2012) used perfluorooctanoic acid (PFOA) and tetrafluoro-1,4-hydroquinone (TFHQ) contaminants for demonstrating the preliminary application of CMP-NMR. This approach was a great potential especially for the *in-situ* study of natural samples in their native state. Likewise, Wheeler et al. (2015) used (CMP)-NMR and discovered that methanol, fatty acids and/or lipids, glutamine, phenylalanine, starch, and nucleic acids were more abundant in *eli1* as compare to WT of *A. thaliana.* Similarly, Mobarhan et al. (2016) found out nearly 40 metabolites in ^{13}C labelled living organism named *Hyallela Azteca.* Multidimensional NMR approach was also used for the detailed assignment of metabolites and structural components *in vivo*. This technology is not limited here, they have been used in intact ^{13}C-labeled seeds (lam et al. 2014) with multidimensional NMR methods again. In the mobile phase, an assortment of metabolites was identified; the gel phase was dominated by triacylglycerides; the semisolid phase was composed of carbohydrate biopolymers, and the solid phase was greatly influenced by starchy endosperm signals.

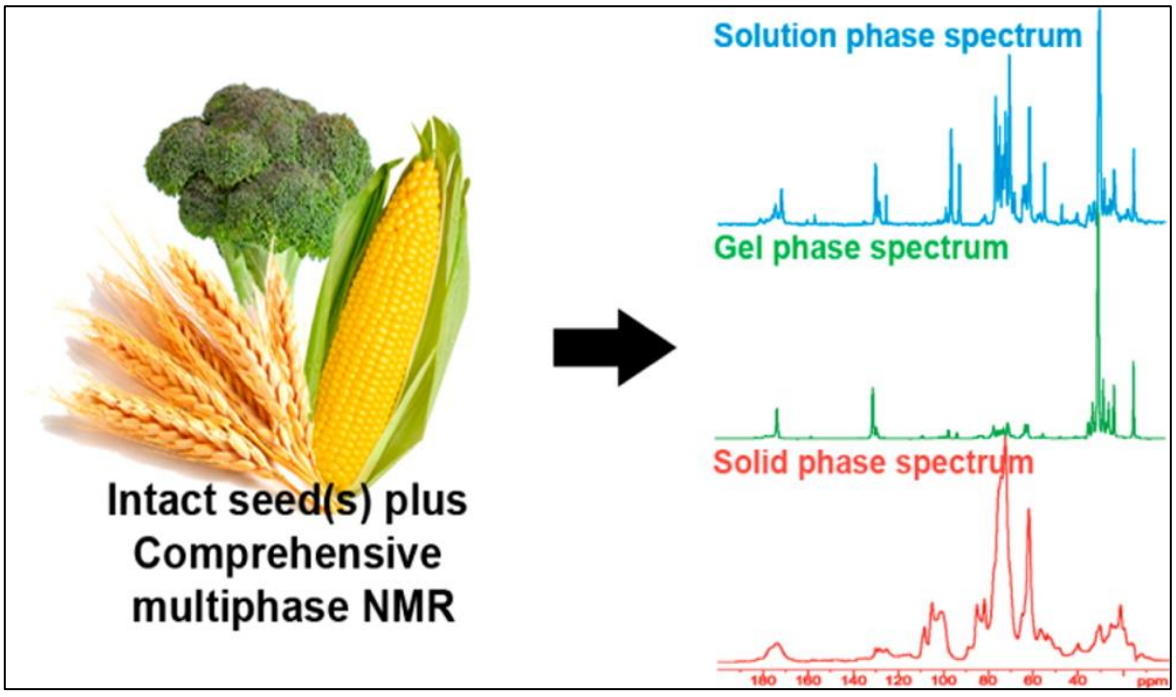

Figure 1.8: Application of CMP-NMR to food chemistry and indicating the feasibility for studying intact heterogeneous samples in three different phases. Source (Lam et al. 2014)

CMP NMR has also been applied in *in-vivo* to understand the binding and fate of contaminants and drugs (Simpson et al. 2007). In many ways it was consider that metabolomics provides an information on the rapid response of an organism to stress, whereas changes to the structural components may occur slower over time and reflect the longer-term impacts. An example could be PFASs; they are ubiquitous in the environment and has been detected in humans, animals and plants (Kannan et al. 2002; Kannan et al. 2004; Martin et al. 2004). Thus, CMP NMR could be used on per fluorinated contaminate due to their increasing environmental importance, distribution and health risk on human being.

References

Ahrens, L., Felizeter, S., Sturm, R., Xie, Z., & Ebinghaus, R. 2009. Polyfluorinated compounds in waste water treatment plant effluents and surface waters along the river elbe, germany. *Marine Pollution Bulletin, 58*(9), 1326-1333. https://doi.org/10.1016/j.marpolbul.2009.04.028.

Ahrens, L., Xie, Z., & Ebinghaus, R. 2010. Distribution of perfluoroalkyl compounds in seawater from Northern Europe, Atlantic Ocean, and Southern Ocean. *Chemosphere*, *78*(8), 1011-1016. https://doi.org/10.1016/j.chemosphere.2009.11.038.

ARPAV (2017). Contaminazione da PFAS.

Ateia, M., Maroli, A., Tharayil, N., & Karanfil, T. 2019. The overlooked short-and ultrashort-chain poly-and perfluorinated substances: A review. *Chemosphere*, *220*, 866-882. https://doi.org/10.1016/j.chemosphere.2018.12.186.

Bao, J., Yu, W. J., Liu, Y., Wang, X., Jin, Y. H., & Dong, G. H. 2019. Perfluoroalkyl substances in groundwater and home-produced vegetables and eggs around a fluorochemical industrial park in China. *Ecotoxicology and environmental safety*, *171*, 199-205. https://doi.org/10.1016/j.ecoenv.2018.12.086.

Bialk, H. M., Simpson, A. J., & Pedersen, J. A. 2005. Cross-coupling of sulfonamide antimicrobial agents with model humic constituents. *Environmental science & technology*, *39*(12), 4463-4473. https://doi.org/10.1021/es0500916.

Birnbaum, L. S., & Grandjean, P. (2015). Alternatives to PFASs: Perspectives on the science. *Environmental Health Perspectives, 123*(5). https://doi.org/10.1289/ehp.1509944.

Blaine, A. C., Rich, C. D., Hundal, L. S., Lau, C., Mills, M. A., Harris, K. M., & Higgins, C. P. 2013. Uptake of perfluoroalkyl acids into edible crops via land applied biosolids: field and greenhouse studies. *Environmental science & technology*, *47*(24), 14062-14069. https://doi.org/10.1021/es403094q.

Blaine, A. C., Rich, C. D., Hundal, L. S., Lau, C., Mills, M. A., Harris, K. M., & Higgins, C. P. 2013a. Uptake of perfluoroalkyl acids into edible crops via land applied biosolids: field and greenhouse studies. *Environmental science & technology*, *47*(24), 14062-14069.

Blaine, A. C., Rich, C. D., Sedlacko, E. M., Hyland, K. C., Stushnoff, C., Dickenson, E. R. V., & Higgins, C. P. 2014. Perfluoroalkyl acid uptake in lettuce (*Lactuca sativa*) and strawberry (*Fragaria ananassa*) irrigated with reclaimed water. *Environmental Science & Technology, https://doi.org/*10.1021/es504150h.

Blum, A., Balan, S. A., Scheringer, M., Trier, X., Goldenman, G., Cousins, I. T., Weber, R. 2015. The madrid statement on poly- and perfluoroalkyl substances (PFASs). *Environmental Health Perspectives, 123*(5). https://doi.org/10.1289/ehp.1509934.

Boxall, A. B., Johnson, P., Smith, E. J., Sinclair, C. J., Stutt, E., & Levy, L. S. 2006. Uptake of veterinary medicines from soils into plants. *Journal of Agricultural and Food Chemistry*, *54*(6), 2288-2297. https://doi.org/10.1021/jf053041t.

Buck, R. C., Franklin, J., Berger, U., Conder, J. M., Cousins, I. T., De Voogt, P., Jensen, A. A., Kannan, k., Mabury, A. S., & van Leeuwen, S. P. 2011. Perfluoroalkyl and polyfluoroalkyl substances in the environment: terminology, classification, and origins. *Integrated environmental assessment and management*, *7*(4), 513-541. https://doi.org/10.1002/ieam.258.

Byrne, S., Begum, T., Miller, P., Seguinot-Medina, S., Waghiyi, V., Buck, C. L., Hippel, V. F. A., & Carpenter, D. O. 2018. Exposure to Perfluoroalkyl Substances and Polybrominated Diphenyl Ethers from Traditionally Harvested Food Animals on St. Lawrence Island, Alaska. In *ISEE Conference Abstracts,* 2018, 1.

Cabello, F. C. 2006. Heavy use of prophylactic antibiotics in aquaculture: a growing problem for human and animal health and for the environment. *Environmental microbiology*, *8*(7), 1137-1144. https://doi.org/10.1111/j.1462-2920.2006.01054.x.

Carter, L. J., Harris, E., Williams, M., Ryan, J. J., Kookana, R. S., & Boxall, A. B. 2014. Fate and uptake of pharmaceuticals in soil–plant systems. *Journal of agricultural and food chemistry*, *62*(4), 816-825. https://doi.org/10.1021/jf404282y.

Carvalho, P. N., Basto, M. C. P., Almeida, C. M. R., & Brix, H. 2014. A review of plant–pharmaceutical interactions: from uptake and effects in crop plants to phytoremediation in constructed wetlands. *Environmental Science and Pollution Research*, *21*(20), 11729-11763. https://doi.org/10.1007/s11356-014-2550-3.

Clara, M., Scharf, S., Weiss, S., Gans, O., & Scheffknecht, C. 2008. Emissions of perfluorinated alkylated substances (PFAS) from point sources—identification of relevant branches. *Water science and technology*, *58*(1), 59-66. https://doi.org/10.2166/wst.2008.641.

Courtier-Murias, D., Farooq, H., Masoom, H., Botana, A., Soong, R., Longstaffe, J. G., Simpson, M., Maas, E. W., Fey, M., Andrew, B., Struppe, J., Hutchins, H., Krishnamurthy, S., Kumar, R., Monette, M., Stronks J. H., Hume, A., & Simpsona, J. A. 2012. Comprehensive multiphase NMR spectroscopy: basic experimental approaches to differentiate phases in heterogeneous samples. *Journal of Magnetic Resonance*, *217*, 61-76. https://doi.org/10.1016/j.jmr.2012.02.009.

Cowieson, A. J., & Kluenter, A. M. 2019. Contribution of exogenous enzymes to potentiate the removal of antibiotic growth promoters in poultry production. *Animal Feed Science and Technology*, *250*, 81-92. https://doi.org/10.1016/j.anifeedsci.2018.04.026.

De Graaf, R. A. 2019. *In vivo NMR spectroscopy: principles and techniques*. John Wiley & Sons.

De Liguoro, M., Poltronieri, C., Capolongo, F., & Montesissa, C. 2007. Use of sulfadimethoxine in intensive calf farming: evaluation of transfer to stable manure and soil. *Chemosphere*, 68(4), 671-676. https://doi.org/10.1016/j.chemosphere.2007.02.009.

Defenbaugh, A. L. 2014. Evaluating Ohio river basin waters: A water quality and water resources internship with the ohio river valley water sanitation commission.

DeWitt, J. C. 2015. *Toxicological effects of perfluoroalkyl and polyfluoroalkyl substances*. Humana Press.

Domingo, J. L., & Nadal, M. 2019. Human exposure to per-and polyfluoroalkyl substances (PFAS) through drinking water: A review of the recent scientific literature. *Environmental Research*, 108648. https://doi.org/10.1016/j.envres.2019.108648.

EFSA Journal. 2008. Opinion of the scientific panel on contaminants in the food chain on perfluorooctane sulfonate (PFOS), perfluorooctanoic acid (PFOA) and their salts. *EFSA Journal, 653*, 1-131.

Eriksen, K. T., Sørensen, M., McLaughlin, J. K., Lipworth, L., Tjønneland, A., Overvad, K., & Raaschou-Nielsen, O. (2009). Perfluorooctanoate and perfluorooctanesulfonate plasma levels and risk of cancer in the general Danish population. *Journal of the National Cancer Institute*, *101*(8), 605-609. https://doi.org/10.1093/jnci/djp041

Farinola Gianluca Maria. 2016. I composti perfluoroalchilici come inquinanti delle acque per consumo umano.

Felizeter, S., McLachlan, M. S., & Voogt, d., P. 2014. Root uptake and translocation of perfluorinated alkyl acids by three hydroponically grown crops. *Journal of Agricultural and Food Chemistry, 62*(15), 3334-3342. https://doi.org/10.1021/jf500674j.

Felizeter, S., McLachlan, M., & de Voogt, P. 2012. Uptake of perfluorinated alkyl acids by hydroponically grown lettuce (*Lactuca sativa*). Environmental Science and Technology, 46(21), 11735-11743. https://doi.org/10.1021/es302398u.

Fernie, A. R. 2003. Metabolome characterisation in plant system analysis. *Functional Plant Biology*, *30*(1), 111-120. https://doi.org/10.1071/FP02163.

Forster, M., Laabs, V., Lamshoft, M., Groeneweg, J., Zuhlke, S., Spiteller, M., Krauss, M. Kaupenjohann, M., & Amelung, W. 2009. Sequestration of manure-applied sulfadiazine residues in soils. *Environmental Science & Technology*, *43*(6), 1824-1830. https://doi.org/10.1021/es8026538.

Frank, R. (1998). The use of biosolids from wastewater treatment plants in agriculture. Environmental Management and Health, 9(4), 165-169.

Fromme, H., Tittlemier, S. A., Völkel, W., Wilhelm, M., & Twardella, D. 2009. Perfluorinated compounds – exposure assessment for the general population in western countries. *International Journal of Hygiene and Environmental Health, 212*(3), 239-270. https://doi.org/10.1016/j.ijheh.2008.04.007.

Fujii, S., Polprasert, C., Tanaka, S., Lien, H., Pham, N., & Qiu, Y. (2007). New POPs in the water environment: distribution, bioaccumulation and treatment of perfluorinated compounds–a review paper. *Journal of Water Supply: Research and Technology-AQUA*. *56*(5), 313-326. https://doi.org/10.2166/aqua.2007.005.

Gelinas, Y., Baldock, J. A., & Hedges, J. I. 2002. Demineralization of marine and freshwater sediments for CP/MAS 13C NMR analysis. *Org. Geochem,* 32 (5), 677−693. https://doi.org/10.1016/S0146-6380(01)00018-3.

Ghisi, R., Vamerali, T., & Manzetti, S. 2018. Accumulation of perfluorinated alkyl substances (PFAS) in agricultural plants: a review. *Environmental research*. https://doi.org/10.1016/j.envres.2018.10.023.

Gobelius, L., Lewis, J., & Ahrens, L. 2017. Plant uptake of per-and polyfluoroalkyl substances at a contaminated fire training facility to evaluate the phytoremediation potential of various plant species. *Environmental science & technology*, *51*(21), 12602-12610. https://doi.org/10.1021/acs.est.7b02926.

Gothwal, R., & Shashidhar, T. 2015. Antibiotic pollution in the environment: a review. *Clean–Soil, Air, Water*, *43*(4), 479-489. https://doi.org/10.1002/clen.201300989.

Grandjean, P., Andersen, E. W., Budtz-Jørgensen, E., Nielsen, F., Mølbak, K., Weihe, P., & Heilmann, C. (2012). Serum vaccine antibody concentrations in children exposed to perfluorinated compounds. *Jama*, *307*(4), 391-397. https://doi.org/10.1001/jama.2011.2034.

Greenpeace 2016. PFC pollution hotspots: how these chemicals are entering our bodies. https://storage.googleapis.com/planet4-international-stateless/2018/06/PFC-Pollution-Hotspots.pdf.

Hekster, F. M., De Voogt, P., Pijnenburg, A. M. C. M., & Laane, R. W. P. M. 2002. Perfluoroalkylated substances: Aquatic environmental assessment. *Rapportnr,* 2002.043.

Herrick Robert L., Buckholz Jeanette, Biro Frank M., Calafat Antonia M., Ye Xiaoyun, Xie Changchun, Pinney Susan M. 2017. Polyfluoroalkyl substance exposure in the mid-ohio river valley, 1991 - 2012. *Environmental Pollution,* 228, 50-60. https://doi.org/10.1016/j.envpol.2017.04.09.

Huschek, G., Hollmann, D., Kurowski, N., Kaupenjohann, M., & Vereecken, H. 2008. Re-evaluation of the conformational structure of sulfadiazine species using NMR and ab initio DFT studies and its implication on sorption and degradation. *Chemosphere*, *72*(10), 1448-1454. https://doi.org/10.1016/j.chemosphere.2008.05.038.

Ingelido, A. M., Abballe, A., Gemma, S., Dellatte, E., Iacovella, N., De Angelis, G., Zampaglioni, F., Marraa, V., Miniero, R., Valentini, S., Russo, F., Vazzoler., M., Testai, E., & De Felipa, E. 2018. Biomonitoring of perfluorinated compounds in adults exposed to contaminated drinking water in the Veneto Region, Italy. *Environment international*, *110*, 149-159. https://doi.org/10.1016/j.envint.2017.10.026.

Janousek, R. M., Lebertz, S., & Knepper, T. P. 2019. Previously unidentified sources of perfluoroalkyl and polyfluoroalkyl substances from building materials and industrial fabrics. *Environmental Science: Processes & Impacts*. https://doi.org/10.1039/C9EM00091G.

Jechalke, S., Kopmann, C., Rosendahl, I., Groeneweg, J., Weichelt, V., Krögerrecklenfort, E., Nikola Brandes, N., Nordwig, M., Ding, G., Siemens, J., Heuer, H., & Smalla, K. 2013. Increased abundance and transferability of resistance genes after field application of manure from sulfadiazine-treated pigs. *Appl. Environ. Microbiol.*, *79*(5), 1704-1711. https://doi.org/10.1128/AEM.03172-12.

Kang, D. H., Gupta, S., Rosen, C., Fritz, V., Singh, A., Chander, Y., Murray, H., & Rohwer, C. 2013. Antibiotic uptake by vegetable crops from manure-applied soils. *Journal of agricultural and food chemistry*, *61*(42), 9992-10001. https://doi.org/10.1021/jf404045m.

Kannan, K., Corsolini, S., Falandysz, J., Fillmann, G., Kumar, K. S., Loganathan, B. G., Ali Mohd, M., Olivero, J., Van Wouwe, N., Ho Yang, J., & Aldous, K. M. 2004. Perfluorooctanesulfonate and related fluorochemicals in human blood from several countries. *Environmental science & technology*, *38*(17), 4489-4495. https://doi.org/10.1021/es0493446.

Karcı, A., & Balcıoğlu, I. A. 2009. Investigation of the tetracycline, sulfonamide, and fluoroquinolone antimicrobial compounds in animal manure and agricultural soils in Turkey. *Science of the total environment*, 407(16), 4652-4664. https://doi.org/10.1016/j.scitotenv.2009.04.047.

Kaufman, D., Sterner, C., Masek, B., Svenningsen, R., & Samuelson, G. 1982. An NMR kinetics experiment. *Journal of chemical Education*, *59*(10), 885.

Kim, H. K., Choi, Y. H., & Verpoorte, R. 2011. NMR-based plant metabolomics: where do we stand, where do we go? *Trends in biotechnology*, *29*(6), 267-275. https://doi.org/10.1016/j.tibtech.2011.02.001.

Krippner, J., Brunn, H., Falk, S., Georgii, S., Schubert, S., & Stahl, T. 2014. Effects of chain length and pH on the uptake and distribution of perfluoroalkyl substances in maize (*Zea mays*). *Chemosphere, 94*, 85-90. https://doi.org/10.1016/j.chemosphere.2013.09.018.

Krippner, J., Falk, S., Brunn, H., Georgii, S., Schubert, S., & Stahl, T. 2015. Accumulation potentials of perfluoroalkyl carboxylic acids (PFCAs) and perfluoroalkyl sulfonic acids (PFSAs) in maize (Zea mays). *Journal of agricultural and food chemistry*, *63*(14), 3646-3653. https://doi.org/10.1021/acs.jafc.5b00012.

Kumar, V., and J. Gupta. 2018. Prevailing practices in the use of antibiotics by dairy farmers in Eastern Haryana region of India. *Veterinary World*, 11 (3), 274-280. https://doi.org/10.14202/vetworld.2018.274-280.

Lam, B., Simpson, A. J. 2008. Direct 1 H NMR spectroscopy of dissolved organic matter in natural waters. *Analyst*, 133 (2), 263−269. https://doi.org/10.1039/B713457F.

Land, M., de Wit, C. A., Bignert, A., Cousins, I. T., Herzke, D., Johansson, J. H., & Martin, J. W. 2018. What is the effect of phasing out long-chain per-and polyfluoroalkyl substances on the concentrations of perfluoroalkyl acids and their precursors in the environment? A systematic review. *Environmental Evidence*, *7*(1), 4. https://doi.org/10.1186/s13750-017-0114-y.

Lechner, M., & Knapp, H. (2011). Carryover of perfluorooctanoic acid (PFOA) and perfluorooctane sulfonate (PFOS) from soil to plant and distribution to the different plant compartments studied in cultures of carrots (Daucus carota ssp. Sativus), potatoes (Solanum tuberosum), and cucumbers (Cucumis Sativus). *Journal of agricultural and food chemistry*, *59*(20), 11011-11018. https://doi.org/10.1021/jf201355y.

Li, M. H. (2009). Toxicity of perfluorooctane sulfonate and perfluorooctanoic acid to plants and aquatic invertebrates. *Environmental Toxicology: An International Journal*, *24*(1), 95-101. https://doi.org/10.1002/tox.20396.

Li, Y., Han, D., Sommerfeld, M., & Hu, Q. 2011. Photosynthetic carbon partitioning and lipid production in the oleaginous microalga Pseudochlorococcum sp. (Chlorophyceae) under nitrogen-limited conditions. *Bioresource Technology*, *102*(1), 123-129. https://doi.org/10.1016/j.biortech.2010.06.036.

Lin, C. Y., Viant, M. R., & Tjeerdema, R. S. 2006. Metabolomics: methodologies and applications in the environmental sciences. *Journal of Pesticide Science*, *31*(3), 245-251. https://doi.org/10.1584/jpestics.31.245.

Lindim, C., Van Gils, J., & Cousins, I. T. 2016. Europe-wide estuarine export and surface water concentrations valseof PFOS and PFOA. *Water research*, *103*, 124-132. https://doi.org/10.1016/j.watres.2016.07.024.

Liu, S., Yang, R., Yin, N., Wang, Y. L., & Faiola, F. 2019. Environmental and human relevant PFOS and PFOA doses alter human mesenchymal stem cell self-renewal, adipogenesis and osteogenesis. *Ecotoxicology and environmental safety*, *169*, 564-572. https://doi.org/10.1016/j.ecoenv.2018.11.064.

Lorenzo, M., Campo, J., & Picó, Y. 2015. Optimization and comparison of several extraction methods for determining perfluoroalkyl substances in abiotic environmental solid matrices using liquid

chromatography-mass spectrometry. *Analytical and bioanalytical chemistry*. *407*(19), 5767-5781. https://doi.org/10.1007/s00216-015-8759-2.

Lu, Z., Na, G., Gao, H., Wang, L., Bao, C., & Yao, Z. 2015. Fate of sulfonamide resistance genes in estuary environment and effect of anthropogenic activities. *Science of the Total Environment*. *527*, 429-438. https://doi.org/10.1016/j.scitotenv.2015.04.101.

Mamsen, L.S., Jönsson, B.A., Lindh, C.H., Olesen, R.H., Larsen, A., Ernst, E., Kelsey, T.W. and Andersen, C.Y., 2017. Concentration of perfluorinated compounds and cotinine in human foetal organs, placenta, and maternal plasma. *Science of the Total Environment*. *596*, 97-105. https://doi.org/10.1016/j.scitotenv.2017.04.058.

Marti, E., Variatza, E., & Balcazar, J. L. 2014. The role of aquatic ecosystems as reservoirs of antibiotic resistance. *Trends in microbiology*, *22*(1), 36-41. https://doi.org/10.1016/j.tim.2013.11.001.

Martin, J. W., Whittle, D. M., Muir, D. C., & Mabury, S. A. 2004. Perfluoroalkyl contaminants in a food web from Lake Ontario. *Environmental Science & Technology*. *38*(20), 5379-5385. https://doi.org/10.1021/es020519q.

Masoom, H., Courtier-Murias, D., Soong, R., Maas, W. E., Fey, M., Kumar, R., Monetter, M., Stronks, J. H., Simpson, J. M., & Simpson, A. J. 2015. From spill to sequestration: the molecular journey of contamination via comprehensive multiphase NMR. *Environmental science & technology*. *49*(24), 13983-13991. https://doi.org/10.1021/acs.est.5b03251.

Mastrantonio, M., Bai, E., Uccelli, R., Cordiano, V., Screpanti, A., & Crosignani, P. 2017. Drinking water contamination from perfluoroalkyl substances (PFAS): an ecological mortality study in the Veneto Region, Italy. *The European Journal of Public Health*, *28*(1), 180-185. https://doi.org/10.1093/eurpub/ckx066.

Michelini, L., La Rocca, N., Rascio, N., & Ghisi, R. 2013. Structural and functional alterations induced by two sulfonamide antibiotics on barley plants. *Plant physiology and biochemistry*. *67*, 55-62. https://doi.org/10.1016/j.plaphy.2013.02.027.

Michelini, L., Reichel, R., Werner, W., Ghisi, R., & Thiele-Bruhn, S. 2012. Sulfadiazine uptake and effects on Salix fragilis L. and Zea mays L. plants. *Water, Air, & Soil Pollution*. *223*(8), 5243-5257. https://doi.org/10.1007/s11270-012-1275-5.

Migliore, L., Rotini, A., Cerioli, N. L., Cozzolino, S., & Fiori, M. 2010. Phytotoxic antibiotic sulfadimethoxine elicits a complex hormetic response in the weed lythrum salicaria L. *Dose-response*, *8*(4), dose-response. https://doi.org/10.2203/dose-response.09-033.Migliore.

Mirzaei, R., Yunesian, M., Nasseri, S., Gholami, M., Jalilzadeh, E., Shoeibi, S., & Mesdaghinia, A. 2018. Occurrence and fate of most prescribed antibiotics in different water environments of Tehran, Iran. *Science of the Total Environment*. *619*, 446-459. https://doi.org/10.1016/j.scitotenv.2017.07.272.

Mobarhan, Y. L., Fortier-McGill, B., Soong, R., Maas, W. E., Fey, M., Monette, M., Henry J. Stronks, H., Schmidt, S., Heumann, H., Norwood, W., & Simpson, A. J. 2016. Comprehensive multiphase NMR applied to a living organism. *Chemical science*. *7*(8), 4856-4866. https://doi.org/10.1039/C6SC00329J.

Möller, A., Ahrens, L., Surm, R., Westerveld, J., van der Wielen, F., Ebinghaus, R., & de Voogt, P. 2010. Distribution and sources of polyfluoroalkyl substances (PFAS) in the river Rhine watershed. *Environmental Pollution. 158*(10), 3243-3250. https://doi.org/10.1016/j.envpol.2010.07.019.

Muir, D., Bossi, R., Carlsson, P., Evans, M., De Silva, A., Halsall, C., Rauert R., Herzke, D., Hung, H., Letcher, R., Rigét, F., & Roos, A., 2019. Levels and trends of poly-and perfluoroalkyl substances in the Arctic environment–An update. *Emerging Contaminants. 5*, 240-271. https://doi.org/10.1016/j.emcon.2019.06.002.

Müller, C. E., LeFevre, G. H., Timofte, A. E., Hussain, F. A., Sattely, E. S., & Luthy, R. G. 2016. Competing mechanisms for perfluoroalkyl acid accumulation in plants revealed using an Arabidopsis model system. *Environmental toxicology and chemistry*. *35*(5), 1138-1147. https://doi.org/10.1002/etc.3251.

Noorlander, C. W., van Leeuwen, Stefan P J, Te Biesebeek, J. D., Mengelers, M. J. B., & Zeilmaker, M. J. 2011. Levels of perfluorinated compounds in food and dietary intake of PFOS and PFOA in the Netherlands. *Journal of Agricultural and Food Chemistry. 59*(13). https://doi.org/10.1021/jf104943p.

Nzeribe, B. N., Crimi, M., Mededovic Thagard, S., & Holsen, T. M. 2019. Physico-Chemical Processes for the Treatment of Per-And Polyfluoroalkyl Substances (PFAS): A review. *Critical Reviews in Environmental Science and Technology. 49*(10), 866-915. https://doi.org/10.1080/10643389.2018.1542916.

OECD/UNEP Global PFC Group, & Environment, Health and Safety, Environment Directorate, OECD. 2013. Synthesis paper on per- and polyfluorinated chemicals (PFCs).

Olsen, G. W. 2015. PFAS biomonitoring in higher exposed populations. In Toxicological Effects of Perfluoroalkyl and Polyfluoroalkyl Substances. *Humana Press, Cham.* 77-125. https://doi.org/10.1007/978-3-319-15518-0_4.

Pan, M., & Chu, L. M. 2016. Adsorption and degradation of five selected antibiotics in agricultural soil. *Science of the Total Environment. 545*, 48-56. https://doi.org/10.1016/j.scitotenv.2015.12.040.

Pan, M., Wong, C. K., & Chu, L. M. 2014. Distribution of antibiotics in wastewater-irrigated soils and their accumulation in vegetable crops in the Pearl River Delta, southern China. *Journal of agricultural and food chemistry*. *62*(46), 11062-11069. https://doi.org/10.1021/jf503850v.

Pautler, B. G., Woods, G. C., Dubnick, A., Simpson, A. J., Sharp, M. J., Fitzsimons, S. J., & Simpson, M. J. 2012. Molecular characterization of dissolved organic matter in glacial ice: coupling natural abundance 1H NMR and fluorescence spectroscopy. *Environmental science & technology*. *46*(7), 3753-3761. https://doi.org/10.1021/es203942y.

Qu, B., Zhao, H., & Zhou, J. 2010. Toxic effects of perfluorooctane sulfonate (PFOS) on wheat (Triticum aestivum L.) plant. *Chemosphere*. *79*(5), 555-560. https://doi.org/10.1016/j.chemosphere.2010.02.012.

Rankin, K., Mabury, S. A., Jenkins, T. M., & Washington, J. W. 2016. A North American and global survey of perfluoroalkyl substances in surface soils: Distribution patterns and mode of occurrence. *Chemosphere. 161*, 333-341. https://doi.org/10.1016/j.chemosphere.2016.06.109.

Rodea-Palomares, I., Leganés, F., Rosal, R., & Fernández-Pinas, F. 2012. Toxicological interactions of perfluorooctane sulfonic acid (PFOS) and perfluorooctanoic acid (PFOA) with selected pollutants. *Journal of hazardous materials*. *201*, 209-218. https://doi.org/10.1016/j.jhazmat.2011.11.061.

Rosendahl, I., Siemens, J., Groeneweg, J., Linzbach, E., Laabs, V., Herrmann, C., Vereecken, H., & Amelung, W. 2011. Dissipation and sequestration of the veterinary antibiotic sulfadiazine and its metabolites under field conditions. *Environmental science & technology. 45*(12), 5216-5222. https://doi.org/10.1021/es200326t.

Russo, F., Vazzoler, M., Tagliapietra, L., Groppi, V., & Simion, M. 2016. Contaminazione da sostanze perfluoroalchiliche nella regione Veneto.

Sajid, M., & Ilyas, M. 2017. PTFE-coated non-stick cookware and toxicity concerns: a perspective. *Environmental Science and Pollution Research*. *24*(30), 23436-23440. https://doi.org/10.1007/s11356-017-0095-y.

Schaefer, C. E., Choyke, S., Ferguson, P. L., Andaya, C., Burant, A., Maizel, A., Strathmann, J. T., & Higgins, C. P. 2018. Electrochemical transformations of perfluoroalkyl acid (PFAA) precursors and PFAAs in groundwater impacted with aqueous film forming foams. *Environmental science & technology*. *52*(18), 10689-10697. https://doi.org/10.1021/acs.est.8b02726.

Scheringer, M., Trier, X., Cousins, I. T., de Voogt, P., Fletcher, T., Wanga, Z., & Webster, T. F. (2014). Helsingør statement on poly- and perfluorinated alkyl substances (PFASs). *Chemosphere.* https://doi.org/10.1016/j.chemosphere.2014.05.044.

Schmidt, B., Ebert, J., Lamshöft, M. A. R. C., Thiede, B., Schumacher-Buffel, R., Ji, R., Corvini, P.F.X., & Schäffer, A. 2008. Fate in soil of 14C-sulfadiazine residues contained in the manure of young pigs treated with a

veterinary antibiotic. *Journal of Environmental Science and Health. Part B*, *43*(1), 8-20. https://doi.org/10.1080/03601230701734824.

Schwarz, J., Aust, M. O., & Thiele-Bruhn, S. 2010. Metabolites from fungal laccase-catalysed transformation of sulfonamides. *Chemosphere*. *81*(11), 1469-1476. https://doi.org/10.1016/j.chemosphere.2010.08.053.

Sepulvado, J. G., Blaine, A. C., Hundal, L. S., & Higgins, C. P. 2011. Occurrence and fate of perfluorochemicals in soil following the land application of municipal biosolids. *Environmental Science & Technology*. *45*(19), 8106-8112. https://doi.org/10.1021/es103903d.

Sharma, V. K., Johnson, N., Cizmas, L., McDonald, T. J., & Kim, H. 2016. A review of the influence of treatment strategies on antibiotic resistant bacteria and antibiotic resistance genes. *Chemosphere*. *150*, 702-714. https://doi.org/10.1016/j.chemosphere.2015.12.084.

Sharon Lerner. PFOA and PFOS cause lower sperm counts and smaller penises, study finds. The Intercept, November 2018. https://theintercept.com/2018/11/30/pfoa-and-pfos-cause-lower-sperm-counts-and-smaller-penises-study-finds/.

Shirzadi, A.; Simpson, M. J., Kumar, R., Baer, A., Xu, Y., Simpson, A. J. 2008. Molecular interactions of pesticides at the soil−water interface. *Environment Science Technology*. 42, 5514−5520. https://doi.org/10.1021/es800115b.

Simpson, A. J., Liaghati, Y., Fortier-McGill, B., Soong, R., & Akhter, M. 2015. Perspective: in vivo NMR–a potentially powerful tool for environmental research. *Magnetic Resonance in Chemistry*. *53*(9), 686-690. https://doi.org/10.1002/mrc.4142.

Simpson, A. J., Simpson, M. J., & Soong, R. 2012. Nuclear magnetic resonance spectroscopy and its key role in environmental research. *Environmental Science and technology*. 11488-11496. https://doi.org/10.1021/es302154w.

Simpson, A.J., Courtier-Murias, D., Longstaffe, J.G., Masoom, H., Soong, R., Lam, L., Sutrisno, A., Farooq, H., Simpson, M.J., Maas, W.E. and Fey, M., 2007. Environmental Comprehensive Multiphase NMR. *eMagRes,* 399-414. https://doi.org/10.1002/9780470034590.emrstm1337.

Stahl, T., Heyn, J., Thiele, H., Hüther, J., Failing, K., Georgii, S., & Brunn, H. 2009. Carryover of perfluorooctanoic acid (PFOA) and perfluorooctane sulfonate (PFOS) from soil to plants. *Archives of environmental contamination and toxicology*, *57*(2), 289-298. https://doi.org/10.1007/s00244-008-9272-9.

Supreeyasunthorn, P., Boontanon, S. K., & Boontanon, N. 2016. Perfluorooctane sulfonate (PFOS) and perfluorooctanoic acid (PFOA) contamination from textiles. *Journal of Environmental Science and Health, Part A*, *51*(6), 472-477. https://doi.org/10.1080/10934529.2015.1128713.

Taniyasu, S., Yamashita, N., Yamazaki, E., Petrick, G., & Kannan, K. 2013. The environmental photolysis of perfluorooctanesulfonate, perfluorooctanoate, and related fluorochemicals. *Chemosphere, 90*(5), 1686-1692. https://doi.org/10.1016/j.chemosphere.2012.09.065.

The Danish Environmental Protection Agency. 2015. Perfluoroalkylated substances: PFOA, PFOS and PFOSA.

Trier, X., Granby, K., & Christensen, J. H. 2011. Polyfluorinated surfactants (PFS) in paper and board coatings for food packaging. *Environmental Science and Pollution Research*, *18*(7), 1108-1120. https://doi.org/10.1007/s11356-010-0439-3.

UNEP, & Stockholm Convention on Persistent Organic Pollutants. 2011. Guidance on alternatives to perfluorooctane sulfonic acid and its derivatives.

Valsecchi, S., Conti, D., Crebelli, R., Polesello, S., Rusconi, M., Mazzoni, M., Aste, F. 2017. Deriving environmental quality standards for perfluorooctanoic acid (PFOA) and related short chain perfluorinated alkyl acids. *Journal of Hazardous Materials, 323*, 84-98. https://doi.org/10.1016/j.jhazmat.2016.04.055.

Verlicchi, P., Al Aukidy, M., & Zambello, E. 2015. What have we learned from worldwide experiences on the management and treatment of hospital effluent? —An overview and a discussion on perspectives. *Science of the Total Environment*, *514*, 467-491. https://doi.org/10.1016/j.scitotenv.2015.02.020.

Viant, M. R., Rosenblum, E. S., & Tjeerdema, R. S. 2003. NMR-based metabolomics: a powerful approach for characterizing the effects of environmental stressors on organism health. *Environmental science & technology*, *37*(21), 4982-4989. https://doi.org/10.1021/es034281x.

Vierke, L., Staude, C., Biegel-Engler, A., Drost, W., & Schulte, C. 2012. Perfluorooctanoic acid (PFOA)—main concerns and regulatory developments in Europe from an environmental point of view. *Environmental Sciences Europe*, *24*(1), 16. https://doi.org/10.1186/2190-4715-24-16.

Walters, A., & Santillo, D. 2006. Uses of perfluorinated substances. *Greenpeace Research Laboratories*.

Wang, Z., Cousins, I. T., Scheringer, M., & Hungerbuehler, K. 2015. Hazard assessment of fluorinated alternatives to long-chain perfluoroalkyl acids (PFAAs) and their precursors: status quo, ongoing challenges and possible solutions. *Environment international*, *75*, 172-179. https://doi.org/10.1016/j.envint.2014.11.013.

Wang, Z., Cousins, I. T., Scheringer, M., & Hungerbuhler, K. 2013. Fluorinated alternatives to long-chain perfluoroalkyl carboxylic acids and their potential precursors. *Environment International. 60*, 242. https://doi.org/10.1016/j.envint.2013.08.021.

Ward, J. L., Baker, J. M., & Beale, M. H. 2007. Recent applications of NMR spectroscopy in plant metabolomics. *The FEBS journal*. 274(5), 1126-1131. https://doi.org/10.1111/j.1742-4658.2007.05675.x.

Wegst-Uhrich, S. R., Navarro, D. A., Zimmerman, L., & Aga, D. S. 2014. Assessing antibiotic sorption in soil: a literature review and new case studies on sulfonamides and macrolides. *Chemistry Central Journal*. *8*(1), 5. https://doi.org/10.1186/1752-153X-8-5.

Wehrhan, A., Streck, T., Groeneweg, J., Vereecken, H., & Kasteel, R. 2010. Long-term sorption and desorption of sulfadiazine in soil: Experiments and modeling. *Journal of environmental quality*. *39*(2), 654-666. https://doi.org/10.2134/jeq2009.0001.

Wei, R., Ge, F., Huang, S., Chen, M., & Wang, R. 2011. Occurrence of veterinary antibiotics in animal wastewater and surface water around farms in Jiangsu Province, China. *Chemosphere*, *82*(10), 1408-1414. https://doi.org/10.1016/j.chemosphere.2010.11.067.

Wheeler, H. L., Soong, R., Courtier-Murias, D., Botana, A., Fortier-Mcgill, B., Maas, W. E., Fey, M., Hutchins, H., Krishnamurthy, S., Kumar, R., Monette, M., Stronks, J.H., Campbell, M.M., Simpson, A. 2015. Comprehensive multiphase NMR: a promising technology to study plants in their native state. *Magnetic Resonance in Chemistry*. *53*(9), 735-744. https://doi.org/10.1002/mrc.4230.

World Health Organization 2016. Keeping our water clean: the case of water contamination in the Veneto Region, Italy.

World Health Organization: Keeping our water clean: the case of water contamination in the Veneto Region. 2017:72. Italy. http://www.euro.who.int/__data/assets/pdf_file/0019/341074/pfas-report-20170606-h1330-print-isbn.pdf?ua=1.

Xu, J., Xu, Y., Wang, H., Guo, C., Qiu, H., He, Y.,Zhang, Y.,li, X., & Meng, W. 2015. Occurrence of antibiotics and antibiotic resistance genes in a sewage treatment plant and its effluent-receiving river. *Chemosphere*. *119*, 1379-1385. https://doi.org/10.1016/j.chemosphere.2014.02.040.

Yang, H. B., Zhao, Y. Z., Tang, Y., Gong, H. Q., Guo, F., Sun, W. H., Liu, S. S., Tan, H., & Chen, F. 2019. Antioxidant defence system is responsible for the toxicological interactions of mixtures: A case study on PFOS and PFOA in Daphnia magna. *Science of the Total Environment*. *667*, 435-443. https://doi.org/10.1016/j.scitotenv.2019.02.418.

Yin, T., Chen, H., Reinhard, M., Yi, X., He, Y., & Gin, K. Y. H. 2017. Perfluoroalkyl and polyfluoroalkyl substances removal in a full-scale tropical constructed wetland system treating landfill leachate. *Water research*. *125*, 418-426. https://doi.org/10.1016/j.watres.2017.08.071.

Yoo, H., Washington, J. W., Jenkins, T. M., & Ellington, J. J. 2011. Quantitative determination of perfluorochemicals and fluorotelomer alcohols in plants from biosolid-amended fields using LC/MS/MS and GC/MS. *Environmental science & technology. 45*(19), 7985-7990. https://doi.org/10.1021/es102972m.

Zafeiraki, E., Costopoulou, D., Vassiliadou, I., Leondiadis, L., Dassenakis, E., Hoogenboom, R L A P, & Leeuwen, v., S.P.J. 2015. Perfluoroalkylated substances (PFASs) in home and commercially produced chicken eggs from the Netherlands and Greece. *Chemosphere. 144*, 2106-2112. https://doi.org/10.1016/j.chemosphere.2015.10.105.

Zhang, S., Gowda, G. N., Asiago, V., Shanaiah, N., Barbas, C., & Raftery, D. 2008. Correlative and quantitative 1H NMR-based metabolomics reveals specific metabolic pathway disturbances in diabetic rats. *Analytical biochemistry*. *383*(1), 76-84. https://doi.org/10.1016/j.ab.2008.07.041.

Zhao, H., Guan, Y., Zhang, G., Zhang, Z., Tan, F., Quan, X., & Chen, J. 2013. Uptake of perfluorooctane sulfonate (PFOS) by wheat (*Triticum aestivum* L.) plant. *Chemosphere. 91*(2), 139-144. https://doi.org/10.1016/j.chemosphere.2012.11.036.

Zhao, H., Qu, B., Guan, Y., Jiang, J., & Chen, X. 2016. Influence of salinity and temperature on uptake of perfluorinated carboxylic acids (PFCAs) by hydroponically grown wheat (*Triticum aestivum* L.). *SpringerPlus*, 5(1), 541. https://doi.org/10.1186/s40064-016-2016-9.

Zhaoyun Zhu, Tieyu Wang, Pei Wang, Yonglong Lu, & John P Giesy. 2013. Perfluoroalkyl and polyfluoroalkyl substances in sediments from south bohai coastal watersheds, china. *Marine Pollution Bulletin. 85*(2), 619-627. https://doi.org/10.1016/j.marpolbul.2013.12.042.

Zheng, G., & Price, W. S. (2012). Direct hydrodynamic radius measurement on dissolved organic matter in natural waters using diffusion NMR. *Environmental science & technology*. *46*(3), 1675-1680. https://doi.org/10.1021/es202809e.

Zhou, W., Zhao, S., Tong, C., Chen, L., Yu, X., Yuan, T., Aimuzi, R., Luo, F., Tian, Y. and Zhang, J., 2019. Dietary intake, drinking water ingestion and plasma perfluoroalkyl substances concentration in reproductive aged Chinese women. *Environment international*. *127*, 487-494. https://doi.org/10.1016/j.envint.2019.03.075.

Zhu, Z., Wang, T., Wang, P., Lu, Y., & Giesy, J. P. 2014. Perfluoroalkyl and polyfluoroalkyl substances in sediments from South Bohai coastal watersheds, China. *Marine pollution bulletin*. *85*(2), 619-627. https://doi.org/10.1016/j.marpolbul.2013.12.042.

Zille, A., & Raoux, S. 2019. Basis for developing a methodology to estimate fluorinated GHG emissions from the fluorinated treatment of textile, carpet, leather, and paper.

Web links

www.arpav.veneto.it.

www.aulss9.veneto.it.

www.faostat.fao.org.

www.legambienteveneto.it

www.mattinopadova.gelocal.it.

www.miteni.com.

www.miteninforma.it/stampa/comunicati.html.

www.ncrpis-gem.agron.iastate.edu

https://ilfattoalimentare.it.

https://www.fosters.com.

CHAPTER 2

EFFECTS OF SDZ IN ARABIDOPSIS

2.1 Publication I

A proteomic and biochemical investigation on the effects of sulfadiazine in *Arabidopsis thaliana*

Nisha Sharma, Giorgio Arrigoni, Leonard Barnabas Ebinezer, Anna Rita Trentin, Cinzia Franchin, Sabrina Giaretta, Paolo Carletti, Sören Thiele-Bruhn, Rossella Ghisi, Antonio Masi. (2019).

Published in Ecotoxicology and Environmental Safety at Volume 178, 30 August 2019, Pages 146-158.

Ecotoxicology and Environmental Safety 178 (2019) 146–158

Contents lists available at ScienceDirect

Ecotoxicology and Environmental Safety

A proteomic and biochemical investigation on the effects of sulfadiazine in *ARABIDOPSIS THALIANA*

Nisha Sharma[a], Giorgio Arrigoni[b,c], Leonard Barnabas Ebinezer[a,*], Anna Rita Trentin[a], Cinzia Franchin[b,c], Sabrina Giaretta[a], Paolo Carletti[a], Sören Thiele-Bruhn[d], Rossella Ghisi[a], Antonio Masi[a]

[a] DAFNAE, University of Padova, Viale Università 16, 30520 Legnaro, PD, Italy

[b] Department of Biomedical Sciences, University of Padova, Via U. Bassi 58/B, Padova, Italy

[c] Proteomics Center, University of Padova and Azienda Ospedaliera di Padova, Italy

[d] Soil Science, Trier University, Behringstraße 21, D-54286, Trier, Germany

ARTICLEINFO

Keywords:

Abiotic stress Antibiotics
Environmental pollution
Peroxidase

Proteomics
Sulfonamides

ABSTRACT

Animal manure or bio-solids used as fertilizers are the main routes of antibiotic exposure in the agricultural land, which can have immense detrimental effects on plants. Sulfadiazine (SDZ), belonging to the class of sulfonamides, is one of the most detected antibiotics in the agricultural soil. In this study, the effect of SDZ on the growth, changes in antioxidant metabolite content and enzyme activities related to oxidative stress were ana- lysed. Moreover, the proteome alterations in Arabidopsis thaliana roots in response to SDZ was examined by means of a combined iTRAQ-LC-MS/MS quantitative proteomics approach. A dose-dependent decrease in leaf biomass and root length was evidenced in response to SDZ. Increased malondialdehyde content at higher con- centration (2 μM) of SDZ indicated increased lipid peroxidation and suggest the induction of oxidative stress. Glutathione levels were significantly higher compared to control, whereas there was no increase in ascorbate content or the enzyme activities of glutathione metabolism, even at higher concentrations. In total, 48 differ- entially abundant proteins related to stress/stimuli response followed by transcription and translation, meta- bolism, transport and other functions were identified. Several proteins related to oxidative, dehydration, salinity and heavy metal stresses were represented. Upregulation of peroxidases was validated with total peroxidase activity. Pathway analysis provided an indication of increased phenylpropanoid biosynthesis. Probable mole- cular mechanisms altered in response to SDZ are highlighted.

1. Introduction

Antibiotics are drugs used against infections and inflammations. Since penicillin was first discovered in 1928 (Fleming, 1944, 1946), antibiotics have been increasingly used worldwide for therapeutic purposes in both human and veterinary medicine leading to the dispersion of these substances in the environment through contaminated excreta. Wastewaters, landfills and industrial and hospital effluents are the major sources of contamination of water resources with such drugs (Karthikeyan and Meyer, 2006; Manzetti and Ghisi, 2014). Soils are mainly contaminated through the application of livestock slurry, manure and sewage sludge as a fertilizer to the soil (Boxall et al., 2002; Sarmah et al., 2006; Carter et al., 2014; Tasho et al., 2016; Thiele-Bruhn, 2003).

Among the antibiotics, sulfadiazines (SDZ) are a group of synthetic antibacterial agents that contain the sulfonamide group (R_1-SO_2NH-R_2) (Huschek et al., 2008). They are used in human medicine and are one of the most sold classes of veterinary antimicrobial compounds in EU countries for their low cost and broad-spectrum antibacterial and anticoccidian activity (De Liguoro et al., 2007). Because of field application of contaminated manure and slurry, extractable concentrations of sulfonamides up to 0.4 mg kg^{-1} in soil have been measured (Karcı and

Abbreviations: ABA, Abscisic acid; ASC, Ascorbate; CDNB, 1-chloro-2, 4-dinitrobenzene; EDTA, Ethylene Diamine Tetra Acetic Acid; ER, Endoplasmic Reticulum; EU, European Union; GGT, Gamma Glutamyl Transferase; GO, Gene Ontology; GSH, Glutathione; GST, Glutathione-S-transferase; iTRAQ, Isobaric Tags for Relative and Absolute Quantification; LC-MS/MS, Liquid chromatography–Tandem mass spectrometry; MDA, Malondialdehyde; PO4, Phosphate; POD, Peroxidase; SBD-F, Ammonium 7-fluoro 2,1,3-benzooxadiazole-4-sulphonate; SDZ, Sulfadiazine; TBA, Thiobarbituric acid; TCA, Trichloroacetic acid

* Corresponding author. Viale dell'Università 16, 30520 Legnaro, PD, Italy.

E-mail address: leonardbarnabas.ebinezer@unipd.it (L.B. Ebinezer).

https://doi.org/10.1016/j.ecoenv.2019.04.008

Balcıoğlu, 2009). The extractability of these compounds from soil decreases with time owing to immobilizing processes, which can involve physical-chemical interactions with soil components (Förster et al., 2009; Wegst-Uhrich et al., 2014; Wehrhan et al., 2010) as well as reactions mediated by oxidoreductase enzymes, such as peroxidases and laccases (Bialk et al., 2005; Schwarz et al.,2010, 2015). However, the total contents of sulfadiazine remain high in contaminated soil for months and years (Rosendahl et al., 2011; Schmidt et al., 2008).

It has been proved that plants are able to incorporate various drugs (Boxall et al., 2006; Carter et al., 2014; Carvalho et al., 2014), thus contributing to the entry of these compounds into the food-chain and spreading antibiotic resistance (Jechalke et al., 2013). Hence, information on the distribution of antibiotics in manure-applied and wastewater-irrigated soils and their uptake and accumulation by plants/crops has been accumulating over the recent years (Kang et al., 2013; Pan et al., 2014; Rosendahl et al., 2011; Schmidt et al., 2008). Antibiotics can directly affect plant physiological processes such as photosynthesis, respiration and root functionality (Carvalho et al., 2014; Li et al., 2011; Michelini et al., 2012, 2013). Regarding plant growth, sulfonamides have been shown as either promoting or in- hibitory substances (hormesis) depending on the plant and the con- centrations used (Migliore et al., 2010; Michelini et al., 2012; Pan and Chu, 2016). The comprehensive information on the global changes in transcriptome, proteome and metabolome in response to antibiotics and related drugs is vital to understand the stress responses induced and the tolerance and detoxification mechanisms in plants. Proteomics, being a powerful tool that yields comprehensive information, it has been ex- tensively applied to understand the effects of emerging environmental pollutants and abiotic stress in plants (Mirzajani et al., 2014; Wang et al., 2019). However, not much is known about the effects of anti- biotics on the proteome of plants. Hitherto, to the best of our knowl- edge, there is no information pertaining to the changes in root pro- teome of *Arabidopsis* and its correlation with the physiological and biochemical effects in response to SDZ. Hence, this study investigates the effects of SDZ on growth, changes in the anti-oxidant metabolites and enzyme activities and the alterations in the proteome occurring in *Arabidopsis thaliana* roots in response to SDZ.

2. Materials and methods

2.1. *Arabidopsis* seed sterilization and growth

Arabidopsis Col-O seeds were surface sterilized by 70% ethanol for 2 min followed by 5% hypochlorite solution for 15 min in microfuge tubes. The seeds were rinsed with sterile water 5 times to ensure that all bleach residues were removed. Then they were grown for 3 weeks, in sterilized half-strength Murashige and Skoog medium at 6% sucrose and 1.4% agarose with SDZ antibiotics at the concentrations 0 μM (Control), 0.5 μM, 1 μM and 2 μM. The exposure concentration was chosen in resemblance to the concentrations of sulfonamide measured in soil (Karcı and Balcıoğlu, 2009). Also in a preliminary experiment, SDZ concentration at 5 μM was tested but resulted in the death of all treated seedlings. Based on Rosendahl et al. (2011), the easily extractable concentration of SDZ and its main metabolites decreases ra- pidly in the environment, with DT_{50} of around 2–3 weeks. Based on this, 21 days were chosen as exposure time in this experiment. Seeds were incubated in vertically oriented Petri dishes in a growth chamber
under short day condition (8.5/15.5 h of light/dark cycle) at a temperature of 22/18 °C, at 50% relative humidity and with a light intensity of 120 $\mu E\ m^{-2}\ s^{-1}$. Root samples were harvested and stored for further analysis.

2.2. MDA content determination

The level of lipid peroxidation in roots was determined by the quantification of malondialdehyde (MDA) based on the spectrophotometric method reported by Heath and Packer (1968) with some modifications. The root tissue sample from five replicates was ground in liquid nitrogen and homogenized with extraction buffer (TCA 0.1% (w/v) in H_2O) in 1:10 ratio. The supernatant was collected after centrifugation at 10000*g* for 10 min. The reaction mix was prepared with sample extract and Thiobarbituric acid (TBA) solution (TCA 20% (w/v) in H_2O, TBA 0.65% (w/v)). The samples were incubated for 15 min at 95 °C, cooled down on the ice and centrifuged at 10000 g for 10 min. The absorbance was read at λ 532 nm, which was subtracted with the unspecific absorbance measured at λ 600 nm. MDA concentration was calculated using the extinction coefficient (157 $mM^{-1}\ cm^{-1}$).

2.3. Extraction for determination of GSH and ascorbate content

The root samples from at least five replicates were harvested, weighed and ground to a fine powder with liquid nitrogen. Extraction buffer was 0.1 M HCl and 1 mmol/L Na_2EDTA in ratio of 1:4 (w/v). After homogenisation, samples were centrifuged at 4 °C at 10000 g for 10 min and the supernatant was collected and immediately used for ascorbate determination and for thiol derivatisation. The ascorbate content was determined spectrophotometrically by measuring the absorbance at λ 265 nm, according to the method of Hewitt and Dickes (1961) that provides total ascorbate, reduced ascorbate and dehydroascorbic acid (Trentin et al., 2015).

Thiol derivatisation followed by isocratic separation and determination by HPLC was carried out as described by Masi et al. (2002) with some minor modifications. 50 μl of thiols extract was derivatized with the ammonium 7-fluoro 2,1,3-benzooxadiazole-4-sulfonate (SBD-F) fluorophore. The derivatized samples were further separated by reversed phase HPLC using a Luna 3 μ C_{18} (2) 150 × 4.60 mm column (Phenomenex), in isocratic conditions with 97% of 75 mM ammonium formate, pH 2.9 and 3% methanol, at a flow rate of 0.3 ml/min at RT.

2.4. Protein extraction and enzyme activity analysis

Proteins were extracted from 150 mg of root samples ground in liquid nitrogen and thereafter the extraction buffer (40 mM Tris-HCl pH 8,3% Triton, 1 mM PMSF, 1 mM Benzamidine, 1 M NaCl) was added in 1:5 (mg/μl) ratio and homogenized thoroughly with the root powder. The mixture was incubated for 1 h in agitation, followed by centrifugation at 10,000 g for 12 min at 4 °C. The protein concentration in the supernatant was quantified by Bradford's method (Bradford, 1976).

The GGT activity was assayed spectrophotometrically according to Huseby and Strömme (1974), where the release of *p*-nitroanilide by the GGT from γ-glutamyl-*p*-nitroanilide (GPNA) substrate was measured. The reaction mix was prepared with protein extract, solution A (4.6 mM GPNA in 100 mM NaH_2PO_4 pH 8.0) and solution B (575 mM gly-gly in 100 mM NaH_2PO_4 pH 8.0) directly in the cuvette. Therefore, the absorbance at λ 407 nm was measured every 5 min for 1 h.

For GST enzyme assays, total protein extracts were prepared as described above. The collected root samples were made fine powder and were homogenized in 1:10 ratio of extraction buffer containing 1% of Polyvinylpolypyrrolidone. The collected extract was then mixed with reaction mixture of PO_4 (200 mM), 1-chloro-2, 4-dinitrobenzene (CDNB) 100 mM, Glutathione (GSH) (100 mM), Ethylenediaminetetraacetic acid (EDTA) 100 mM, was then incubated at 30 °C for 5 min. The absorbance was measured at λ 340 nm (Giaretta et al., 2017).

The activity of syringaldazine POD was determined by measuring the increase in absorbance at λ 530 mm of the reaction mixture containing leaf extracts with 100 mM Na-K phosphate buffer, pH 6.0, 2.5 mM H_2O_2 and 2 mM syringaldazine (Ranieri et al., 2000).

Data from all the technical replicates of biochemical assays were tested for statistical significance (at $p < 0.05$) using ANOVA followed by Post Hoc analysis with Van der Waerden (Normal score test) and

Friedman's test using R studio.

2.5. Protein Extraction for iTRAQ labelling and MS analysis

The method described in Tolin et al. (2013) was followed to obtain total root proteins. After quantification, 50 μg of samples were loaded in a 12% homemade gel. The electrophoretic run was stopped when the protein extracts entered the running gel, single bands were excised, cut in small pieces, washed with 50 mM triethylammonium bicarbonate (TEAB), and dried under vacuum. Protein reduction, alkylation and trypsin digestion were carried out as described in Resmini et al. (2017). Peptides were extracted from the gel with 3 changes (50 μL each) of 50% acetonitrile in water and samples dried under vacuum.

2.6. iTRAQ labelling

The method described by Tolin et al. (2013) was followed with few modifications. Labelling was done with an iTRAQ® Reagents 4-plex Kit (AB Sciex, MA, USA). The iTRAQ experiment was performed on protein samples derived from roots collected from 1 μM SDZ concentration and control. Peptides from control and treated samples were re-suspended in an iTRAQ-compatible buffer (TEAB 0.5 M, SDS 0.1%) to a final concentration of 2 μg/μL and labelled with the iTRAQ tags according to manufacturer's instructions. Before mixing the samples, LC-MS/MS analysis was performed on each sample to assess labelling efficiency. All peptides were correctly iTRAQ-modified at the N-terminus and at each lysine residue. Samples were finally pooled and dried under vacuum.

2.7. Strong cation exchange fractionation

Strong cation exchange chromatography (SCX) was performed on a SCX cartridge (AB Sciex). Labelled sample was dissolved in 500 μL of buffer A (10 mM KH_2PO_4, 25% acetonitrile, pH 2.9) and loaded onto the cartridge using a syringe pump with a 50 μL/min flow rate, according to Trentin et al. (2015). The cartridge was washed with 500 μL of buffer A and peptides were eluted in a stepwise manner with 500 μL of KCl in buffer A at the following concentrations: 25, 50, 100, 200, and 350 mM. Samples were desalted using C_{18} cartridges (Sep-Pack, C_{18}, Waters, Milford, MA, USA) according to the manufacturer's instructions and dried under vacuum.

2.8. LC-MS/MS analysis and database search

Each sample was suspended in H_2O/0.1% formic acid and LC-MS/MS analysis was performed with an LTQ-Orbitrap XL mass spectrometer (Thermo Fisher Scientific) coupled online with a nano-HPLC Ultimate 3000 (Dionex-Thermo Fisher Scientific). Chromatographic and instrumental conditions were as described in De Rosa et al. (2015).

Raw files were analysed using Proteome Discoverer 1.4 (Thermo Fisher Scientific). The software was connected to a Mascot Search Engine server, version 2.2.4 (Matrix Science, London, UK). Spectra were searched against an *A. thaliana* database (downloaded from UniProt, version October 2015). Trypsin was selected as enzyme with 1 missed cleavage allowed. Peptide and fragment tolerances were 20 ppm and 0.6 Da, respectively. Methylthiocysteine, 4-plex iTRAQ (N-term and Lys) were set as fixed modifications, while methionine oxidation was selected as variable modification. False discovery rates (FDR) were calculated by the software with the algorithm Percolator and data were filtered to keep only proteins identified with at least two unique peptides with high confidence (FDR 1%). The quantification was performed normalizing the results on the median value of all measured iTRAQ reporter ratios. The ratios of treated-to-control values were averaged and subjected to a two-tailed Z-test ($p \leq 0.05$). A ratio of treated to control ≥ 1.5 or ≤ 0.67 was set as the threshold for increased and de- creased abundance, respectively.

2.9. Bioinformatic analyses

All identified proteins were functionally categorized based on UniProt (https://www.uniprot.org/). Pathway analysis using KEGG Mapper - Search & Colour Pathway (Kanehisa et al., 2017) was performed using UniProt accessions against *A. thaliana* database. The amino acid sequences of the identified proteins obtained from UniProt were subjected to multiple bioinformatic servers DeepLoc-1.0 (http://www.cbs.dtu.dk-/services/DeepLoc/) and SignalP (http://www.cbs.dtu.dk/services/SignalP/) to predict sub-cellular localization and proteins secreted by classical (with signal peptide). SecretomeP (http://www.cbs.dtu.dk/services/SecretomeP-2.0/) was used to predict proteins secreted by non-classical pathways (without signal peptide). Integrated Interactome System (IIS) platform 3 (Carazzolle et al., 2014) was used to build the protein interactomes with only differentially regulated proteins limiting to only first neighbours' nodes. Cytoscape 3.5.1 software (Shannon et al., 2003) was used to visualise and analyse the interactome data output from IIS as reported in Roomi et al. (2018).

3. Results and discussion

3.1. Effects on seedling growth, leaf biomass and root length

There was no significant difference in the seed germination per- centage with respect to the SDZ concentrations studied. The effect of different concentrations of SDZ (0.5, 1 and 2 μM) on *Arabidopsis* growth was evaluated after three weeks of treatment. Morphologically, there was a reduction in the overall growth and a considerable decrease in the number of leaves and root growth in a dose-dependent manner (Fig. 1A). A significant decrease in lateral root growth was also noticed. Root growth and length were notably reduced in plants treated with 1 μM and 2 μM SDZ already after 10 days of treatment (Fig. 1B). There was a noticeable reduction in overall growth with poorly developed roots during the treatment at the highest SDZ dose (2 μM).

No hormetic effect was observed in the concentration range analysed. Consistent with our observation, sulfonamide class of antibiotics have been reported to reduce the root and stem growth, lower the number of leaves and biomass production in several crops and non-crop plants (Migliore et al., 1995, 1997, 2010). In addition to observing that SDZ was mainly stored inside the roots of willow (*Salix fragilis* L.) and maize (*Zea mays* L.), it was reported to decrease stem length, development and also result in death in *Zea mays* at higher concentrations (Michelini et al., 2012).

3.2. Changes in malondialdehyde content

In order to ascertain if the SDZ treatment induced oxidative stress, changes in MDA content in response to different SDZ concentrations were measured. MDA is one of the final products of oxidative modification of lipids, resulting in damage of membrane integrity and hence considered as a biochemical marker for oxidative stress (Hodges et al., 1999). There was a gradual increase in MDA content with response to SDZ concentration. At 2 μM concentration, the MDA content was significantly higher compared to 0.5 μM and control indicating lipid peroxidation due to oxidative stress after 21 days of treatment (Table 1). Increased MDA content was also reported in wheat seedlings treated with SDZ (Xu et al., 2017).

3.3. Changes in ascorbate and glutathione levels

ROS scavenging system in plants consists of enzymatic and non-enzymatic antioxidant components (Scandalios, 2005). Ascorbate and glutathione are non-enzymatic antioxidants that are an integral part of this system, crucial for the survival of the plant (Mittler et al., 2004; Foyer and Noctor, 2005). Although ascorbate and glutathione function invariably in a compensatory and synergistic manner, there is evidence

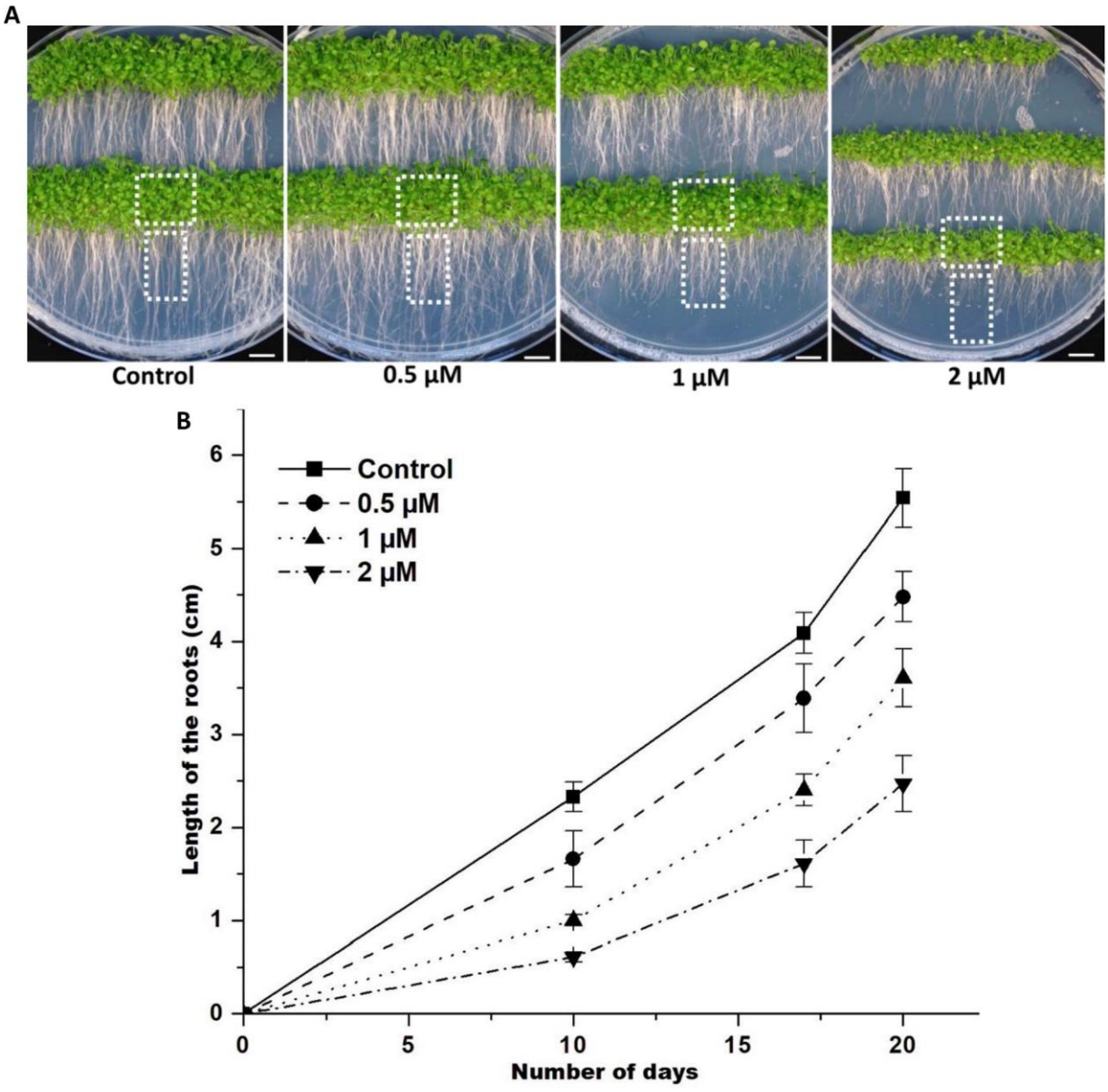

Fig. 1. A Effects of SDZ on *Arabidopsis thaliana* growth, leaf biomass and root length after 3 weeks of treatment. Boxes are of same dimensions highlighting the dose-dependent decrease in leaf biomass, root length and lateral root growth. Fig. 1B Effect of different concentrations of SDZ (0.5, 1, 2 µM) on root length in comparison to control over a period of 3 weeks. Error bars represent standard error (n = 5).

that suggests that they are differentially influenced by environmental stimuli and their interdependence and independence in peroxide me- tabolism have also been elaborated (Foyer and Noctor, 2011). Here we quantified both ascorbate and dehydroascorbate, but we found that ascorbate was 99% reduced. This supports the notion that sulfadiazine is not altering the ascorbate redox state, at least in our experimental conditions at the concentrations and exposure times we have used. SDZ did not induce significant changes to the ascorbate levels but the GSH content was consistently higher than the control at all concentrations (Table 1). These results indicate that the GSH could be one of the major anti-oxidant metabolites in *Arabidopsis* roots responding to oxidative stress induced by SDZ.

Table 1 Changes in the different biochemical parameters and enzyme activities in *ARABIDOPSIS* roots in response to different concentrations of SDZ in growth medium after 21 days of treatment.

Treatment	MDA (%)	Total ASC (mol*g^{-1} FW)	GSH (mol*g^{-1} FW)	Total Protein (mg prot*g^{-1} FW)	GGT (U*mg prot^{-1})	GST (U*mg prot^{-1})	POD (µmol quinone*min^{-1}mg prot)
Control	100 ± 25.92^{ab}	0.66 ± 0.22^{a}	50.6 ± 9.10^{b}	3.21 ± 0.54^{b}	0.013 ± 0.003^{a}	22.59 ± 3.07^{a}	0.69 ± 0.15^{b}
0.5µM	89.67 ± 22.43^{b}	0.51 ± 0.09^{a}	72.10 ± 13.64^{a}	3.63 ± 0.50^{ab}	0.012 ± 0.003^{a}	21.00 ± 5.36^{a}	1.25 ± 0.85^{ab}
1µM	106.79 ± 20.52^{ab}	0.63 ± 0.22^{a}	74.69 ± 12.25^{a}	3.77 ± 0.53^{ab}	0.012 ± 0.001^{a}	24.84 ± 7.06^{a}	1.10 ± 0.15^{a}
2µM	125.54 ± 13.12^{a}	0.55 ± 0.16^{a}	78.41 ± 10.52^{a}	4.05 ± 0.46^{a}	0.013 ± 0.003^{a}	23.61 ± 7.72^{a}	0.96 ± 0.24^{ab}

Values after ± indicate standard deviation and different letters indicate statistically significant difference at $p < 0.05$ according to Van der Waerden (Normal score test) and Friedman's tests.

Table 2

Summary of the list of proteins identified.

S.No.	Accession[a]	Protein description[a]	Mascot Score[b]	No. Of unique peptides/ PSMs[b]	% Coverage[b]	Experimental kDa/*pI*[b]	Fold change[b]	Subcellular localization[c]	CS/NCS[d]	Functional category[a]
	P24102	Peroxidase 22 (PER 22)	614.43	3/29	19.77	38.1/6.0	2.522	EX	CS	Stress and stimuli response
	Q9LHB9	Peroxidase 32 (PER 32)	1131.76	8/58	42.90	38.8/6.67	2.395	EX	CS	
	Q9SUT2	Peroxidase 39 (PER 39)	30.87	3/5	10.43	35.6/6.98	1.767	EX	CS	
	Q9SMU8	Peroxidase 34 (PER 34)	144.76	3/9	17.0	38.8/7.64	1.731	EX	CS	
	F4JFY4	L-ascorbate peroxidase S (sAPX)	48.34	2/2	8.38	37.4/9.06	2.128	PL	NCS	
	P42763	Dehydrin ERD14 (ERD14)	159.57	1/6	11.35	20.8/5.48	4.20	NU	–	
	P31168	Dehydrin COR47 (COR47)	69.37	3/7	18.49	29.9/4.77	1.495	NU	–	
	Q9ZVF3	MLP-like protein 328 (MLP328)	1907.37	7/100	60.93	17.5/5.73	1.846	CY	–	
	Q9ZVF2	MLP-like protein 329 (MLP329)	1061.50	5/43	60.93	17.6/5.55	1.596	CY	–	
	Q9FIX1	AIG2-like protein (AIG2LB)	85.18	4/5	20.35	20.0/5.10	1.508	CY	–	
	Q9SIE7	PLAT domain-containing protein 2 (PLAT2)	326.33	4/19	26.78	20.10/5.31	1.569	ER	CS	
	F4JHJ0	HSP20-like chaperone (HSP20)	275.91	5/13	25	25.3/4.56	1.848	NU	–	
	P31265	Translationally-controlled tumour protein homolog (TCTP)	311.67	7/19	31.55	18.9/4.64	2.051	CY	NCS	
	O64517	Metacaspase-4 (AMC4)	240.16	4/7	9.57	45.5/4.82	1.480	CY	–	
	Q8L4N1	Universal stress protein (USP)	45.37	2/3	8.46	28.1/6.25	1.874	CY	–	
	Q9LXC9	Soluble inorganic pyrophosphatase 6 (PPA6)	181.31	4/5	15.0	33.4/6.01	1.998	PL	NCS	
	Q9LHG9	Nascent polypeptide-associated complex subunit alpha-like protein 1 (NAC)	404.70	6/13	40.89	22.0/4.48	1.494	NU	–	
	Q9FGT8	Temperature-induced lipocalin-1 (TIL)	94.40	2/3	9.68	21.4/6.35	1.453	CY	–	
	Q8RUD6	Rhodanese-like domain-containing protein 19, mitochondrial (HAC)	33.35	2/2	17.16	19.0/6.79	1.494	MI	–	
	F4IHK9	Glycine-rich RNA-binding protein 7 (GRP7)	133.59	2/8	23.27	15.5/5.60	1.845	NU	–	
	F4JVC0	Glycine-rich RNA-binding protein 8 (GRP8)	233.43	2/10	35.87	10.2/4.79	2.366	CY	NCS	
	Q9FKA5	PLD-regulated protein 1 (PLDrp1)	387.04	8/16	35.70	43.5/4.78	2.375	NU	–	
	Q9SYT0	Annexin D1 (ANN1)	1491.69	22/70	68.45	36.20/5.38	0.64	CY	–	
	Q9ZVA4	Curculin-like (Mannose-binding) lectin family protein (EP1GP)	1060.40	18/36	41.50	49.0/7.65	0.65	EX	CS	

O80950	Jacalin-related lectin 22 (JAL22)	479.92	10/22	28.82	50.4/5.30	0.54	CY	–	
O82762	F17H15.1/F17H15.1 (KHdp)	113.41	2/3	4.11	64.6/5.49	3.448	NU	–	Transcription and
Q9XI36	Methyl-CpG-binding domain-containing protein (MBD)	45.81	2/2	7.81	42.3/4.67	1.784	NU	–	translation
Q9LYK9	40S ribosomal protein S26-3 (RPS26C)	79.96	2/5	18.46	14.6/11.09	1.598	CY	–	
O23515	60S ribosomal protein L15-1 (RPL15A)	139.01	5/7	27.45	24.2/11.44	1.585	CY	–	
Q9LZH9	60S ribosomal protein L7a-2 (RPL7AB)	469.74	2/31	43.75	29.0/10.15	1.582	CY	–	
Q9S9P1	40S ribosomal protein S12-1 (RPS12A)	85.27	2/4	13.19	15.4/5.55	1.510	CY	NCS A8MS83	60S
ribosomal protein L23a-2 (RPL23AB)		217.17	5/10	35.81	16.7/10.17	1.503	CY	NCS P49692	60S ribosomal protein L7a-1
(RPL7AA) 492.22 3/30 47.86 29.1/10.13 1.452 CY –									
O49499	Caffeoyl-CoA O-methyltransferase1 (CCOAOMT1)	412.52	7/15	30.89	29.1/5.29	1.631	CY	–	Metabolism
Q0WP12	Thiocyanate methyltransferase 1, Isoform 2 (HOL1)	528.25	7/18	38.33	25.3/4.82	1.671	CY	–	
O82179	Glycine cleavage system H protein 2 (GDH2)	136.49	2/4	12.82	17.1/5.11	1.809	MI	–	
Q42599	NADH dehydrogenase [ubiquinone] iron-sulfur protein 8-A (NADHD)	54.68	3/3	14.86	25.5/5.41	1.655	MI	NCS	
Q8GUN2	Adenylylsulfatase (HINT1)	58.09	2/3	21.77	16.0/7.20	2.319	MI	NCS	
Q8GW53	Phosphorylase superfamily protein (PSP)	158.57	4/5	14.50	36.9/8.75	0.66	EX	CS	
O65398	Lactoyl-glutathione lyase (GLX1)	641.22	10/28	36.04	31.9/5.27	0.62	CY	–	
O82089	Copper transport protein (CCH)	249.09	3/9	32.23	13.0/4.93	2.628	CY	–	Transport
B3H438	MD-2-related lipid recognition domain-containing protein (MRO11.13)	149.35	3/6	13.04	17.8/4.56	1.542	EX	CS	
Q8VYM2	Inorganic phosphate transporter 1-1 (PHT1-1)	84.40	4/7	7.63	57.6/9.01	0.64	LY/VA	TM	

(*continued on next PAGE*)

Table 2 (*continued*)

S.No.	Accession[a]	Protein	Mascot Score[b]	No. Of unique peptides/ PSMs[b]	% Coverage[b]	Experimental kDa/*pI*[b]	Fold change[b]	Subcellular localization[c]	CS/NCS[d]	Functional category[a]
	F4K8S2	2S seed storage protein CRU1 (CRA1) SOUL	108.89	3/3	9.12	31.6/8.8	4.335	CY	NCS	Other
	F4IRX0	Heme-binding-like protein (SOUL-1) FAM10			24.44	1		MI	–	
	Q93YI4	family protein (FAM10)	106.48	4/4			1.496	CY		
	Q95J81					24.9/8.8		CM	–	
	F4J9K5	Fasciclin-like arabinogalactan protein 7 (FLA7)	237.33	5/7	15.87	1	3.080	NU	–	

[a] - Accession, proteins description and functional categorization are based on UniProt; Corresponding gene names from UniProt were used as abbreviations; b - Information obtained from iTRAQ-LC-MS/MS and Mascot search; c - Subcellular localization (DeepLoc 1.0): EX - Extracellular, PL - Plastid, NU - Nucleus, CY - Cytoplasm, ER - Endoplasmic Reticulum, MI - Mitochondria, LY/VA - Lysosome/Vacuole, CM - Cell membrane; d - Prediction of classical (CS) and non-classical secretory (NCS) pathway (SignalP and SecretomeP).

3.4. Changes in the total protein content and enzyme activities of GST and GGT

An increasing trend in the total protein content in response to SDZ treatment was observed (Table 1). Increased as well as decreased total protein content in crops under abiotic stress have been reported (Hendawey and Kamel, 2015; Jahanbakhsh et al., 2017). Hence, it is reasonable to presume that the change in total protein content depends on the plant species, its inherent varietal tolerance to a specific stress, type of stress and the duration of stress. Nevertheless, it could be correlated in general with the proteome level changes that occur in response to stress, whereby the majority of proteins were upregulated several folds in comparison to untreated control plants. Total protein content is usually considered as a proxy for plant growth. However, protein content accounts for the protein concentration in a tissue, which might be at least partially unrelated to higher biomass. In this study, root growth was reduced in response to SDZ treatment compared to control, while the root protein content increased. Higher protein content not necessarily relates to structural proteins needed for plant growth, it might account for higher levels of proteins related to stress responses, as evidenced in the proteome analysis.

Considering the increase in GSH content, the activities of GST - an enzyme involved in xenobiotic detoxification using GSH as co-substrate (Dixon and Edwards, 2010) and GGT - an enzyme related to GSH metabolism (Masi et al., 2015) were determined. Enzyme activities of both GST and GGT expressed on a protein basis did not show any significant differences between the control and the SDZ treated roots (Table 1). This could possibly indicate that there were other alternate routes of detoxifying the ROS induced by SDZ or that these crucial enzymes were already present in abundance to regulate and maintain the ROS homeostasis. Hence, there could be only subtle changes in these enzymes under such conditions, which might not have been reflected in the total enzyme activity assay.

3.5. Proteome level alterations in Arabidopsis roots in response to SDZ

A quantitative iTRAQ experiment was carried out to understand the alterations that occur at the protein level in *Arabidopsis* roots in response to SDZ. In total, 48 proteins were found to be differentially abundant, of which 42 were upregulated and 6 were downregulated (Table 2). List of all the proteins identified with peptides used for identification and other relevant parameters used for quantification and statistical testing is provided as supplementary material (Table S1). Based on the functional categorization, the differentially regulated proteins represented stress and stimuli response, transcription and translation, metabolism, transport and other functions (Fig. S1). Subcellular localization prediction indicated that the majority of the proteins were localized in the cytoplasm followed by the nucleus and extracellular proteins (Fig. S2). It also indicated that several proteins were intracellularly transported or secreted by non-classical secretory pathway (Table 2).

3.5.1. Proteins related to stress and stimuli response

3.5.1.1. Proteins related to multiple abiotic stress. Two major latex protein (MPL)-like proteins 328 and 329 (MLP328 and MLP329) found to be upregulated in our study were reported to be differentially regulated in response to plant hormones (Yang et al., 2015) and various other abiotic stresses (Stanley Kim et al., 2005; Chen and Dai, 2010; Zhang et al., 2018). Similarly, AIG2-like protein (AIG2LB) reported to be upregulated in response to water deficit and salt stress (Reymond et al., 2000; Qiu et al., 2017). Further, AIG2-like protein also functions as a gamma-glutamylcyclotransferase, which is involved in protecting *Arabidopsis* plants from heavy metal toxicity by ensuring sufficient GSH turnover by recycling glutamate to maintain GSH homeostasis during stress (Paulose et al., 2013).

A PLAT domain-containing protein 2 (**P**olycystin, **L**ipoxygenase,

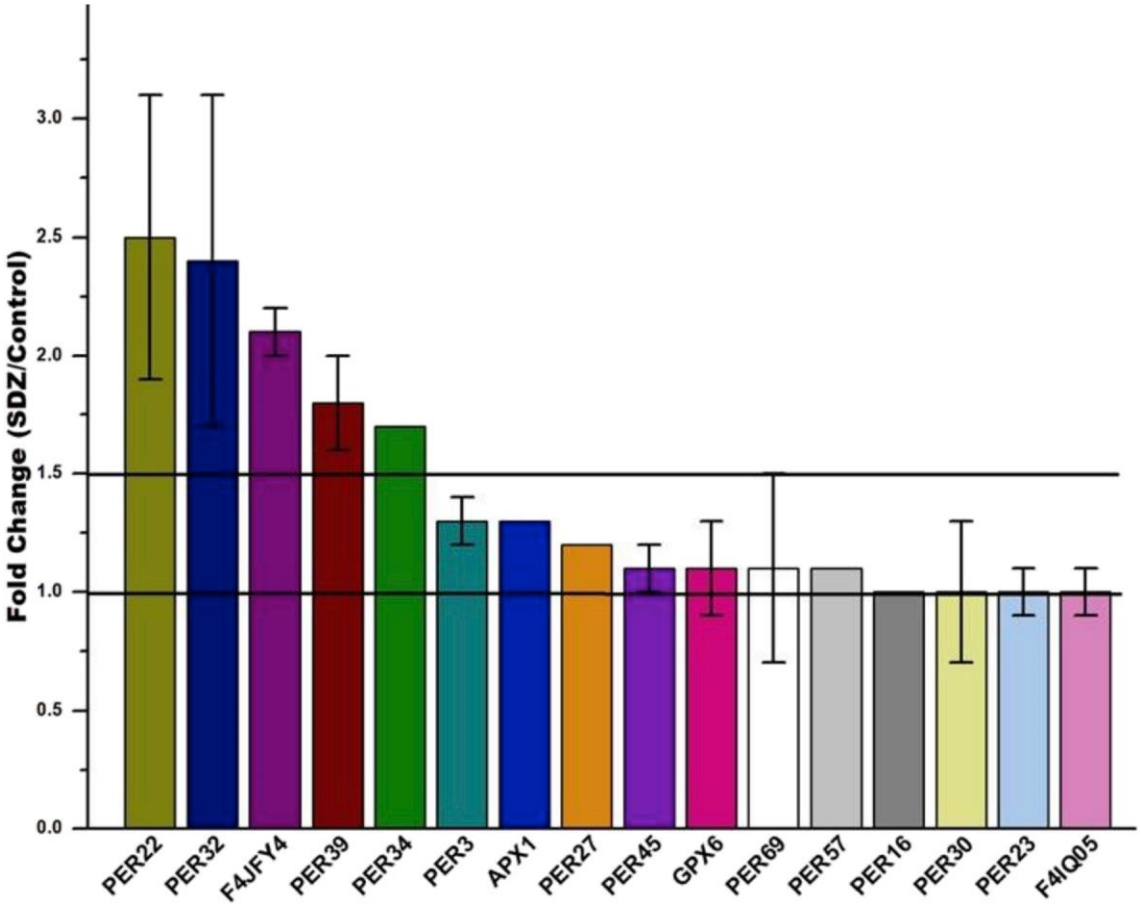

Fig. 2. Fold change variation for peroxidase enzymes in SDZ versus control roots. Error bars indicate standard deviation.

Alpha-toxin and **T**riacylglycerol lipase) (PLAT2) was found to be upregulated 1.6 folds compared to control and it has been reported that overexpression of PLAT domain-containing proteins conferred tolerance to abiotic stress (cold, drought and salt) (Hyun et al., 2014). An HSP20-like chaperone (HSP20), which was upregulated (1.8 folds) primarily functions by avoiding protein denaturation, maintaining native conformation and reorganizing denatured proteins and hence, is induced largely in response to heat, cold, salinity, oxidative and osmotic stresses (Park and Seo et al., 2015). The translationally controlled tumour protein homolog (TCTP) upregulated in this study was reported to be differentially expressed and regulated in abiotic stress conditions such as water limitation, cold and salinity (Lee and Lee, 2003; Vincent et al., 2007).

Universal Stress Protein (USP) was found to be upregulated and belongs to a class of stress-responsive proteins shown to be differentially regulated in salt, drought, cold, heat, and oxidative stress (Kerk et al., 2003; Ndimba et al., 2005; Persson et al., 2007). Inorganic pyrophosphatases (PPA6) are involved in germination, development and stress adaptive responses. Transgenic overexpression of PPA6 has been shown to enhance tolerance to abiotic stress (Gutiérrez-Luna et al., 2018). Similarly, a Nascent polypeptide-associated complex (NAC) protein and a Phospholipase D (PLD) - regulated protein 1 (PLDrp1) were upregulated, both of which were strongly induced in dehydration and salt stress (Karan and Subudhi, 2012; Ufer et al., 2017).A rhodanese-like domain-containing protein, also known as High

Arsenic Content 1 (HAC) protein, was upregulated. In addition, to being responsive to arsenate, it facilitates efflux of toxic arsenic from roots thereby preventing its accumulation and transport (Chao et al., 2014). Glycine-rich RNA binding proteins (GRP7 and GRP8) upregulated in our study have been shown to be induced during oxidative stress (Schmidt et al., 2010) and these GRPs confer stress tolerance in *Arabidopsis* under dehydration and high salt stress conditions (Kim et al., 2008). Higher expression of transcripts and upregulation of dehydrins, specifically ERD14 and COR47, upregulated in this study, were reported in response to low temperature, salinity and in response to abscisic acid (ABA) (Nylander et al., 2001).

It is interesting that Jacalin-related lectin protein (JAL22) associated with response to various abiotic stresses was downregulated in our study. Similarly, Abebe et al. (2005) reported its downregulation in response to drought, dehydration and ABA.

3.5.1.2. Proteins related to ROS scavenging. Increased ROS generation has been reported in response to various abiotic stresses including antibiotics (Thounaojam et al., 2012; Xu et al., 2017). Increased MDA content in our study suggests that there was lipid peroxidation induced by oxidative stress in response to SDZ (Table 1). The proteome analysis indicated that several proteins related to oxidative stress with direct ROS-scavenging roles were upregulated in response to SDZ in comparison to the untreated control.

In total, there were four type III peroxidases (PODs) (PER 22, PER 32, PER 34 and PER 39) and one stromal ascorbate peroxidase (sAPX) found to be upregulated, while Annexin D1 (ANN1) with POD activity was downregulated in response to SDZ (Table 2). PODs are one of the major classes of antioxidant enzymes that directly catalyse the oxidation of certain electron donors concomitant with the disintegration of H_2O_2.

At the transcriptome level, several type III POD genes were highly expressed in *Arabidopsis* roots due to oxidative stress in response to salinity (Jiang and Deyholos, 2006). APX, a class I heme-peroxidases is one of the key enzymes in the ascorbate-glutathione cycle, one of the crucial hydrogen peroxide-detoxification systems in plant chloroplasts.

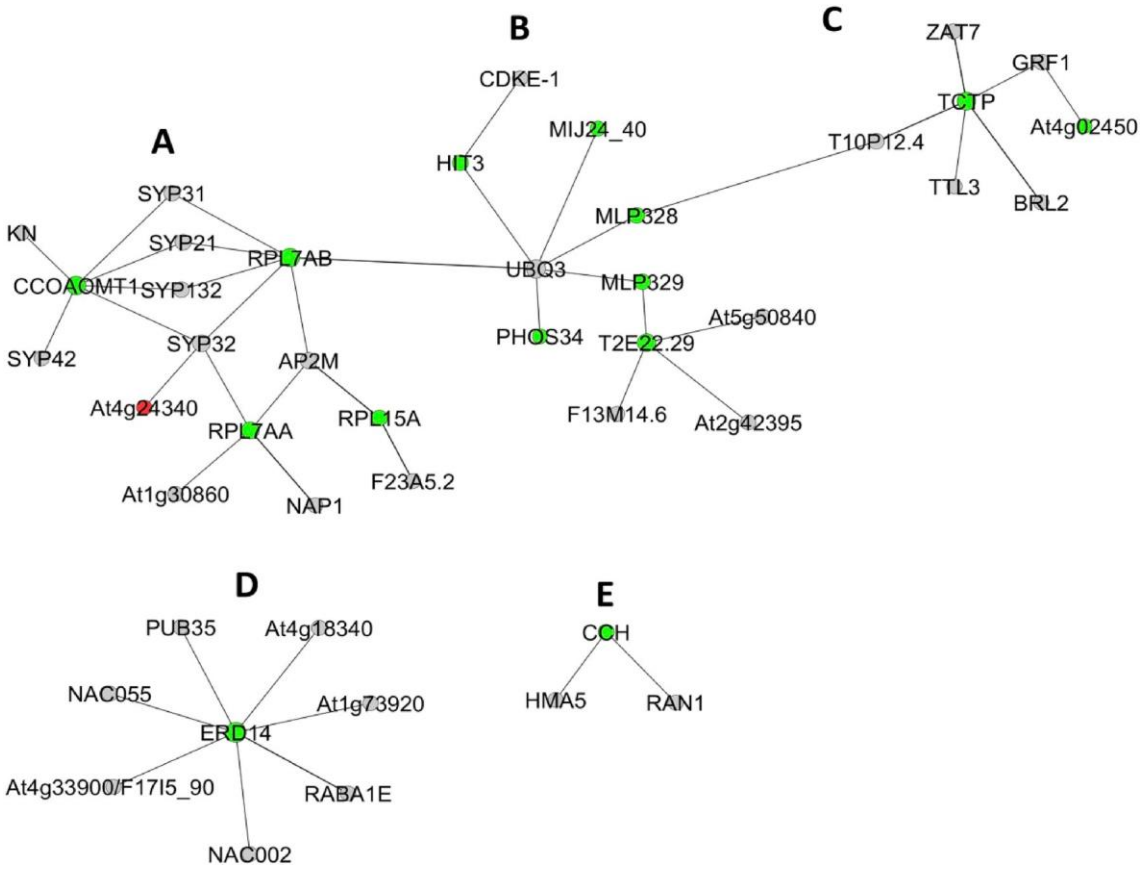

Fig. 3. Interactome analysis of the identified proteins. Colours indicate up regulated (Green), down regulated (Red) and experimentally determined interacting partners (Grey) from the database. Gene names are displayed. (For interpretation of the references to colour in this figure legend, the reader is referred to the Web version of this article.)

Hence, is also considered as a marker for oxidative stress (Asada, 1992).

The sAPX identified in our study was upregulated 2 folds compared to the control (Table 2), supporting our notion of SDZ induced oxidative stress. Caverzan et al. (2012) reported differential regulation of specific isoforms of APXs in response to various environmental stress/stimuli.

To obtain an overall profile, fold change values of all the PODs identified in this study were compared (Fig. 2). In total, sixteen PODs were identified. Five PODs (PER 22, PER 32, sAPX, PER 39, PER 34) were found to be upregulated more than 1.5 folds compared to control. With a less stringent threshold to determine the fold change (> 1.2), three other PODs (PER 3, APX 1, PER 27) were found to be upregulated, while other PODs were unaltered and interestingly, not downregulated (Fig. 2). Thus, it is evident that the expression of several isoforms of PODs are stimulated in response to SDZ treatment in *Arabidopsis* roots, suggesting that PODs could be the major antioxidant enzymes functioning toward mitigating SDZ induced stress.

In addition to PODs, dehydrins ERD14, COR47 and Temperature induced lipocalin 1 (TIL) were found to be upregulated. Dehydrins are multifunctional proteins and their role in direct ROS scavenging and oxidative stress tolerance have been reported (Heyen et al., 2002; Jaffe et al., 2008).

3.5.1.3. Proteins with cytoprotective function. Abiotic stresses such as drought, high salinity, high temperature and cold ultimately lead to reduced free water available in the cell and result in dehydration. Dehydrins, including ERD14 and COR47 (upregulated 4.2 and 1.5 folds, respectively), are primarily induced in dehydration stress conditions and hence, are considered as molecular markers for identifying drought/dehydration stress and tolerance in plants (Graether and Boddington, 2014). Like other Late Embryogenesis Abundant (LEA) proteins, dehydrins are also accumulated in cells to maintain the cell volume and prevent cell collapse in response to dehydration (Hanin et al., 2011).

12S seed storage protein CRU1 (CRA1) belongs to the cupin superfamily of proteins. Although it is predominantly considered as a nutrient reservoir, upregulation in response to abiotic stress has also been reported (Wang et al., 2014). Considering that CRA1 had the highest fold change (4.3), we speculate that this protein could have similar roles to that of LEA proteins like dehydrins in preventing cell collapse.

3.5.1.4. Proteins related to PCD. TCTP is a multifunction protein that regulates several cellular processes. This protein, upregulated in this study, has been reported to prevent or inhibit the progression of programmed cell death (PCD) in *Arabidopsis* plants treated with PCD activators (Hoepflinger et al., 2013). Coherently, a metacaspase 4 (AMC4) was found to be upregulated and Curculin-like (Mannose- binding) lectin family protein (EP1GP) was downregulated in response to SDZ. Both these proteins are involved in regulating PCD (Hwang and Hwang, 2011; Watanabe and Lam, 2011). Regulation of these proteins suggests that PCD mechanisms are being modulated in response to stress conditions induced by SDZ.

3.5.2. Proteins related to metabolism

Caffeoyl-CoA O-methyltransferase 1 (CCOAOMT1), a protein related to phenylpropanoid pathway was upregulated. It catalyses monolignol formation, thus involved in lignification. It is also a crucial enzyme in various other phenylpropanoid metabolite biosynthesis including scopoletin and suberin, which were directly associated with abiotic stress response (Döll et al., 2018; Franke et al., 2012; Koeppe

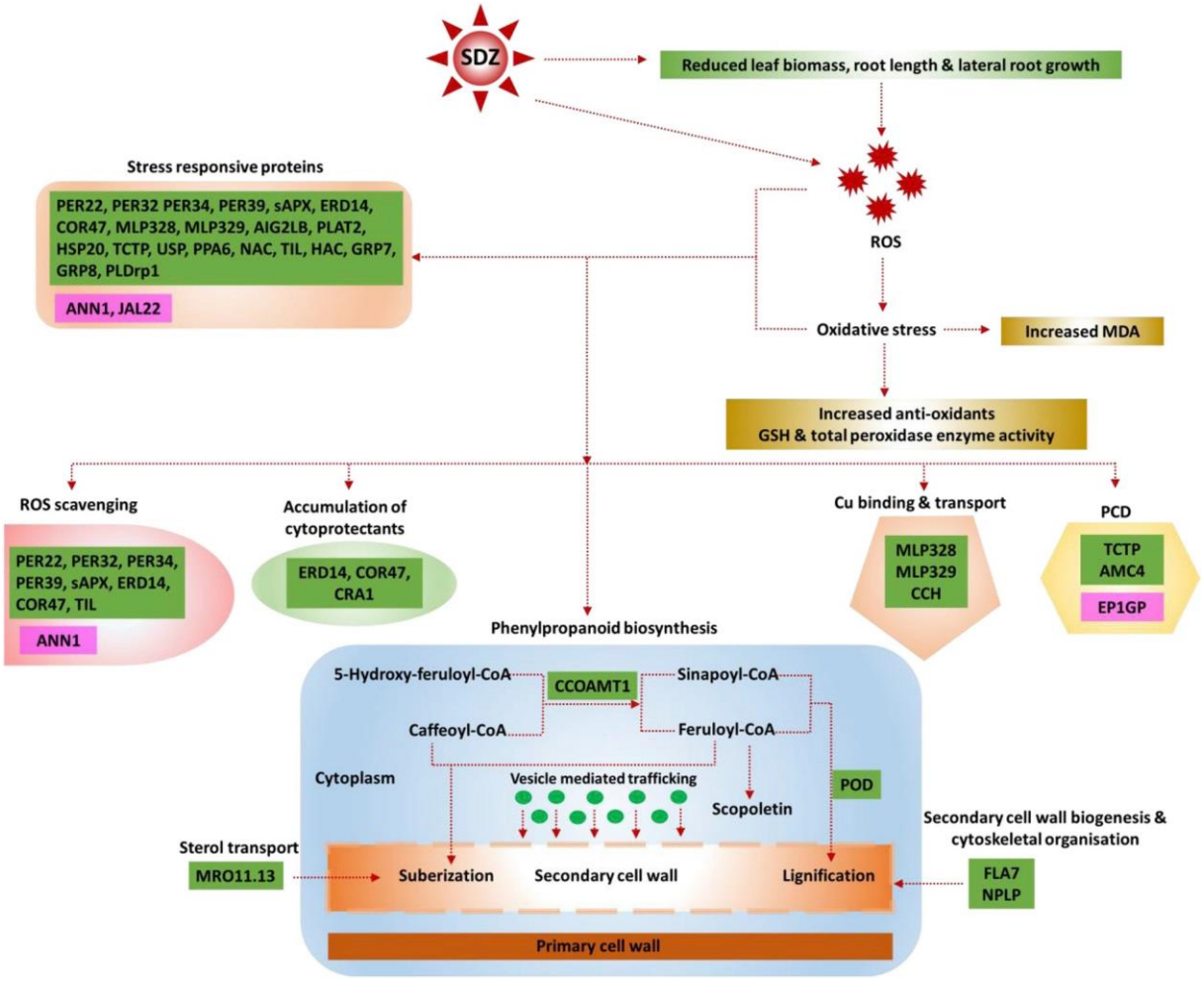

Fig. 4. Conceptual overview highlighting the probable molecular mechanisms modulated in response to SDZ in *Arabidopsis* roots.

et al., 1970).

Elevated levels of glucosinolate could be correlated with the accumulation of osmoprotective compounds (del Carmen Martínez-Ballesta et al., 2013). Thiocyanate methyltransferase 1 (HOL1), a key enzyme in the glucosinolate metabolism was upregulated in our study.

A glycine cleavage system H protein 2 (GDH2) involved in glyoxylate metabolism and glycine degradation and a NADH dehydrogenase [ubiquinone] iron-sulfur protein 8-A (NADHD) associated with the mitochondrial respiratory chain complex I assembly were upregulated. In addition, adenylylsulfatase (HINT1), which belongs to HIS triad family protein associated with purine ribonucleotide metabolism and sulfur metabolism was also upregulated. While a Phosphorylase superfamily protein (PSP) with nucleoside phosphorylase domain related to nucleoside metabolic process and lactoyl-glutathione lyase (GLX1) related to methylglyoxal degradation were downregulated.

In addition to ROS scavenging, type III PODs identified in this study could also be involved in several physiological, cellular and metabolic processes including auxin catabolism, lignification, and suberization in response to stress (Degenhardt and Gimmler, 2000).

3.5.3. Proteins related to transport

Copper transport protein (CCH), upregulated in our study, is involved in copper (Cu) homeostasis and transport. It was reported that this protein was upregulated in response to salt stress and cadmium exposure (Sarry et al., 2006; Jiang et al., 2007). Xu et al. (2017) examined the individual and combined effects of SDZ and copper on wheat seedlings and suggested that amending Cu at specific concentrations in soil could alleviate SDZ induced stress. Interestingly, MDA content was lower in plants treated with SDZ and with Cu at lower concentrations, indicating that Cu could have reduced the oxidative stress induced by SDZ. The mechanism underpinning the Cu mediated alleviation of SDZ induced stress is yet to be understood. Nonetheless, upregulation of this Cu transport protein in our study could be an indication supporting this observation.

An MD-2-related lipid recognition domain-containing protein (MRO11.13) associated with intercellular sterol transport was upregulated suggesting a probable increase in sterol transport. The significance of sterols in drought tolerance and regulation of ROS have been established in *Arabidopsis* (Posé et al., 2009). Inorganic phosphate transporter 1-1 (PHT1-1) is a transmembrane protein, which acts as a high-affinity transporter for inorganic phosphate and was shown that the overexpression of this symporter conferred arsenate sensitivity as it increased arsenate uptake (LeBlanc et al., 2013). Downregulation of this protein in our study suggests that altered preference in the transmembrane transporters could be one of the many mechanisms employed by plants to avoid or limit the import of hazardous compounds including SDZ.

3.5.4. Proteins related to transcription and translation

The protein F17H15.1/F17H15.1 (KHdp) upregulated 3.4 folds in this study consists of a KH domain with putative RNA binding function and has been reported to be an important upstream regulator of stress-responsive gene expression in *Arabidopsis* (Guan et al., 2013). A Methyl-CpG-binding domain (MBD) containing protein, found to be

upregulated in our study, was reported as an important factor that regulates DNA methylation, which is associated with transcriptional level silencing (Lang et al., 2015).

Structural constituents of ribosomes (RPS26C, RPL15A, RPL7AB, RPS12A, RPL23AB, RPL7AA) involved in translation were upregulated indicating a thrust in the protein synthesis, which can be corroborated to the observed increase in the total protein content (Table 1) and the upregulation of several proteins (42) (Table 2).

3.5.5. *Proteins with other functions*

A SOUL heme-binding-like protein (SOUL-1), which was upregulated is regarded as a cytosolic tetrapyrrole-carrier protein associated with free heme homeostasis (Lee et al., 2012). Upregulation of CRA1 - the 12S seed storage protein in response to SDZ in *Arabidopsis* roots is intriguing as these proteins are generally regarded as a nutrient reservoir for germinating seeds and its possible role as a cytoprotectant is discussed above. FAM10 family protein (FAM10) related to chaperone cofactor-dependent protein refolding, Fasciclin-like arabinogalactan protein 7 (FLA7) and Neurofilament like protein (NPLP) related secondary cell wall biogenesis and cytoskeleton structure, respectively were also upregulated.

3.6. *Pathway analysis of the identified proteins*

Among the identified proteins, CCOAOMT1 and POD superfamily were mapped to the phenylpropanoid biosynthetic pathway (Fig. S3), indicating that this pathway could be induced in response to SDZ. CCOAOMT1 is a crucial enzyme in monolignol biosynthesis catalysing the formation of feruloyl- CoA (substrate for scopoletin and suberin biosynthesis) and sinapoyl-CoA (substrate for syringyl lignin biosynthesis). Scopoletin accumulates in roots in response to osmotic stress with proposed function in ROS scavenging and forming a protective barrier (Döll et al., 2018); while increased deposition of suberin on roots with protective roles has been reported in drought, osmotic and heavy metal stress (Franke et al., 2012). PODs are involved in oxidative polymerization of monolignols to lignin and a positive association of lignification in response to various abiotic stress has been reported (Le Gall et al., 2015). Lignification and suberization are one of the primary responses of the plant, especially in roots, in response to drought, salinity and heavy metal stress (Franke et al., 2012; Le Gall et al., 2015). In accordance with the increased lignification observed in the roots of barley plants exposed to sulfonamide antibiotics (Michelini et al., 2013), it is probable that lignification and suberization of root cells could also be involved in the responses to SDZ in *Arabidopsis*.

3.7. *Interactome of the identified proteins*

Of the identified proteins, 26 proteins were found to be interacting with other proteins. Interestingly, several proteins were found to be interacting with Syntaxins associated with SNARE complex involved in vesicle fusion and docking - mediated intracellular transport (Fig. 3A).

This, in turn, redirects to the sub-cellular localization data where several proteins were predicted to be extracellularly secreted and intracellularly transported via the non-classical secretory pathway (Table 2). In addition, CCOAMT1 catalysing the formation of monolignols interacting with the SNARE complex proteins suggests that the monolignols could also be trafficked through vesicles to the secondary cell wall, wherein it is oxidatively polymerised to lignin by peroxidases.

Similarly, it has been indicated that constituents for the suberin biosynthesis are also transported through vesicles (Barros et al., 2015; Vishwanath et al., 2015). Multiple upregulated proteins were found to interact with a polyubiquitin protein (UBQ3) (Fig. 3B) suggesting that there could be ubiquitination-mediated degradation of these proteins to maintain protein homeostasis. TCTP1 - a multifunctional protein, which regulates several crucial cellular processes was found to be interacting with proteins related to auxin signalling and homeostasis, cell redox homeostasis, proteins involved in regulation of hormonal induction in response to stress and other proteins with direct/indirect roles in abiotic stress (Fig. 3C). Dehydrin ERD 14 was found to be interacting with crucial enzymes related to carbohydrate and lipid metabolism, a peroxisomal membrane protein and proteins involved in phosphorylation, jasmonic acid and ABA signalling pathways (Fig. 3D). Dehydrin - a multifunctional protein is established to interact with proteins and enzymes and maintain its native confirmation especially during dehydration and other abiotic stresses. Further, proteins involved in Cu binding and transport were also found to be interacting (Fig. 3E). In the interactome, several proteins related to ABA, auxin, jasmonic acid and brassinosteroid signalling pathways with a known interaction with SDZ-induced proteins evidenced in the present work were found. This suggests that there could be multiple phytohormonal signalling cascades operating with probable cross-talks at various levels.

3.8. *Changes in peroxidase enzyme activity*

To substantiate the involvement of PODs in response to SDZ and validate the proteomic results, the total POD enzyme activity was determined. There was an overall increase in the POD activity in all the concentrations of SDZ with the highest at 0.5 μM (Table 1), supporting the observed upregulation of PODs (PER 22, PER 32, PER 34 and PER 39) (Table 2; Fig. 2). Increased anti-oxidant enzyme activities were observed in plants exposed to antibiotics (Xie et al., 2011; Nie et al., 2013) and increased POD activity was reported in wheat seedlings treated with SDZ (Xu et al., 2017). It is ascertained that PODs are in- volved in the responses to SDZ treatment either in ROS-detoxification or in other responses such as lignification and suberization. Bialk et al. (2005) provided direct evidence of PODs-mediated covalent cross- coupling of the sulfonamide sulfamethazine with phenolic substances. This leads to the notion if such sequestration mechanisms mediated by PODs would exist in plants to limit uptake, bioavailability and biological activity of SDZ.

4. Conceptual overview and concluding remarks

Results from this study might be depicted as a comprehensive conceptual snapshot (Fig. 4). There was a significant reduction in leaf biomass, root length and lateral root growth. Congruently, Xu et al. (2017) have reported that SDZ adversely affects the leaf biomass, root formation and length. As a consequence of impaired root growth and function, water uptake and balance would be disturbed, mimicking water deficit-like conditions. This could have resulted in excessive ROS generation as evidenced by increased MDA content, indicating oxidative stress and in turn ROS-induced lipid peroxidation. This was further substantiated by upregulation of several proteins related to oxidative stress and increased anti-oxidants (GSH and PODs). ROS could be one of the primary signalling molecules inducing a cascade of stress responses resulting in upregulation of several stress-related proteins. Their crucial role as stress signalling molecules has been well established (Choudhury et al., 2017).

Comprehensively, in response to SDZ, several proteins related to drought, salinity and heavy metal stress were upregulated, many of which had direct ROS-scavenging roles, notably PODs and dehydrins. Upregulation of dehydrins (ERD14, COR47) and CRA1 - the seed storage protein with a putative cytoprotective function was also observed. There was also an indication of phenylpropanoid biosynthesis. The final outcome of CCOAMT1 and POD is lignification, suberization and accumulation of stress-responsive metabolites such as scopoletin. Along with peroxide detoxification and oxidative cross-linking of monolignols, a possible role of POD in cross-coupling SDZ to phenolic compounds as a means of transformation to limit bioavailability and mobility has also been hypothesised. The interactome analysis also provided an indication of the existing proposed model of lignin monomers and suberin constituents transported through vesicles to the

secondary cell wall. Further, there was an upregulation of proteins in- volved in sterol transport, secondary cell wall architecture and cytos- keletal organization indicating that there could be rearrangements in the cell wall, possibly by lignification and suberization in response to SDZ. Proteins related to Cu binding and transport and proteins asso- ciated with PCD were also upregulated. We contemplate that these could be a few of the mechanisms among the intricate, intertwined and multifaceted responses induced by SDZ in *ARABIDOPSIS* roots.

SDZ at higher concentrations reduced the overall growth, leaf bio- mass and root length. Biochemical analysis suggested that there is oxidative stress in response to SDZ. Taking into considerations the possible cytotoxic effects of SDZ, the exact mechanism triggering the oxidative stress upon treatment needs to be determined. Increased GSH levels and upregulation of several PODs validated with total POD en- zyme activity suggest that these could be the major anti-oxidants re- sponding to SDZ treatment. Proteome analysis indicated that the major proportion of the upregulated proteins were multifunctional stress-re- sponsive proteins. It is possible that SDZ treatment triggers multiple stress responsive pathways in *ARABIDOPSIS* roots.

5. Declarations of interest

None.

6. Acknowledgements

This work was supported by the grant of the University of Padova, Italy (DOR1621018). The authors wish to thank the Cassa di Risparmio di Padova e Rovigo (Cariparo) Holding for funding the acquisition of the LTQ-Orbitrap XL mass spectrometer. Nisha Sharma was supported by a Cariparo Fellowship for Foreign students. Leonard Barnabas Ebinezer was supported by the grant of the University of Padova (BIRD188182).

Appendix A. Supplementary data

Supplementary data to this article can be found online at https:// doi.org/10.1016/j.ecoenv.2019.04.008.

References

Abebe, T., Skadsen, R.W., Kaeppler, H.F., 2005. A proximal upstream sequence controls tissue-specific expression of Lem 2, a salicylate-inducible barley lectin-like gene. Planta 221 (2), 170–183. https://doi.org/10.1007/s00425-004-1429-9.

Asada, K., 1992. Ascorbate peroxidase-a hydrogen peroxide-scavenging enzyme in plants. Physiol. Plantarum 85 (2), 235–241. https://doi.org/10.1111/j.1399-3054.1992. tb04728.x.

Barros, J., Serk, H., Granlund, I., Pesquet, E., 2015. The cell biology of lignification in higher plants. Ann. Bot. 115 (7), 1053–1074. https://doi.org/10.1093/aob/mcv046.

Bialk, H.M., Simpson, A.J., Pedersen, J.A., 2005. Cross-coupling of sulfonamide anti-microbial agents with model humic constituents. Environ. Sci. Technol. 39 (12), 4463–4473. https://doi.org/10.1021/es0500916.

Boxall, A.B., Blackwell, P., Cavallo, R., Kay, P., Tolls, J., 2002. The sorption and transport of a sulphonamide antibiotic in soil systems. Toxicol. Lett. 131 (1–2), 19–28. https:// doi.org/10.1016/S0378-4274(02)00063-2.

Boxall, A.B., Johnson, P., Smith, E.J., Sinclair, C.J., Stutt, E., Levy, L.S., 2006. Uptake of veterinary medicines from soils into plants. J. Agric. Food Chem. 54 (6), 2288–2297. https://doi.org/10.1021/jf053041t.

Bradford, M.M., 1976. A rapid and sensitive method for the quantitation of microgram quantities of protein utilizing the principle of protein-dye binding. Anal. Biochem. 72 (1–2), 248–254. https://doi.org/10.1016/0003-2697(76)90527-3.

Carazzolle, M.F., de Carvalho, L.M., Slepicka, H.H., Vidal, R.O., Pereira, G.A.G., Kobarg, J., et al., 2014. IIS - integrated Interactome System: a web-based platform for the annotation, analysis and visualization of protein-metabolitegene-drug interactions by integrating a variety of data sources and tools. PLoS One 9, e100385. https://doi.org/ 10.1371/journal.pone.0100385.

Carter, L.J., Harris, E., Williams, M., Ryan, J.J., Kookana, R.S., Boxall, A.B., 2014. Fate and uptake of pharmaceuticals in soil–plant systems. J. Agric. Food Chem. 62 (4), 816–825. https://doi.org/10.1021/jf404282y.

Carvalho, P.N., Basto, M.C.P., Almeida, C.M.R., Brix, H., 2014. A review of plant–-pharmaceutical interactions: from uptake and effects in crop plants to phytor-emediation in constructed wetlands. Environ. Sci. Pollut. Control Ser. 21 (20), 11729–11763. https://doi.org/10.1007/s11356-014-2550-3.

Caverzan, A., Passaia, G., Rosa, S.B., Ribeiro, C.W., Lazzarotto, F., Margis-Pinheiro, M., 2012. Plant responses to stresses: role of ascorbate peroxidase in the antioxidant protection. Genet. Mol. Biol. 35 (4), 1011–1019. https://doi.org/10.1590/S1415-47572012000600016.

Chao, D.Y., Chen, Y., Chen, J., Shi, S., Chen, Z., Wang, C., Salt, D.E., 2014. Genome-wide association mapping identifies a new arsenate reductase enzyme critical for limiting arsenic accumulation in plants. PLoS Biol. 12 (12), e1002009. https://doi.org/10.1371/journal.pbio.1002009.

Chen, J.-Y., Dai, X.-F., 2010. Cloning and characterization of the *Gossypium hirsutum* major latex protein gene and functional analysis in *ARABIDOPSIS THALIANA*. Planta 231 (4), 861–873. https://doi: 10.1007/s00425-009-1092-2.

Choudhury, F.K., Rivero, R.M., Blumwald, E., Mittler, R., 2017. Reactive oxygen species, abiotic stress and stress combination. Plant J. 90 (5), 856–867. https://doi: 10.1111/ tpj.13299.

De Liguoro, M., Poltronieri, C., Capolongo, F., Montesissa, C., 2007. Use of sulfadi-methoxine in intensive calf farming: evaluation of transfer to stable manure and soil. Chemosphere 68 (4), 671–676. https://doi.org/10.1016/j.chemosphere.2007.02. 009.

De Rosa, E., Checchetto, V., Franchin, C., Bergantino, E., Berto, P., Szabò, I., Costantini, P., 2015. [NiFe]-hydrogenase is essential for cyanobacterium *Synechocystis* sp. PCC 6803 aerobic growth in the dark. Sci. Rep. 5, 12424. https://doi.org/10.1038/srep12424.

Degenhardt, B., Gimmler, H., 2000. Cell wall adaptations to multiple environmental stresses in maize roots. J. Exp. Bot. 51 (344), 595–603. https://doi.org/10.1093/jexbot/51.344.595.

del Carmen Martínez-Ballesta, M., Moreno, D.A., Carvajal, M., 2013. The physiological importance of glucosinolates on plant response to abiotic stress in Brassica. Int. J. Mol. Sci. 14 (6), 11607–11625. https://doi.org/10.3390/ijms140611607.

Dixon, D.P., Skipsey, M., Edwards, R., 2010. Roles for glutathione transferases in plant secondary metabolism. Phytochemistry 71 (4), 338–350. https://doi.org/10.1016/j.phytochem.2009.12.012.

Döll, S., Kuhlmann, M., Rutten, T., Mette, M.F., Scharfenberg, S., Petridis, A., Mock, H.P., 2018. Accumulation of the coumarin scopolin under abiotic stress conditions is mediated by the *ARABIDOPSIS THALIANA* THO/TREX complex. Plant J. 93 (3), 431–444. https://doi.org/10.1111/tpj.13797.

Fleming, A., 1944. The discovery of penicillin. Br. Med. Bull. 2 (1), 4–5.

Fleming, A., 1946. Penicillin. Its Practical Application. Butterworth And Co. Publishers Ltd., London.

Förster, M., Laabs, V., Lamshoft, M., Groeneweg, J., Zuhlke, S., Spiteller, M., Amelung, W., 2009. Sequestration of manure-applied sulfadiazine residues in soils. Environ. Sci. Technol. 43 (6), 1824–1830. https://doi.org/10.1021/es8026538.

Foyer, C.H., Noctor, G., 2005. Oxidant and antioxidant signalling in plants: a re-evaluation of the concept of oxidative stress in a physiological context. Plant Cell Environ. 28 (8), 1056–1071. https://doi.org/10.1111/j.1365-3040.2005.01327.x.

Foyer, C.H., Noctor, G., 2011. Ascorbate and glutathione: the heart of the redox hub. Plant Physiol. 155 (1), 2–18. https://doi.org/10.1104/pp.110.167569.

Franke, R.B., Dombrink, I., Schreiber, L., 2012. Suberin goes genomics: use of a short living plant to investigate a long lasting polymer. Front. Plant Sci. 3, 4. https://doi.org/10.3389/fpls.2012.00004.

Giaretta, S., Prasad, D., Forieri, I., Vamerali, T., Trentin, A.R., Wirtz, M.,, et al., 2017.Apoplastic gamma-glutamyl transferase activity encoded by GGT1 and GGT2 is important for vegetative and generative development. Plant Physiol. Biochem. 115, 44–56. https://doi.org/10.1016/j.plaphy.2017.03.007.

Graether, S.P., Boddington, K.F., 2014. Disorder and function: a review of the dehydrin protein family. Front. Plant Sci. 5, 576. https://doi.org/10.3389/fpls.2014.00576.

Guan, Q., Wen, C., Zeng, H., Zhu, J., 2013. A KH domain-containing putative RNA-binding protein is critical for heat stress-responsive gene regulation and thermotolerance in Arabidopsis. Mol. Plant 6 (2), 386–395. https://doi.org/10.1093/mp/sss119.

Gutiérrez-Luna, F.M., Hernández-Domínguez, E.E., Valencia-Turcotte, L.G., Rodriguez-Sotres, R., 2018. Pyrophosphate and pyrophosphatases in plants, their involvement in stress responses and their possible relationship to secondary metabolism. Plant Sci. 267, 11–19. https://doi.org/10.1016/j.plantsci.2017.10.016.

Hanin, M., Brini, F., Ebel, C., Toda, Y., Takeda, S., Masmoudi, K., 2011. Plant dehydrins and stress tolerance: versatile proteins for complex mechanisms. Plant Signal. Behav. 6 (10), 1503–1509. https://doi.org/10.4161/psb.6.10.17088.

Heath, R.L., Packer, L., 1968. Photoperoxidation in isolated chloroplasts: I. Kinetics and stoichiometry of fatty acid peroxidation. Arch. Biochem. Biophys. 125 (1), 189–198. https://doi.org/10.1016/0003-9861(68)90654-1.

Hendawey, M.H., Kamel, H.A., 2015. Distribution and bioaccumulation of radiocarbon (14C) into biochemical components of wheat in relation to antioxidant system under saline stress conditions. J. Am. Sci. 11 (10), 8–21. https://doi:10.7537/marsjas111015.02.

Hewitt, E.J., Dickes, G.J., 1961. Spectrophotometric measurements on ascorbic acid and their use for the estimation of ascorbic acid and dehydroascorbic acid in plant tissues. Biochem. J. 78 (2), 384.

Heyen, B.J., Alsheikh, M.K., Smith, E.A., Torvik, C.F., Seals, D.F., Randall, S.K., 2002. The calcium-binding activity of a vacuole-associated, dehydrin-like protein is regulated by phosphorylation. Plant Physiol. 130 (2), 675–687. https://doi.org/10.1104/pp.002550.

Hodges, D.M., DeLong, J.M., Forney, C.F., Prange, R.K., 1999. Improving the thiobarbituric acid-reactive-substances assay for estimating lipid peroxidation in plant tissues containing anthocyanin and other interfering compounds. Planta 207 (4), 604–611. https://doi.org/10.1007/s004250050524.

Hoepflinger, M.C., Reitsamer, J., Geretschlaeger, A.M., Mehlmer, N., Tenhaken, R., 2013. The effect of translationally controlled tumour protein (TCTP) on programmed cell death in plants. BMC Plant Biol. 13, 135. https://doi.org/10.1186/1471-2229-13- 135.

Huschek, G., Hollmann, D., Kurowski, N., Kaupenjohann, M., Vereecken, H., 2008. Re-evaluation of the conformational structure of sulfadiazine species using NMR and ab initio DFT studies and its implication on sorption and degradation. Chemosphere 72 (10), 1448–1454. https://doi.org/10.1016/j.chemosphere.2008.05.038.

Huseby, N.E., Stromme, J.H., 1974. Practical points regarding routine determination of γ-glutamyl transferase (γ-GT) in serum with a kinetic method at 37 C. Scand. J. Clin. Lab. Investig. 34 (4), 357–363. https://doi.org/10.3109/00365517409049892.

Hwang, I.S., Hwang, B.K., 2011. The pepper mannose-binding lectin gene CaMBL1 is required to regulate cell death and defense responses to microbial pathogens. Plant Physiol. 155 (1), 447–463. https://doi.org/10.1104/pp.110.164848.

Hyun, T.K., van der Graaff, E., Albacete, A., Eom, S.H., Großkinsky, D.K., Böhm, H., Roitsch, T., 2014. The Arabidopsis PLAT domain protein 1 is critically involved in abiotic stress tolerance. PLoS One 9 (11), e112946. https://doi.org/10.1371/journal. pone.0112946.

Jaffe, R., Charron, T., Puley, G., Dick, A., Strauss, B.H., 2008. Microvascular obstruction and the no-reflow phenomenon after percutaneous coronary intervention. Circulation 117 (24), 3152–3156. https://doi.org/10.1161/circulationaha.107.742312

Jechalke, S., Kopmann, C., Rosendahl, I., Groeneweg, J., Weichelt, V., Krögerrecklenfort, E., Heuer, H., 2013. Increased abundance and transferability of resistance genes after field application of manure from sulfadiazine-treated pigs. Appl. Environ. Microbiol. 79 (5), 1704–1711. https://doi.org/10.1128/AEM.03172-12.

Jiang, Y.Q., Deyholos, M.K., 2006. Comprehensive transcriptional profiling of NaCl-stressed *Arabidopsis* roots reveals novel classes of responsive genes. BMC Plant Biol. 6, 25. https://doi.org/10.1186/1471-2229-6-25.

Jiang, Y., Yang, B., Harris, N.S., Deyholos, M.K., 2007. Comparative proteomic analysis of NaCl stress-responsive proteins in Arabidopsis roots. J. Exp. Bot. 58 (13), 3591–3607. https://doi.org/10.1093/jxb/erm207.

Kanehisa, M., Furumichi, M., Tanabe, M., Sato, Y., Morishima, K., 2017. KEGG: new perspectives on genomes, pathways, diseases and drugs. Nucleic Acids Res. 45, D353–D361. https://doi.org/10.1093/nar/gkw1092.

Kang, D.H., Gupta, S., Rosen, C., Fritz, V., Singh, A., Chander, Y., et al., 2013. Antibiotic uptake by vegetable crops from manure-applied soils. J. Agric. Food Chem. 61 (42), 9992–10001. https://doi.org/10.1021/jf404045m.

Karan, R., Subudhi, P.K., 2012. Overexpression nascent polypeptide associated gene complex (*SaBNAC*) of Spartine alternifora improves tolerance to salinity and drought in transgenic Arabidopsis. Biochem. Biophys. Res. Commun. 424 (4), 747–752. https://doi.org/10.1016/j.bbrc.2012.07.023.

Karcı, A., Balcıoğlu, I.A., 2009. Investigation of the tetracycline, sulfonamide, and fluoroquinolone antimicrobial compounds in animal manure and agricultural soils in Turkey. Sci. Total Environ. 407 (16), 4652–4664. https://doi.org/10.1016/j.scitotenv.2009.04.047.

Karthikeyan, K.G., Meyer, M.T., 2006. Occurrence of antibiotics in wastewater treatment facilities in Wisconsin, USA. Sci. Total Environ. 361 (1–3), 196–207. https://doi.org/ 10.1016/j.scitotenv.2005.06.030.

Kerk, D., Bulgrien, J., Smith, D.W., Gribskov, M., 2003. *Arabidopsis* proteins containing similarity to the universal stress protein domain of bacteria. Plant Physiol. 131 (3), 1209–1219. https://doi.org/10.1104/pp.102.016006.

Kim, J.S., Jung, H.J., Lee, H.J., Kim, K.A., Goh, C.H., Woo, Y., Kang, H., 2008. Glycine-rich RNA-binding protein 7 affects abiotic stress responses by regulating stomata opening and closing in *Arabidopsis thaliana*. Plant J. 55 (3), 455–466. https://doi.org/10.1111/j.1365-313X.2008.03518.x.

Koeppe, D.E., Rohrbaugh, L.M., Rice, E.L., Wender, S.H., 1970. The effect of age and chilling temperature on the concentration of scopolin and caffeoylquinic acids in tobacco. Physiol. Plantarum 23 (2), 258–266. https://doi.org/10.1111/j.1399-3054. 1970.tb06415.x.

Lang, Z., Lei, M., Wang, X., Tang, K., Miki, D., Zhang, H., Yan, J., 2015. The methyl-CpG-binding protein MBD7 facilitates active DNA demethylation to limit DNA hyper-methylation and transcriptional gene silencing. Mol. Cell 57 (6), 971–983. https://doi.org/10.1016/j.molcel.2015.01.009.

Le Gall, H., Philippe, F., Domon, J.M., Gillet, F., Pelloux, J., Rayon, C., 2015. Cell wall metabolism in response to abiotic stress. Plants 4 (1), 112–166. https://doi.org/10. 3390/plants4010112.

LeBlanc, M.S., McKinney, E.C., Meagher, R.B., Smith, A.P., 2013. Hijacking membrane transporters for arsenic phytoextraction. J. Biotechnol. 163 (1), 1–9. https://doi.org/ 10.1016/j.jbiotec.2012.10.013.

Lee, J.Y., Lee, D.H., 2003. Use of serial analysis of gene expression technology to reveal changes in gene expression in *Arabidopsis* pollen undergoing cold stress. Plant Physiol. 132 (2), 517–529. https://doi.org/10.1104/pp.103.020511.

Lee, H.J., Mochizuki, N., Masuda, T., Buckhout, T.J., 2012. Disrupting the bimolecular binding of the haem-binding protein 5 (AtHBP5) to haem oxygenase 1 (HY1) leads to oxidative stress in Arabidopsis. J. Exp. Bot. 63 (16), 5967–5978. https://doi.org/10.1093/jxb/ers242.

Li, Y., Han, D., Sommerfeld, M., Hu, Q., 2011. Photosynthetic carbon partitioning and lipid production in the oleaginous microalga Pseudochlorococcum sp. (Chlorophyceae) under nitrogen-limited conditions. Bioresour. Technol. 102 (1), 123–129. https://doi.org/10.1016/j.biortech.2010.06.036.

Manzetti, S., Ghisi, R., 2014. The environmental release and fate of antibiotics. Mar. Pollut. Bull. 79 (1–2), 7–15. https://doi.org/10.1016/j.marpolbul.2014.01.005.

Masi, A., Ghisi, R., Ferretti, M., 2002. Measuring low-molecular-weight thiols by detecting the fluorescence of their SBD-derivatives: application to studies of diurnal and UV-B induced changes in *Zea mays* L. J. Plant Physiol. 159 (5), 499. https://doi.org/10.1078/0176-1617-00655.

Masi, A., Trentin, A.R., Agrawal, G.K., Rakwal, R., 2015. Gamma-glutamyl cycle in plants: a bridge connecting the environment to the plant cell? Front. Plant Sci. 6, 252. https://doi.org/10.3389/fpls.2015.00252.

Michelini, L., Reichel, R., Werner, W., Ghisi, R., Thiele-Bruhn, S., 2012. Sulfadiazine uptake and effects on *Salix fragilis* L. and *Zea mays* L. plants. Water, Air, Soil Pollut. 223 (8), 5243–5257. https://doi.org/10.1007/s11270-012-1275-5.

Michelini, L., La Rocca, N., Rascio, N., Ghisi, R., 2013. Structural and functional alterations induced by two sulfonamide antibiotics on barley plants. Plant Physiol. Biochem. 67, 55–62. https://doi.org/10.1016/j.plaphy.2013.02.027.

Migliore, L., Brambilla, G., Cozzolino, S., Gaudio, L., 1995. Effect on plants of ulphadimethoxine used in intensive farming (Panicum miliaceum, Pisum sativum and Zeamays). Agric. Ecosyst. Environ. 52 (2–3), 103–110. https://doi.org/10.1016/0167- 8809(94)00549-T.

Migliore, L., Civitareale, C., Brambilla, G., Di Delupis, G.D., 1997. Toxicity of several important agricultural antibiotics to Artemia. Water Res. 31 (7), 1801–1806. https:// doi.org/10.1016/S0043-1354(96)00412-5.

Migliore, L., Rotini, A., Cerioli, N.L., Cozzolino, S., Fiori, M., 2010. Phytotoxic antibiotic sulfadimethoxine elicits a complex hormetic response in the weed *Lythrum salicaria* L. Dose Res. 8, 414–427. https://doi.org/10.2203/dose-response.09-033.

Mirzajani, F., Askari, H., Hamzelou, S., Schober, Y., Römpp, A., Ghassempour, A., Spengler, B., 2014. Proteomics study of silver nanoparticles toxicity on *Oryza sativa* L. Ecotoxicol. Environ. Saf. 108, 335–339. https://doi.org/10.1016/j.ecoenv.2014.07.013.

Mittler, R., Vanderauwera, S., Gollery, M., Van Breusegem, F., 2004. Reactive oxygen gene network of plants. Trends Plant Sci. 9 (10), 490–498. https://doi.org/10.1016/j. tplants.2004.08.009.

Ndimba, B.K., Chivasa, S., Simon, W.J., Slabas, A.R., 2005. Identification of rabidopsis salt and osmotic stress responsive proteins using two-dimensional difference gel electrophoresis and mass spectrometry. Proteomics 5 (16), 4185–4196. https://doi. org/10.1002/pmic.200401282.

Nie, X.P., Liu, B.Y., Yu, H.J., Liu, W.Q., Yang, Y.F., 2013. Toxic effects of erythromycin, ciprofloxacin and sulfamethoxazole exposure to the antioxidant system in *Pseudokirchneriella subcapitata*. Environ. Pollut. 172, 23–32. https://doi.org/10.1016/j.envpol.2012.08.013.

Nylander, M., Svensson, J., Palva, E.T., Welin, B.V., 2001. Stress-induced accumulation and tissue-specific localization of dehydrins in *Arabidopsis thaliana*. Plant Mol. Biol. 45 (3), 263–279. https://doi: 10.1023/A:1006469128280.

Pan, M., Chu, L.M., 2016. Adsorption and degradation of five selected ntibiotics in agricultural soil. Sci. Total Environ. 545, 48–56. https://doi.org/10.1016/j.scitotenv. 2015.12.040.

Pan, M., Wong, C.K., Chu, L.M., 2014. Distribution of antibiotics in wastewater-irrigated soils and their accumulation in vegetable crops in the Pearl River Delta, Southern China. J. Agric. Food Chem. 62 (46), 11062–11069. https://doi.org/10.1021/jf503850v.

Park, C.J., Seo, Y.S., 2015. Heat shock proteins: a review of the molecular chaperones for plant immunity. Plant Pathol. J. 31 (4), 323. https://doi.org/10.5423/PPJ.RW.08.2015.0150.

Paulose, B., Chhikara, S., Coomey, J., Jung, H.I., Vatamaniuk, O., Dhankher, O.P., 2013. A γ-glutamyl cyclotransferase protects Arabidopsis plants from heavy metal toxicity by recycling glutamate to maintain glutathione homeostasis. Plant Cell tpc-113. https://doi.org/10.1105/tpc.113.111815.

Persson, Ö., Valadi, Å., Nyström, T., Farewell, A., 2007. Metabolic control of the Escherichia coli universal stress protein response through fructose-6-phosphate. Mol. Microbiol. 65 (4), 968–978. https://doi.org/10.1111/j.1365-2958.2007.05838.x.

Posé, D., Castanedo, I., Borsani, O., Nieto, B., Rosado, A., Taconnat, L., Botella, M.A., 2009. Identification of the Arabidopsis dry 2/sqe1-5 mutant reveals a central role for sterols in drought tolerance and regulation of reactive oxygen species. Plant J. 59 (1), 63–76. https://doi.org/10.1111/j.1365-313X.2009.03849.x.

Qiu, N., Liu, Q., Li, J., Zhang, Y., Wang, F., Gao, J., 2017. Physiological and transcriptomic responses of Chinese cabbage (Brassica rapa L. ssp. pekinensis) to salt stress. Int. J. Mol. Sci. 18 (9), 1953. https://doi.org/10.3390/ijms18091953.

Ranieri, A., Petacco, F., Castagna, A., Soldatini, G.F., 2000. Redox state and peroxidase system in sunflower plants exposed to ozone. Plant Sci. 159 (1), 159–167. https://doi. org/10.1016/S0168-9452(00)00352-6.

Resmini, G., Rizzo, S., Franchin, C., Zanin, R., Penzo, C., Pegoraro, S., Manfioletti, G., 2017. HMGA1 regulates the Plasminogen activation system in the secretome of breast cancer cells. Sci. Rep. 7 (1), 11768. https://doi.org/10.1038/s41598-017-11409-4.

Reymond, P., Weber, H., Damond, M., Farmer, E.E., 2000. Differential gene expression in response to mechanical wounding and insect feeding in Arabidopsis. Plant Cell 12 (5), 707–719. https://doi.org/10.1105/tpc.12.5.707.

Roomi, S., Masi, A., Conselvan, G.B., Trevisan, S., Quaggiotti, S., Pivato, M., et al., 2018. Protein profiling of *Arabidopsis* roots treated with humic substances: insights into the metabolic and interactome networks. Front. Plant Sci. 9 (1812). https://doi.org/10. 3389/fpls.2018.01812.

Rosendahl, I., Siemens, J., Groeneweg, J., Linzbach, E., Laabs, V., Herrmann, C., Amelung, W., 2011. Dissipation and sequestration of the veterinary antibiotic sulfadiazine and its metabolites under field conditions. Environ. Sci. Technol. 45 (12), 5216–5222. https://doi.org/10.1021/es200326t.

Sarmah, A.K., Meyer, M.T., Boxall, A.B., 2006. A global perspective on the use, sales, exposure pathways, occurrence, fate and effects of veterinary antibiotics (VAs) in the environment. Chemosphere 65 (5), 725–759. https://doi.org/10.1016/j.chemosphere.2006.03.026.

Sarry, J.E., Kuhn, L., Ducruix, C., Lafaye, A., Junot, C., Hugouvieux, V.,, et al., 2006. The early responses of Arabidopsis thaliana cells to cadmium exposure explored by protein and metabolite profiling analyses. Proteomics 6 (7), 2180–2198. https://doi.org/10.1002/pmic.200500543.

Scandalios, J.G., 2005. Oxidative stress: molecular perception and transduction of signals triggering antioxidant gene defenses. Braz. J. Med. Biol. Res. 38 (7), 995–1014. https://doi.org/10.1590/S0100-79X2005000700003

.Schmidt, B., Ebert, J., Lamshöft, M.A.R.C., Thiede, B., Schumacher-Buffel, R., Ji, R., Schäffer, A., 2008. Fate in soil of 14C-sulfadiazine residues contained in the manure of young pigs treated with a veterinary antibiotic. J. Environ. Sci. Health 43 (1),8–20. https://doi.org/10.1080/03601230701734824.

Schmidt, F., Marnef, A., Cheung, M.K., Wilson, I., Hancock, J., Staiger, D., Ladomery, M., 2010. A proteomic analysis of oligo (dT)-bound mRNP containing oxidative stress-induced Arabidopsis thaliana RNA-binding proteins ATGRP7 and ATGRP8. Mol. Biol. Rep. 37 (2), 839–845. https://doi.org/10.1007/s11033-009-9636-x.

Schwarz, J., Aust, M.O., Thiele-Bruhn, S., 2010. Metabolites from fungal laccase-catalysed transformation of sulphonamides. Chemosphere 81 (11), 1469–1476. https://doi. org/10.1016/j.chemosphere.2010.08.053.

Shannon, P., Markiel, A., Ozier, O., Baliga, N.S., Wang, J.T., Ramage, D., et al., 2003. Cytoscape: a software environment for integrated models of biomolecular interaction networks. Genome Res. 13, 2498–2504. https://doi.org/10.1101/gr.1239303.

Stanley Kim, H., Yu, Y., Snesrud, E.C., Moy, L.P., Linford, L.D., Haas, B.J., Quackenbush, J., 2005. Transcriptional divergence of the duplicated oxidative stress-responsive genes in the Arabidopsis genome. Plant J. 41 (2), 212–220. https://doi.org/10.1111/ j.1365-313X.2004.02295.x.

Tasho, R.P., Cho, J.Y., 2016. Veterinary antibiotics in animal waste, its distribution in soil and uptake by plants: a review. Sci. Total Environ. 563, 366–376. https://doi.org/10. 1016/j.scitotenv.2016.04.140.

Thounaojam, T.C., Panda, P., Mazumdar, P., Kumar, D., Sharma, G.D., Sahoo, L., Sanjib, P., 2012. Excess copper induced oxidative stress and response of antioxidants in rice. Plant *Physiol. Biochem.* 53, 33–39. https://doi.org/10.1016/j.plaphy.2012.01.006.

Thiele-Bruhn, S., 2003. Pharmaceutical antibiotic compounds in soils. J. Plant Nutr. Soil Sci. 166 (2), 145–167. https://doi.org/10.1002/jpln.200390023.

Tolin, S., Arrigoni, G., Trentin, A.R., Veljovic-Jovanovic, S., Pivato, M., Zechman, B., Masi, A., 2013. Biochemical and quantitative proteomics investigations in Arabidopsis ggt1 mutant leaves reveal a role for the gamma-glutamyl cycle in plant's adaptation to environment. Proteomics 13 (12–13), 2031–2045. https://doi.org/10. 1002/pmic.201200479.

Trentin, A.R., Pivato, M., Mehdi, S.M., Barnabas, L.E., Giaretta, S., Fabrega-Prats, M., Masi, A., 2015. Proteome readjustments in the apoplastic space of Arabidopsis thaliana ggt1 mutant leaves exposed to UV-B radiation. Front. Plant Sci. 6, 128. https://doi: 10.3389/fpls.2015.00128.

Ufer, G., Gertzmann, A., Gasulla, F., Röhrig, H., Bartels, D., 2017. Identification and characterization of the phosphatidic acid-binding A. thaliana phosphoprotein PLD rp1 that is regulated by PLD α1 in a stress-dependent manner. Plant J. 92 (2), 276–290. https://doi.org/10.1111/tpj.13651.

Vincent, D., Ergül, A., Bohlman, M.C., Tattersall, E.A., Tillett, R.L., Wheatley, M.D., Schooley, D.A., 2007. Proteomic analysis reveals differences between Vitis vinifera L. cv. Chardonnay and cv. Cabernet Sauvignon and their responses to water deficit and salinity. J. Exp. Bot. 58 (7), 1873–1892. https://doi.org/10.1093/jxb/erm012.

Vishwanath, S.J., Delude, C., Domergue, F., Rowland, O., 2015. Suberin: biosynthesis, regulation, and polymer assembly of a protective extracellular barrier. Plant Cell Rep. 34 (4), 573–586. https://doi.org/10.1007/s00299-014-1727-z.

Wang, X., Zhang, H., Gao, Y., Sun, G., Zhang, W., Qiu, L., 2014. A comprehensive analysis of the Cupin gene family in soybean (Glycine max). PLoS One 9 (10), e110092. https://doi.org/10.1371/journal.pone.0110092.

Wang, Y., Peng, X., Salvato, F., Wang, Y., Yan, X., Zhou, Z., Lin, J., 2019. Salt-adaptive strategies in oil seed crop *Ricinus communis* early seedlings (cotyledon vs. true leaf) revealed from proteomics analysis. Ecotoxicol. Environ. Saf. 171, 12–25. https://doi. org/10.1016/j.ecoenv.2018.12.046.

Watanabe, N., Lam, E., 2011. *ARABIDOPSIS* metacaspase 2d is a positive mediator of cell death induced during biotic and abiotic stresses. Plant J. 66 (6), 969–982. https:// doi.org/10.1111/j.1365-313X.2011.04554.x.

Wegst-Uhrich, S.R., Navarro, D.A., Zimmerman, L., Aga, D.S., 2014. Assessing antibiotic sorption in soil: a literature review and new case studies on sulfonamides and mac- rolides. Chem. Cent. J. 8 (1), 5. https://doi.org/10.1186/1752-153X-8-5.

Wehrhan, A., Streck, T., Groeneweg, J., Vereecken, H., Kasteel, R., 2010. Long-term sorption and desorption of sulfadiazine in soil: experiments and modeling. J. Environ. Qual. 39 (2), 654–666. https://doi.org/10.2134/jeq2009.0001.

Xie, X., Zhou, Q., Lin, D., Guo, J., Bao, Y., 2011. Toxic effect of tetracycline exposure on growth, antioxidative and genetic indices of wheat (Triticum aestivum L.). Environ. Sci. Pollut. Control Ser. 18 (4), 566–575. https://doi.org/10.1007/s11356-010-0398-8.

Xu, Y., Yu, W., Ma, Q., Zhou, H., Jiang, C., 2017. Toxicity of sulfadiazine and copper and their interaction to wheat (*Triticum AESTIVUM* L.) seedlings. Ecotoxicol. Environ. Saf. 142, 250–256. https://doi: 10.1016/j.ecoenv.2017.04.007.

Yang, C.L., Liang, S., Wang, H.Y., Han, L.B., Wang, F.X., Cheng, H.Q., Xia, G.X., 2015. Cotton major latex protein 28 functions as a positive regulator of the ethylene re- sponsive factor 6 in defense against *Verticillium DAHLIAE*. Mol. Plant 8 (3), 399–411. https://doi.org/10.1016/j.molp.2014.11.023.

Zhang, N., Li, R., Shen, W., Jiao, S., Zhang, J., Xu, W., 2018. Genome-wide volutionary characterization and expression analyses of major latex protein (MLP) family genes in *Vitis VINIFERA*. Mol. Genet. Genom. 1–15. https://doi.org/10.1007/s00438-018-1440-7.

CHAPTER 3

PHYTOREMEDIATION of PFAAs

3.1 Publication II

Accumulation and effects of perfluoroalkyl substances in three *Salix* L. species

Nisha Sharma, Giuseppe Barion, Inisa Shrestha, Leonard Barnabas Ebinezer, Anna Rita Trentin, Teofilo Vamerali, Giustino Mezzalira, Antonio Masi, Rossella Ghisi

Submitted in Ecotoxicology and Environmental Safety on 12 September 2019 and now it is under minor revision.

Accumulation and effects of perfluoroalkyl substances in three hydroponically grown Salix L. species

Nisha Sharma[1], Giuseppe Barion[1], Inisa Shrestha[1], Leonard Barnabas Ebinezer[1]*, Anna Rita Trentin[1], Teofilo Vamerali[1], Giustino Mezzalira[2], Antonio Masi[1], Rossella Ghisi[1]

[1]Department of Agronomy, Food, Natural resources, Animals and Environment (DAFNAE), University of Padova, Italy

[2] Veneto Agricoltura, Padova, Italy

Abbreviations: A, Net CO_2 assimilation rate; Ci, intercellular CO_2; dpt, Days post-treatment; ETR, Electron transport rate; ESI, electron spray ionization; Fm', Maximum chlorophyll fluorescence; Fs, Steady-state chlorophyll fluorescence; Fv/Fm, photosynthesis efficiency; Fv'/Fm', photosynthesis efficiency net of NPQ losses; FRCF, foliage to root concentration factor; gsw, stomatal conductance to water vapor; MPF, multiphase flash fluorescence protocol; NPQ, non-photochemical quenching; PhiCO_2, molecules of CO_2 fixed per photon; PFAAs, perfluoroalkyl acids; PFCA, perfluorinated carboxylic acid; PFASs, perfluoroalkyl and polyfluoroalkyl substances; PFBA, perfluorobutanoic acid; PFBS, perfluorobutane sulfonate; PFDA, perfluorodecanoic acid; PFDoA, perfluoro dodecanoic acid; PFHpA, perfluoroheptanoic acid; PFHxA, perfluorohexadecanoic acid; PFNA, perfluorononanoic acid; PFOA, perfluorooctanoic acid; PFOS, perfluorooctanesulfonate; PFPeA, perfluoro-n-pentanoic acid; PFSA, perfluorinated sulfonic acid; PFUnA, perfluoroundecanoic acid; POPs, persistent organic pollutants; Rd, Dark respiration rate; RGR, relative growth rate; SRM, single-reaction monitoring.

Highlights:

- PFAAs treatment tended to reduce the growth rate of willow
- Net photosynthesis and stomatal conductance were increased by PFAAs
- Leaf concentration of PFAAs decreased with increasing C-chain length
- Long-chain PFAAs were preferentially retained in roots
- Higher removal of individual PFAAs was observed in *S. eleagnos* and *S. purpurea*

Abstract:

The potential of young rooted cuttings of three Salix L. species plants to accumulate a mixture of eleven perfluoroalkyl substances (PFASs), in particular, perfluoroalkyl acids (PFAAs), from the nutrient solution and their effects on plant growth and photosynthesis were assessed in an 8-day experiment. Willow plants exposed to the PFAA mixture tended to show a decline in the growth rate after 2 days of treatment, with significant reductions in S. triandra. Regarding photosynthesis, the gas exchange parameters were affected more than those related to chlorophyll fluorescence, with significant increase of the net CO2 assimilation rate and parameters related to stomatal conductance. A decreasing trend in the PFAA concentration in leaves with increasing carbon chain length was observed, whereas long-chain PFAAs showed higher concentrations in roots. Accordingly, the foliage to root concentration factor highlighted that PFAAs with shorter carbon chain length (C ≤ 7) translocated and accumulated relatively more in leaves compared to roots. Removal efficiency of individual PFAAs for leaves and roots were comparatively higher with S. e*leagnos* and S. *purpurea* than S*. triandra,* with mean removal values at the whole plant level ranging around 10 % of the amount initially spiked, suggesting their potential for phytoremediation of PFASs.

1. Introduction

Perfluoroalkyl and polyfluoroalkyl substances (PFASs), most notably perfluoroalkyl acids (PFAAs) such as perfluorooctane sulfonic acid (PFOS) and perfluorooctanoic acid (PFOA), have been detected at elevated concentrations in surface waters, sediments, groundwater and drinking water near to airports, firefighter training areas and industrial and landfill sites of several countries (Ahrens et al. 2011; Busch et al. 2010; Higgins and Luthy, 2006; Moody and Field, 1999; Castiglioni et al, 2015). Soil can also be contaminated by PFAAs, mainly from the use of contaminated irrigation water and biosolids (Blaine et al. 2014; Sepulvado et al. 2011).

Among PFASs, PFAAs are a unique group of chemicals with a perfluoroalkyl backbone, typically with carbon-chain lengths ranging from 4 to 14 (linear or branched) and with a functional group, commonly carboxylic and sulfonic, but also sulfinic, phosphonic, and phosphinic (Buck et al. 2011). The presence of a hydrophilic moiety and a fluorinated backbone in the same molecule imparts these compounds with unique properties such as water and oil repellency and surfactant properties (Huang et al. 2007). It has been clear that PFAAs behave differently from nonpolar and slightly polar organic micro-pollutants and neither accumulate in fatty substances nor adsorb to organic matter solely due to hydrophobic interactions (Key et al. 1997). Furthermore, the high strength of the carbon-fluorine bond and the large size of the fluorine atom which hides the C-C bonds to microorganisms, give the fluoroalkyl moieties their high thermal, chemical and biochemical stability (Krafft and Riess, 2015; O'Hagan, 2008).

The most widely studied PFAAs are the eight carbon compounds perfluorooctanoic acid (PFOA) and perfluorooctane sulfonic acid (PFOS). These substances have received most attention because of their persistence (Buck et al. 2011; Parson et al. 2008), toxic effects to mammals (Stahl et al. 2011), strong tendency for bioaccumulation (Conder et al. 2008; Haukas et al. 2007) and bio magnification in food chain (Kannan et al. 2005; Kelly et al. 2009;). PFAAs also showed some interaction with blood proteins and are suspected of causing several pathological responses, including cancer (De Witt et al. 2015). For the concerns about the potential environmental and toxicological impact of long-chain PFAAs, PFOS has been added to the persistent organic pollutants (POPs) list of the Stockholm Convention in May 2009 resulting in global restriction of its production (UNEP, 2009), whereas PFOA is expected

to be added shortly to this banned list (Stockholm convention, 2018). In recent years, fluorinated alternatives have come on the market to replace the legacy of long-chain PFAAs in specific applications. However, short-chain PFAAs and other fluorinated alternatives possess high environmental stability and mobility, and some of them are toxic, therefore they are likely to pose global risks to humans and the environment as well (Wang et al. 2015).

The main dietary exposure routes to these substances are considered to be contaminated water, fish and vegetables (D'Holliver et al. 2010; Tittlemier et al. 2007). Twelve different PFAAs were detected in 21 samples of food and beverages (Haug et al. 2010), with the most prominent being PFOS and PFOA.

The existing information suggests that PFAS contaminated irrigation water and soil are a source for their entry into the food chain. Hence, it is important to identify appropriate technologies to remove PFASs from plant growth matrices. Physicochemical techniques are expensive, especially if they are to be applied on a large scale and can produce undesirable by-products and alter soil characteristics. On the other hand, due to the high stability of perfluorinated compounds, the application of microbial degradation is still unfeasible. It has been shown that different plant species are able to accumulate PFAAs (Gobelius et al. 2017; Ghisi et al. 2019 for a review on agricultural plants), thus laying the foundations for the use of bioremediation techniques. Phytoremediation is an eco-friendly technology, which uses plants and associated rhizosphere microorganisms to remove, transform, or detoxify organic and inorganic pollutants in soils, sediments, ground water, surface water and the atmosphere (Dhankher et al. 2012; Susarla et al. 2002; Sandermann, 1994). In the evaluation of plant species to be used in phytoremediation processes, phytotoxicity of pollutants is just as important as plant uptake capacity and understanding plant responses to contaminant stress defines whether a plant has the potential to transform and tolerate toxic chemicals, which would enhance phytoremediation (Carvalho et al. 2014; Medina et al. 2003).

Willow (*Salix spp. L.)* is one of the species commonly studied and used in phytoremediation projects, owing to their high biomass production, high evapotranspiration and a pronounced capability of taking up heavy metals and removing organic pollutants (Marmiroli et al. 2011; Vervaeke et al. 2003). However, to the best of our knowledge, the are no reports on the accumulation and effects of PFAAs on willow plants. In order to evaluate the possibility of using willow plants for the phytoremediation of PFAAs, in the present study,

we investigated the effects of a mixture of 11 PFAAs on biomass accumulation, growth rate and photosynthetic parameters in an eight-day hydroponic experiment. Accumulation and distribution of PFAAs among roots and leaves of willow plants were also assessed. Three willow species, i.e. *Salix eleagnos L., S. purpurea L.* and *S. triandra L.* were considered to examine species-specific effects and differences in accumulation of PFAAs.

2. Material and Methods

2.1 Chemicals

The PFAAs included in the experiment are: perfluorobutanoic acid (PFBA), perfluoro-n-pentanoic acid (PFPeA), perfluoroheptanoic acid (PFHpA), perfluorooctanoic acid (PFOA), perfluorononanoic acid (PFNA), perfluorodecanoic acid (PFDA), perfluoroundecanoic acid (PFUnA), perfluorohexadecanoic acid (PFHxA), Perfluoro dodecanoic acid (PFDoA), perfluorobutane sulfonate (PFBS) and perfluorooctanesulfonate (PFOS) (Sigma Aldrich, St. Louis, MS, USA). Mass labelled $^{13}C_2$-PFDA, $^{13}C_4$-PFBA, $^{13}C_5$-PFPeA, $^{13}C_5$-PFNA,$^{13}C_4$-PFBS, $^{13}C_6$-PFHxA, $^{13}C_7$-PFHpA, $^{13}C_4$-PFOA, $^{13}C_4$-PFOS, $^{13}C_{10}$-PFDoA, and $^{13}C_{11}$-PFUnA (Wellington laboratories, Guelph, ON, Canada) were used at a fixed concentration as internal standards (IS) in mass spectrometry (MS) for identification and quantification of all PFAAs.

2.2 Plant growth and treatment

Cuttings (~30 cm in length) of *S. eleagnos L., S. purpurea L.* and *S. triandra L.* (15 per species) collected from the Plant Biodiversity and Agroforestry Center of Veneto Agricoltura, (Montecchio Precalcino, Vicenza, Italy) were grown in water for three weeks under greenhouse conditions to induce optimal root and shoot growth. After rooting and with leaves, 10 plants per species (5 for controls and 5 for PFAA treatments) were carefully selected for uniformity and transferred for some days to a modified Hoagland nutrient solution (Hoagland 1933) (one plant per 1 L pot) in a growth chamber (12/12 hrs light/dark period, 25/20 °C temperature and 300 µmol photons m^{-2} s^{-1} of photosynthetic active radiation, PAR) to allow them to adapt to the new conditions, before the nutrient solution was changed and spiked or not with PFAAs. Treated plants were exposed to a mixture of eleven PFAAs (PFBA, PFPeA, PFHxA, PFHpA, PFOA, PFNA, PFDoA, PFUnA, PFBS, PFOS), each at 10 µg L^{-1} concentration for 8 days.

2.3 Determination of relative growth rate, dry weight and photosynthetic parameters

Individual plants from control and treated groups were carefully weighed during the experiment for assessing the relative growth rate (RGR). Nutrient solution volumes were also measured. Time point before treatment indicated as '-1' was used as the reference to calculate RGR, 0 was the day of the treatment with PFAAs, whereas 2, 4, 6, and 8 indicate days post treatment (dpt).

RGR % was calculated according to the formula:

$$RGR\ \% = [(ln\ Wt_x - ln\ Wt_{-1}) / t_x - t_{-1}] * 100$$

where Wt_x refers to the plant weight at a specific time point during the experiment and Wt_{-1} refers to the weight on the day before treatment.

For determining the dry weight, roots and leaves from control and treated plants were dried in an oven at 50 °C till constant weight was attained.

Photosynthetic gas exchange parameters and chlorophyll fluorescence measurements were performed on 7 dpt and 8 dpt with Li-6800 (Li-Cor Inc., Lincoln, Nebraska, USA). Measurements were performed thrice on the middle portion of the youngest fully expanded leaf for five plants per treatment using the methods described by Stinziano et al. (2018). Actinic light composition was varied between 100% blue (470 nm) and 100% red (625 nm). The instrument was configured with flow rate 500 $\mu mols^{-1}$, 400 µmol mol^{-1} CO_2, leaf temperature 27°C and 51 % humidity. The negative ϕ PSII values were set to 0 for the measurement of fully saturated reaction centers. Dark respiration rate (Rd) was measured at the end of the light response curve and gross CO_2 assimilation was approximated as [CO_2 assimilation rate (A) + dark respiration rate (Rd)]. All fluorescence measurements were made using the multiphase flash fluorescence protocol (MPF) with a saturating intensity of 8,000 µmol m^{-2} s^{-1} with 1000 ms duration and 100 Hz output rate. Steady-state chlorophyll fluorescence (Fs) was measured at 50 kHz. Maximum chlorophyll fluorescence (Fm') was measured at 250 kHz during the saturating pulse, and fluorescence was detected at >700 nm (Evans et al. 2017). At the end of the experimental period, i.e. on the 8 dpt, leaf and root tissues from control and treated plants were weighed, rapidly frozen in liquid nitrogen and stored at -80 °C until analysis.

Within the software MS Excel XLSTAT (Addinsoft, Paris, France), factorial discriminant analysis (MDA, Multi-group Discriminant Analysis, with Wilks lambda and Pillai trace tests)

(Coley and Lohnes, 1971) and Principal Component Analysis (PCA) were applied after data standardization (by subtracting the mean and dividing by standard deviation). Multivariate data normality was preliminarily verified by the Shapiro test with the public domain software R 2.9.2 (package mvnorm-R; Ihaka and Gentleman, 1996).

2.4 Extraction and determination of PFAAs in leaves and roots by LC-MS/MS

Extraction of PFAAs from the roots and leaves of control and treated plants were carried out using the extraction methodology described by Gobelius et al. (2017), with some minor modifications. Briefly, 0.2 g samples were ground to a fine powder with liquid nitrogen, then 100 mM sodium hydroxide in 80 % methanol with ^{13}C PFAAs (internal standard at 3 µg/L final concentration) was added in 1:5 ratio and mixed thoroughly. Samples were sonicated for 10 min and were incubated with shaking for 60 min, room temperature (RT) and then centrifuged at 2800 x g for 15 min at RT to collect the supernatants. To ensure maximal recovery of PFAAs, the extraction was repeated twice with the resultant pellets using the same extraction solution without the internal standard. To the supernatants, 1M HCl was added (1:10), mixed thoroughly and centrifuged at 2800 x g, 15 min, RT. The resulting supernatants from the three sequential extractions were combined and filtered using 0.22 µM RC and further stored at -20 °C until analysis.

2.5 Instrumental analysis

MS analysis was performed with a high-performance liquid chromatograph (Ultimate 3000 UHPLC, Dionex, Sunnyvale, CA, USA) coupled to an electrospray ionization tandem mass spectrometer (TSQ Quantiva Triple Quadrupole, Thermo Scientific, San Jose, CA, USA). Separation of PFAAs based on their polarity was carried out using a C18 column Luna Omega PS (50 x 2.1, L x ID; particle size: 1.6 µm; pore size: 100 Å, Phenomenex). The mobile phase was 10 mM ammonium formiate aqueous solution (A) and methanol (B). The gradient started at 10% B and was maintained for 2 min, then changed to 100% B in 2 min and maintained for 6 min, then returned to 10% B and equilibrated for 3 min. Flow rate was 0.40 mL/min. The injection volume was 10 µL. The electrospray ionization (ESI) source was set to negative mode. The optimized parameters for mass spectrometric detection were: vaporized and ion transfer tube temperature to 300°C, CID argon pressure was 1.5 mTorr, sheath gas 50 (Arb), auxiliary gas 15 (Arb), and sweep gas 2 (Arb). (Xcalibur 3.0 (Thermo Scientific)

software was used for instrument control, data acquisition and quantification. Data acquisition was performed in single-reaction monitoring (SRM) mode.

2.6 Quality assurance and quality control

During the whole experiment, from sample extraction to LC-MS/MS analysis, the presence of any fluorine containing compounds as external potential contaminants was carefully avoided to prevent artifactual results. The linearity range of each PFAAs was tested with a standard mixture (Wellington laboratories, Guelph, ON, Canada) spiked with isotope-labeled internal standard to evaluate the accuracy, limits of detection and limits of quantification. Also, all the samples were spiked with an isotope-labeled internal standard at a fixed concentration. Quantification of each molecule was carried out using the corresponding calibration curve.

2.7 Foliage to root concentration factor and removal efficiency percentage

Foliage to root concentration factor (FRCF) was calculated by dividing the concentration of PFAAs in foliage by the concentration of PFAAs in roots, both on a fresh weight (FW) basis (Felizeter et al. 2012). Removal efficiency % of PFAAs was calculated as described by Zhang et al. (2019) with the equation below.

$$\text{Removal efficiency \%} = [\text{Mass of PFAAs in plant tissues}/\text{Total mass of PFAAs added initially}] \times 100$$

2.8 Data Analysis

All experiments were conducted with at least 5 biological and 3 technical replicates. All data were analyzed by One-way ANOVA and Tukey's HSD test to assess the significance of treatment effects. Differences at $p<0.05$ were considered as statistically significant. Statistical analysis was performed using R studio. Origin 6.0 was used to construct the graphs.

3 Results and Discussion

PFAAs are one of the most persistent and globally distributed groups of organic pollutants. Following the alarming reports on the detection of PFAAs, especially PFOA and PFOS in several cereals and vegetables (Stahl et al. 2009), research in the recent years was addressed towards bio-accumulation and partitioning of PFAAs in different parts of various vegetable

crops (extensively reviewed by Ghisi et al. 2019). Nonetheless, little information is available on the direct phytotoxicity of a mixture of PFAAs on plants and their effects on *Salix* L. species have not been reported yet. In the present study, the accumulation and effects of 11 PFAAs (each at 10 µg L^{-1} concentration) on three *Salix L.* species were investigated. The experimental set up was based on the considerations that PFAAs exist in the environment predominantly as a mixture, and the chosen concentrations are in the range of what is detected in waters in highly industrialized areas (Ahrens et al. 2011; Valsecchi et al. 2015; Wang et al. 2019).

3.1 Effects of PFAAs on plant growth, shoot and root biomass

Growth analysis indicated that the application of PFAAs had a transient stimulatory effect on *S. eleagnos* at 1 and 2 dpt, with a similar trend in *S. purpurea* and in *S. triandra* at 1 dpt. Consistently after 2 dpt, a decline in growth rate was observed across all the species for both control and treated plants. Significant reduction in growth rate was observed with *S. triandra* at 4 and 8 dpt, suggesting that this species could be comparatively more sensitive to PFAAs and that the effects of these substances can vary depending on the species (Fig. 1).

Some reduction and a decreasing trend was observed with the fresh weight of foliage and roots in response to PFAAs across the three species. Foliage to root ratio suggested that the biomass reduction was more pronounced in the leaves than in the roots in *S. triandra* compared to the other species, which had no significant deviations from the control (Fig. S1 A, B, C). Similarly, in *Arabidopsis thaliana,* the fresh weight of leaves and roots and the root length were significantly reduced with PFOA treatment, although at concentrations i.e. above 10 µmol L^{-1} (equivalent to 4.14 mg L^{-1}) (Yang et al. 2015). Ding et al. (2011) evaluated the phytotoxic effects of seven PFASs on lettuce and green algae (*Pseudokirchneriella subcapitata*) and reported that perfluorobutanoic acid (PFBA) was more toxic to the photosynthetic green algae than to lettuce among the other PFASs. This suggests that PFAAs could vary in their phytotoxicity and have distinctive effects depending on the plant species. Hence, the observed reduction in fresh weight of leaves and roots in our study could be due to specific PFAAs, as evidenced in *A. thaliana* and the green algae or a combinational effect of the PFAAs dependent on the *Salix L.* species.

No significant differences were observed among the dry weights of leaves and roots of control and treated plants in all the three *Salix* species considered here, even if a subtle increase in the dry weight of the roots of *S. eleagnos* and *S. purpurea* treated with PFAAs compared to control was noticed (Table S1). Similarly, Wen et al. (2013) reported no increase in shoot and root dry weight in maize plants treated with 1 mg L^{-1} PFOS or PFOA, but at higher concentrations (10 to 200 mg L^{-1}) a significant reduction in dry weight was observed. Contrastingly, an increase in averaged dry weights of roots and leaves of plants treated with lower concentrations of PFOS (at 0.1 and 1 mg L^{-1}) (Qu et al. 2010) and PFOA (at 0.02 and 0.2 mg kg^{-1}) (Zhou et al. 2016) was reported in wheat seedlings. This suggests that the phytotoxic effects on growth rate, fresh and dry weights depend on the PFAAs to which the plants are exposed, their concentration and the plant species.

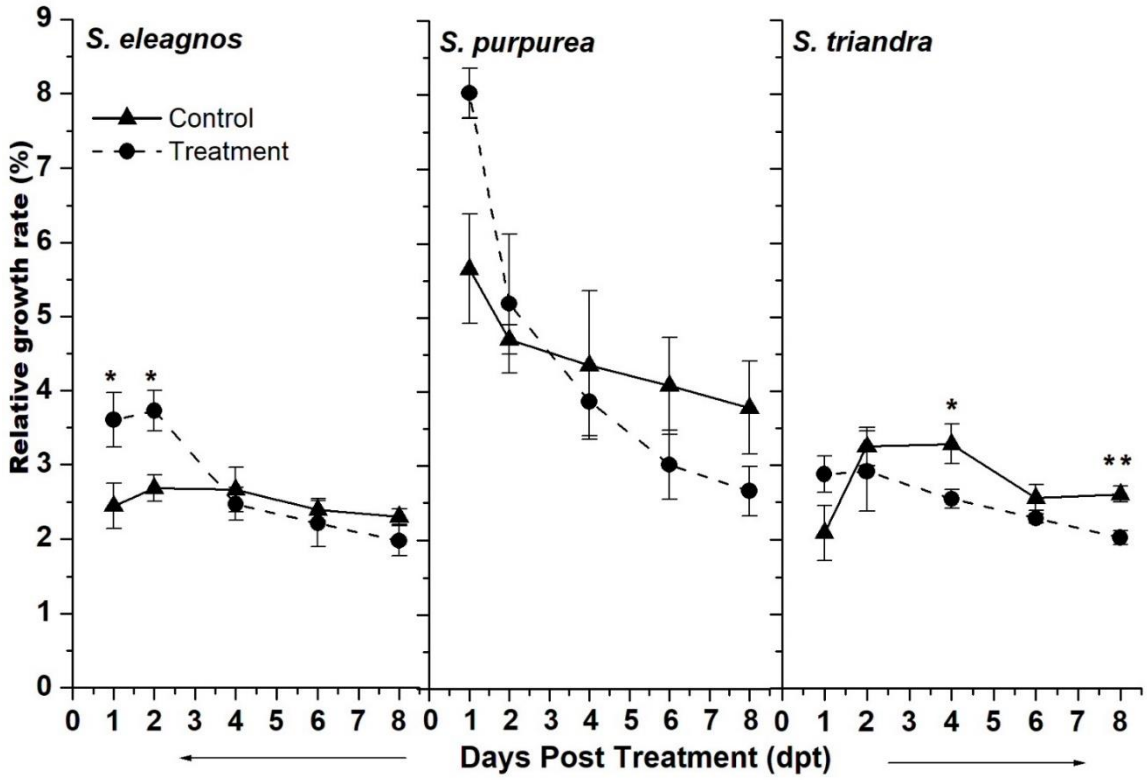

Fig. 3.1. Percentage RGR of the three willow species treated with PFAAs in comparison with control over the course of the experimental duration. RGR was determined with respect to the weight of the plants before treatment. Error bars represent mean standard error (n=5). *, ** indicate *P*<0.05 and 0.01, respectively, as determined with One-way ANOVA.

3.2 Effects of PFAAs on photosynthesis

The influence of PFAAs on photosynthesis has been poorly investigated and is still not fully understood. Examining the effects of PFAAs on photosynthesis in this study, it was evident that the gas exchange parameters were more affected than those related to chlorophyll fluorescence. Significant increase in net CO_2 assimilation rate (*A*) was observed in all the three *Salix spp* treated with PFAAs compared to controls (Fig. 3.2A). While intriguingly, the intercellular CO_2 (*Ci*) was reduced in all species with statistical significance in *S. eleagnos* and *S. purpurea* (Fig. 2B). Conversely, other parameters associated with *A* such as photosynthetic efficiency (*Fv/Fm*), photosynthesis efficiency net of NPQ losses (*Fv'/Fm'*), electron transport rate (*ETR*), molecules of CO_2 fixed per photon ($PhiCO_2$) and non-photochemical quenching (*NPQ*) values did not significantly change in treated plants compared to controls (Fig. S2).

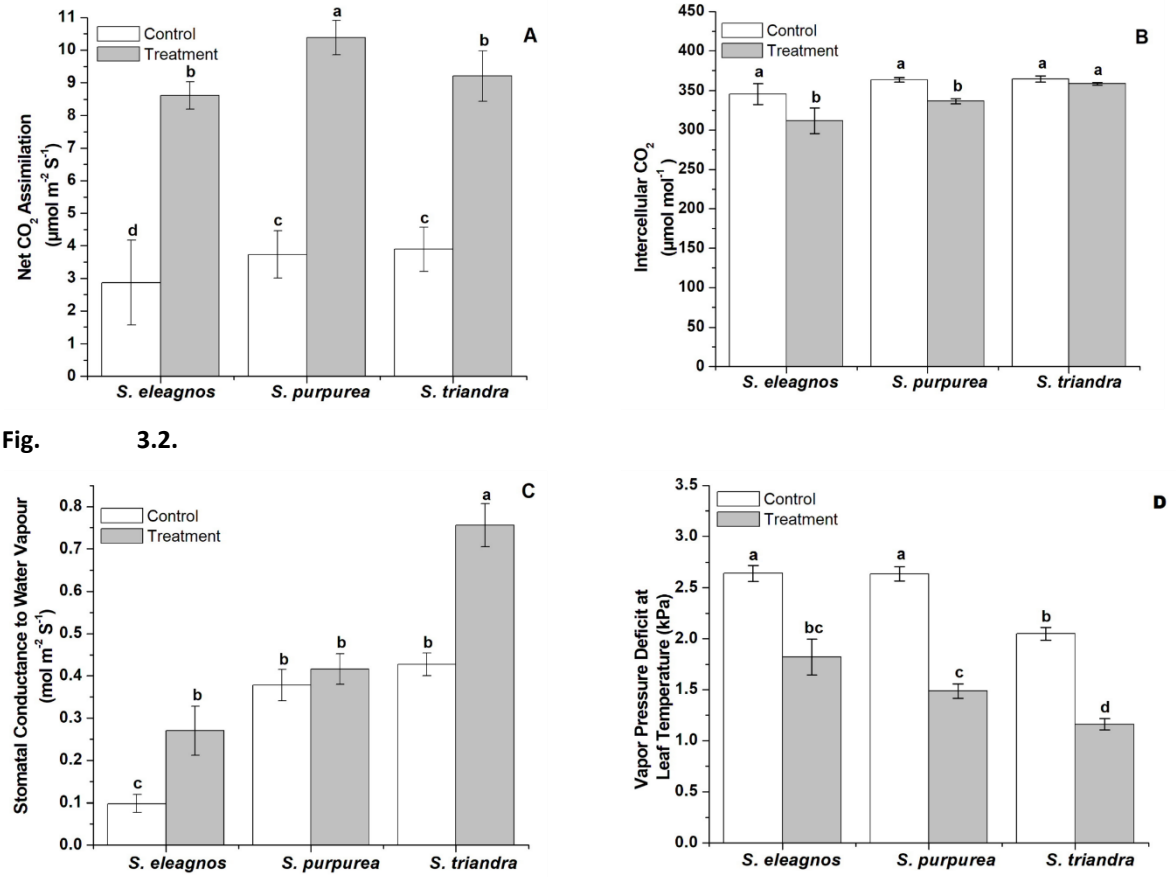

Fig. 3.2.

Differences in the photosynthetic parameters in the three *Salix* L. species at the end of the experimental period. Error bars represent mean standard error (n=5). Different letters indicate significant differences as determined by Tukey's HSD test at $p < 0.05$.

Interestingly, stomatal conductance to water vapor (*gsw*) was increased with significant differences in *S. eleagnos* and *S. triandra* (Fig. 3.2C). In addition, vapor pressure deficit at leaf temperature (*VPD*) values were significantly reduced in all the three treated willow species

(Fig. 3.2D). Contrary to these responses of willow plants to PFAAs, reduced stomatal conductance in plants treated with organic and inorganic pollutants are frequently observed (Iori et al. 2013; Li et al. 2011; Michelini et al. 2015; Pietrini et al. 2010). This seems to indicate that PFAAs interact with plants in a different way compared to other pollutants, probably due to their particular physico-chemical characteristics, and specifically their surfactant properties.

Regarding *Fv/Fm* values, one of the widely accepted photosynthetic parameters to indicate if the plant is under stress, they were not significantly changed in response to PFAAs treatment (Fig. 3.S2) in any willow species at the experimented concentration. This indicates that the photosynthetic machinery of willow plants doesn't seems to be impaired by the exposure of plants to PFAAs in our experimental setup.

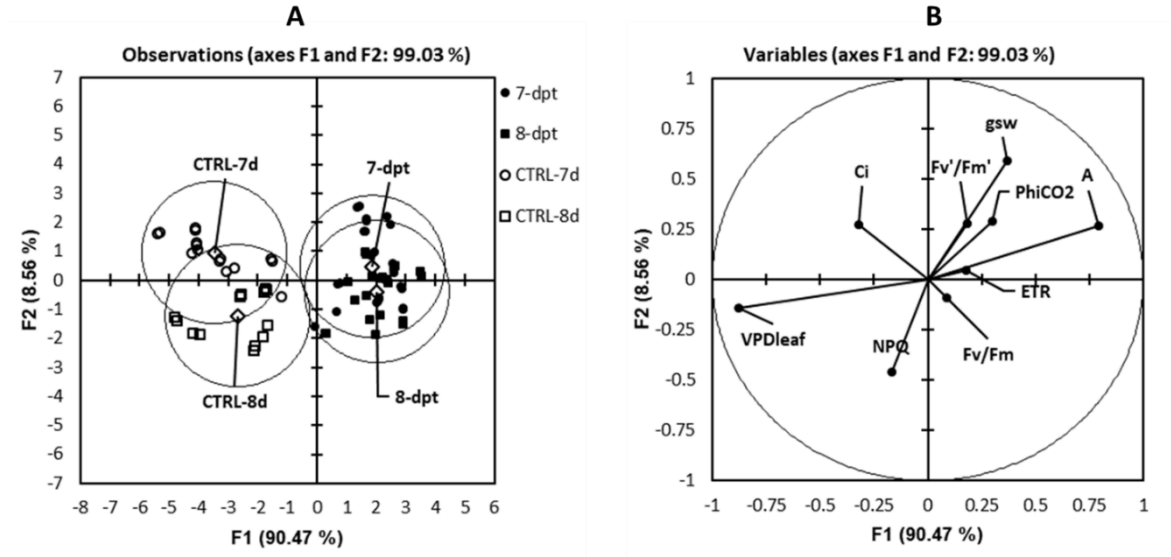

Fig. 3.3. Discriminant analysis (A) and Principal component analysis (B) of the photosynthetic parameters of the three willow species (average of *S. eleagnos*, *S. purpurea*, *S. triandra*) at 7 and 8 dpt with PFAAs. CTRL denotes control.

PCA of the photosynthetic parameters highlighted two synthetic variables, of which major part of variability (90.47 %) was with F1. Variables associated with 7 and 8 dpt with PFAAs segregated into distinct clusters away from their respective controls indicating an overall difference in the measured photosynthetic parameters and there were not major variations among the measured parameters between these time points (7 and 8 dpt) (Fig. 3.3A).

Photosynthetic parameters with high lodging (> 0.35) explaining high fractions of variability were *VPD leaf* and *A,* followed by *gsw* (Table S2). As indicated by the shift towards

the opposite quadrants, as a consequence of PFAA application there was a significant increase in *A* and *gsw* and a decrease in *VPD leaf* values (Fig. 3.3B). Interestingly, a slight increase in the light-dependent photosynthetic reactions (*PhiCO$_2$, Fv/Fm, Fv'/Fm', ETR*) and a decrease in *NPQ* and *Ci* were noticed in response to PFAA treatment. Increased *gsw* (lodging value +0.366 in F1) could be associated with the high lodging values (> 0.75) observed with *VPD leaf* and *A*. Increased conductance - related parameters can lead to increased CO_2 influx (*A*) (Fig. 3.2A) and consequently water loss, as indicated by significantly reduced *VPD leaf* values (Fig. 3.2D).

It was evidenced that several PFAAs are taken up by the root and translocated to the leaves through the transpiration stream. As these compounds have a low volatility and are not degraded, they can remain as residues in the leaves (Blaine et al. 2014; Felizeter et al. 2014). Conceivably, PFAAs may accumulate in the hypo-stomatal cavity where the xylem sap is finally directed to, and also as a consequence of water evaporation and transpiration. While there is no information on this pertaining to plants, the existing hypotheses for the mechanism of bioaccumulation and distribution of PFAAs in mammals, birds and fishes include partitioning to membrane phospholipids and interaction with specific proteins (Ng and Hungerbuehler, 2013, Ng and Hungerbuhler, 2014; Armitage et al. 2012). While being transported through the xylem vessels and accumulating in the hypo-stomatal cavity, it is possible that PFAAs may interact with lignocellulosic constituents, phospholipids and specific proteins. As surfactants~~,~~ the possibility of PFAAs to alter the surface tension of the transpiration stream and thus, the xylem hydraulic conductivity may not be excluded; however, no studies have been carried out to this end.

Considering these inferences, we speculate that PFAAs could alter xylem hydraulic conductivity and accumulate in the hypo-stomatal cavity altering its surface properties, which are strongly implicated in the gas exchange parameters. In a possible scenario which is compatible with our experimental results, lowering the water surface tension would result in an increased water evaporation rate in the hypo-stomatal cavity, which in turn would lower the measurable *VPD*. Conversely, the bundle sheath and mesophyll cells adjacent to the hypo-stomatal cavity would be in a more hydrated state because of the PFAAs accumulation and the water-repelling properties of these pollutants, which we speculate would lead to ABA-mediated stomatal opening. As an effect of increased stomatal

conductance, there would be a greater CO_2 influx into the hypo-stomatal cavity leading to an increase in the measured net CO_2 assimilation rate. It has been shown that PFAAs tend to accumulate and get concentrated in the air-water interface (Felizeter et al. 2012; Reth et al. 2011) and hence, their possible accumulation in the hypo-stomatal cavity (air-water interface in the leaves) could perturb CO_2 permeability, leading to a lower intercellular CO_2 (*Ci*), which can be also due to the higher rate of CO_2 assimilation (*A*) in treated plants. However, additional experiments are required to confirm the localization of PFAAs to further establish the underlying mechanism. It seems clear to us, that the effects of these environmental pollutants on plant growth are likely to involve altered plant-water relation, affecting the stomatal opening and CO_2 assimilation. The increase in measurable CO_2 assimilation rate (*A*) should not be interpreted as a direct stimulatory effect on photosynthesis, and in fact, it is quite paradoxical to the observed reduction in RGR. It could rather be considered as a compensatory mechanism, where part of the carbon fixed with photosynthesis could be used by willow plants in adaptation mechanisms to the presence of PFAAs. For example, the exposure to PFAAs stimulated the antioxidative defense system in *Juncus effusus* shoots (Zhang et al. 2019), whereas PFOS stimulated superoxide dismutase (SOD) activity in *Acorus calamus* and *Phragmites communis* (Qian et al. 2019).

3.3 Differential accumulation of PFASs in leaves and roots

The volume of the nutrient solution over the course of the experiment was monitored to assess if PFASs affect the uptake of the nutrient solution. In all species the nutrient solution volume decreased during the experimental period, with *S. eleagnos* showing the lowest reduction in both control and treated plants. Despite the higher stomatal conductance in treated plants, the residual nutrient solution volume at the end of the experiment was not lower compared to controls, and in treated plants of *S. triandra* the volume was even significantly greater at 2, 4 and 8 dpt (Fig. 3.4).

Therefore, it is likely that PFAAs altered the plant-water relations and, alternately, it can be hypothesized that PFAAs can limit the root permeability to water influx or alter the hydrophilicity of conductive elements from roots to stomata, thus limiting the uptake of nutrient solution, which could have contributed to the significant reduction in RGR and leaf biomass in *S. triandra* (Fig. 1 and S1A). There is also reported evidence of root exudates altering the physical and chemical properties of rhizosphere, mediating chelation, complexation and deposition of pollutants (Kuang et al. 2003; Pilon-Smits 2005), which may alter plant water uptake and evaporation too.

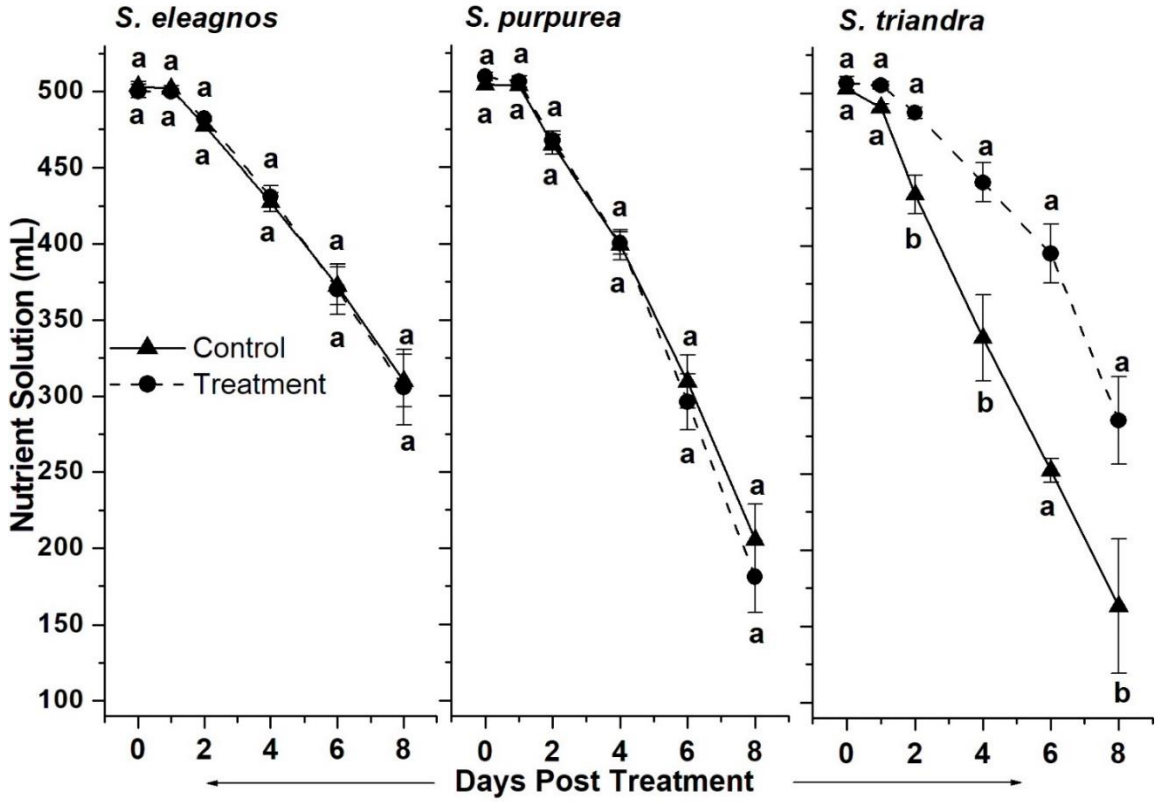

Fig. 3.4. Changes in the nutrient solution volumes during the experimental period for the three willow species. Error bars represent standard error of the mean (n=5). Different letters indicate significant differences as determined by Tukey's HSD test at $p < 0.05$.

There has been mounting evidence that PFAAs tend to translocate and accumulate in various plant tissues, according to their chain length and functional group (Ghisi et al. 2019 for a review). In this study a decreasing trend in the concentration of PFAAs dependent on the increasing carbon-chain length was observed in the leaves of all the three willow species (Fig. 3.5A). Regarding perfluorinated sulfonic acids (PFSAs), they were accumulated to a lower extent than perfluorinated carboxylic acids (PFCAs) with equal number of carbon atoms. Among the willow species, significantly higher concentrations of PFBA, PFOA, PFNA, PFDA &

PFOS were observed in *S. eleagnos* leaves (Fig. 3.5A). Irrespective of the type of PFASs, lowest concentrations were always detected in *S. triandra* compared to the other willow species.

With respect to the roots, PFCAs with higher carbon chain length, i.e. PFDoA followed by PFNA and PFDA were detected at higher concentrations, with PFUnA as an exception (Fig. 3.5B). Regarding PFSAs an opposite trend was observed in respect to the leaves, with high concentration of PFOS and low concentrations of PFBS being detected in the roots of all the willow species.

The foliage to root concentration factors (FRCF) suggests that PFBA, PFPeA, PFHxA, PFHpA and PFBS translocated and accumulated relatively more in the leaves than in the roots, as they showed FRCF values higher than 1. PFCAs accumulated more in leaves of all the three willow species compared to PFSAs (Fig. 3.5C).

Consistent with our findings, highest concentration of PFBA followed by PFPeA was observed in lettuce leaves, and FRCFs exponentially decreased with increasing chain length of PFCAs and PFSAs (Felizeter et al. 2012). Similarly, the leaf concentration factor of cabbage, zucchini and tomato indicated that all PFCAs, except for the long chain ones (C >10) were translocated and accumulated more in the leaves of these species (Felizeter et al. 2014). Higher root concentration factors (RCF) (by a factor of 2 to 3) were observed with all PFSAs than the PFCAs with the same number of fluorinated carbon atoms and hence, the authors suggested the uptake of PFASs is also governed by the functional group in addition to the carbon chain length.

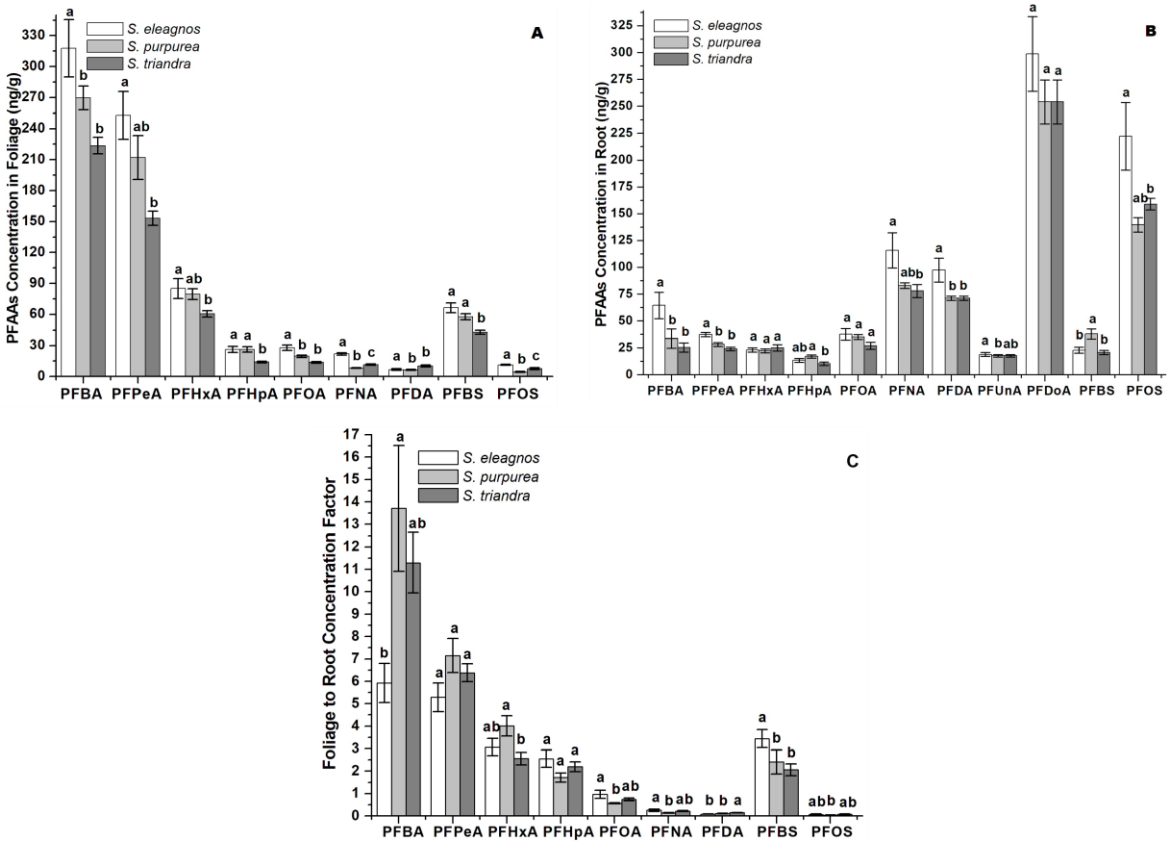

Fig. 3.5. Concentration of PFAAs in foliage (A) and roots (B) and foliage to root concentration factor (FRCF) (C) of three willow species, on FW basis. Error bars represent standard error of the mean (n=5). Different letters indicate significant differences within the three willow species, as determined by Tukey's HSD test at $p < 0.05$.

Krippner et al. (2014) also stated that the uptake rate of PFCAs and PFSAs were dependent on the carbon chain length in hydroponically grown maize plants reporting that a shoot to root ratio > 2 was observed with PFBA, PFBS, PFPeA, PFHxA and PFHpA, whereas PFOA, PFNA, PFDA, PFHxS and PFOS were retained more in the roots (shoot to ratio < 1). In agreement with our results, longer-chain PFASs were more retained in the maize roots and the shoot to root concentration ratio decreased with increasing chain lengths of PFASs. Garcia-Valcarcel et al. (2014) investigated the uptake of some PFCAs (PFBA, PFOA, PFDA) and PFSAs (PFBS, PFHxS, PFOS) in *Bromus diandrus* grown in nutrient solution reporting that the uptake and concentration of PFAAs decreased with an increase in the carbon chain length. Zhao et al. (2016) assessed the uptake of PFCAs (i.e., PFBA, PFHpA, PFOA, PFDoA) in hydroponically grown wheat plants subjected to different salinities and temperatures. Considering the dataset of the plants grown with PFCAs and not subjected to salinity and temperature, the observations coincide with our results and interestingly, PFDoA was retained in wheat roots as observed with willow in this study (Fig. 3.5B). In a recent study,

Zhao et al. (2017) have reported the comparative uptake of PFCAs by wheat plantlets grown in nutrient solution and concluded that with increasing carbon chain length, the RCF increased while the shoot to root concentration factor (SRCF) decreased. It is interesting that there is similarity in the uptake and accumulation trend of PFASs, irrespective of the plant species. The existing hypotheses for the chain-length and functional group-dependent uptake and translocation of PFASs include (i) a decrease in their ability to cross the Casparian strip and an increase in their sorption to root components with increasing carbon chain length; (ii) higher sorption of perfluorinated surfactant sulfonates than their carboxylic analogues to root surface tissue (Felizeter et al. 2012; 2014).

Significantly higher values of removal efficiency % were observed for *S. eleagnos* and *S. purpurea* leaves compared to *S. triandra* for PFCAs - PFBA, PFPeA, PFHxA, PFHpA and PFOA, and only for PFBS among the PFSAs (Fig. 3.6A). Significantly higher values were noticed with *S. eleagnos* leaves compared to *S. purpurea* for PFNA and PFOS. Removal efficiency % associated with roots indicated a similar trend only for PFBA, PFPeA, PFOA and PFNA, wherein significantly higher values were observed with *S. eleagnos* and *S. purpurea* compared to *S. triandra.* Interestingly, higher values were observed for PFHxA, PFHpA and PFBS with *S. purpurea* roots compared to the other willow species (Fig. 3.6B).

The removal efficiency of total PFASs by the whole plant ranged from 6 to 11 % and there were no significant differences noticed between the willow species; however, *S. purpurea* followed by *S. eleagnos* had higher removal efficiency compared to *S. triandra* (Fig. 6C). Zhang et al. (2019) assessed the removal efficiency of hydroponically grown *Juncus effusus* plants treated with PFPA, PFBS, PFHxA, PFHpA, PFHxS, PFOA and PFOS (spiked at different concentrations) over a period of 21 days and concluded that the concentration of PFASs in the growth medium and the exposure time are the major factors affecting removal efficiency. Albeit the concentration of PFASs spiked in our study was much lower, we inferred that the removal efficiency of total PFASs by *S. eleagnos* (9 %) and *S. purpurea* (11 %) were higher compared to *J. effusus* plants (6 %) grown for 7 days at the concentration denoted as 1X concentration (Total PFAS concentration: 4635 μg L^{-1}). This suggests that willow plants could possess higher removal efficiency under hydroponic experimental conditions and hence, could be a potential candidate for phytoremediation of PFAS-contaminated sites;

however, systematic studies are required to assess their efficiency to uptake and accumulate PFASs from contaminated soil.

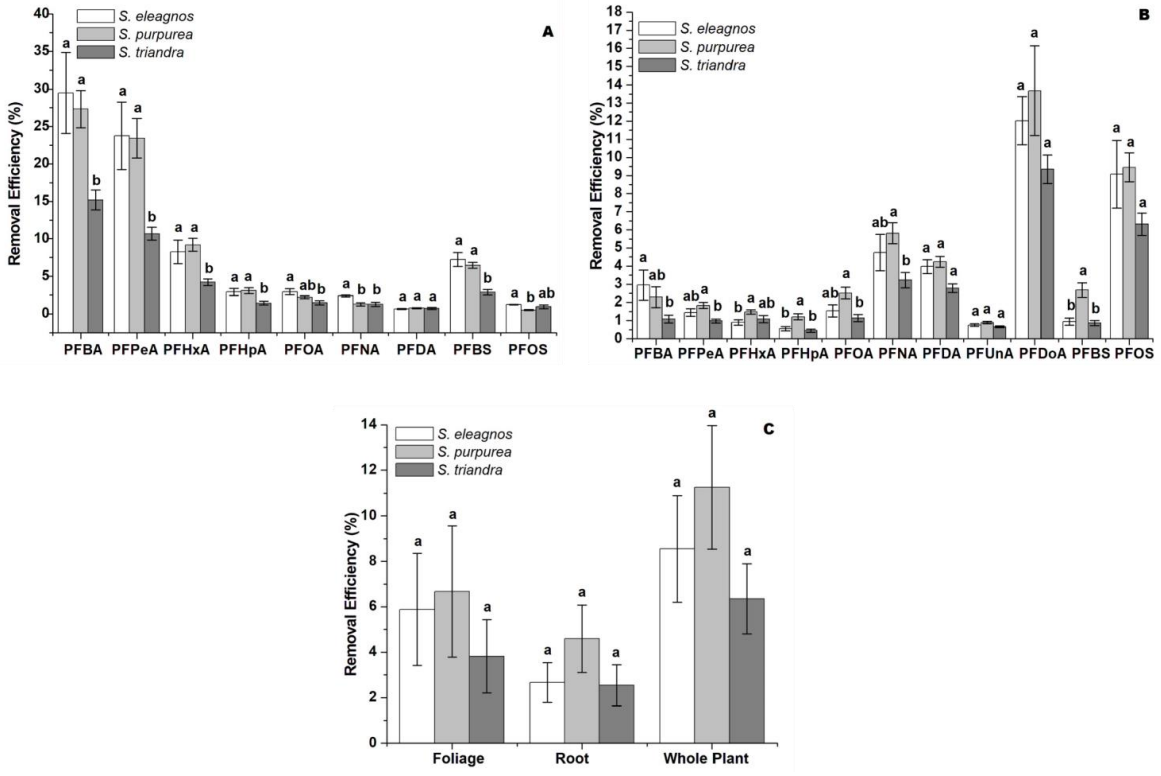

Fig. 3.6. Removal efficiency % of individual PFAAs - Foliage (A) & Root (B) and of total PFAAs (C). Error bars represent standard error of the mean. Different letters indicate significant differences within the three willow species as determined by Tukey's HSD test at $p < 0.05$.

Concluding remarks

As PFASs predominantly exist as a mixture, our study gains significance as it addresses their combined effects on plant growth at an environmentally relevant concentration. Results from our study suggest that PFAAs in combination had a species-specific effect on the growth of the three willow species. Interesting effects of PFAAs on the photosynthesis were observed but the perspectives discussed require further research to thoroughly understand them. The general trend in uptake and accumulation of PFAAs depending on the carbon chain length and the functional group also evidenced in our study could be interesting for future development of uptake/phytoremediation models. Considering that PFAAs in the nutrient solution are taken up by roots and then distributed in the plant through the transpiration stream, it would be interesting to examine their effects on plant-water relations, which could have a larger impact when plants are grown on soil. While our hydroponic-based study provided novel insights and indicated the potential of willow plants

to uptake and accumulate PFAAs, their applicability under field condition needs to be assessed. However, taking into consideration the great ability of willow to adapt to wetland conditions, this would have promising implications for future phytoremediation projects targeting PFASs.

Declarations of interest: None

Acknowledgements

This project was supported by the University of Padova BIRD165880/16 funding. Nisha Sharma was supported by a CARIPARO fellowship for graduate foreign students. Inisa Shrestha was supported by an Erasmus+ KA107 fellowship. Leonard Barnabas Ebinezer was supported by the postdoctoral grant by the University of Padova. The authors also wish to thank the University of Padova for supporting the acquisition of the TSQ Quantiva mass spectrometer by 2015/CPDB15489 funding.

References

Ahrens, L. 2011. Polyfluoroalkyl compounds in the aquatic environment: a review of their occurrence and fate. *Journal Environment Monitoring*. 13, 20–31. http://doi.org/10.1039/C0EM00373E.

Armitage, J. M., Arnot, J. A., & Wania, F. 2012. Potential role of phospholipids in determining the internal tissue distribution of perfluoroalkyl acids in biota. https://doi.org/10.1021/es304430r.

Blaine, A. C., Rich, C. D., Sedlacko, E. M., Hyland, K. C., Stushnoff, C., Dickenson, E. R., & Higgins, C. P. 2014. Perfluoroalkyl acid uptake in lettuce (*Lactuca sativa*) and strawberry (*Fragaria ananassa*) irrigated with reclaimed water. *Environmental science & technology.* 48(24), 14361-143. https://doi.org/10.1021/es504150h.

Buck, R. C., Franklin, J., Berger, U., Conder, J. M., Cousins, I. T., De Voogt, P., & van Leeuwen, S. P. 2011. Perfluoroalkyl and polyfluoroalkyl substances in the environment: terminology, classification, and origins. *Integrated environmental assessment and management*. 7(4), 513-541. https://doi.org/10.1002/ieam.258.

Busch, J., Ahrens, L., Sturm, R., & Ebinghaus, R. 2010. Polyfluoroalkyl compounds in landfill leachates. *Environmental Pollution.* 158(5), 1467-1471. https://doi.org/10.1016/j.envpol.2009.12.03.

Carvalho, P. N., Basto, M. C. P., Almeida, C. M. R., & Brix, H. 2014. A review of plant–pharmaceutical interactions: from uptake and effects in crop plants to phytoremediation in constructed wetlands. *Environmental Science and Pollution Research*. 21(20), 11729-11763. https://doi.org/10.1007/-s11356-014-2550-3.

Castiglioni, S., Valsecchi, S., Polesello, S., Rusconi, M., Melis, M., Palmiotto, M., Manenti, A., Davoli, E., & Zuccato, E. 2015. Sources and fate of perfluorinated compounds in the aqueous environment and in drinking water of a highly urbanized and industrialized area in Italy. *Journal of hazardous materials*. 282, 51-60. https://doi.org/10.1016/j.jhazmat.2014.06.007.

Coley, W.W., & Lohnes, P.R. 1971. Multivariate Data Analysis Wiley, New York.

Conder, J. M., Hoke, R. A., Wolf, W. D., Russell, M. H., & Buck, R. C. 2008. Are PFCAs bio-accumulative? A critical review and comparison with regulatory criteria and persistent lipophilic compounds. *Environmental science & technology*. 42, 995-1003. https://doi.org/10.1021/es070895g.

D'Hollander, W., de Voogt, P., De Coen, W., & Bervoets, L. 2010. Perfluorinated substances in human food and other sources of human exposure. *In Reviews of Environmental Contamination and Toxicology.* 208, 179-215. https://doi.org/10.1007/978-1-4419-6880-7_4.

DeWitt, J. C. (Ed.). 2015. Toxicological effects of perfluoroalkyl and polyfluoroalkyl substances, Springer International Publishing, Switzerland. https://doi.org/10.1007/978-3-319-15518-0.

Dhankher, O. P., Pilon-Smits, E. A., Meagher, R. B., & Doty, S. 2012. Biotechnological approaches for phytoremediation. *In Plant biotechnology and agriculture*. 309-328. https://doi.org/10.1016/B978-0-12-381466-1.00020-1.

Ding, G., Wouterse, M., Baerselman, R., & Peijnenburg, W. J. 2001. Toxicity of polyfluorinated and perfluorinated compounds to lettuce (*Lactuca sativa*) and green algae (*Pseudokirchneriella subcapitata*). *Archives of environmental contamination and toxicology*. 62(1), 49-55. https://doi.org/10.1007/s00244-011-9684-9.

Evans, John R., Patrick B. Morgan, & Susanne von Caemmerer. 2017. Light quality affects chloroplast electron transport rates estimated from Chl fluorescence measurements. *Plant and Cell Physiology*. 58(10), 1652-1660. https://doi.org/10.1093/pcp/pcx103.

Felizeter, S., McLachlan, M. S., & De Voogt, P. 2012. Uptake of perfluorinated alkyl acids by hydroponically grown lettuce (*Lactuca sativa*). *Environmental science & technology*. 46(21), 11735-11743. https://doi.org/10.1021/es302398u.

Felizeter, S., McLachlan, M. S., & De Voogt, P. 2014. Root uptake and translocation of perfluorinated alkyl acids by three hydroponically grown crops. *Journal of agricultural and food chemistry*. 62(15), 3334-3342. https://doi.org/10.1021/jf500674j.

Garcia-Valcarcel, A. I., Molero, E., Escorial, M. C., Chueca, M. C., & Tadeo, J. L. 2014. Uptake of perfluorinated compounds by plants grown in nutrient solution. *Science of the Total Environment.* 472, 20-26. https://doi.org/10.1016/j.scitotenv.2013.10.054.

Ghisi, R., Vamerali, T., & Manzetti, S. 2018. Accumulation of perfluorinated alkyl substances (PFAS) in agricultural plants: A review. *Environmental research*. https://doi.org/10.1016/j.envres.2018.10.023.

Gobelius, L., Lewis, J., & Ahrens, L. 2017. Plant uptake of per-and polyfluoroalkyl substances at a contaminated fire training facility to evaluate the phytoremediation potential of various plant species. *Environmental science & technology*. 51(21), 12602-12610. https://doi.org/10.1021/acs.est.7b02926.

Haug, L. S., Salihovic, S., Jogsten, I. E., Thomsen, C., van Bavel, B., Lindström, G., & Becher, G. 2010. Levels in food and beverages and daily intake of perfluorinated compounds in Norway. *Chemosphere*. 80(10), 1137-1143. https://doi:10.1016/j.chemosphere.2010.06.023.

Haukås, M., Berger, U., Hop, H., Gulliksen, B., & Gabrielsen, G. W. 2007. Bioaccumulation of per-and polyfluorinated alkyl substances (PFAS) in selected species from the Barents Sea food web. *Environmental Pollution*. 148(1), 360-371. https://doi.org/10.1016/j.envpol.2006.09.021.

Higgins, C. P., & Luthy, R. G. 2006. Sorption of perfluorinated surfactants on sediments. *Environmental science & technology.* 40(23), 7251-7256. https://doi.org/10.1021/es061000n.

Hoagland, D. R. 1933. Nutrition of strawberry plant under controlled conditions. (a) Effects of deficiencies of boron and certain other elements, (b) susceptibility to injury from sodium salts. In Proc. *American Society of Horticulutre Science*. 30, 288-294. https://doi.org/10.1016/j.chemosphere.2019.05.258.

Huang, J. Q., Meng, W. D., & Qing, F. L. 2007. Synthesis and repellent properties of vinylidene fluoride-containing polyacrylates. *Journal of Fluorine Chemistry*. 128(12), 1469-1477. https://doi.org/10.1016/j.jfluchem.2007.08.005.

Ihaka, R., & Gentleman, R. 1996. R: a language for data analysis and graphics. *Journal of computational and graphical statistics.* 5(3), 299-314. https://doi.org/10.1080/10618600.1996.10474713.

Iori, V., Zacchini, M., & Pietrini, F. 2013. Growth, physiological response and phytoremoval capability of two willow clones exposed to ibuprofen under hydroponic culture. *Journal of hazardous materials.* 262, 796-804. https://doi.org/10.1016/j.jhazmat.2013.09.017.

Kannan, K., Tao, L., Sinclair, E., Pastva, S. D., Jude, D. J., & Giesy, J. P. 2005. Perfluorinated compounds in aquatic organisms at various trophic levels in a Great Lakes food chain. *Archives of Environmental Contamination and Toxicology.* 48, 559–566. https://doi.org/10.1007/s00244-004-0133-x.

Kelly, B. C., Ikonomou, M. G., Blair, J. D., Surridge, B., Hoover, D., Grace, R., & Gobas, F. A. 2009. Perfluoroalkyl contaminants in an Arctic marine food web: trophic magnification and wildlife exposure. *Environmental science & technology*. 43(11), 4037-4043. https://doi.org/10.1021/es9003894.

Key, Blake D., Robert D. Howell, & Craig S. Criddle. 1997. Fluorinated organics in the biosphere. *Environmental Science & Technology*. 31(9), 2445-2454. https://doi.org/10.1021/es961007c.

Krafft, M.P., & Riess, J.G. 2015. Selected physicochemical aspects of poly-and perfluoroalkylated substances relevant to performance, environment and sustainability Part one. *Chemosphere*. 129, 4–19. https://doi.org/10.1016/j.chemosphere.2014.08.039.

Krippner, J., Brunn, H., Falk, S., Georgii, S., Schubert, S., & Stahl, T. 2014. Effects of chain length and pH on the uptake and distribution of perfluoroalkyl substances in maize (*Zea mays*). *Chemosphere*. 94, 85-90. https://doi.org/10.1016/j.chemosphere.2013.09.018.

Kuang, Y., Wen, D., Zhong, C., & Zhou, G. 2003. Root exudates and their roles in phytoremediation. *Acta Phytoecological Sinica*. 27(5), 709-717.

Li, Z. J., Xie, X. Y., Zhang, S. Q., & Liang, Y. C. 2011. Negative effects of oxytetracycline on wheat (*Triticum aestivum* L.) growth, root activity, photosynthesis, and chlorophyll contents. *Agricultural Sciences in China.* 10(10), 1545-1553. https://doi.org/10.1016/S1671-2927(11)60150-8.

Marmiroli, M., Pietrini, F., Maestri, E., Zacchini, M., Marmiroli, N., & Massacci, A. 2011. Growth, physiological and molecular traits in *Salicaceae* trees investigated for phytoremediation of heavy metals and organics. *Tree Physiology*. 31(12), 1319-1334. https://doi.org/10.1093/treephys/tpr090.

Medina, V. F., Maestri, E., Marmiroli, M., Dietz, A. C., & McCutcheon, S. C. 2003. Plant tolerances to contaminants. In: McCutcheon S.C. and Schnoor J.L. (Eds) *Phytoremediation: transformation and control of contaminants.* 189-232.

Michelini, L., Meggio, F., Reichel, R., Thiele-Bruhn, S., Pitacco, A., Scattolin, L., Montecchio L., Alberghini S., Squartini S. & Ghisi, R. 2015. Sulfadiazine uptake and effects in common hazel (*Corylus avellana* L.). *Environmental Science and Pollution Research*. 22(17), 13362-13371. https://doi.org/10.1007/s11356-015-4560-1.

Moody, C. A., & Field, J. A. 1999. Determination of perfluorocarboxylates in groundwater impacted by fire-fighting activity. *Environmental science & technology.* 33(16), 2800-2806. https://doi.org/10.1021/es981355.

Ng, C. A., & Hungerbühler, K. 2013. Bioconcentration of perfluorinated alkyl acids: how important is specific binding? *Environmental science & technology*. 47(13), 7214-7223. https://doi.org/10.1021/es400981a.

Ng, C. A., & Hungerbühler, K. 2014. Bioaccumulation of perfluorinated alkyl acids: observations and models. *Environmental science & technology*. 48(9), 4637-4648. https://doi.org/10.1021/es404008g.

O'Hagan, D. 2008. Understanding organofluorine chemistry. An introduction to the C–F bond. *Chemical Society Review*. 37, 308–319. https://doi.org/10.1039/B711844A.

Parsons, J. R., Sáez, M., Dolfing, J., & De Voogt, P. 2008. Biodegradation of perfluorinated compounds. *In Reviews of Environmental Contamination and Toxicology.* 196, 53-71. Springer, New York, NY. https://doi.org/10.1007/978-0-387-78444-1_2.

Pietrini, F., Zacchini, M., Iori, V., Pietrosanti, L., Bianconi, D., & Massacci, A. 2010. Screening of poplar clones for cadmium phytoremediation using photosynthesis, biomass and cadmium content analyses. *International Journal of Phytoremediation.* 12, 105–120. https://doi.org/10.1080/15226510902767163.

Pilon-Smits, E. (2005). Phytoremediation. *Annu. Rev. Plant Biol*., 56, 15-39. https://doi.org/10.1146/-annurev.arplant.56.032604.144214.

Qian, J., Lu, B., Chen, H., Wang, P., Wang, C., Li, K., Tian, X., Jine, W., He, X., & Chen, H. 2019. Phytotoxicity and oxidative stress of per fluorooctanesulfonate to two riparian plants: *Acorus calamus* and *Phragmites communis. Ecotoxicology and environmental safety*. *180*, 215-226. https://doi.org/10.1016/j.ecoenv.2019.04.078.

Qu, B., Zhao, H., & Zhou, J. 2010. Toxic effects of perfluorooctane sulfonate (PFOS) on wheat (*Triticum aestivum* L.) plant. *Chemosphere.* 79(5), 555-560. https://doi.org/10.1016/j.chemosphere.2010.02.012.

Reth, M., Berger, U., Broman, D., Cousins, I. T., Nilsson, E. D., & McLachlan, M. S. 2011. Water to air transfer of perfluorinated carboxylates and sulfonates in a sea spray simulator. *Environmental. Chemistry.* 8(4), 381-388. https://doi.org/10.1071/EN11007_AC.

Sandermann, J. H. 1994. Higher plant metabolism of xenobiotics: the'green liver'concept. *Pharmacogenetics.* 4(5), 225-241.

Sepulvado, J. G., Blaine, A. C., Hundal, L. S., & Higgins, C. P. 2011. Occurrence and fate of perfluorochemicals in soil following the land application of municipal biosolids. *Environmental Science & Technology.* 45(19), 8106-8112. https://doi.org/10.1021/es103903d.

Stahl, T., Heyn, J., Thiele, H., Hüther, J., Failing, K., Georgii, S., & Brunn, H. 2009. Carryover of perfluorooctanoic acid (PFOA) and perfluorooctane sulfonate (PFOS) from soil to plants. *Archives of environmental contamination and toxicology*. 57(2), 289-298. https://doi.org/10.1007/s00244-008-9272-9.

Stahl, T., Mattern, D., & Brunn, H. 2011. Toxicology of perfluorinated compounds. *Environmental Sciences Europe*. 23(1), 38. https://doi.org/10.1186/2190-4715-23-38.

Stinziano, J. R., Morgan, P. B., Lynch, D. J., Saathoff, A. J., McDermitt, D. K., & Hanson, D. T. 2017. The rapid A–Ci response: photosynthesis in the phenomic era. *Plant, cell & environment.* 40(8), 1256-1262. https://doi.org/10.1111/pce.12911.

Stockholm Convention. 2018. Fourteenth meeting of the Persistent Organic Pollutants Review Committee (POPRC.14). http://chm.pops.int/TheConvention/POPsReviewCommittee/Meetings/POPRC14/Overview/tabid/7398/Default.aspx.

Susarla, S., Medina, V. F., & McCutcheon, S. C. 2002. Phytoremediation: an ecological solution to organic chemical contamination. *Ecological Engineering*. 18(5), 647-658. https://doi.org/10.1016/S0925-8574(02)00026-5.

Tittlemier, S. A., Pepper, K., Seymour, C., Moisey, J., Bronson, R., Cao, X. L., & Dabeka, R. W. 2007. Dietary exposure of Canadians to perfluorinated carboxylates and perfluorooctane sulfonate via consumption of meat, fish, fast foods, and food items prepared in their packaging. *Journal of agricultural and food chemistry*. 55(8), 3203-3210. https://doi.org/10.1021/jf0634045.

United Nations Environment Programme. 2009. *The Environment in the News.* from http://www.unep.org/cpi/briefs/(12/01/2010).

Valsecchi, S., Rusconi, M., Mazzoni, M., Viviano, G., Pagnotta, R., Zaghi, C.,Serrini, G. & Polesello, S. 2015. Occurrence and sources of perfluoroalkyl acids in Italian river basins. *Chemosphere*. 129, 126-134. https://doi.org/10.1016/j.chemosphere.2014.07.044.

Vervaeke, P., Luyssaert, S., Mertens, J., Meers, E., Tack, F. M. G., & Lust, N. 2003. Phytoremediation prospects of willow stands on contaminated sediment: a field trial. *Environmental pollution.* 126(2), 275-282. https://doi.org/10.1016/S0269-7491(03)00189-1.

Wang, Q., Tsui, M. M., Ruan, Y., Lin, H., Zhao, Z., Ku, J. P., Sun, H. & Lam, P. K. 2019. Occurrence and distribution of per-and polyfluoroalkyl substances (PFASs) in the seawater and sediment of the South China sea coastal region. *Chemosphere.* 231, 468-477. https://doi.org/10.1016/j.chemosphere.2019.05.162.

Wang, Z., Cousins, I. T., Scheringer, M., & Hungerbuehler, K. 2015. Hazard assessment of fluorinated alternatives to long-chain perfluoroalkyl acids (PFAAs) and their precursors: status quo, ongoing challenges and possible solutions. *Environment international.* 75, 172-179. https://doi.org/10.1016/j.envint.2014.11.013.

Wen, B., Li, L., Liu, Y., Zhang, H., Hu, X., Shan, X. Q., & Zhang, S. 2013. Mechanistic studies of perfluorooctane sulfonate, perfluorooctanoic acid uptake by maize (*Zea mays* L. cv. TY2). *Plant and soil*. 370(1-2), 345-354. https://doi.org/10.1007/s11104-013-1637-9.

Yang, X., Ye, C., Liu, Y., & Zhao, F. J. 2015. Accumulation and phytotoxicity of perfluorooctanoic acid in the model plant species Arabidopsis thaliana. *Environmental pollution*. 206, 560-566. https://doi.org/10.1016/j.envpol.2015.07.050.

Zhang, W., Zhang, D., Zagorevski, D. V., & Liang, Y. 2019. Exposure of *Juncus effusus* to seven perfluoroalkyl acids: Uptake, accumulation and phytotoxicity. *Chemosphere*. https://doi.org/10.1016/j.chemosphere.2019.05.258.

Zhao, H., Qu, B., Guan, Y., Jiang, J., & Chen, X. 2016. Influence of salinity and temperature on uptake of perfluorinated carboxylic acids (PFCAs) by hydroponically grown wheat (*Triticum aestivum* L.). *Springer Plus*. 5(1), 541. https://doi.org/10.1186/s40064-016-2016-9.

Zhao, S., Fan, Z., Sun, L., Zhou, T., Xing, Y., & Liu, L. 2017. Interaction effects on uptake and toxicity of perfluoroalkyl substances and cadmium in wheat (*Triticum aestivum* L.) and rapeseed (*Brassica campestris* L.) from co-contaminated soil. *Ecotoxicology and environmental safety*. 137, 194-201.https://doi.org/10.1016/j.ecoenv.2016.12.007.

Zhou, L., Xia, M., Wang, L., & Mao, H. 2016. Toxic effect of perfluorooctanoic acid (PFOA) on germination and seedling growth of wheat (*Triticum aestivum* L.). *Chemosphere*. 159, 420-425. https://doi.org/10.1016/j.chemosphere.2016.06.045.

CHAPTER 4

PFAAs IN CROP PLANT: MAIZE (ZEA MAYS)

4.1 Publication IV

Accumulation, Physiological and morphological alterations induced by PFAAs in Maize (*Zea mays*) plants

Nisha Sharma, Sara De Vecchi, Leonard Barnabas Ebinezer, Anna Rita Trentin, Teofilo Vamerali, Antonio Masi, Rossella Ghisi

This manuscript is under review for the submission.

Accumulation, Physiological and morphological alterations induced by PFAAs in Maize (*Zea mays*) plants

Nisha Sharma[1], Sara De Vecchi[1], Giuseppe Barion [1],Leonard Barnabas Ebinezer[1], Anna Rita Trentin[1], Teofilo Vamerali[1], Rossella Ghisi[1,] Antonio Masi[1]

[1]Department of Agronomy, Food, Natural resources, Animals and Environment (DAFNAE), University of Padova, Italy.

Keywords: *Zea mays*, Seed germination, Perfluoroalkyl Substances (PFAAs), hydroponic, Photosynthesis, root growth, carbon chain

Highlight

- Seed germination was inhibited due to mixture of PFAAs in the dose dependent manner.
- Mixture of PFAAs affected the root growth and biomass of the maize seedlings
- The depletion trend of each PFAAs in the nutrient solution was acting differently.

Abbreviation: PFAAs, Polyfluoroalkyl substances; FW, Fresh Weight; DW, Dry Weight; RGR, Relative Growth Rate; Dpt, Days Post Treatment; PS II, PhotoSystem 2; PFASs, per- and polyfluoroalkyl substances; PFDoA, Tricosafluorododecanoic acid; PFOS, Perfluorooctanesulfonic acid; PFBS, Nonafluorobutane-1-sulfonic acid; PFOA, Pentadecafluorooctanoic acid; PFBA, Heptafluorobutyric acid; PFPeA, Perfluoropentanoic acid; PFHxA, Undecafluorohexanoic acid; PFHpA, Perfluoroheptanoic acid; PFNA, Perfluorononanoic acid; PFDeA, Perfluorodecanoic acid; PFUnA, Perfluoroundecanoic acid; PFDoA Tricosafluorododecanoic acid; A, Assimilation Rate; E, Transpiration Rate; Gsw, Stomatal Conductance; Fv'/Fm', Photosynthesis efficiency net of NPQ losses; ETR, Electron Transport Rate; NPQ, Non-photochemical Quenching; PhiCO2, Molecules of CO2 fixed per Photon; PhiPS2, Photochemistry II; VPD leaf, Vapor pressure deficit at leaf temperature.

Abstract

Per -and Polyfluoroalkyl substances (PFASs) have been recognized as emerging pollutants and are found ubiquitously in the environment including humans, animals and plants due to their multiple uses in industry and consumer products. A large number of investigations has been carried out on PFAAs effects, fate and accumulation by plants., The aim of the following study was to determine the effects of mixture of 11 PFAAs on the growth of Maize (*Zea mays*) and depletion of PFAAs in nutrient solution. Maize, a staple food cultivated widely through the world for human consumption and animal fodder, was taken as a model plant for this study which was grown hydroponically spiked with mixture of 11 PFAAs at 100 µg/L each. The effects of PFAAs on plants were studied by the growth parameters (fresh weight (FW), dry weight (DW) and relative growth rate percentage (RGR), the measurements of gas exchange characteristics, fluorescence parameters, and depletion of PFAAs in the nutrient solution. The total plant biomass (g) of PFAAs treated maize seedlings declined as compared to control (without treatment) demonstrating that PFAAs are toxic to plants. Likewise, the photosynthesis parameters were altered, as well as the concentration of PFAAs having shorter carbon chain were less abundant in nutrient solution, which suggests that they have entered into the plant system.

1. Introduction

Per- and polyfluoroalkyl substances (PFASs) have a unique physicochemical property such as water, oil and grease-repellence and high thermal stability. Due to this reason, PFASs are being widely used in various industries such as textile coatings, paper treatments, pesticides and fire-fighting foams, and have led to their widespread occurrence and persistence in the environment. They do not degrade in the environment (Liu et al. 2013) and thus can be found ubiquitously in air, water, soil, sediment, sludge from wastewater treatment plants, biosolids for agricultural application, and house dust (Prevedouros et al. 2006; DeWitt 2015; Ahrens, 2011). However, some of the properties of PFAAs are contributing to make them problematic environmental contaminants.

The strong C–F chemical bond makes PFAS extremely resistant to thermal (Moody et al. 2003), chemical (Yang et al. 2015) and biological degradation (Zhao et al. 2011), which results in bioaccumulation in the environment and persistence in human tissues for years. PFAAs have been detected in human blood and breast milk, (Karrman et al., 2010) which is of concern because some PFAAs have been proven or are suspected to have adverse effects on animal and human health. Few studies have been done on how humans are exposed and still little is known so far about PFAAs exposure. Although human exposure to PFAAs may occur through different pathways, dietary intake seems to be the main route of exposure to these compounds (D'Hollander et al. 2010; Domingo et al. 2012). Because of the interest that this topic generates in both public opinion and the scientific community.

In recent years, several researchers have determined the concentrations of PFASs in foodstuffs, whereas some studies have also assessed the dietary intake of some of the most well-known PFASs, mainly PFOS and PFOA. In 2011, the state-of-the-art regarding human health risks of the dietary exposure to PFASs were assessed (Ericson et al. 2008).

Most of the studies focused on PFAAs, especially PFOS and PFOA, even though some studies have shown that other PFAAs might be even more abundant in the environment. There are very few data published on hydroponic uptake of PFAAs on crops. Even though hydroponic conditions are an artificial system, they can provide interpretable results regarding the depletion of PFAAs from the nutrient medium without any soil component interference (Ghisi et al. 2018). The limitation of hydroponic studies is that they do not include any effects of soil on modulating chemical availability.

The maize being one of the most important food crops in the world (Shiferaw et al. 2011), was used (*Zea mays,* B_{73}) as a model plant for our experimental work. In a recently published study, nutrient solution experiments were performed on maize plants for studying the uptake mechanism of PFAAs differing in chain lengths and functional group (Krippner et al. 2014). Also, Felizeter et al. (2014) studied PFAS accumulation in lettuce, tomato, cabbage and zucchini plants grown in a nutrient solution containing a mixture of PFASs. These plants tended to accumulate molecules with shorter carbon chain length in the leaf and higher chain lengths in roots. Other studies have been carried out to investigate the toxic effects (Stahl et al. 2009), uptake and accumulation of PFAAs by plants (Wen et al. 2013), and the toxic effects on a freshwater alga by flow cytometry and photosynthesis efficiency (liu et al. 2008). However, detailed photosynthesis and proteomics studies on the effects of PFAAs on maize plantlets have not been reported yet.

The aim of the present study was to investigate the effects of PFAAs on *Zea mays* L., as it is a major crop in the Veneto region, which is one of the four major PFAAs contaminated sites in the world. The experiments were conducted with maize plants grown in a hydroponic system to investigate the phytotoxic effects, morphological alterations of root system and depletion of PFAAs from the nutrient solution. The comparison was carried out between plants grown in a nutrient medium spiked by mixture of PFAAs and control (no spiking of PFAAs).

2. Materials and methods

2.1 Chemicals

The PFAAs included in the experiment are perfluorobutanoic acid (PFBA), perfluoro-n-pentanoic acid (PFPeA), perfluoroheptanoic acid (PFHpA), perfluorooctanoic acid (PFOA), perfluorononanoic acid (PFNA), perfluorodecanoic acid (PFDA), perfluoroundecanoic acid (PFUnA), perfluorohexadecanoic acid (PFHxA), Perfluoro dodecanoic acid (PFDoA), perfluorobutane sulfonate (PFBS) and perfluorooctanesulfonate (PFOS) (Sigma Aldrich, St. Louis, MS, USA). Mass labelled $^{13}C_2$-PFDA, $^{13}C_4$-PFBA, $^{13}C_5$-PFPeA, $^{13}C_5$-PFNA,$^{13}C_4$-PFBS, $^{13}C_6$-PFHxA, $^{13}C_7$-PFHpA, $^{13}C_4$-PFOA, $^{13}C_4$-PFOS, $^{13}C_{10}$-PFDoA, and $^{13}C_{11}$-PFUnA (Wellington laboratories, Guelph, ON, Canada) were used at a fixed concentration as internal standards (IS) for identification and quantification of all PFAAs.

2.2 Surface sterilization of seeds and germination test

The maize (B73) seeds grown in the University of Padova farm "L. Toniolo" in Legnaro city, were used for the experiment. The *Zea mays* (B73) seeds were thoroughly washed with tap water for 2 to 3 times, followed by 70 % ethanol. The surface sterilized seeds were further soaked overnight in the water. The plants were further grown for seed germination test and for PFAAs exposure experiments.

A germination test was conducted to check the effects of the PFAA on seed germination and to decide the concentration for the hydroponic treatment. The sterilized B73 maize seeds were placed in Petri dishes with an absorbent paper. 20 seeds were carefully stowed in each Petri dish with 6 mL of ½ strength Murashige and Skoog Nutrient Solution spiked with eleven PFAAs (PFBS, PFBA, PFPeA, PFHxA, PFHpA, PFOA, PFOS, PFNA, PFDA, PFDoA, PFUnA) at three different concentrations (10 µg/L, 100 µg/L, 1000 µg/L) and one without any treatment (control). Petri dishes were sealed with parafilm and were placed in a germination chamber at 25 °C for three nights.

At 4 days post treatment (dpt), 20 germinated maize seedlings from each treatment were randomly selected. First, seedlings were carefully removed intact from the paper; second, the seedlings were evenly spread apart in a water layer on a transparent tray (30 cm × 20 cm) and lastly, all the separated germinated seedlings were imaged at a resolution of 400 dpi (dots per inch) with an EPSON Expression 11000 XL PRO scanning system. Root images were analyzed for the total root length (cm), root surface area (cm^2), root volume (cm^3) and the diameter(mm) by using WinRHIZO software V5.0.

The total length and the average diameter of the roots was determined by the following formulas:

Length = (number of pixels in the radical skeleton / Image Resolution

Diameter = [(projection area / Total Length)] * (1 / Image Resolution)

2.3 Plant Culture and Exposure Experiments

Based on the results from seed germination experiment, the concentration of PFAAs was decided for growing the maize plantlets hydroponically. The sterilized seeds were rolled into wet paper and put in a beaker, incubated at 25 °C for three nights. The germinated seeds

were transferred to 50 ml falcon tube with tap water, and then to ½ strength MS Nutrient Solution under controlled conditions (70 % humidity, 25±1 Temperature and 350 µE m^{-2} s^{-1}, 10 hours of light) until plantlets reached an optimal growth for the PFAAs treatment.

One set of plants (10 plants) were transferred to full strength MS nutrient Solution spiked with eleven PFAAs (PFBS, PFBA, PFPeA, PFHxA, PFHpA, PFOA, PFOS, PFNA, PFDA, PFDoA, PFUnA) at 100 µg/L each. The other set (10 plants) were transferred only with full-strength MS medium without any PFAAs for the comparison. The treated and control plants were harvested at 8 dpt. Also, 500 µL of nutrient solution was collected from each falcon at the following time intervals: 0 dpt, 4 dpt, and 8 dpt, to evaluate the depletion of PFAAs from the nutrient solution through HPLC-MS/MS. Based on the depletion kinetics, the concentration of each PFAAs was estimated which might have been taken up by the plants during the treatment.

The control and treated maize plants were randomly selected and separated into leaves and roots. The separated radicles were placed in a water layer on a transparent tray for imaging from WinRhizo scanner in the same way as above.

2.4 Determination of relative growth rate and dry weight

Randomly, 20 plants were selected from control and treated groups and were carefully weighed during the experiment for assessing the relative growth rate (RGR). The plants were separated into foliage and roots to determine the physical parameters by an EPSON Expression 11000 XL PRO scanner, as mentioned above. The volume of the nutrient solution was also measured at the same time.

Time point before treatment denoted as '-1', used as the reference to calculate RGR, 0 was the day of the treatment with PFAAs, whereas 2, 4, 6, and 8 indicate dpt. RGR % was calculated according to the formula:

$$RGR\ \% = [(ln\ Wt_x - ln\ Wt_{-1}) / t_x - t_{-1}] * 100$$

where Wt_x refers to the weight at a specific time point during the experimental duration and

Wt_{-1} refers to the weight on the day before treatment.

10 plants were selected again for determining the dry weight. The roots and leaves from control and treated plants were dried in an oven at 50 °C till a constant weight was attained.

2.5 Leaf Gas exchange and Chlorophyll fluorescence measurement

Photosynthetic gas exchange parameters and chlorophyll fluorescence measurements were performed on 8 dpt with Li-6800 instrument (Li-Cor Inc., Lincoln, Nebraska, USA). Measurements were performed thrice on the middle portion of the second fully expanded leaf for five plants per condition (control and treatment) using the methods described by Stinziano et al. (2017). Actinic light composition was varied between 100% blue (470 nm) and 100% red (625 nm). The instrument was configured with flow rate 500 $\mu mols^{-1}$, 400 µmol mol^{-1} CO_2, leaf temperature 27°C and 51 % humidity. The negative ϕ PSII values were set to 0 for the measurement of fully saturated reaction centers. Dark respiration rate (Rd) was measured at the end of the light response curve and gross CO_2 assimilation was approximated as [CO_2 assimilation rate (A) + dark respiration rate (Rd)]. All fluorescence measurements were made using the multiphase flash fluorescence protocol (MPF) with a saturating intensity of 8,000 µmol m^{-2} s^{-1} with 1000 ms duration and 100 Hz output rate. Steady-state chlorophyll fluorescence (Fs) was measured at 50 kHz. Maximum chlorophyll fluorescence (Fm') was measured at 250 kHz during the saturating pulse, and fluorescence was detected at >700 nm (Evans et al. 2017). At the end of the experimental period, i.e. on the 8 dpt, leaf and root tissues from control and treated plants were weighed, rapidly frozen in liquid nitrogen and stored at -80 °C until analysis.

2.6 Protein Extraction from Root Tissues and iTRAQ labeling

The protein was extracted from root tissue following the protocol from Lan et al. (2011) with few modifications. The protein pellets were extracted using protein extraction buffer composed of 8 M urea and 50 mM triethylammonium bicarbonate, pH 8.5. The protein was collected, and protein concentration was determined by Bradford protein estimation assay. The protein quality and quantification of both the control and treated roots were also carried out by Sodium Dodecyl Sulphate-Polyacrylamide Gel Electrophoresis (SDS-PAGE) following the method of Laemmli (1970) in a Mini Protean II cell (Bio-Rad). The protein intensity of maize roots will be assessed before iTRAQ labeling. The 2.3.02 version of the Mascot software (Matrix Science) will be used to simultaneously identify and quantify the proteins. In this version, only unique peptides used for protein quantification will be chosen, which is more precise to quantify proteins.

2.7 Chemical analysis: HPLC-MS/MS

For further PFAAs analysis, the nutrient solution from both the conditions (Control and Treatment) were collected at time "0", at 4 dpt and at 8 dpt for the uptake of PFAAs by plant system. The nutrient solution from 0, 4 and 8 dpt were filtered and injected in the MS for analysis.

Reversed-phase HPLC was used to separate the different PFAA compounds based on polarity. Chromatographic separation was done using Ultimate 3000 UHPLC (Dionex, Italy) equipped with RS pump, RS autosampler and RS column compartment. The stationary phase was Phenomenex Luna_Omega PS C_{18} (Length, 50 mm; internal diameter, 2.1 mm; particle size, 1.6 µm; pore size, 100 Å). Gradient elution was performed using 0.1% formic acid in water as 1st eluent and methanol as 2nd eluent. The mobile phase flow rate was maintained constant at 0.40 mL/min. The injection volume was 5 µL.

MS analysis was performed by using TSQ Quantiva (Thermo Scientific, Waltham, MA, USA). The working optimized ESI parameter values were: Ion source type H-ESI, spray voltage, 2.5 kV, sheath gas flow rate, 50 (arbitrary unit, arb); aux gas flow rate, 20 (arb); Ion transfer tube temperature, 300°C; Vaporazer Temperature, 350 °C. Data were processed using the accompanying software Thermo Xcalibur 2.2 Qual browser (Thermo Scientific).

2.8 Data Analysis

All experiments were conducted with at least 10 biological replicates. All data were analyzed by One-way ANOVA and Tukey's test to assess the significance of the treatment effects. Differences at $p<0.05$ were considered as statistically significant. Statistical analysis was performed using R studio. Origin 6.0 was used to construct the graphs.

2. Results and discussion

3.1 PFAAs effects on Maize seed germination

PFAAs inhibited seed germination in a dose dependent manner. The germination rates and the root lengths were decreased in a dose dependent manner with the concentration of PFAAs (figure 4. 1C). Morphologically, the radicles of the treated plants were deformed and smaller as compare to untreated one (control) at 4 dpt. Physiological effects increased in a dose dependent manner with the concentration of PFAAs. The seed germination was highly

affected here at the higher concentration (1000 µg/L) of PFAAs, which might be due to physiological stresses.

From the EPSON scanner, the total length, the surface area, the total volume and the diameter of the radicles were determined. There was a trend of decrement with an increase in concentration of PFAA from 10 µg/L to 1000 µg/L for length, surface area and volume but there were not any differences in diameter of treated radicles as compare to control (figure 4. 2B & C).

Since seed germination is a critical stage in plant development (Seneviratne et al. 2017; Talukdar 2011), the effect of environmental pollutants on plants should be investigated in detail at this stage.

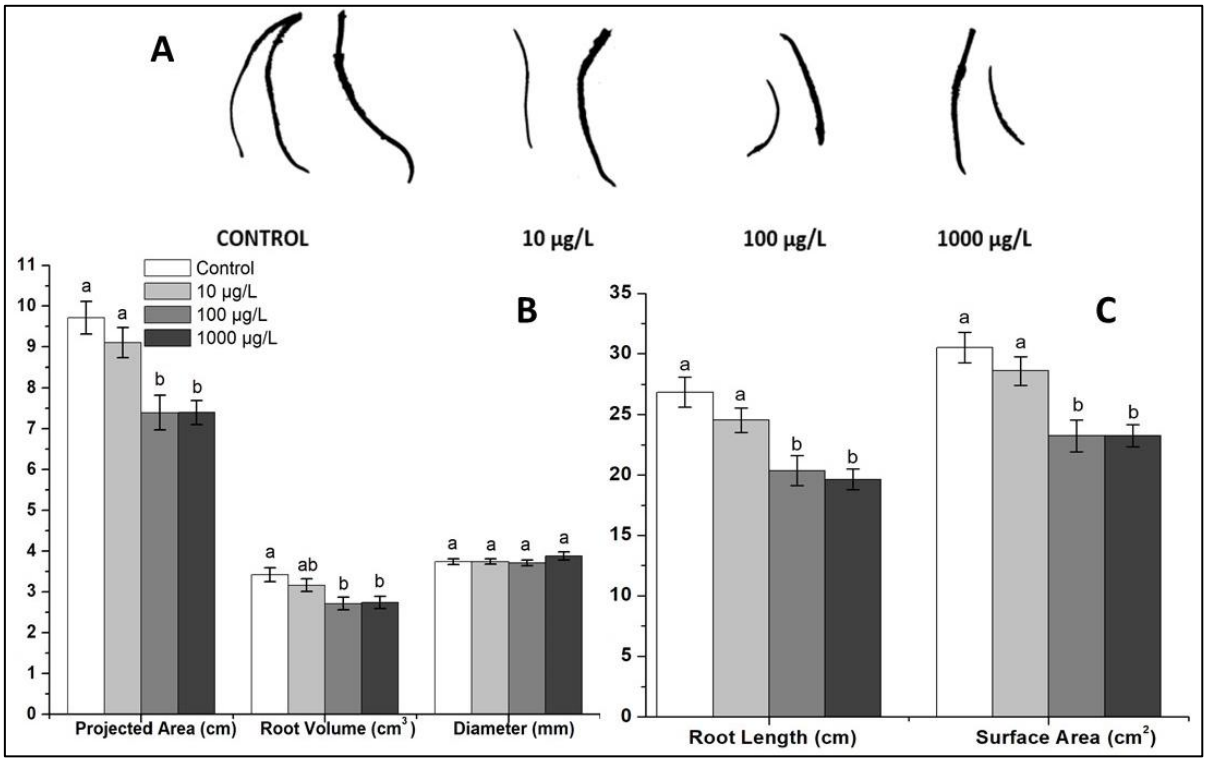

Figure 4.1: The Mean values of projected area, volume, diameter (B), root length and surface area (C), of maize seedlings from the EPSON Expression 11000 XL PRO scanner (A). The maize seeds were germinated in Nutrient Solution spiked with mixture of PFAAs at 0 µg/L, 10 µg/L, 100 µg/L and 1000 µg/L. The error bars represent the standard error (n=15-20). The different letters indicate significant differences as tested by Tukey-HSD test at $p < 0.05$ done between control and treated plants for each parameter separately.

3.2 Effects of PFAAs on maize growth

The relative growth rate percentage of the treated maize plants, hydroponically grown was significantly different from control (ANOVA, Tukey test, $p > 0.05$) (Figure 4.2); the growth started to decline slowly from 4 dpt of the treatment. The negative effect on RGR following

the treatment was further confirmed by dry weight and fresh weight of the maize leaf and root.

In facts, following PFAAs exposure, differences in the biomass of both shoots and roots (FW) were significant, compared with the control. This suggests that maize growth was hindered by the PFAAs treatment at 100 µg/L. As mentioned by Zhao et al. 2016, the decreased biomass could be due to cell damage in roots and shoots plantlets by high level of PFAAs contaminants. Yet, we know from Wen et al. (2013), that PFOS and PFOA significantly inhibited the maize root growth at higher concentration (10 mg/l). Since roots are the first point of contact with the nutrient solution containing PFAAs, they could be affected more than the shoots. As the growth of roots was inhibited, the uptake of nutrients might also be restrained, and resulted in decrease of the plant biomass.

Also, the dry weight of a sample was determined after drying to constant weight at 50 °C overnight in an oven. No significant differences were detected among the roots and leaves of the treatment with control plants (Table 4.1). Krippner et al. (2014) also detected no significant differences among the plant dry weights of PFAAs treatment.

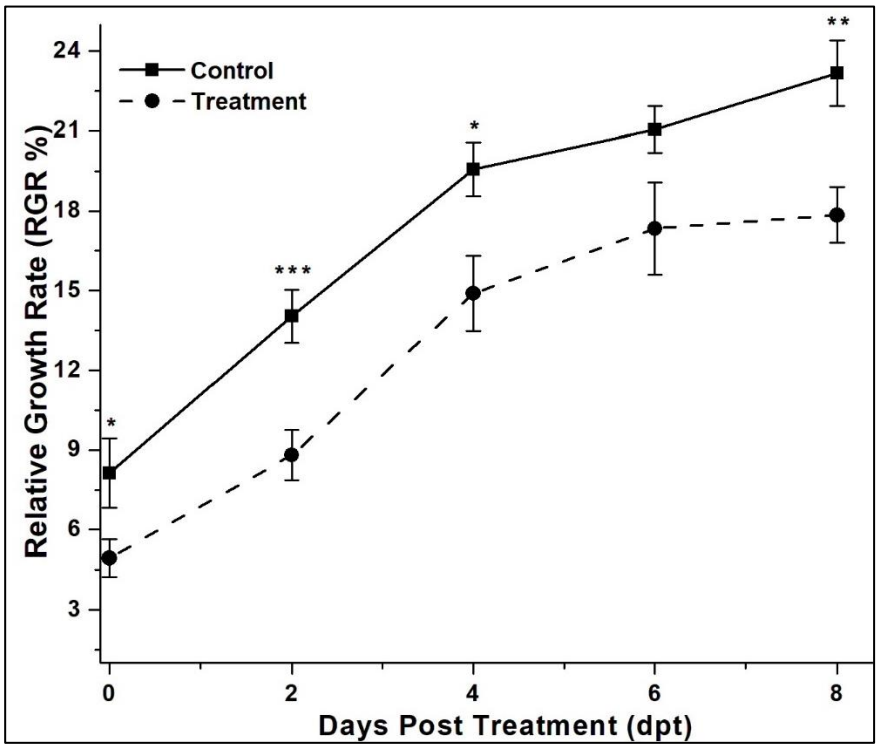

Figure 4.2: Effects of mixture of PFAAs on the relative growth rate in maize plants. Plants were grown in nutrient solution containing 11 PFAAs at 1.1 ppm for 8 dpt. "0" dpt represents the day of the treatment and 8 dpt is the end of the experiment. Error bars represent the mean standard error (n=18-20). Asterisks indicate the

significant differences between the treatments and the control ($p < 0.05$) at each dpt, as determined with One-way ANOVA

Table 4.1: The dry and wet weight of the maize roots and leaves treated with mixture of 11 PFAAs with control in nutrient solution for 8 dpt. The data show the mean ± standard error (n=4-5). The different letters indicate significant differences as tested by Tukey-HSD test at $p < 0.05$, between control and treated plants.

	WET WEIGHT (g)		DRY WEIGHT (g)	
	Weight of the Roots	**Weight of the Leaves**	**Weight of the Roots**	**Weight of the Leaves**
Control	0.262 ±0.01[a]	0.4258 ±0.02[a]	0.0176±0.002[a]	0.0431±0.002[a]
Treatment	0.196 ±0.01[b]	0.3467 ±0.01[b]	0.0147±0.001[a]	0.0354±0.003[a]

3.3 Morphological Changes in Maize roots under PFAAs treatment

It can be seen from the Table 4.2 that the root growth parameters of the maize plants were significantly inhibited under PFAAs treatment. Compared with the control, the treatment decreased the root length, root surface area and root volume by 47.47 %, 46.96 % and 46.19 % respectively. There was an increase in root average diameter by 3.7 %, yet not statistically different.

This negative effects by nearly 50 % on maize root length, area and volume could be related to the acute toxicity of PFAA on radicles. Toxic effects have been mentioned also by Joensen et al. (2009), Lau et al. (2007) in wildlife and humans and thus, the number for environmental monitoring studies has been increasing (Wen et al. 2016).

PFOS and PFOA toxicity in 3 different plant species was also previously demonstrated (Mei-Hui, 2008). Several other studies on phytotoxicity of PFOS and PFOA in aquatic species and plant species have been reported too (Hekster et al. 2003). However, the effects of a mixture of PFAAs on maize plants has not been reported yet, which may be more environmentally relevant given the simultaneous presence of several PFAAs species in contaminated sites.

Table 4.2: The dry and fresh weight of the maize roots and leaves treated with mixture of 11 PFAAs at 100 µg/L each with control in nutrient solution. The data show the mean ± standard error (n=4-5). The different letters indicate significant differences as tested by Tukey-HSD test at $p < 0.05$, between control and treated plants.

	Root Length (cm)	**Root Surface Area (cm^2)**	**Root Volume(cm^3)**	**Root Average Diameter (mm)**
Control	139.457 ±13[a]	26.208±2.6[a]	0.394±0.04[a]	0.598±0.02[a]
Treatment	73.250 ±10.6[b]	13.899±1.6[b]	0.212±0.02[b]	0.620±0.03[a]
%	-47.475	-46.967	-46.193	+3.715

3.4 Effect on Gas Exchange and chlorophyll fluorescence responses to PFAAs

The presence of physiological stress conditions under PFAAs treatment can be assessed by the estimation of photosynthesis related parameters, notably. Gas exchange parameters like Net photosynthesis rate (A), stomatal conductance (gsw), transpiration (E) and some fluorescence variables were monitored. We clearly observed that gas exchange parameters of treated plants were affected more than the parameters related to the fluorescence (Table 4.3) at 8 dpt (end of PFAAs treatment). Among them, A and phiCO_2 has increased significantly in treated plants compared to control. Net photosynthesis increased by 31.3 % and phiCO_2 by 40.1 %. Interestingly, vapor pressure deficit at leaf temperature (VPD) values were significantly decreased (Table 4.3). The observed increased level of *VPD leaf* and *A*. can be relate to parameters which can lead to increased CO_2 influx (*A*) and consequently water loss, as indicated by significantly reduced *VPD leaf* values.

Table 4.3. Photosynthetic parameters of the Maize (Zea mays) plants treated with mixture of 11 PFAAs and Control (without treatment). The data show the mean ± standard error (n=4-5). The different letters indicate significant differences as tested by Tukey-HSD test at $p < 0.05$, between control and treated plants. The column with percentage (%) indicates the increased percentage of PFAAs treated plants comparing to control.

Gas exchange variables	**Control**	**Treatment**	**%**
Assimilation Rate (A) (µmol m^{-2} s^{-1})	6.68±0.33[b]	8.78±0.65[a]	+31.3
Transpiration Rate (E), (mol m^{-2} s^{-1})	0.00076±0.00[a]	0.00095±0.00[a]	+25.3
Stomatal Conductance (gsw) (mol m^{-2} s^{-1})	0.033±0.00[a]	0.040±0.00[a]	+22.6
Fluorometer variables			
Fv/Fm	0.708±0.00[a]	0.717±0.01[a]	+1.2
Photosynthesis efficiency net of NPQ losses (Fv'/Fm')	0.439±0.01[a]	0.446±0.01[a]	+1.7
Electron Transport Rate (ETR) (µmol m^{-2} s^{-1})	58.172±1.94[a]	63.518±3.69[a]	+9.1
Non-photochemical Quenching (NPQ)	1.659±0.03[a]	1.542±0.08[a]	-7.0
Molecules of CO2 fixed per Photon (PhiCO_2)	0.020±0.00[b]	0.029±0.00[a]	+40.1
Photochemistry II (Phi$PS_{2)}$	0.276±0.01[a]	0.301±0.02[a]	+9.18
Vapor pressure deficit at leaf temperature (VPD leaf)	2.393±0.04[a]	2.192±0.03[b]	-8.35

3.5 Physiological effects of PFAAs exposure at proteomic level

To understand the effect of PFAAs on the plant metabolism, proteomic study will be carried out to show the alterations induced by the mixture of PFAAs treatment on metabolic pathways. The work of protein extraction, quantification and purification from maize root has already been concluded, whereas the MS experiments are currently being carried out at the Proteomic Center of the University of Padova.

3.6 Uptake of PFAAs in plants

Along the observation period, the PFAAs containing nutrient solution had a slightly different decrement from the control, as shown in Figure 4.2. In facts, the initial level of the nutrient solution in the falcon tube at day 0 was 50 mL for the control, but at the end of the treatment the final mean level value was 38.25 mL. Regarding the treatment, the final mean volume value was 40.36 ml.

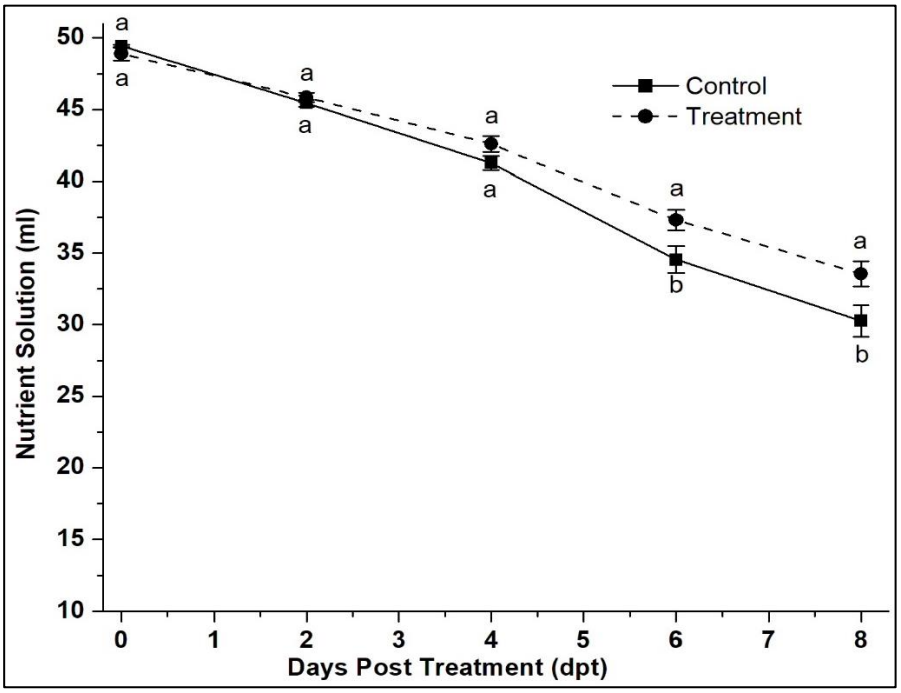

Figure 4.3 Uptake of the nutrient solution during the experimental period by the maize plants. Error bars represent standard error of the mean (n=20). Different letters indicate significant differences as tested by Tukey-HSD test at $p < 0.05$, between control and treated plants at each dpt.

The Tukey-HSD test gave a statistically significant difference with a P value equal to 0.0329 (< 0.05), which means that the absorption rate of the nutrient solution by the control differs from treated plants. The PFAAs, taken up by the roots via the transpiration stream (Felizeter et al. *2014*), inhibit the root uptake of nutrient solution. The water together with PFAAs, is taken up by the roots and is translocated to the leaves, where the water transpiration results in local accumulation of PFAAs.

3.7 Depletion of PFAAs in Nutrient Solution

HPLC-MS/MS analysis shows that depletion of each PFAA occurs from the nutrient solution during the observation period. The treated plants were spiked with mixture of 11 PFAAs, and among them two were not detected at all (PFUnA and PFDoA). As we can see in the Figure

4.4 A, each compound has a different decrement trend from 0 dpt to 8 dpt, which indicates that the plants could absorb a different amount of each PFAAs in a different way. Each compound was taken up by the plant in uneven way, which might be due to the difference in molecular characteristics of each PFAAs.

From the very beginning of the treatment, PFOS, PFNA and PFOA were three compounds which continuously decreased from 0 dpt to 4 dpt and at 8 dpt but PFDA was the one which showed abrupt decrease from 4 dpt in the nutrient solution. A higher percentage (36.40 %) of PFOS was monitored in the nutrient solution at the end of the experiment (8 dpt). Similarly, the results by Krippner et al. (2014), mentioned that PFOS was taken up significantly at higher rate by maize plants than all the other ten PFAAs examined. The second compound was PFNA, where 53.70 % was remained in the nutrient solution. The order of percentage of each PFAAs compound remained in nutrient solution was PFPeA > PFHxA> PFBA> PFBS> PFHpA> PFDA > PFOA > PFNA>PFOS.

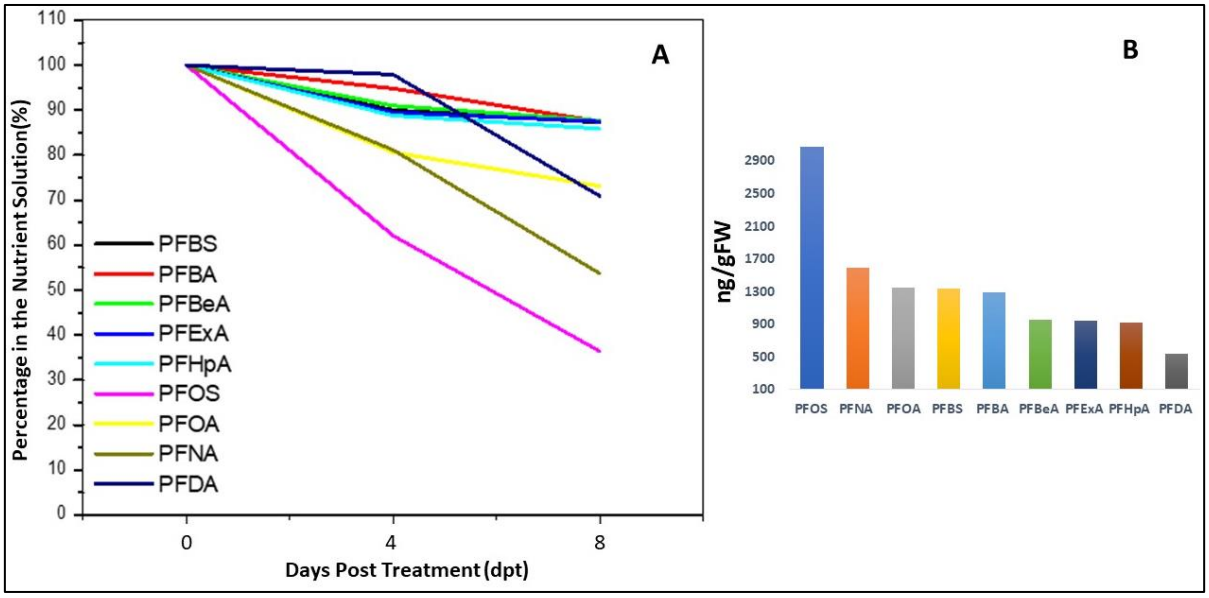

Figure 4.4 Depletion trend of each studied PFAA at 0, 4 and 8 dpt, in the nutrient solution (A) and estimated concentration of each PFAAs taken up by plants (B).

The percentage that was possibly taken up by the whole plant from the nutrient solution was calculated, based on the percentage of each PFAAs compound that were not detected in nutrient solution (Fig 4.4 B). The possible amount of each PFAAs expected to be found in the plant system (roots and leaves together), was expressed in ng/g FW. As expected, the higher concentration of PFOS was calculated in the plant, estimated value with 3071.25 ng/g FW. Likewise, the order of the concentration of each PFAAs was in the following order: PFOS >

PFNA> PFOA> PFBS> PFBA>PFBeA> PFeXA> PFHpA> PFDA. The uptake rates of PFAAs by maize plants are very much different, which might be due to carbon chain length of each PFAAs. Similar findings were observed by Felizeter et al. (2012), who mentioned that the concentration of PFAAs in shoots decreased with increasing chain length of PFCAs and PFSAs. Similarly, leaf concentration factors of cabbage, zucchini and tomato indicated that all PFCAs except the long chain ones were translocated and accumulated in the plants (Felizeter et al. 2014).

3. Conclusions

The basic growth parameters such as relative growth rate of the plants, biomass of the maize plants, photosynthetic efficiency measurements such as fluorescence and gas exchange measurement and the depletion of PFAAs in nutrient solution were studied in maize plants grown hydroponically with a mixture of PFAAs at 100 µg/L each compared with control (no PFAAs). Proteomics studies are in progress to highlight the effects of PFAAs at metabolic level.

The results of this study showed that mixture of 11 different PFAAs at a concentration of 100 µg/L each have significant effects on the growth of maize plants, affecting the uptake of the nutrient solution. Moreover, data showed that PFAAs having higher carbon number like PFHxA could not enter the plants and remain in the nutrient solution. But at the same time PFAAs having small carbon number might have entered into the plant system, thus affecting the plant's growth. I could conclude that PFAAs in combination are potentially phytotoxic and could be accumulated by plant system, if they are grown in PFAAs contaminated area. As a result, the maize plant, as well as crops, may contribute to increase human PFAA exposure, with toxic effect for human beings and animals, when grown in hot-spot regions, like Veneto region in Italy.

REFERENCES

Ahrens, L. 2011. Polyfluoroalkyl compounds in the aquatic environment: a review of their occurrence and fate. *Journal Environment Monitoring*. 13, 20–31. http://doi.org/10.1039/C0EM00373E.

Blaine, A. C., Rich, C. D., Sedlacko, E. M., Hyland, K. C., Stushnoff, C., Dickenson, E. R., & Higgins, C. P. 2014. Perfluoroalkyl acid uptake in lettuce (*Lactuca sativa*) and strawberry (*Fragaria ananassa*) irrigated with reclaimed water. *Environmental science & technology.* 48(24), 14361-143. https://doi.org/10.1021/es504150h.

Blaine, A. C., Rich, C. D., Sedlacko, E. M., Hyland, K. C., Stushnoff, C., Dickenson, E. R., & Higgins, C. P. 2014. Perfluoroalkyl acid uptake in lettuce (Lactuca sativa) and strawberry (Fragaria ananassa) irrigated with reclaimed water. *Environmental science & technology*. 48(24), 14361-14368. https://doi.org/10.1021/es504150h.

Buck, R. C., Franklin, J., Berger, U., Conder, J. M., Cousins, I. T., De Voogt, P., & van Leeuwen, S. P. 2011. Perfluoroalkyl and polyfluoroalkyl substances in the environment: terminology, classification, and origins. *Integrated environmental assessment and management*. 7(4), 513-541. https://doi.org/10.1002/ieam.258.

Chang, C., Bowman, J. L., & Meyerowitz, E. M. 2016. Field guide to plant model systems. *Cell*, *167*(2), 325-339. https://doi.org/10.1016/j.cell.2016.08.031.

D'Hollander, W., de Voogt, P., De Coen, W., & Bervoets, L. (2010). Perfluorinated substances in human food and other sources of human exposure. In Reviews of Environmental Contamination and Toxicology Volume 208, 179-215. *Springer, New York, NY*. https://doi.org/10.1007/978-1-4419-6880-7_4.

DeWitt, J. C. (Ed.). 2015. Toxicological effects of perfluoroalkyl and polyfluoroalkyl substances, Springer International Publishing, Switzerland. https://doi.org/10.1007/978-3-319-15518-0.

Domingo, J. L. 2012. Health risks of dietary exposure to perfluorinated compounds. *Environment international*, 40, 187-195. https://doi.org/10.1016/j.envint.2011.08.001.

Ericson, I., Martí-Cid, R., Nadal, M., Van Bavel, B., Lindström, G., & Domingo, J. L. 2008. Human exposure to perfluorinated chemicals through the diet: intake of perfluorinated compounds in foods from the Catalan (Spain) market. *Journal of agricultural and food chemistry,* 56(5), 1787-1794. https://doi.org/10.1021/jf0732408.

Evans, J. R., Morgan, P. B., & von Caemmerer, S. (2017). Light Quality Affects Chloroplast Electron Transport Rates Estimated from Chl Fluorescence Measurements. *Plant and Cell Physiology*, *58*(10), 1652-1660. https://doi.org/10.1093/pcp/pcx103.

Felizeter, S., McLachlan, M. S., & De Voogt, P. 2012. Uptake of perfluorinated alkyl acids by hydroponically grown lettuce (*Lactuca sativa*). *Environmental science & technology*. 46(21), 11735-11743. https://doi.org/10.1021/es302398u.

Felizeter, S., McLachlan, M. S., & De Voogt, P. 2014. Root uptake and translocation of perfluorinated alkyl acids by three hydroponically grown crops. *Journal of agricultural and food chemistry*. 62(15), 3334-3342. https://doi.org/10.1021/jf500674j.

Ghisi, R., Vamerali, T., & Manzetti, S. (2018). Accumulation of perfluorinated alkyl substances (PFAS) in agricultural plants: a review. *Environmental research.*

Joensen, U. N., Bossi, R., Leffers, H., Jensen, A. A., Skakkebæk, N. E., & Jørgensen, N. 2009. Do perfluoroalkyl compounds impair human semen quality?. *Environmental health perspectives*, *117*(6), 923-927. https://doi.org/10.1289/ehp.0800517.

Kärrman, A., Domingo, J. L., Llebaria, X., Nadal, M., Bigas, E., van Bavel, B., & Lindström, G. 2010. Biomonitoring perfluorinated compounds in Catalonia, Spain: concentrations and trends in human liver and milk samples. *Environmental Science and Pollution Research*, 17(3), 750-758. https://doi.org/10.1007/s11356-009-0178-5.

Krippner, J., Brunn, H., Falk, S., Georgii, S., Schubert, S., & Stahl, T. 2014. Effects of chain length and pH on the uptake and distribution of perfluoroalkyl substances in maize (*Zea mays*). *Chemosphere*. 94, 85-90. https://doi.org/10.1016/j.chemosphere.2013.09.018.

Laemmli, U. K. 1970. Cleavage of structural proteins during the assembly of the head of bacteriophage T4. *Nature, 227*, 680-685.

Lan, P., Li, W., Wen, T. N., Shiau, J. Y., Wu, Y. C., Lin, W., & Schmidt, W. 2011. iTRAQ protein profile analysis of Arabidopsis roots reveals new aspects critical for iron homeostasis. *Plant physiology*. 155(2), 821-834. https://doi.org/10.1104/pp.110.169508.

Lau, C., Anitole, K., Hodes, C., Lai, D., Pfahles-Hutchens, A., & Seed, J. 2007. Perfluoroalkyl acids: a review of monitoring and toxicological findings. *Toxicological sciences*, *99*(2), 366-394. https://doi.org/10.1093/toxsci/kfm128.

lHekster, F. M., Laane, R. W., & de Voogt, P. 2003. Environmental and toxicity effects of perfluoroalkylated substances. In *Reviews of Environmental Contamination and Toxicology* (pp. 99-121). Springer, New York, NY.

Liu, J., & Avendaño, S. M. 2013. Microbial degradation of polyfluoroalkyl chemicals in the environment: a review. *Environment International,* 61, 98-114. https://doi.org/10.1016/j.envint.2013.08.022.

Liu, W., Chen, S., Quan, X., & Jin, Y. H. 2008. Toxic effect of serial perfluorosulfonic and perfluorocarboxylic acids on the membrane system of a freshwater alga measured by flow cytometry. *Environmental Toxicology and Chemistry: An International Journal*. 27(7), 1597-1604. https://doi.org/10.1897/07-459.1.

Me Li. H. 2009. Toxicity of perfluorooctane sulfonate and perfluorooctanoic acid to plants and aquatic invertebrates. *Environmental Toxicology: An International Journal*. 24(1), 95-101. https://doi.org/10.1002/tox.20396.

Moody, C. A., Hebert, G. N., Strauss, S. H., & Field, J. A. 2003. Occurrence and persistence of perfluorooctanesulfonate and other perfluorinated surfactants in groundwater at a fire-training area at Wurtsmith Air Force Base, Michigan, USA. *Journal of Environmental Monitoring*, *5*(2). 341-345.

Prevedouros, K., Cousins, I. T., Buck, R. C., & Korzeniowski, S. H. 2006. Sources, fate and transport of perfluorocarboxylates. *Environmental science & technology.* 40(1), 32-44. https://doi.org/10.1021/es0512475.

Seneviratne, M., Rajakaruna, N., Rizwan, M., Madawala, H. M. S. P., Ok, Y. S., & Vithanage, M. 2017. Heavy metal-induced oxidative stress on seed germination and seedling development: a critical review. *Environmental geochemistry and health*. 1-19. https://doi.org/10.1007/s10653-017-0005-8.

Shiferaw, B., Prasanna, B. M., Hellin, J., & Bänziger, M. 2011. Crops that feed the world 6. Past successes and future challenges to the role played by maize in global food security. *Food Security*, *3*(3), 307. https://doi.org/10.1007/s12571-011-0140-5.

Stahl, T., Heyn, J., Thiele, H., Hüther, J., Failing, K., Georgii, S., & Brunn, H. 2009. Carryover of perfluorooctanoic acid (PFOA) and perfluorooctane sulfonate (PFOS) from soil to plants. *Archives of environmental contamination and toxicology*. *57*(2), 289-298. https://doi.org/10.1007/s00244-008-9272-9.

Stinziano, J. R., Morgan, P. B., Lynch, D. J., Saathoff, A. J., McDermitt, D. K., & Hanson, D. T. 2017. The rapid A–Ci response: photosynthesis in the phenomic era. *Plant, cell & environment.* 40(8), 1256-1262. https://doi.org/10.1111/pce.12911.

Strable, J., & Scanlon, M. J. 2009. Maize (*Zea mays*): a model organism for basic and applied research in plant biology. *Cold spring harbor protocols*. 10, 132. http://doi.org/10.1101/pdb.emo132.

Talukdar, D. 2011. Morpho-physiological responses of grass pea (Lathyrus sativus L.) genotypes to salt stress at germination and seedling stages. *Legume Research: An International Journal*. 34(4).

Wen, B., Li, L., Liu, Y., Zhang, H., Hu, X., Shan, X. Q., & Zhang, S. 2013. Mechanistic studies of perfluorooctane sulfonate, perfluorooctanoic acid uptake by maize (*Zea mays* L. cv. TY2). *Plant and soil*. 370(1-2), 345-354. https://doi.org/10.1007/s11104-013-1637-9.

Wen, B., Li, L., Liu, Y., Zhang, H., Hu, X., Shan, X. Q., & Zhang, S. 2013. Mechanistic studies of perfluorooctane sulfonate, perfluorooctanoic acid uptake by maize (*Zea mays* L. cv. TY2). *Plant and soil*. 370(1-2), 345-354. https://doi.org/10.1007/s11104-013-1637-9.

Wen, B., Wu, Y., Zhang, H., Liu, Y., Hu, X., Huang, H., & Zhang, S. 2016. The roles of protein and lipid in the accumulation and distribution of perfluorooctane sulfonate (PFOS) and perfluorooctanoate (PFOA) in

plants grown in biosolids-amended soils. *Environmental pollution*. 216, 682-688. https://doi.org/10.1016/j.envpol.2016.06.032.

Yang, B., Jiang, C., Yu, G., Zhuo, Q., Deng, S., Wu, J., & Zhang, H. 2015. Highly efficient electrochemical degradation of perfluorooctanoic acid (PFOA) by F-doped Ti/SnO2 electrode. *Journal of hazardous materials*. *299*, 417-424.

Zhao, H., Chen, C., Zhang, X., Chen, J., & Quan, X. 2011. Phytotoxicity of PFOS and PFOA to Brassica chinensis in different Chinese soils. *Ecotoxicology and environmental safety*, *74*(5), 1343-1347. https://doi.org/10.1016/j.ecoenv.2011.03.007.

Zhao, H., Guan, Y., Zhang, G., Zhang, Z., Tan, F., Quan, X., & Chen, J. 2013. Uptake of perfluorooctane sulfonate (PFOS) by wheat (*Triticum aestivum* L.) plant. *Chemosphere*, *91*(2), 139-144. https://doi.org/10.1016/j.chemosphere.2012.11.036.

Zhao, H., Qu, B., Guan, Y., Jiang, J., & Chen, X. 2016. Influence of salinity and temperature on uptake of perfluorinated carboxylic acids (PFCAs) by hydroponically grown wheat (*Triticum aestivum* L.). *Springer Plus*. 5(1), 541. https://doi.org/10.1186/s40064-016-2016-9.

Zhou, L., Xia, M., Wang, L., & Mao, H. 2016. Toxic effect of perfluorooctanoic acid (PFOA) on germination and seedling growth of wheat (*Triticum aestivum* L.). *Chemosphere*. 159, 420-425. https://doi.org/10.1016/j.chemosphere.2016.06.045.

CHAPTER 5

NMR STUDY OF PFAAS TREATED SEEDLINGS

Publication III

5.1 Focusing on "the important" through targeted NMR experiments: an example of selective 13C–12C bond detection in complex mixtures.

Amy Jenne,[a] Ronald Soong,[a] Wolfgang Bermel,[b] Nisha Sharma,[c] Antonio Masi,[c] Maryam Tabatabaei Anaraki[a] and Andre Simpson*[a]

[a]Environmental NMR Centre, University of Toronto, 1265 Military Trail, Toronto, ON, Canada

[b]Bruker BioSpin GmbH, Silberstreifen 4, Rheinstetten, Germany

[c]Department of Agronomy, Food, Natural Resources, Animals and the Environment, University of Padova, Padova, Italy.

Published in Faraday discussion, 2018

Publication IV

5.2 The study on Perfluroalkyl acids contaminated *Arabidopsis thaliana* with a powerful approach: Comprehensive Multiphase NMR Spectroscopy.

Nisha Sharma, Stefano Dall'Acqua, Stefania Sut, Leonard Barnabas Ebinezer, Antonio Masi, Andrea Simpson

This manuscript is under submission

Summary

NMR is a unique technology having many applications in the plant science. The main advantage of NMR is to identify the metabolites by comparing the NMR data with references or by structure elucidation using two-dimensional NMR without the need for any separation. The metabolite fingerprint provided by NMR is a convenient, and an effective tool which could be used to compare the groups of samples and for discriminating between groups of related samples. Likewise, here in my study (part of the thesis), I introduced the novel spectroscopy approach called CMP-NMR which is based on metabolomics to elucidate the significant metabolic changes in the metabolome of *Arabidopsis thaliana* upon exposure to PFOA, PFOS at 10 ppm separately and 11 mixture of PFASs with the control (no PFAAs exposure).

First, a protocol was optimized in collaboration with Prof. Simpson at the University of Toronto (Canada) for growing *Arabidopsis thaliana* heterotrophically in the dark and in presence of ^{13}C–glucose as the sole primary carbon source. The results of this work have been presented in the paper "Focusing on the important" through targeted NMR experiments: an example of selective ^{13}C–^{12}C bond detection in complex mixtures" published in "Faraday Discussion" journal (Jenne et al. 2019), where I am co-author.

The optimized protocol was further used to obtain a list of metabolites that are differentially abundant in *A. thaliana* seedlings upon exposure to PFAAs in the mixture and with individual PFAAs as compared to control. First, the seedlings were sterilized by a chlorine gas method and were grown in the nutrient solution in presence of $^{13}C_6$-glucose and spiked with PFAAs at three different conditions: i) PFOA at 10 ppm; ii) PFOS at 10 ppm; and iii) mixture of 11 PFAAs at 11 ppm. The sterilized seeds were transferred to the dark for 14 days at 21 °C. The presence of $^{13}C_6$-glucose as the sole carbon source resulted in all metabolites in the seedlings to be labeled with ^{13}C, which enables the study by CMP-NMR spectroscopy. Hence, two metabolites (Alanine and Glutamine) were identified which were significantly altered in the mixture of 11 PFAAs as compared to control. This result indicates that amino acid metabolism is a possible target of PFAAs in plants. A possible explanation is that the plants are under stress due to PFAAs exposure and are adapting to cope with the pollutant.

Faraday Discussions

Cite this: *Faraday Discuss.*, 2019, 218, 372

PAPER

View Article Online

Focusing on “the important” through targeted NMR experiments: an example of selective $^{13}C–^{12}C$ bond detection in complex mixtures

Amy Jenne,[a] Ronald Soong,[a] Wolfgang Bermel,[b] Nisha Sharma,[c] Antonio Masi,[c] Maryam Tabatabaei Anaraki[a] and Andre Simpson *[a]

Received 29th November 2018, Accepted 5th December 2018

DOI: 10.1039/c8fd00213d

Current research is attempting to address more complex questions than ever before. As such, the need to follow complex processes in intact media and mixtures is becoming commonplace. Here, a targeted NMR experiment is introduced which selectively detects the formation of $^{13}C–^{12}C$ bonds in mixtures. This study introduces the experiment on simple standards, and then demonstrates the potential on increasingly complex processes including: fermentation, *Arabidopsis thaliana* germination/early growth, and metabolism in *Daphnia magna* both *ex vivo* and *in vivo*. As signals from the intact ^{12}C and ^{13}C pools are themselves filtered out, correlations are only observed when a component from each pool combines (*i.e.* new $^{13}C–^{12}C$ bonds) in the formation of new structures. This targeted approach significantly reduces the complexity of the mixtures and provides information on the fate and reactivity of carbon in environmental and biological processes. The experiment has application to follow bond formation wherever two pools of carbon are brought together, be it the incorporation of ^{13}C enriched food into a living organism’s biomass, or the degradation of ^{13}C enriched plant material in soil.

Introduction

Questions in science research are becoming increasingly complex, with biological and environmental relevance always at the forefront of discussion. Almost every natural sample, including soils, atmospheric particles, plants, aquatic dissolved organic matter, and animals, can be thought of as complex mixtures. Often, isolation or fractionation can reduce complexity and make mixtures more amenable to a wider range of instrumental analyses. Conversely, it can be argued

[a]*Environmental NMR Centre, University of Toronto, 1265 Military Trail, Toronto, ON, Canada, M1C 1A4. E-mail: andre.simpson@utoronto.ca*

[b]*Bruker BioSpin GmbH, Silberstreifen 4, Rheinstetten, Germany*

[c]*Department of Agronomy, Food, Natural Resources, Animals and the Environment, University of Padova, Padova, Italy*

that it is often the synergism between components and phases in complex samples such as soil and living organisms that gives rise to the overall structure and function, and therefore must be kept intact.[1]

Nuclear Magnetic Resonance (NMR) spectroscopy is unique in that it is highly versatile and can be applied to liquids, gels, and solids. Thus it has applications to study both intact mixtures/systems or extracted/isolated sub-components.[2] NMR spectroscopy combines very high resolving capabilities and a diverse range of experiments to measure structure, dynamics, and interactions, while being non- invasive, and non-destructive.[3–6] The high resolving potential of NMR spectros- copy is often underestimated, but summarized beautifully by Hertkorn *et al.* The authors estimate 1D ^{1}H and ^{13}C NMR spectroscopy have peak capacities of ~3000 and 30 000, while 2D ^{1}H–^{13}C increases to ~2 000 000 and 3D NMR to ~100 000 000.[7] On extrapolation to 7D NMR spectroscopy, which has recently been demonstrated on disordered proteins *via* sparse sampling approaches, the peak capacity can potentially reach on the order of 10^{18}.[8–10] Of course, in most environ- mental and biological samples, the limiting factor is a lack of sensitivity when dispersing signals into a larger number of higher dimensions. However, as NMR sensitivity continues to increase and sparse sampling approaches improve,[11] NMR experiments of high dimensionality become more feasible, and will therefore likely become central to the next generation of complex mixture research.[12] Arguably, one of the most impressive applications to date on environmental systems is by Bell *et al.*[13] Humic substances in soil have been described by many as the most complex known mixture.[14] Bell *et al.* combined selective labelling and 4D NMR spectroscopy to gain exquisite information on the lignin derived components from soil, with the approach identifying many of the exact structures for the first time.[13]

When performing mixture-based research there are two avenues that can be pursued, namely targeted and non-targeted analysis, for which NMR spectroscopy has strong capabilities in both. However, many analytical approaches are avail- able for targeted analysis, while NMR spectroscopy's high reproducibility, non- destructive, and non-selective nature (*i.e.* any compounds containing an NMR active nucleus can be detected) make it uniquely suited for non-targeted anal- ysis.[15] Deciding on a targeted or non-targeted approach is most commonly driven by the research question itself. For example, if the question is "what is the molecular composition of aquatic organic matter?", it would make sense that a researcher applies the highest resolution molecular tools available and tries to evaluate what components make up the mixture as a whole in a non-targeted fashion.[16–18] Conversely, if the goal is to follow the fate of specific contaminants in soil, then having an NMR nucleus such as ^{19}F allows targeted monitoring of the contaminant and its interactions, providing information specific to the target of interest.[19] The study of Bell *et al.* was successful in identifying novel structural units because the ^{13}C enrichment targeted the lignin components in the soil organic matter.[13] In turn, this reduced the overlap with carbohydrates and allowed a wealth of new information to be uncovered. In both of the targeted examples above, a specific NMR nucleus (^{13}C or ^{19}F) was introduced to provide the selectivity. In the current study, a slightly different approach is explored. Instead of monitoring a label selectively, the filtering is built into the NMR experiment itself. Here, a new experiment is developed that specifically targets the formation of ^{13}C–^{12}C bonds, where ^{13}C–^{13}C bonds and ^{12}C–^{12}C bonds are not detected by the experiment. This experiment could have widespread implications for any studies

that bring two separate pools of carbon together and complements other exper- iments that are currently used for isotopic tracing by NMR spectroscopy.[20–22] For example, in 2006 a year-long study was performed following the fate of ^{13}C plant biomass as it degraded using HR-MAS NMR spectroscopy.[23] While humic substances are now thought to be largely complex mixtures,[24,25] at the time humic substances were thought to be chemically distinct, and formed from crosslinking components within soil organic matter.[26] As such, one of the goals of the 2006 study was to see if new bonds were formed. However, as the study followed just the fate of the ^{13}C enriched plant biomass, and as the material was so complex, while it was possible to see general changes (*i.e.* carbohydrates degraded fast, aliphatics accumulated, *etc.*), it was not possible to deftnitely see if crosslinks formed between the ^{13}C enriched plant biomass and other components in the soil.[23] If this were to be repeated with the experiment introduced here, it should be possible to target only the new bonds between ^{13}C and ^{12}C, which would help unravel how molecules are degraded, and if any novel recalcitrant structures do form within soil during humiftcation. Additionally, the approach could have huge implications for monitoring and understanding the transfer of carbon in food webs. For example, *Daphnia magna* is a keystone aquatic species (a key food source for many ftsh) but it cannot synthesize many lipids and sterols *de novo*, and is reliant on algae for nutrition.[27] As such, *D. magna* is one of the most studied species in ecology, yet details as to the individual molecular species, their sources, and their impact on growth are still not fully understood.[28] We anticipate that by utilizing targeted experiments that focus on ^{13}C–^{12}C bond formation, then detailed studies, that for example feed ^{13}C enriched *Daphnia* with ^{12}C algae (or *vice versa*), could provide insight on exactly how these organisms utilize food, and likely provide a better understanding of the biochemical pathways involved. Another example of a speciftc NMR experiment tailored for selective detection would be the amino acid-only experiment developed to selectively observe amino acid-proftles in living organisms.[29]

This study introduces the selective ^{13}C–^{12}C experiment, ftrst on simple stan- dards, and then demonstrates its potential on processes of increasing complexity, including fermentation, plant growth, and *Daphnia* metabolism both *ex vivo* and *in vivo*. We anticipate that due to the versatility of NMR spectroscopy, many more targeted experiments can be developed in the future that examine speciftc components or processes within complex environmental samples.

Experimental

Ethanol fermentation

Ten milligrams of 1-^{13}C-glucose (Sigma Aldrich) were dissolved into a 1.5 mL 90 : 10 water and D_2O solution. Baker's yeast (produced by ACH Food Companies Inc.) was added to the mixture, which was then vortexed for 30 seconds, and allowed to settle. The remaining suspension was then placed into a 5 mm NMR tube (Norell Inc. NJ, USA) and monitored inside the NMR instrument over 24 hours.

Daphnia magna culturing

D. magna was cultured from a colony originally purchased from Ward's Scientiftc and maintained at 20 °C, with a water hardness of 124 mg $CaCO_3$ per L, and pH

7.5–8.5, consistent with local freshwater conditions. The cultures were kept under a 16 : 8 light/dark cycle. The species were fed 99% ^{13}C enriched *Chlamydomonas reinhardtii* (purchased from Silantes, GmbH)[30] as their sole food source for 14 days starting at birth, to produce enriched ^{13}C organisms. The daphnids were fed three times a week, and at the same time the water was changed to ensure sufficient oxygen content. The *D. magna* was also provided vitamin B_{12} (Sigma Aldrich, 2 mg L^{-1}) once a week to help with growth. Prior to the NMR studies, the organisms were placed in clean, aged water (dechlorinated *via* bubbling for one week) for 30 minutes to clear off residual algae. During the NMR experiments, the food source was switched to unenriched *Chlamydomonas reinhardtii* cultured in the lab using Bold's Basal Medium and following the Ministry of Ontario's standard operating procedure for algae culturing.

Sterilization and growth of *Arabidopsis thaliana*

The wild-type Columbia (Col-0) *Arabidopsis thaliana* seeds (originally from TAIR, OH, USA) were sterilized by a chlorine gas method. This method does not affect the seed viability, but removes microbial contaminants present on the seed surface.[31] The seeds were placed in Eppendorf tubes and with the cap open, were added to the desiccator. 100 mL of bleach and 6 mL of concentrated HCL (both from Sigma Aldrich) were placed inside the desiccator separately in a beaker. All the processes were performed inside the fume hood. After six hours of sterilization, the seeds were collected and stored in the freezer. The sterilized wild-type Columbia (Col-0) *Arabidopsis thaliana* was grown in sterilized Murashige and Skoog (MS) growth medium containing 1% (w/v) glucose. For the NMR experi- ments, uniformly labelled $^{13}C_6$-glucose at 99% ^{13}C enrichment (Silantes, GmbH) was used. The seeds were then cold-stratified for three days. The plates with sterilized seeds were transferred to the dark for seven days at 21 °C. Seedlings were collected on day zero, day one, day three, and day seven for NMR analysis.

Sample preparation and extraction of *D. magna* and *A. thaliana*

20 fully labelled *D. magna* were removed from the culture, flash frozen with liquid nitrogen, and lyophilized. The remaining organisms were switched to natural abundance ^{13}C algae as their food source, and sampling was repeated every 24 hours for four days. Metabolites were extracted following the protocol by Nagato *et al.*[32] using 3.2 mg of dried sample in 65 mL of buffer and placed in 1.75 mm capillary tubes (Hirschmann, Eberstadt, Germany) for 2D NMR analysis.

The *A. thaliana* samples were extracted using the protocol above prior to measurement, using 3.2 mg in 65 mL of buffer, and also in 1.75 mm tubes.

NMR spectroscopy

NMR experiments on extractions. NMR experiments on extractions were per- formed using a Bruker Avance III 500 MHz NMR spectrometer equipped with a ^{1}H–^{13}C–^{15}N TXI 1.7 mm microprobe fitted with an actively shielded gradient. The selective ^{13}C–^{12}C experiment is discussed in the main text. Data were collected with 98 increments, each with 16 scans (1-^{13}C-glucose, 1,2-^{13}C-glucose, and fermentation), and 64 increments with 832 scans (plants), and 896 scans (daphnids), 2048-time domain points, a recycle delay of one second, a 30 ms or 80 ms (see main text) TOCSY mixing time, a ^{1}J ^{1}H–^{13}C coupling of 145 Hz, and GARP-

4 for decoupling. Presaturation (~100 Hz bandwidth) was applied during the recycle delay to help reduce large water signals when required. The 90° pulses were determined in each sample. Data were processed with a sine-squared function phase shifted by 90° in both dimensions and a zero-filling factor of 2.

In vivo flow system. A low-volume flow system was utilized for these experiments. This was accomplished using the system and method created by Tabata- baei Anaraki *et al.*[33] 40 *Daphnia*, all 14 days old (fed only ^{13}C algae from birth), were placed in a high-precision, thin-walled 5 mm NMR tube (Wilmad-LabGlass, NJ, USA), with a Teflon plug (machined in-house) placed in the bottom of the NMR tube to prevent the daphnids from swimming outside the coil region. The top plug was created out of Teflon to keep the injection capillary glass and D_2O capillary in place (created in-house), and to keep all the daphnids within the coil region, maximizing the signal. The flow rate was set at 0.25 mL min^{-1}, and the reservoir contained oxygenated water and unenriched algae. This enables the daphnids to survive and remain in a low-stress environment in the instrument by providing consistent food and oxygen. The entire system was placed inside the NMR spectrometer and kept at 5 °C to slow down the movement of the daphnids, enabling better water suppression and a more stable signal. Separate *in vivo* NMR experiments were conducted for 24 hours on fully enriched ^{13}C *Daphnia*, and *Daphnia* after being fed ^{12}C algae outside of the instrument for nine days.

In vivo NMR experiments. Experiments were performed on a Bruker Avance III HD 500 MHz (^{1}H) NMR spectrometer using a ^{1}H–^{13}C–^{15}N TCI Prodigy cryoprobe fitted with an actively shielded *z*-gradient. The external D_2O capillary lock (~5 mL) was integrated into the flow system and all experiments were run locked. The ^{13}C–^{12}C experiment was performed as with the extracts, with the exception that the reversed editing block was removed to increase the SNR and reduce relaxa- tion. Presaturation (~100 Hz bandwidth) was applied during the recycle delay to help reduce the large water signal. 90° pulses determined in each sample and a TOCSY mixing time of 30 ms was used. A total of 128 increments were collected, each with 480 scans, 2048-time domain points, and a recycle delay of one second. The INEPT transfer was based on ^1J ^{1}H–^{13}C coupling of 145 Hz. Data were pro- cessed with a sine-squared function phase shifted by 90° in both dimensions and a zero-filling factor of 2.

Spectral assignments. Compound identification and assignment were done using AMIX (analysis of MIXtures software package, version 3.9.15, Bruker BioSpin), in combination with the Bruker Bio-reference NMR databases version 2-0- 0 through 2-0-5. Spectra were calibrated against the Bruker Bio-reference NMR databases using tyrosine and $_D$-glucose resonances for reference. Assignment was performed using a procedure previously described.[34,35]

Results and discussion

Basic pulse sequences and spectra

Fig. 1 shows the basic sequence used for the selective detection of ^{13}C–^{12}C bonds. In practice, sequences A and B are acquired in an interleaved fashion such that slice one of the 2D is the result from sequence A, and slice two is the result of sequence B. The data sets are split after acquisition to yield separate data sets. As A is essentially a "reference" for B it is important to collect the data sets at similar time points which is the purpose of interleaving the acquisition.

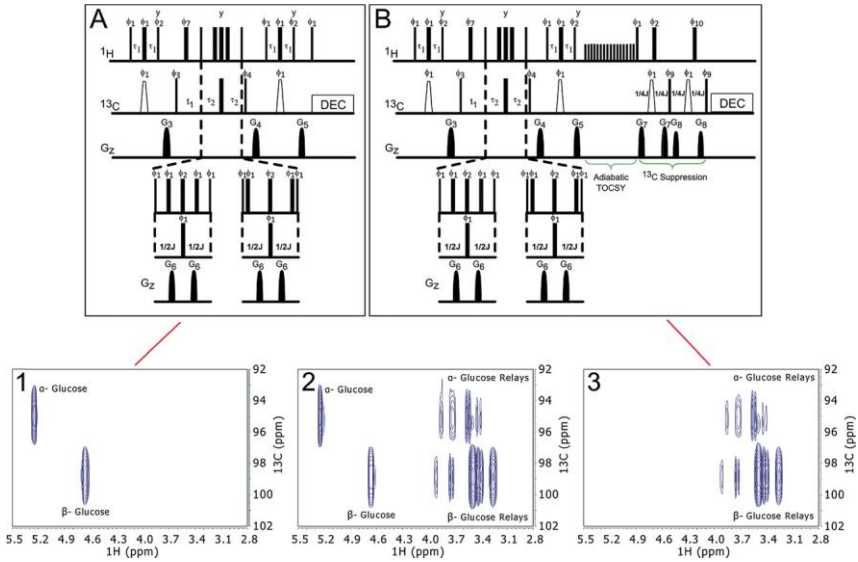

Fig. 1 The basic qualitative sequence. (A) A reverse HSQC spectrum. Narrow rectangles indicate a 90° pulse, whereas wide rectangles indicate a 180° pulse. Unless otherwise stated, pulses are applied along the *x*-axis. Open trapezoids represent smoothed chirp pulses for inversion with a pulse length of 500 ms, a sweep width of 60 kHz, defined with 1000 points and with a 20% smoothing of the amplitude on either end. The pulsed field gradients are indicated as filled sine envelopes and are 1 ms in length. The amplitudes of the gradient pulses have the following ratio: G_3 ¼ 60%, G_4 ¼ 40%, G_5 ¼ 31%, G_6 ¼ 19%, G_7 ¼ 23%, and G_8 ¼ 13% (with 100% being 53.5 G cm^{-1}). The pulsed field gradients are applied along the *z*-axis followed by a gradient recovery delay of 200 ms. The following phase cycling was used for the pulse sequences: $\mathbf{f}_1$ ¼ 0, $\mathbf{f}_2$ ¼ 1, $\mathbf{f}_3$ ¼ 0 2, $\mathbf{f}_4$ ¼ 0 000222 2, $\mathbf{f}_7$ ¼ 00 00 22 2 2, $\mathbf{f}_8$ ¼ 00 2 2, $\mathbf{f}_9$ ¼ 012 3, $\mathbf{f}_{10}$ ¼ 1 1 2 2, and $\mathbf{f}_{rec}$ ¼ 2 0 20 02 0 2. (B) An adiabatic TOCSY which consists of 16 adiabatic processes (ca-WURST, 300 ms, 27.3 KHz pulses) with the following phase cycle, 0 0 2 2 0 2 2 0 2 2 2 0 0 2 0 0 2, precedes this sequence, and the additional pulses in panel B are appended. In this part of the sequence the following phase cycling was used: $\mathbf{f}_1$ ¼ 0, $\mathbf{f}_2$ ¼ 1, $\mathbf{f}_9$ ¼ 0 1 2 3, $\mathbf{f}_{10}$ ¼ 1 1 2 2, and $\mathbf{f}_{rec}$ ¼ 0 2 2 2 0 2 0 0 2. The bottom panel shows the results of these sequences on 1-^{13}C-glucose. Sequence A leads to panel 1 in which only the one bond ^{1}H–^{13}C bonds are detected. Panel 2 shows the result of data collected after the TOCSY block in B. At this point the data resemble an HSQC-TOCSY experiment (note this data is not actually collected but is included for clarity). Panel 3 shows the result of sequence B. In this case, the ^{1}H–^{13}C bonds are subtracted, leaving only the signal from ^{1}H–^{12}C that is in the same spin system as a ^{13}C. In practice, the data collection is interleaved with sequence A being collected for the first slice and then sequence B being collected for the second slice and so on. The data are then split at the end of the experiment to give panels 1 and panels 3.

The result of sequence A is a standard reverse HSQC spectrum where the CH_2 moieties are reflected around the carbon offset (O_2P).[36] The advantage is that in complex samples the editing improves the spectral dispersion and helps reduce overlap especially in the aliphatic region where the chemical shift overlap between $CH/CH_2/CH_3$ is common. The added dispersion will become clearer in more complex samples shown later in the manuscript (see Fig. 4 as an example).

Fig. 1 (inset 1) shows the results from sequence A on glucose labelled with ^{13}C at the 1-position (1-^{13}C-glucose). As position one is a C–H group, the result from

sequence A in this case is the same as a conventional HSQC spectrum and two cross peaks arise, one from a-glucose and one from b-glucose. In Fig. 1 (inset 2) the adiabatic TOCSY block is activated, and protons attached to ^{13}C are now allowed to mix with all other protons in the sample (both those attached to ^{13}C and those attached to ^{12}C). The result is similar to an HSQC-TOCSY experiment, with relays along the horizontal plane. Readers should note that the data set in Fig. 1 (inset 2) is not actually recorded using sequence B, but is included as an additional step to make it easier to visualize how the experiments work (*i.e.* progressing from Fig. 1 (inset 1) through (inset 3)). An adiabatic TOCSY[37] is used as it shows superior mixing in complex natural samples over MLEV and DIPSI.[3,38] The result of the full sequence B is shown in Fig. 1 (inset 3). After the TOCSY block and additional ^{13}C filter is applied between Fig. 1 (inset 2) and (inset 3), the signals from any protons attached to ^{13}C are cancelled. The final result is the ^{1}H atoms attached to ^{12}C are selectively detected. It is important to note that for peaks to occur in the first place they must be in the same $^{1}H–^{1}H$ spin system as a ^{13}C nucleus. If a molecule contained only $^{1}H–^{12}C$ then the protons would not be selected by the first block. If a molecule contains all ^{13}C then the last filter would cancel the signals such that they are not detected. As such, the experiment selectively detects $^{13}C–^{12}C$ in proximity (albeit *via* their attached protons as ^{12}C is NMR inactive). The maximum number of bonds between the ^{13}C and ^{12}C that can be detected is determined by the TOCSY mixing time. In this first example, 80 ms are used, as such, correlations from the ^{13}C labelled 1-position relay around most of the glucose ring and a number of short (COSY), and long (TOCSY) correlations are seen. However, if the TOCSY mixing time is reduced to 30 ms, mainly COSY type interactions are emphasized. In complex samples this can reduce crowding in data and make it a little easier to interpret. Conversely, additional long range TOCSY correlations can be useful in aiding spectral assignment.

Fig. 2 shows the results of sequence B performed on 1-^{13}C-glucose using a 30 ms mixing time for comparison to Fig. 1, such that only the COSY correlations to ^{12}C show. The result being that only the ^{12}C atoms directly adjacent to ^{13}C atoms are selected. When the results of sequence A (Fig. 2A) and sequence B (Fig. 2B) are overlaid (Fig. 2C), the one bond $^{1}H–^{13}C$ cross peaks are blue while correlations to the ^{12}C adjacent are shown in red. We find this differential colouring approach

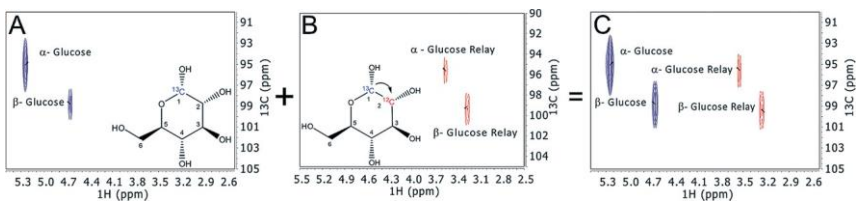

Fig. 2 Examining the process of monitoring $^{13}C–^{12}C$ bonds using 1-^{13}C-glucose. (A) 2D reverse HSQC spectrum that only detects ^{13}C atoms (*i.e.* the result from sequence 1A), the glucose molecule contains the labelled carbon atom in blue. (B) 2D $^{13}C–^{12}C$ sequence with a 30 ms TOCSY mixing time that selectively detects COSY-like relays and subtracts the signals from ^{13}C (*i.e.* the result from sequence 1B). (C) The overlaid spectra of 2A and 2B. ^{13}C atoms are show in blue while relays to ^{12}C atoms are shown in red. With a 30 ms TOCSY mixing time, if a blue cross peak is seen on the same row as the red cross peak it means they are directly bonded in the molecule.

very convenient for visualizing data sets, if a red and blue cross peak appear on the same horizontal row, this indicates a ^{13}C and ^{12}C unit are directly bonded. Interpretation from assigned NMR databases is easy, as HSQC cross peaks are commonly labelled with the corresponding structural position (H1/C1, H2/C2, *etc.*). In the example shown in Fig. 2, first the blue cross peaks (one bond correlations of $^{1}H–^{13}C$) are identified and then, using the assigned molecular structure, the cross peak (and thus chemical shifts) of the adjacent $^{1}H–^{12}C$ unit is found. If the molecule selected for assignment is indeed correct, then the proton chemical shift of the relay should match the proton chemical shift at the same position in the molecule of interest. In the case of 1-^{13}C-glucose, the relays match exactly with the proton chemical shift of carbon 2 in both α-glucose and β-glucose as expected. If assigned molecules are not available in a database, then assignments could be performed by referring to the HSQC and COSY (or TOCSY when a longer mixing time is used) data in combination. The one bond correlation would be identified from the HSQC data and the chemical shift of the proton relay from the COSY data. Whichever way the assignment is performed, the experiment gives a convenient approach to monitor the formation of $^{13}C–^{12}C$ bonds.

A simple process: fermentation

To demonstrate the concept further, 1-^{13}C-glucose was allowed to ferment in the presence of baker's yeast (*Saccharomyces cerevisiae*) to form ethanol over 24 hours inside the NMR spectrometer. Fig. 3A shows the overlaid one-bond/relay data before the experiment began, which is essentially identical to that shown in Fig. 2C. After 24 hours of fermentation, ethanol has formed. In Fig. 3B, it can be seen that the CH_3 group in the ethanol molecule has been derived from the ^{13}C

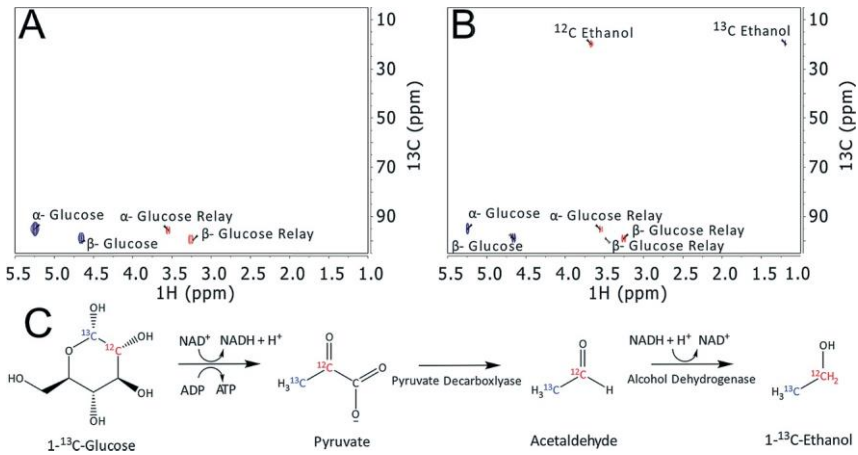

Fig. 3 Following the simple process of fermentation. 1-^{13}C-glucose was mixed with baker's yeast (*Saccharomyces cerevisiae*) for 24 hours inside the NMR spectrometer to monitor the formation of 1-^{13}C-ethanol. Carbons 1 and 2 in glucose are used to form ethanol through fermentation. (A) The same overlaid spectrum from Fig. 2C prior to the fermentation reaction. (B) 24 hours after the addition of yeast. ^{13}C is seen in blue, and the ^{12}C relays are in red. In this case, ethanol is formed with the methylene group from ^{12}C and the methyl group from ^{13}C. (C) Simplified fermentation process with 1-^{13}C-glucose.

labelled 1-position (blue contour), while the CH_2 group is from ^{12}C (red contour). This is consistent with the well understood process of fermentation of glucose. Under anaerobic conditions, glucose breaks down to form ethanol, with the help of ATP and NADP/H. Through this process the six-membered ring breaks, resulting in two 3-carbon pyruvate derivatives, which are then broken down into 2-ethanol. Through this process, the result is a ^{13}C atom in the 1 position, and a ^{12}C atom in the 2 position.[39,40] A simplified mechanism of the fermentation process can be seen in Fig. 3C.

A complex process: *Daphnia magna ex vivo*

Fig. 4 demonstrates the approach in a much more complex system. In this case, *Daphnia magna* have been fed 99% ^{13}C enriched algae two weeks from birth such that the overwhelming majority of carbon in their biomass is ^{13}C. After this they were fed ^{12}C algae (natural abundance ^{13}C) for 96 h. During this time, it is expected that ^{13}C–^{12}C bonds will form as their new ^{12}C food is incorporated into their ^{13}C biomass. A TOCSY time of 80 ms is used in this example such that both long- and short-range correlations are observed. Samples were taken every 24 hours over four days and extracted using a phosphate buffer. Fig. 4A shows the result after 96 hours. The CH_2 groups in the reversed HSQC spectrum are flipped around the carbon offset (100 ppm in this case) and appear in the lower right quadrant of the data set. The CH_3 and CH groups appear as they would in a conventional HSQC experiment. The data are highly complex, and the full analysis is beyond the scope of this paper. However, five regions of interest have been highlighted.

Region one is consistent with a relay from the adenine group to the ribose ring in the energy molecules (*i.e.* ATP, ADP, and AMP). This indicates the adenine is coming from the older ^{13}C carbon pool while the ribose has been synthesized from the ^{12}C biomass introduced over the last 96 hours.[41,42] In this case, the adenine and ribose link *via* a quaternary N center and protons on each side of this (one from adenine and one from ribose) TOCSY correlate due to the 80 ms mixing. This has been confirmed by cross-checking the TOCSY spectra of the energy molecules (ATP, ADP, AMP) in Bruker bio-reference databases, which all show this correlation.[35] The formation of energy molecules from carbon coming from different pools is consistent with the glycolysis and glycogenesis pathways used by *D. magna* for energy formation. These are major energy-creating pathways in crustaceans, producing vital ATP and NAD/H.[43] Pyruvate is formed from the breakdown of the glucose contained within the algae, and given the cyclic nature of the tricarboxylic acid (TCA) cycle, these pyruvate molecules can come from either labelled or non-labelled algae. These pyruvate molecules then form into new energy-containing molecules that are used by *D. magna*. This process has been studied extensively using cell flux analysis with *E. coli* and *S. cerevisiae*. Upon adding labelled glucose into the system, energy metabolism can be monitored and is seen to occur *via* the glycolysis/glycogenesis pathway.[42,44–46] By our estimate, this may be the first time this process has been examined directly in *D. magna*.

Region two is consistent with relays from ^{13}C enriched lipids to ^{12}C lipids containing double bonds. *Daphnia* are known to assimilate most of their lipids from their diet and cannot synthesize many essential fatty acids from scratch.[27,47–49] As the food source is changed to unenriched algae, the *Daphnia*

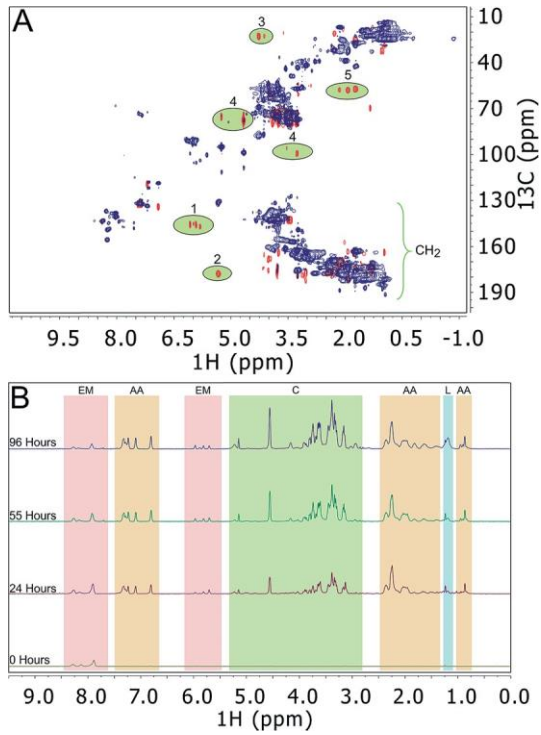

Fig. 4 Sequence applied to *Daphnia magna* extracts. The organisms were enriched for two weeks from birth with 99% ^{13}C enriched algae. They were then switched to natural abundance ^{12}C algae and monitored for four days. Samples were taken every 24 hours and extracted using a phosphate buffer. (A) Overlaid 2D NMR spectrum of the 96 hour sample. Blue is the ^{13}C remaining in the organisms and red is the ^{12}C relays to the new bonds formed. There are five regions of interest highlighted in green. (1) Adenine from ^{13}C bonding with ^{12}C ribose from the algae used in energy formation, (2) ^{13}C lipids containing ^{12}C unsaturation indicative of lipid synthesis, (3) protons in the ^{13}C lipid chains relaying to ^{12}C adjacent to oxygen atoms, (4) carbohydrate components including a mix of carbon enrichment in glucose as it moves through the TCA cycle and glycogenesis, and (5) a mixture of glutamate and glutamine amino acids. (B) 1D ^{1}H projections for all the time points showing the uptake and use of ^{12}C in the *Daphnia*. EM ¼ energy molecules, AA ¼ amino acids. C ¼ carbohydrates. and L ¼ lipids.

begin to form lipids from the new food source. Acetyl CoA, derived from pyruvate and the degradation of glucose, is used as a primer for the carbon chain, and elongated by the repeating condensation of malonyl-CoA yielding lipid pools.[50,51] As well, some dietary fatty acids are able to be desaturated in the carboxyl direction, as opposed to the methyl direction and then elongated to form poly- unsaturated fatty acids.[50] The correlation between ^{13}C and ^{12}C in the lipid chains suggests existing lipids are being modifted with units derived from the new ^{12}C food source. Region three is consistent with protons in the ^{13}C lipid chains relaying to the ^{12}C atoms adjacent to an oxygen atom, such as in a phospholipid head or even an ester group. This follows the above explanation where the formation of phospholipids to lipids occurs through dietary routing, which is the process of linking

together multiple fatty acid or lipid chains through digestion, where the chains can be from different carbon pools.[50]

Region four is carbohydrates including glucose breakdown and formation. As the experiment uses an 80 ms TOCSY spinlock, coupling around the entire hexose ring is expected. As such, the correlations indicate that ^{12}C and ^{13}C are being brought together to form the carbohydrates. This is consistent with the process explained above for the breakdown of glucose through glycolysis and then the re- formation through glycogenesis. As there will be pools of ^{13}C pyruvate and ^{12}C pyruvate, the glucose can get re-formed with ^{12}C theoretically in any position, resulting in $^{13}C–^{12}C$ relays observed within glucose.[52]

Region five is consistent with a-protons in amino acids relaying to the side chains. The peaks are the closest match for a mixture of glutamine and glutamate. This is consistent with studies in rat brains, which quickly assimilate glucose into glutamate.[46,53] After this, glutamine can be formed from the glutamate by glutamine synthetase.[54,55] The fact that ^{13}C and ^{12}C are found in the same system suggests that both ^{12}C and ^{13}C are feeding the glutamate–glutamine cycle, which produces amino acids containing both isotopes.[56] Glutamine and glutamate are used by *Daphnia magna* to aid in glucose metabolism, similar to a wide range of species.[56]

While the 2D NMR data contains a wealth of information down to the exact bonds involved in key processes, the ^{1}H projections represent a complementary source of information. As explained above, the only ^{1}H signal remaining at the end of pulse sequence B is relays to $^{1}H–^{12}C$ that are in close proximity to ^{13}C. As such, the ^{1}H projection essentially gives a simple visual as to the fate of ^{12}C as a process progresses. Consider, for example, the ^{13}C *Daphnia* feeding on ^{12}C algae. At the start of the experiment, the *Daphnia* are fully ^{13}C enriched so no signal is expected in the $^{13}C–^{12}C$ experiment or its ^{1}H projection. However, overtime as the

Daphnia utilize the ^{12}C, new molecules are formed bringing together both ^{13}C and ^{12}C, and a signal will appear in the $^{13}C–^{12}C$ experiment. In turn, the ^{1}H projection shows the fate of the ^{12}C and what types of molecules it has become incorporated into. Fig. 4B shows the ^{1}H projections over time as the *Daphnia* utilize ^{12}C. At time zero the spectrum is essentially blank, as expected. However, some small signals are present consistent with an adenine group. Prior to lyophilizing, the *Daphnia* were transferred and stored in aged water (which itself contains an algal background) for ~30 min. It is likely the *Daphnia* used this ^{12}C to start making adenine, the precursor required for energy molecules such as ADP/ATP/AMP.

After 24 hours of exposure to the unenriched food, ^{12}C has been incorporated into a range of structural categories. Signals from energy molecules have become much stronger, and key ribose signals around 6 ppm start to appear indicating a portion of both the adenine and ribose units are being made from ^{12}C substrates and are being brought in proximity to ^{13}C. In addition, a range of amino acid and carbohydrate signals also appear. It is important to remember that to appear in the spectrum a ^{13}C atom and a ^{12}C atom must be bonded together somewhere in the molecule, as such the experiment selectively detects new molecules that had to have been synthesized *de novo* from the food source. After 55 hours the spectral profile is relatively similar with the exception of carbohydrates that have ~doubled in intensity, consistent with the newly introduced C biomass being combined with ^{13}C likely for energy *via* glycolysis.[42,46] After 96 hours a distinct broad signal is noted around 1.2 ppm, consistent with $(CH_2)_n$ in lipids. This

indicates the *Daphnia* are modifying ^{13}C lipids using ^{12}C from their food source. This is particularly interesting; as mentioned above, *Daphnia* cannot synthesize many lipids and they rely on their food to assimilate many essential fatty acids. In addition, the lipids incorporated from their diets are key for reproduction. As *Daphnia* reproduce asexually, the lipid content is required for egg formation, and spikes immediately prior to birth, which is on average every 2–3 days.[57] Daphnids without proper lipid content stop producing viable offspring, and will often start to convert to sexual reproduction.[58] Thus, the use of lipids in *Daphnia* is key to their survival. Further, as *Daphnia* are keystone species, the stable reproductive cycles are imperative for many species' survival. *Daphnia* are found in almost every fresh water body worldwide, and are the food source for many other aquatic species.[48,59,60] Therefore, the use of lipids is not only key to *Daphnia* survival, but also has many potential negative consequences to higher trophic levels (*i.e.* fish and higher predators) based on available food sources. As such, the ^{13}C–^{12}C experiment introduced here specifically targets the modification of existing ^{13}C lipids by ^{12}C, and could be quite important in uncovering a better understanding of lipid modification and utilization in key species such as *Daphnia*.

Working in reverse: $^{13}C_6$-glucose in *Arabidopsis thaliana*

Fig. 5 depicts the germination and early growth of ^{12}C *Arabidopsis thaliana* seeds in the dark using $^{13}C_6$-glucose as the sole carbon source as previously described.[61] This study has been designed as the reverse of the *Daphnia* study, such that the process begins with ^{12}C, and ^{13}C is added into the system. As the plants are stored in the dark, photosynthesis does not occur, and the seeds grow *via* ^{13}C sorption through their husk and later uptake *via* roots after initial germination. In this situation, the question becomes "what does the plant synthesize from the ^{12}C stored in its seeds?" As the original biomass in the seeds is the only source of ^{12}C, the only way structures can appear is if the carbon from the seed biomass is combined with ^{13}C derived from the glucose, forming a new structure. After one

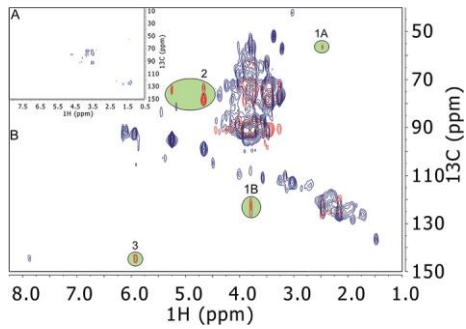

Fig. 5 *Arabidopsis thaliana* grown in the dark with $^{13}C_6$-glucose as the primary carbon source. (A) One day of growth with ^{13}C in blue and an absence of relays due to the lack of new bond formation. (B) Seven-day growth of the plants with ^{13}C in blue and ^{12}C relays in red. Three areas of interest are highlighted in green. (1A) a^{13}C–b^{12}C glutamate relays, (1B) a^{12}C–b^{13}C glutamate relays, an essential amino acid in plants, (2) relays from glucose from glycolysis and the TCA cycle, and (3) the formation of energy molecules derived from the glucose and TCA cycle.

day of germination/growth, no new signals are seen (see small inset, Fig. 5A). However, after one week of growth, the plant extract shows three main types of signals arising from several different pathways. There are three sections that are worth highlighting in Fig. 5B.

In region one, the new peaks arise from the synthesis of glutamate. This amino acid is crucial for the health of plants as it is used for assimilation and dissimi- lation of ammonia that is then transferred to all other amino acids in the plant.[62] As well, glutamate has been shown to be the precursor to chlorophyll synthesis in developing leaves.[62] Glutamate, like many of the metabolites under examination, is formed through the TCA cycle in plants and animals, therefore it also has implications in regards to energy formation.[56,63] Given the importance of this amino acid to plant health, it is expected that its formation would occur relatively quickly in the growth of *Arabidopsis*. In this experiment $a^{13}C–b^{12}C$ (peak 1A) and $a^{12}C–b^{13}C$ relays (peak 1B) are seen for glutamate, indicating ^{12}C and ^{13}C pools are likely brought together from isotopically different sources *via* the TCA cycle. Region two represents relays from the ^{13}C portions of glucose to ^{12}C at the 1- position. As a TOCSY mixing time of 80 ms was used for the plant study, long range interactions around the ring will be observed. Plants, like all living things, use glucose as an energy source for ATP formation, and without light, the glycolysis process occurs much like in *Daphnia*. The glucose gets broken down into two pyruvate molecules, and then moves through the TCA cycle to form ATP.[64,65] However, pyruvate can also move 'backwards' through gluconeogenesis to reform glucose, but the two pyruvates can be from different carbon sources.

This results in a glucose molecule with C1–3 with one isotope and C4–6 as another.

Region three represents energy molecules such as ATP/ADP/AMP with a ^{13}C adenine connecting to a ^{12}C ribose ring. Much like in the *Daphnia*, the plants utilize the glucose through the TCA cycle to create energy molecules.[44,45] The results here indicate that a portion of the energy molecules is created when adenine derived from the $^{13}C_6$-glucose is combined with ribose derived from the seed (^{12}C).

Daphnia magna in vivo

To further test the applicability of the $^{13}C–^{12}C$ experiment, the sequence was applied to a flow system containing living *Daphnia* raised on ^{13}C from birth. The main difference here is that the editing step has been removed from the sequence in Fig. 1B such that the CH_2 groups are not flipped around the ^{13}C offset. The reason for this is that in intact samples, such as living *Daphnia*, relaxation is very fast. Therefore, it is prudent to reduce the pulse sequence length as much as possible. When the CH_2 edited step was removed, it was found the signal intensity doubled over the edited version *in vivo*. Due to the additional signal, the non-edited version was applied to the *in vivo* system.

Fig. 6A shows a conventional HSQC experiment for reference, which represents all the $^{1}H–^{13}C$ bonds in the sample. Fig. 6B shows the result of the $^{13}C–^{12}C$ experiment of the *Daphnia* grown solely with ^{13}C algae since birth. As the organisms contain only ^{13}C, no signals appear in the $^{13}C–^{12}C$ experiment. Note, the vertical streak centered around 5 ppm is the breakthrough of residual water due to the fact that the organisms are swimming in 100% pure H_2O and 90% of

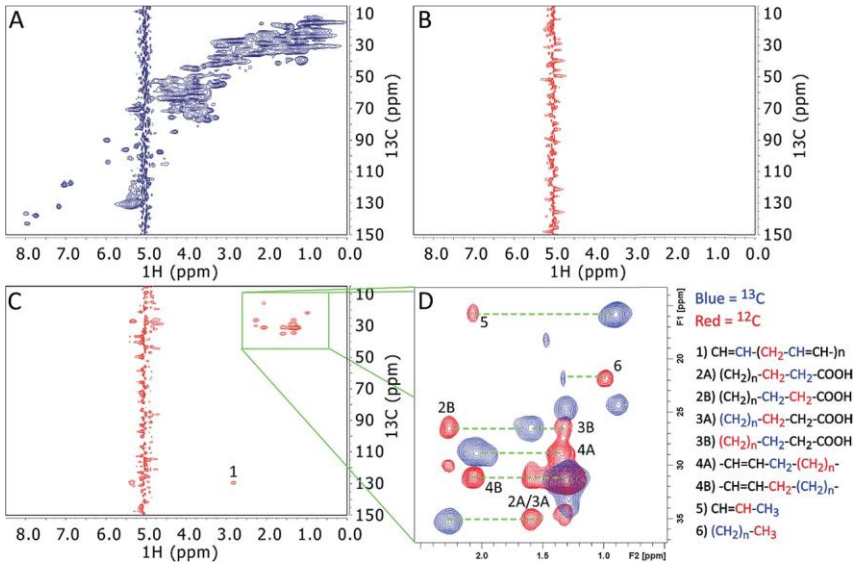

Fig. 6 Testing the ^{13}C–^{12}C sequence on an *in vivo* sample of *Daphnia magna*. In this case, the *Daphnia* were cultured from birth for two weeks using 99% enriched ^{13}C algae, and then switched to natural abundance ^{12}C algae for 9 days. (A) 2D HSQC spectrum of day zero *Daphnia* (*i.e.* not ^{12}C fed), (B) ^{13}C–^{12}C spectrum at day zero, no relays were detected due to the lack of ^{12}C in the system (note the streak at 5 ppm is residual water), (C) ^{13}C–^{12}C relays of *Daphnia* after nine days of exposure to ^{12}C algae as the food source. Relays have started to appear due to the assimilation of the new food into their biomass. (D) An expansion of the lipid region highlighting the new bonds that are formed.

their bodies are also water, making perfect water suppression incredibly difficult. Fig. 6C shows the same culture of organisms after nine days of being fed ^{12}C carbon. As can be seen, ^{12}C has been incorporated into the original ^{13}C biomass at various sites. Interestingly, despite the complexity of the system, all the correla- tions are relatively easy to assign based on the literature,[66–68] and arise from the modification of lipids (see Fig. 6D). Various structures can be identified, most of which appear twice with the relative locations of the ^{13}C and ^{12}C switched. This suggests that the *Daphnia* can utilize the ^{12}C and ^{13}C pools in similar ways. For example, it indicates the organisms can modify ^{13}C lipids from their own biomass with ^{12}C from their new diet. It also suggests they can modify ^{13}C lipids from their new diet using ^{12}C derived from their own biomass.

As discussed previously, *Daphnia* are limited in the lipids they can make, thus lipid incorporation from their diet is very important.[48,57,58] The expectation is that modification of their food source and lipids from their own biomass will result in new peaks formed using this sequence. For example, as the organism digests the algae, the lipids are broken down into single chain fatty acids that can then be desaturated and elongated using carbon already in the system.[50] Such lipids can be utilized to make more complex chains of lipids with additional carbon coming from either the diet (^{12}C) or biomass (^{13}C) pools.[69,70] This would occur relatively quickly and in higher concentrations compared to other metabolites due to the energy requirement from the lipids, and the inability to synthesize them inter- nally. This experiment is a powerful approach for providing information on

a complex *in vivo* system for processes such as lipid modification that are currently not well understood.[28]

The future potential for quantification

The ability to quantify the ratio of $^{12}C/^{13}C$ at a given position in a molecule would be extremely useful in constrained metabolic models, and tracing pathways.[71,72] Using the sequence outlined in Fig. 1B, it is not possible to quantify the $^{12}C/^{13}C$ ratio as the intensity of the cross peaks depends on both the efficiency of the TOCSY transfer and the abundance of ^{12}C in the peaks. Unfortunately, a rigorous implementation of a quantitative approach is beyond the scope of this paper and would likely take years of research to implement thoroughly in complex systems. That said, it is worthwhile to consider the future potential for quantification on a standard that paves the way for development and further discussion.

Fig. 7 shows two pulse sequences that when used in combination, in theory, should permit quantification of site specific $^{13}C/^{12}C$ ratios. The result of Fig. 7B is in fact identical to Fig. 1B (*i.e.* relays to ^{12}C remain, while ^{13}C is subtracted). Fig. 7A is derived from Fig. 7B with the goal to keep the pulses, durations, and timing identical between the two sequences. After the TOCSY proton magnetisation is excited and the CH coupling evolves for 1/2J, either block A or B is executed. In the case of B, the first ^{13}C 90° pulse converts the magnetisation into unobservable zero and double quantum coherence. The remaining proton mag- netisation can again evolve into CH antiphase magnetisation, which then is also converted into unobservable magnetisation by a second ^{13}C 90° pulse, thus enhancing the efficiency of the filter. For block A, the position of the second 90° pulse (of B) is changed (moved to the beginning). These two ^{13}C 90° pulses now act as a 180° pulse and reverse the J evolution so that at the end of block A all the magnetisation is back in phase and no filtering takes place. The net result is that the sequence in Fig. 7A now allows both protons attached to both $^{1}H–^{13}C$ and $^{1}H–^{12}C$ signals to pass, while the sequence in Fig. 7B blocks the $^{1}H–^{13}C$ signals. As the timing in both sequences is identical, Fig. 7A acts as a reference for the sequence shown in Fig. 7B. As such, we will refer to the sequence in Fig. 7A as the "quantitative reference" while we will refer to the sequence in Fig. 7B as the "^{12}C- only sequence." The TOCSY transfer in both will be identical, as such, the difference in signal intensity between the reference and the ^{12}C-only sequence will be from the subtraction of the ^{13}C signal. The concept is best explained on a standard. Fig. 7, panel 1 shows the result from 99% 1,2-^{13}C-glucose. Two horizontal bands appear, the upper band representing correlations between the 2-^{13}C position and protons around the ring, with the lower band representing correlations between the 1-^{13}C position and the ring protons. As there is no X filter, both protons attached to ^{12}C and ^{13}C appear in the spectrum. Fig. 8A (top spectrum) shows the proton projection from the experiment. Conversely, Fig. 7, panel 2 shows the result with the X filter turned on, such that the ^{13}C signals subtract. The corresponding projection is shown in Fig. 8A (bottom spectrum). Fig. 8B shows the spectra superimposed and it is clear that the intensities from the protons on ^{12}C are near identical in both experiments, while those from ^{13}C are completely suppressed. As such, the ratio between the two spectra indicates that the ^{13}C positions are essentially fully labelled (99%) while the ^{12}C positions are essentially ^{13}C free. In reality, of course, the ^{12}C position will be at natural

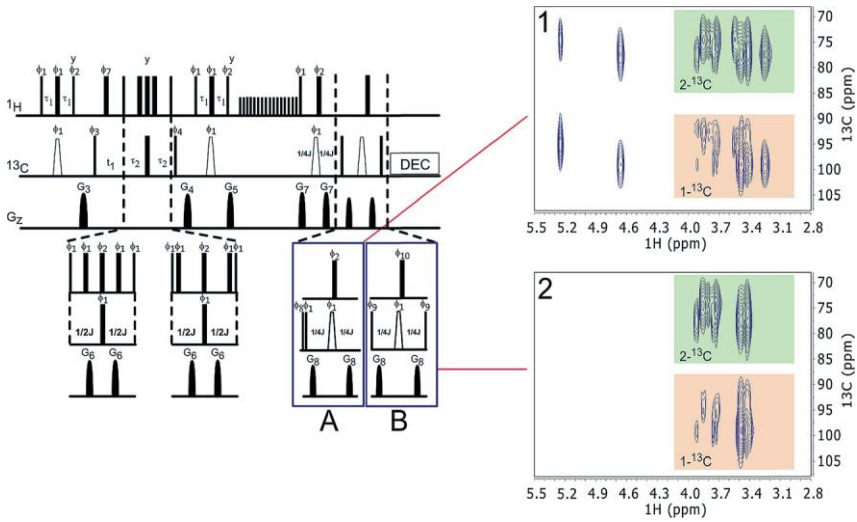

Fig. 7 The basic quantitative sequence. Block B produces the same result as Fig. 1B in that the ^{13}C signals are subtracted to leave only relays to $^{1}H–^{12}C$. (A) is derived from (B) with the goal to keep the pulses, durations and timing identical between the two sequences. By reorganizing the X filter element (block B) to become a spin-echo on carbon, and eliminating the carbon phase cycling (*i.e.* $\mathbf{f}_8$ 0¼in block A), block A essentially does nothing and allows signals from both $^{1}H–^{12}C$ and $^{1}H–^{13}C$ to pass. The data from A and B are collected in an interleaved fashion. The narrow rectangles indicate a 90° pulse whereas the wide rectangles indicate a 180° pulse. Unless otherwise stated, pulses are applied along the *x*-axis. The open trapezoids represent smoothed chirp pulses for inversion with a pulse length of 500 ms, a sweep width of 60 kHz, defined by 1000 points and with a 20% smoothing of the amplitude on either end. The pulsed field gradients are indicated as filled sine envelopes and are 1 ms in length. The amplitudes of the gradient pulses have the following ratio: G_3 60%, G_4 40%, G_5 ¼31%, G_6 ¼19%, G_7 ¼22%, and G_8 ¼13% (with 100% being 53.5 G cm^{-1}). The pulsed field gradients are applied along the *z*-axis followed by a gradient recovery delay of 200 ms. The following phase cycling was used for the pulse sequences: $\mathbf{f}_1$¼0, $\mathbf{f}_2$¼1, $\mathbf{f}_3$¼0 2, $\mathbf{f}_4$¼0 0 0 0 2 2 2 2, $\mathbf{f}_7$¼0 0 0 0 2 2 2 2, $\mathbf{f}_8$¼0, $\mathbf{f}_9$¼0 1 2 3, $\mathbf{f}_{10}$¼1, and $\mathbf{f}_{rec}$¼0 2 0 2 2 0 2 0. The adiabatic TOCSY is comprised of 16 adiabatic processes (ca-WURST, 300 ms, 27.3 KHz pulses) with the following phase cycle, 0 0 2 2 0 2 2 0 2 2 0 0 2 0 0 2. Sequence A results in spectra one, where both the ^{13}C and ^{12}C are acquired. In this case, 1,2-^{13}C-glucose was used. Sequence B subtracts the ^{13}C informa- tion leaving only the ^{12}C, as can be seen in spectra two. This allows for quantification by examining signal loss between (A) (the control) and (B) (the ^{12}C-only spectrum), the difference being the % ^{13}C at a specific site.

abundance and should contain 1.1% ^{13}C. Looking at the peaks, there is a very slight reduction that is consistent with a 1% reduction in signal at the "^{12}C- position", but the accuracy and reproducibility of this would need to be the subject of a much more extensive study. Future work would need to focus on standards with different levels of ^{13}C enrichment to assess how well ratios can be determined and the errors associated with such measurements, before measurements in complex systems would be meaningful. The goal here is simply to introduce one possible route towards isotope ratio quantification in products that are formed when ^{12}C and ^{13}C are bonded together in a complex process, that is a natural extension of the qualitative experiments introduced in the main body of this work.

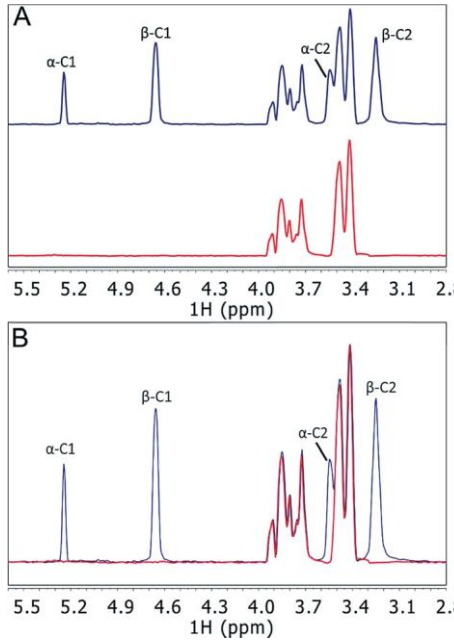

Fig. 8 A simple example of the potential for quantification on 1,2-^{13}C-glucose. (A) The top spectrum is the ^{1}H projection from the quantitative reference (both protons on ^{12}C and ^{13}C appear), and the bottom is the ^{12}C-only sequence (only ^{1}H on ^{12}C are observed). (B) The superimposed spectra show the ^{13}C signals completely cancel, resulting in the red ^{12}C signals. This theoretically allows for quantification by measuring the signal loss in the ^{12}C-only sequence relative to the reference which represents the % ^{13}C at that specific position within the molecule.

Conclusions

A new method for examining new bond formation using targeted 2D NMR spectroscopy has been explored. With this new sequence, ^{13}C–^{12}C bond formation can be selectively observed. To show the concept, processes from simple fermentation to complex metabolic examination in *Daphnia magna* and *Arabi- dopsis thaliana* were examined both *ex vivo* and *in vivo*. The results provide insight into how these species utilize food and energy sources and synthesize new molecules such as glutamate, ATP, and lipids. Quantiftcation is briefly considered, and the sequence is modifted to provide site specifttc ^{13}C/^{12}C ratios within a simple standard. However, additional further characterization with partially labelled standards is required to determine the error of such measurements before application to complex systems.

In summary, the approach provides a unique insight into the fate and reac- tivity of carbon in environmental and biological samples. After detailed spectral interpretation, it should be a useful tool for understanding how organisms utilize, store, and transform carbon. Similarly, in environmental research, the trans- formation and fate of organic matter are of widespread interest. If an enriched substrate (for example, ^{13}C enriched plant biomass, ^{13}C enriched biochar, or a ^{13}C enriched contaminant) is introduced in soil, sediment or water, the experiment should identify when these materials become functionalized, or degraded and recombined with ^{12}C from their environment. In turn, this should provide better insight into carbon sequestration, carbon cycling, humification, and contaminant fate.

Conflicts of interest

There are no conflicts to declare.

Acknowledgements

Andre Simpson would like to thank the Strategic (STPGP 494273-16) and Discovery Programs (RGPIN-2014-05423), the Canada Foundation for Innovation (CFI), the Ontario Ministry of Research and Innovation (MRI), the Krembil Foundation for providing funding, and the Government of Ontario for an Early Researcher Award.

Notes and references

1 A. J. Simpson, Y. Liaghati, B. Fortier-McGill, R. Soong and M. Akhter, Perspective: *in vivo* NMR – a potentially powerful tool for environmental research, *Magn. Reson. Chem.*, 2015, 53, 686–690.

2 D. Courtier-Murias, H. Farooq, H. Masoom, A. Botana, R. Soong, J. G. Longstaffe, M. J. Simpson, W. E. Maas, M. Fey, B. Andrew, J. Struppe, H. Hutchins, S. Krishnamurthy, R. Kumar, M. Monette, H. J. Stronks, A. Hume and A. J. Simpson, Comprehensive multiphase NMR spectroscopy: Basic experimental approaches to differentiate phases in heterogeneous samples, *J. Magn. Reson.*, 2012, 217, 61–76.

3 A. J. Simpson, D. J. McNally and M. J. Simpson, NMR spectroscopy in environmental research: From molecular interactions to global processes, *Prog. Nucl. Magn. Reson. Spectrosc.*, 2011, 58, 97–175.

4 P. R. L. Markwick, T. Malliavin and M. Nilges, Structural Biology by NMR: Structure, Dynamics, and Interactions, *PLoS Comput. Biol.*, 2008, 4, e1000168.

5 R. Ghose, in *eLS*, John Wiley & Sons, Ltd, Chichester, UK, 2017, pp. 1–20.

6 M. Nilsson, Diffusion NMR, *Magn. Reson. Chem.*, 2017, 55, 385.

7 N. Hertkorn, C. Ruecker, M. Meringer, R. Gugisch, M. Frommberger, E. M. Perdue, M. Witt and P. Schmitt-Kopplin, High-precision frequency measurements: indispensable tools at the core of the molecular-level analysis of complex systems, *Anal. Bioanal. Chem.*, 2007, 389, 1311–1327.

8 S. Żerko and W. Kozmí ński, Six- and seven-dimensional experiments by combination of sparse random sampling and projection spectroscopy dedicated for backbone resonance assignment of intrinsically disordered proteins, *J. Biomol. NMR*, 2015, 63, 283–290.

9 X. Yao, S. Becker and M. Zweckstetter, A six-dimensional alpha proton detection-based APSY experiment for backbone assignment of intrinsically disordered proteins, *J. Biomol. NMR*, 2014, 60, 231–240.

10 S. Hiller, C. Wasmer, G. Wider and K. Wüthrich, Sequence-Specifc Resonance Assignment of Soluble Nonglobular Proteins by 7D APSY-NMR Spectroscopy, *J. Am. Chem. Soc.*, 2007, 129, 10823–10828.

11 M. Mobli, M. W. Maciejewski, A. D. Schuyler, A. S. Stern and J. C. Hoch, Sparse sampling methods in multidimensional NMR, *Phys. Chem. Chem. Phys.*, 2012, 14, 10835–10843.
12 C. Pontoizeau, T. Herrmann, P. Toulhoat, B. Elena-Herrmann and L. Emsley, Targeted projection NMR spectroscopy for unambiguous metabolic profiling of complex mixtures, *Magn. Reson. Chem.*, 2010, 48, 727–733.
13 N. G. A. Bell, A. A. L. Michalchuk, J. W. T. Blackburn, M. C. Graham and D. Uhrín, Isotope-Filtered 4D NMR Spectroscopy for Structure Determination of Humic Substances, *Angew. Chem., Int. Ed.*, 2015, 54, 8382– 8385.
14 I. M. Young and J. W. Crawford, Interactions and self-organization in the soil-microbe complex, *Science*, 2004, 304, 1634–1637.
15 J. L. Markley, R. Brüschweiler, A. S. Edison, H. R. Eghbalnia, R. Powers, D. Raftery and D. S. Wishart, The future of NMR-based metabolomics, *Curr. Opin. Biotechnol.*, 2017, 43, 34–40.
16 N. Hertkorn, M. Frommberger, M. Witt, B. P. Koch, P. Schmitt-Kopplin and E. M. Perdue, Natural Organic Matter and the Event Horizon of Mass Spectrometry, *Anal. Chem.*, 2008, 80, 8908–8919.
17 B. P. Koch, M. Witt, R. Engbrodt, T. Dittmar and G. Kattner, Molecular formulae of marine and terrigenous dissolved organic matter detectedby electrospray ionization Fourier transform ion cyclotron resonance mass spectrometry, *Geochim. Cosmochim. Acta*, 2005, 69, 3299–3308.
18 N. Hertkorn, M. Harir, B. P. Koch, B. Michalke and P. Schmitt-Kopplin, High-field NMR spectroscopy and FTICR mass spectrometry: powerful discovery tools for the molecular level characterization of marine dissolved organic matter, *Biogeosciences*, 2013, 10, 1583–1624.
19 H. Masoom, D. Courtier-Murias, R. Soong, W. E. Maas, M. Fey, R. Kumar, M. Monette, H. J. Stronks, M. J. Simpson and A. Simpson, From Spill to Sequestration: The Molecular Journey of Contamination *via* Comprehensive Multiphase NMR, *Environ. Sci. Technol.*, 2015, 49, 13983–13991.
20 I. A. Lewis, R. H. Karsten, M. E. Norton, M. Tonelli, W. M. Westler and J. L. Markley, NMR Method for Measuring Carbon-13 Isotopic Enrichment of Metabolites in Complex Solutions, *Anal. Chem.*, 2010, 82, 4558–4563.
21 P. N. Reardon, C. L. Marean-Reardon, M. A. Bukovec, B. E. Coggins and N. G. Isern, 3D TOCSY-HSQC NMR for Metabolic Flux Analysis Using Non- Uniform Sampling, *Anal. Chem.*, 2016, 88, 2825–2831.
22 T. W. M. Fan and A. N. Lane, NMR-based stable isotope resolved metabolomics in systems biochemistry, *J. Biomol. NMR*, 2011, 49, 267–280.
23 B. P. Kelleher, M. J. Simpson and A. J. Simpson, Assessing the fate and transformation of plant residues in the terrestrial environment using HR- MAS NMR spectroscopy, *Geochim. Cosmochim. Acta*, 2006, 70, 4080–4094.
24 B. P. Kelleher and A. J. Simpson, Humic Substances in Soils: Are They Really Chemically Distinct?, *Environ. Sci. Technol.*, 2006, 40, 4605–4611.
25 M. W. I. Schmidt, M. S. Torn, S. Abiven, T. Dittmar, G. Guggenberger, I. A. Janssens, M. Kleber, I. Kögel-Knabner, J. Lehmann, D. A. C. Manning, P. Nannipieri, D. P. Rasse, S. Weiner and S. E. Trumbore, Persistence of soil organic matter as an ecosystem property, *Nature*, 2011, 478, 49–56.
26 M. H. B. Hayes, *Humic substances II: in search of structure*, J. Wiley, 1st edn, 1989.

27 N. Sengupta, D. C. Reardon, P. D. Gerard and W. S. Baldwin, Exchange of polar lipids from adults to neonates in *Daphnia magna*: Perturbations in sphingomyelin allocation by dietary lipids and environmental toxicants, *PLoS One*, 2017, 12, 1–25.

28 D. Martin-Creuzburg, E. von Elert and K. H. Hoffmann, Nutritional constraints at the cyanobacteria- *Daphnia magna* interface: The role of sterols, *Limnol. Oceanogr.*, 2008, 53, 456–468.

29 D. Lane, R. Soong, W. Bermel, W. Maas, S. Schmidt, H. Heumann and A. Simpson, in *57th Experimental NMR Conference*, Pittsburg, 2016.

30 R. Soong, E. Nagato, A. Sutrisno, B. Fortier-Mcgill, M. Akhter, S. Schmidt, H. Heumann and A. J. Simpson, *In vivo* NMR spectroscopy: toward real time monitoring of environmental stress, *Magn. Reson. Chem.*, 2015, 53, 774–779.

31 B. E. Lindsey, L. Rivero, C. S. Calhoun, E. Grotewold and J. Brkljacic, Standardized Method for High-throughput Sterilization of Arabidopsis Seeds, *J. Visualized Exp.*, 2017, 128, e56587.

32 E. G. Nagato, B. P. Lankadurai, R. Soong, A. J. Simpson and M. J. Simpson, Development of an NMR microprobe procedure for high-throughput environmental metabolomics of *Daphnia magna*, *Magn. Reson. Chem.*, 2015, 53, 745–753.

33 M. Tabatabaei Anaraki, R. Dutta Majumdar, N. Wagner, R. Soong, V. Kovacevic, E. J. Reiner, S. P. Bhavsar, X. Ortiz Almirall, D. Lane, M. J. Simpson, H. Heumann, S. Schmidt and A. J. Simpson, Development and Application of a Low-Volume Flow System for Solution-State *in vivo* NMR, *Anal. Chem.*, 2018, 90, 7912–7921.

34 G. C. Woods, M. J. Simpson, P. J. Koerner, A. Napoli and A. J. Simpson, HILIC-NMR: Toward the Identification of Individual Molecular Components in Dissolved Organic Matter, *Environ. Sci. Technol.*, 2011, 45, 3880–3886.

35 J. J. Ellinger, R. A. Chylla, E. L. Ulrich and J. L. Markley, Databases and Software for NMR-Based Metabolomics, *Curr. Metabolomics*, 2013, 1, 28–40.

36 P. Sakhaii and W. Bermel, A different approach to multiplicity-edited heteronuclear single quantum correlation spectroscopy, *J. Magn. Reson.*, 2015, 259, 82–86.

37 W. Peti, C. Griesinger and W. Bermel, Adiabatic TOCSY for C,C and H,H J-transfer, *J. Biomol. NMR*, 2000, 18, 199–205.

38 H. Farooq, D. Courtier-Murias, R. Soong, W. Bermel, W. M. Kingery and A. J. Simpson, HR-MAS NMR Spectroscopy: A Practical Guide for Natural Samples, *Curr. Org. Chem.*, 2013, 17, 3013–3031.

39 D. E. Koshland and F. H. Westheimer, Mechanism of Alcoholic Fermentation. The Fermentation of Glucose-1-C14, *J. Am. Chem. Soc.*, 1950, 72, 3383–3388.

40 J. L. Galazzo and J. E. Bailey, Fermentation pathway kinetics and metabolic flux control in suspended and immobilized Saccharomyces cerevisiae, *Enzyme Microb. Technol.*, 1990, 12, 162–172.

41 M. Ikeda, R. Katsumata and O. Zelder, Hyperproduction of tryptophan by Corynebacterium glutamicum with the modified pentose phosphate pathway, *Appl. Environ. Microbiol.*, 1999, 65, 2497–2502.

42 J. M. Buescher, M. R. Antoniewicz, L. G. Boros, S. C. Burgess, H. Brunengraber, C. B. Clish, R. J. DeBerardinis, O. Feron, C. Frezza, B. Ghesquiere, E. Gottlieb, K. Hiller, R. G. Jones, J. J. Kamphorst, R. G. Kibbey, A. C. Kimmelman, J. W. Locasale, S. Y. Lunt, O. D. K. Maddocks, C. Malloy, C. M. Metallo,

E. J. Meuillet, J. Munger, K. Nöh, J. D. Rabinowitz, M. Ralser, U. Sauer, G. Stephanopoulos, J. St-Pierre, D. A. Tennant, C. Wittmann, M. G. Vander Heiden, A. Vazquez, K. Vousden, J. D. Young, N. Zamboni and S.-M. Fendt, A roadmap for interpreting (13)C metabolite labeling patterns from cells, *Curr. Opin. Biotechnol.*, 2015, 34, 189–201.

43 W. M. De Coen, C. R. Janssen and H. Segner, The Use of Biomarkers in *Daphnia magna* Toxicity Testing V. *In Vivo* Alterations in the Carbohydrate Metabolism of *Daphnia magna* Exposed to Sublethal Concentrations of Mercury and Lindane, *Ecotoxicol. Environ. Saf.*, 2001, 48, 223–234.

44 W. Wiechert, 13C Metabolic Flux Analysis, *Metab. Eng.*, 2001, 3, 195–206.

45 A. Marx, A. A. de Graaf, W. Wiechert, L. Eggeling and H. Sahm, Determination of the □uxes in the central metabolism of Corynebacterium glutamicum by nuclear magnetic resonance spectroscopy combined with metabolite balancing, *Biotechnol. Bioeng.*, 1996, 49, 111–129.

46 C. Zwingmann, N. Chatauret, D. Leibfritz and R. F. Butterworth, Selective increase of brain lactate synthesis in experimental acute liver failure: Results of a [^{1}H–^{13}C] nuclear magnetic resonance study, *Hepatology*, 2003, 37, 420–428.

47 A. Wacker and D. Martin-Creuzburg, Allocation of essential lipids in *Daphnia magna* during exposure to poor food quality, *Funct. Ecol.*, 2007, 21, 738–747.

48 M. Bastawrous, A. Jenne, M. Tabatabaei Anaraki and A. Simpson, *In Vivo* NMR Spectroscopy: A Powerful and Complimentary Tool for Understanding Environmental Toxicity, *Metabolites*, 2018, 8, 35.

49 C. E. Goulden and A. R. Place, Fatty acid synthesis and accumulation rates in daphniids, *J. Exp. Zool.*, 1990, 256, 168–178.

50 L. Ruess and P. M. Chamberlain, The fat that matters: Soil food web analysis using fatty acids and their carbon stable isotope signature, *Soil Biol. Biochem.*, 2010, 42, 1898–1910.

51 J. A. G. Duarte, F. Carvalho, M. Pearson, J. D. Horton, J. D. Browning, J. G. Jones and S. C. Burgess, A high-fat diet suppresses *de novo* lipogenesis and desaturation but not elongation and triglyceride synthesis in mice, *J. Lipid Res.*, 2014, 55, 2541–2553.

52 C. Ettenhuber, T. Radykewicz, W. Kofer, H.-U. Koop, A. Bacher and W. Eisenreich, Metabolic □ux analysis in complex isotopolog space. Recycling of glucose in tobacco plants, *Phytochemistry*, 2005, 66, 323–335.

53 R. Gruetter, E. J. Novotny, S. D. Boulware, G. F. Mason, D. L. Rothman, G. I. Shulman, J. W. Prichard and R. G. Shulman, Localized ^{13}C NMR Spectroscopy in the Human Brain of Amino Acid Labeling from $_{D}$-[1-^{13}C] Glucose, *J. Neurochem.*, 2002, 63, 1377–1385.

54 M. D. McCoole, B. T. D'Andrea, K. N. Baer and A. E. Christie, Genomic analyses of gas (nitric oxide and carbon monoxide) and small molecule transmitter (acetylcholine, glutamate and GABA) signaling systems in *Daphnia pulex*, *Comp. Biochem. Physiol., Part D: Genomics Proteomics*, 2012, 7, 124–160.

55 N. R. Sibson, A. Dhankhar, G. F. Mason, K. L. Behar, D. L. Rothman and R. G. Shulman, In vivo 13 C NMR measurements of cerebral glutamine synthesis as evidence for glutamate-glutamine cycling (hyperammonemianeurotransmitter cycledetoxi□cation), *Neurobiology*,1997, 94, 2699–2704.

56 L. Hertz, The Glutamate–Glutamine (GABA) Cycle: Importance of Late Postnatal Development and Potential Reciprocal Interactions between Biosynthesis and Degradation, *Front. Endocrinol.*, 2013, 4, 59.

57 A. Bunescu, J. Garric, B. Vollat, E. Canet-Soulas, D. Graveron-Demilly and F. Fauvelle, In vivo proton HR-MAS NMR metabolic profile of the freshwater cladoceran *Daphnia magna*, *Mol. BioSyst.*, 2010, 6, 121–125.

58 A. Putman, D. Martin-Creuzburg, B. Panis and L. De Meester, A comparative analysis of the fatty acid composition of sexual and asexual eggs of *Daphnia magna* and its plasticity as a function of food quality, *J. Plankton Res.*, 2015, 37, 752–763.

59 M. Kariuki, E. Nagato, B. Lankadurai, A. Simpson and M. Simpson, Analysis of Sub-Lethal Toxicity of Perfluorooctane Sulfonate (PFOS) to *Daphnia magna* Using 1H Nuclear Magnetic Resonance-Based Metabolomics, *Metabolites*, 2017, 7, 1–13.

60 V. Kovacevic, A. J. Simpson and M. J. Simpson, 1H NMR-based metabolomics of *Daphnia magna* responses after sub-lethal exposure to triclosan, carbamazepine and ibuprofen, *Comp. Biochem. Physiol., Part D: Genomics Proteomics*, 2016, 19, 199–210.

61 H. L. Wheeler, R. Soong, D. Courtier-Murias, A. Botana, B. Fortier-Mcgill, W. E. Maas, M. Fey, H. Hutchins, S. Krishnamurthy, R. Kumar, M. Monette, H. J. Stronks, M. M. Campbell and A. Simpson, Comprehensive multiphase NMR: a promising technology to study plants in their native state, *Magn. Reson. Chem.*, 2015, 53, 735–744.

62 B. G. Forde and P. J. Lea, Glutamate in plants: metabolism, regulation, and signalling, *J. Exp. Bot.*, 2007, 58, 2339–2358.

63 V. R. Young and A. M. Ajami, Glutamate: An Amino Acid of Particular Distinction, *J. Nutr.*, 2000, 130, 892S–900S.

64 R. A. Harris and E. T. Harper, in *eLS*, John Wiley & Sons, Ltd, Chichester, UK, 2015, pp. 1–8.

65 U. Sonnewald, N. Westergaard, B. Hassel, T. B. Müller, G. Unsgård, F. Fonnum, L. Hertz, A. Schousboe and S. B. Petersen, NMR spectroscopic studies of 13C acetate and 13C glucose metabolism in neocortical astrocytes: evidence for mitochondrial heterogeneity, *Dev. Neurosci.*, 1993, 15, 351–358.

66 L. Lam, R. Soong, A. Sutrisno, R. De Visser, M. J. Simpson, H. L. Wheeler, M. Campbell, W. E. Maas, M. Fey, A. Gorissen, H. Hutchins, B. Andrew, J. Struppe, S. Krishnamurthy, R. Kumar, M. Monette, H. J. Stronks, A. Hume and A. Simpson, Comprehensive Multiphase NMR Spectroscopy of Intact 13C-Labeled Seeds, *J. Agric. Food Chem.*, 2014, 62, 107–115.

67 A. P. Deshmukh, A. J. Simpson and P. G. Hatcher, Evidence for cross-linking in tomato cutin using HR-MAS NMR spectroscopy, *Phytochemistry*, 2003, 64, 1163–1170.

68 R. K. Adosraku, G. T. Choi, V. Constantinou-Kokotos, M. M. Anderson and W. A. Gibbons, NMR lipid profiles of cells, tissues, and body fluids: proton NMR analysis of human erythrocyte lipids, *J. Lipid Res.*, 1994, 35, 1925–1931.

69 M. J. DeNiro and S. Epstein, Mechanism of carbon isotope fractionation associated with lipid synthesis, *Science*, 1977, 197, 261–263.

70 N. Blair, A. Leu, E. Muñoz, J. Olsen, E. Kwong and D. Des Marais, Carbon isotopic fractionation in heterotrophic microbial metabolism, *Appl. Environ. Microbiol.*, 1985, 50, 996–1001.

71 T. W.-M. Fan and A. N. Lane, Applications of NMR spectroscopy to systems biochemistry, *Prog. Nucl. Magn. Reson. Spectrosc.*, 2016, 92–93, 18–53.
72 T. W.-M. Fan and A. N. Lane, Structure-based proftling of metabolites and isotopomers by NMR, *Prog. Nucl. Magn. Reson. Spectrosc.*, 2008, 52, 6

The study on Perfluroalkyl acids contaminated *Arabidopsis thaliana* with a powerful approach: Comprehensive Multiphase NMR Spectroscopy

Nisha Sharma[1], Stefano Dall'Acqua[2], Stefania Sut[2], Leonard Barnabas Ebinezer[1], Antonio Masi[1], Andre Simpson[3]

[1]DAFNAE, University of Padova, Viale Università 16, 30520 Legnaro, PD, Italy
[2]Department of Pharmaceutical Sciences, University of Padova, Via Marzolo 5, 35131 PD, Italy
[3]Department of Chemistry, University of Toronto, 1265 Military Trail, Toronto, Ontario M1C 1A4, Canada

Keywords: Perfluoroalkyl and Polyfluoroalkyl Substances (PFASs), CMP NMR, Alanine, Glutamine, A. *thaliana*

Highlights

1. Two metabolites glutamine and alanine were more abundant in PFAAs contaminated *A. thaliana* seedlings.
2. The mixture of 11 different PFAAs was more toxic to seedlings as compared to individual PFOS and PFOA treatment

Abbreviations: PFAAs, Perfluoroalkyl acids; PFSAs, Perfluoroalkyl sulfonic acids; PFCAs, Perfluoroalkyl carboxylic acids; CMP-NMR, Comprehensive Multiphase-Nuclear Magnetic Resonance; NMR, Nuclear magnetic resonance spectroscopy; PFCs, Fluorinated compounds; UNEP, United Nations Environment Programme; POPs, Persistent organic pollutant; PFBA, Perfluorobutanoic acid; PFPeA, Perfluoro-n-pentanoic acid; PFHpA, Perfluoroheptanoic acid; PFOA, Perfluorooctanoic acid; PFNA, Perfluorononanoic acid; PFDA, Perfluorodecanoic acid; PFUnA, Perfluoroundecanoic acid; PFHxA, Perfluorohexadecanoic acid; PFDoA, Perfluoro dodecanoic acid; PFBS, Perfluorobutane sulfonate; PFOS, Perfluorooctanesulfonate; MS, Murashige and Skoog; WT, Col-0, Wild-type Columbia; ppm, Parts per Million. HSQC, Heteronuclear single-quantum coherence

Abstract:

Nuclear magnetic resonance (NMR) spectroscopy, has become a key method for high throughput comparative analysis in plant metabolomics. In the recent year, Comprehensive Multiphase-Nuclear Magnetic Resonance (CMP-NMR) was proposed as new approach presenting great potential for the *in-situ* study of natural samples in their native state without sample destruction (Courtier-Murias et al. 2012). This new technology gives unique opportunity to observe the stress biology and acclimation response in plants by identifying different compounds, toxicity, its mode of action, contaminate fate and the remediation (Simpson et al. 2012). PFAAs contamination has been so far studied mainly for effects on humans but few papers deal with effects on plant metabolism. The overall aim of my study

was to assess which metabolites can be influenced in *A. thaliana,* by perfluoroalkyl acids (PFAAs) exposure. In this context, three experimental setups were established using Arabidopsis as a model plant. PFOS and PFOA at 10 ppm each separately, and a mixture of 11 different PFAAs at total 11ppm concentration, were compared with the control conditions without any treatment. The plates with sterilized seeds were transferred to the dark for fourteen days at 21 °C and grown in the presence of 13C glucose to increase NMR response; finally, plants were collected and prepared for NMR analysis. The CMP-NMR approach allows the monitoring of soluble compounds as well as the metabolites present in the cell wall and in non-soluble part of the tissues. Obtained data were compared in control versus the different treatment groups (PFOS, PFOA and PFAAs MIX).

The overall results indicated that the annotated metabolites levels are not modified when plant seedlings are treated with PFOA, PFOS at the selected concentration and in the proposed experimental conditions. On the other hand, the mixture of the 11 different pollutants showed the significant modification of Alanine and Glutamine levels with an increase of 30 and 10-fold compared with the control.

1. INTRODUCTION

Perfluoroalkyl acids (PFAAs) are the group of highly persistent environmental contaminants, globally distributed (Liou et al. 2010, Zhi et al. 2015). They are considered one of the persistent organic pollutants (POPs) (Ji et al. 2012), which consist of the presence of different positions being linked to fluorine by C-F bonds and a functional acid group in the chain (Buck et al. 2011). Due to these physiochemical properties, they are used in industries like building materials, textiles (Bečanová et al. 2016), consumer products like shampoo, clothes, shoes and food packaging products (ye et al. 2015, Xia et al. 2001) and fire fighting foams (Moody et al. 2000) for decades. The most widely detected PFAAs in the environment are perfluorooctane sulfonate (PFOS) and perfluorooctanoate (PFOA) (Hekster et al. 2003, Jin et al. 2009, Xiao et al. 2013) posing toxic effects to the plants (Li et al. 2009, Ghisi et al. 2018) and high risk on human health (reviews in OECD, 2002, Mazzoni et al. 2019). Due to its hazardous effects to organisms (Giesy and Kannan 2001), their long persistence, potential accumulation in food webs, United Nations Environment Programme (UNEP) has listed PFOS and PFOA and its related substances as persistent organic pollutant (POPs) under the Stockholm Convention.

PFOS and PFOA consists of a hydrophobic alkyl chain and a hydrophilic end-group. PFOS belongs to the perfluoroalkyl sulfonic acids (PFSAs), whereas PFOA belongs to the perfluoroalkyl carboxylic acids (PFCAs). These two compounds are the two common perfluorinated compounds (PFCs) detected in lakes (Yeung et al., 2013), fish (Suominen et al. 2011), animal (Zafeiraki et al. 2016), soils (Li et al. 2010), human beings and plants (Ghisi et al. 2017) at the range of ng/L–µg/L but also in mg/l range near the PFASs contaminated sites. However, toxicity effects of PFOS, PFOA and PFAAs mixture on the plants are very intermittent. Thus, analyzing the metabolites in response to PFAAs contamination exposure in the model plant comparing to control (without PFAAs exposure) may provide some understanding of this chemical. Therefore, developing high- throughput analytical methods could measure the PFAA exposure responses in the plants may be essential.

Nuclear magnetic resonance (NMR) spectroscopy, being a powerful technique has become a key method for high throughput comparative analysis in plant metabolomics. For the plant metabolites, there has been high resolution NMR like ^{1}H NMR. Further, this technology has also been used in human samples. They have been powerful tools for plant sample also. Thus, a novel NMR approach named Comprehensive Multiphase-Nuclear Magnetic Resonance

(CMP-NMR) possessing a great potential for the in-situ study of natural samples in their native state without sample destruction (Courtier-Murias et al. 2012). This new technology has helped to understand the stress biology and acclimation response in plants by identifying different compounds, toxicity, its mode of action, contaminate fate and the remediation (Simpson et al. 2012). Thus, this spectroscopy is used in PFAAs treated plants to study liquid, gel and solid state of intact ^{13}C labeled Arabidopsis seedlings where all the organic components are explored. To overcome the poor sensitivity of the instrument, the seedlings were uniformly labeled with 13C and to ensure the complete labeling of all the metabolites the plants were grown in complete dark, excluding all the photosynthetic metabolic pathways. Thus, due to experimental conditions, seedlings were forced to uptake the ^{13}C for synthetizing 13C enriched metabolites that can be analysed with high sensitivity by NMR allowing the observation of the possible metabolic changes induced by the different studied PFAAs plant exposure.

Arabidopsis thaliana is taken as a model plant in the plant research era due to its small and complete genome sequence, easy cultivation and high- level seed production (Wixon, 2001). Thus, it has been widely used to monitor the toxicity and accumulation and translocation of PFOA individually at 181 - 1811 µM PFOA-F, exposure in the agar plate which affected the shoot and root growth (Yang et al. 2015). And even Jun et al. (2005) discussed the future role of stable isotope labeling using *A. thaliana* for the NMR based metabolomics approach. There has been considerable research on PFASs on soil, food, animals, humans and plants to study its effects, accumulation and translocation. However, up to our knowledge no studies have considered the metabolic changes induced in *A. thaliana* seedlings grown in the presence of single or mixture of PFASs. Here, I introduced CMP NMR to determine the effects of eleven different PFAAs in plant as in the open environment I encounter with many kinds of PFAAs. The study focuses on the stress metabolites on plants which might be due to PFAAs treatment. And I believe that this is only work reported till now which gives molecular interactions of 11 different PFAAs with individual PFAAs separately (PFOS and PFOA) comparing with control (seedlings without PFAAs treatment). CMP-NMR was chosen for my experiment to understand the various phases, which might provide full information on the membranes, as-well as to explore and eventually to annotate and identify a wide range of metabolites due to PFAAs stress on seedlings.

There have been few studies carried out in toxicological profile of PFAAs on plants; however, little information on the histological alterations and accumulation patterns has been compared for different PFAAs at different exposure levels. Here, I proposed to use the CMP-NMR, a new NMR technology to study the effects of PFAAs on *A. thaliana* seedlings at molecular level using both single and mixture of PFAAs and considering that the exposure of the pollutant in the seeds during the germination stage thus aiming to observe the possible metabolic modifications without the destruction of the sample.

2. Methods and Materials

2.1 Chemicals and Standards

The PFAAs included in the experiment are perfluorobutanoic acid (PFBA), perfluoro-n-pentanoic acid (PFPeA), perfluoroheptanoic acid (PFHpA), perfluorooctanoic acid (PFOA), perfluorononanoic acid (PFNA), perfluorodecanoic acid (PFDA), perfluoroundecanoic acid (PFUnA), perfluorohexadecanoic acid (PFHxA), Perfluoro dodecanoic acid (PFDoA), perfluorobutane sulfonate (PFBS) and perfluorooctanesulfonate (PFOS) (Sigma Aldrich, St. Louis, MS, USA). H_2O_2, methanol and high purity water purchased from Sigma Aldrich Co (USA). Standard solutions of test compounds were prepared in methanol.

2.2 Plant growth and experimental setup

The sterilization of wild-type Columbia (WT, Col-0) *Arabidopsis thaliana* were initially sterilized by a chlorine gas method. 100 ml of bleach and 6 ml of concentrated HCL were placed in the desiccator with the cap open Eppendorf containing seeds. After six hours, the seeds were removed and stored in the freezer until use. The seeds were grown in sterilized Murashige and Skoog (MS) growth medium containing 1% (w/v) glucose, a uniformly labelled $^{13}C_6$-glucose at 99% ^{13}C enrichment (Silantes, GmbH). The seeds were then cold-stratified for three days, transferred to the dark for fourteen days at 21 °C.

The experiment was conducted in 12 well culture plate containing sterilized MS medium which were spiked with PFOS at 10 ppm, PFOA at 10 ppm and third condition was 11 different PFAAs (PFBA, PFPeA, PFHpA, PFOA, PFNA, PFDA, PFUnA, PFHxA, PFDoA, PFBS and PFOS) at 11 ppm.

2.3 Nuclear magnetic resonance spectroscopy

The CMP-NMR samples were prepared as described in previous studies Wheeler et al. 2015, Ning et al. 2018). Briefly, 20mg *A. thaliana* seedlings were carefully picked and placed into a 4mm zirconia rotor. 30 µL of deuterium oxide (D_2O, Cambridge Isotope, MA) was added as the lock solvent, as well as to swell the sample. The rotor was then sealed with Kel-F insert and plug screws and was left being swollen for 12 hours.

All experiments were performed on a 500MHz Bruker Avance III spectrometer with a 4mm H-D-C-N CMP probe fitted with actively shielded gradient along the magic angle direction. The rotor was spun at 6666 Hz and the relaxation time (T1) was measured using inversion recovery. All samples were run with a recycle delay 5 times that of the measure T1. Phase differentiation was performed as described previously (Courtier-Murias et al. 2016) by using various delays and gradient to selectively detect compounds in the targeted phase.

3. Results and Discussion

The effect of PFAAs on growth of 14 days *A. thaliana* seedlings under PFAAs exposure was assessed in terms of weight of the seedlings. The observation on the PFAAs treatment resulted in reduction of the growth attributes of seedlings; the weight was declined by 31.9 % in sample of 11 different PFAAs mixture, 18.9 % in seedlings treated with 10 ppm PFOS and 1.18 % in 10 ppm PFOA as compared with untreated group (control). Both Post hoc analysis and Tukey test revealed the significant differences between seedlings treated with mixture of 11 PFAAs and seedlings treated with PFOS as compared to control (Graph 5.1). The results were consistent with the several other studies reporting that, PFOS is more toxic than PFOA to plants and aquatic invertebrates (Li et al. 2009); to a zooplankton community (Sanderson et al. 2004) and to the rats (Cui et al. 2009). But still uptake, accumulation and effects of each PFAAs compounds on plants might have different mechanisms as compared to aquatic animals.

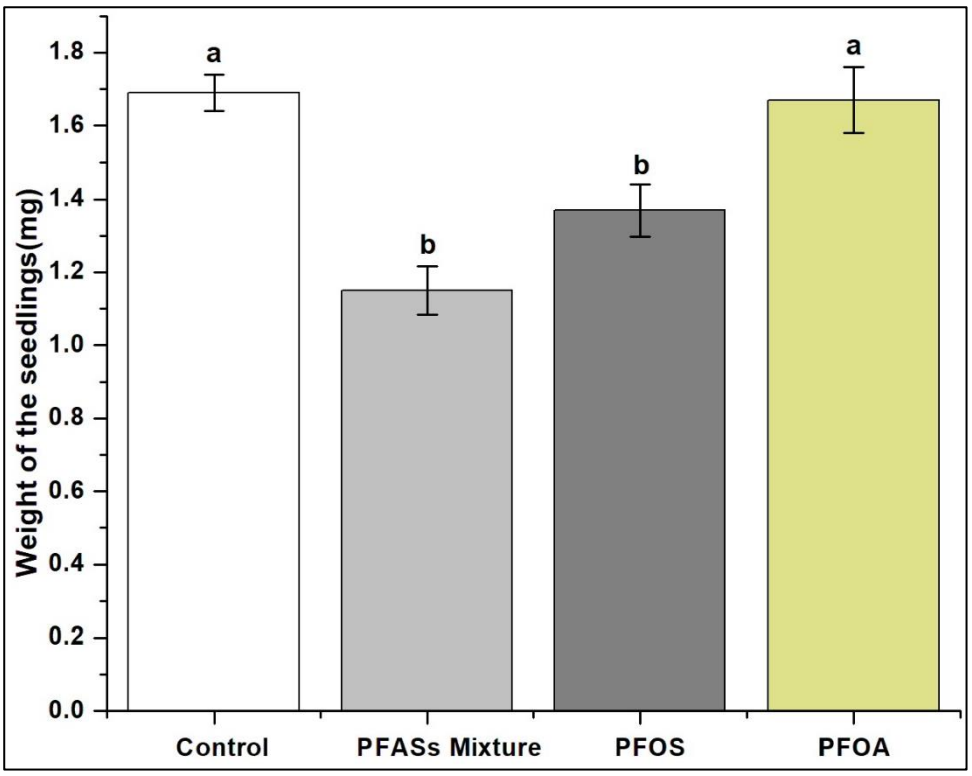

Graph 5.1: The weight of the PFAAs treated A. thaliana seedlings after 14 days. Error bars represent standard error of the mean (n=10). Different letters indicate significant differences as tested by Tukey-HSD test at $p < 0.05$.

3.1 2D ^{1}H-^{13}C correlation Heteronulclear Single Quantum Coherence (HSQC) NMR of *Arabidopsis thaliana* seedlings treated with PFAAs

The detail overview of the metabolite profile of the seedlings was observed from the 2D ^{1}H-^{13}C heteronuclear single quantum coherence (HSQC) NMR, this measurement allows to observe the chemical shifts of directly bonded ^{1}H and ^{13}C nuclei (Wheeler et al. 2015; McGill et al. 2017). As such, HSQC mostly emphasizes in the mobile components (dissolved, and dynamic solids such as gels and swollen materials), thought of as a high resolution (theoretical peak capacity as a measure of resolution per unit is reported as ~2000 000 for HSQC) fingerprint of the H–C framework in a complex mixture. The result presented here is a 'fingerprint' of a wide range of metabolites from the contaminated seedlings (Table 5.1. and Figure 5. 2), indicating that the seedlings contained similar profiles of metabolites. Some of the metabolites identified here in the spectra are consistent with previous NMR studies of plant extracts (Wheeler et al. 2015; McGill et al. 2017) and living organism (Mobarhan et al. 2016). In total 13 metabolites, including amino acids such as alanine, arginine, glutamine, tyrosine as well as carbohydrates and nucleotide, were identified via 2D-NMR (Table 5.1). But as expected there were few metabolites, like galactose, glutamine, alanine, tyrosine and uridine, which were in higher abundance.

Table 5.1: Proton (^{1}H) and Carbon (^{13}C) Chemical Shift Assignment of Amino acids and carbohydrates of a Single ^{13}C-Labeled A. thaliana Seedlings.

	AMINO ACID			
SN	**Annotation**	**Intensity**	**f2 (ppm)**	**f1 (ppm)**
1	Alanine	3372627,8	4,05	54,6
2	Alanine	14711691	1,48	19,37
3	Arginine	3480217,5	3,17	44,34
4	Arginine	8719626	3,03	42,24
5	Glutamine	19186286	2,46	33,82
6	Glutamine	18212240	2,15	29,36
7	Glutamine	7978999,5	3,81	57,48
8	L arginine	2692028,5	1,91	26,36
9	Tyrosine	265470,9	7,17	133,64
10	Tyrosine	304175,2	6,87	118,52
11	Tyrosine	7084984,5	2,94	37,54
	CARBOHYDRATES			
SN	**Annotation**	**Intensity**	**^{1}H (ppm)**	**^{13}C (ppm)**
1	D galactose	9605732,0	4,66	99,13
2	D galactose	6613024,0	5,25	95,15
3	D galactose	5676318,5	3,94	72,10
4	D glucosamine	648151,70	4,85	96,59
5	D glucosamine	9268337,0	3,48	78,98
6	Fructose	682612,4	4,07	84,33
7	Fructose	2855100,0	3,97	79,56
8	Fructose	2559819,5	4,11	78,26
9	Glucosamine	9757071,0	3,41	72,80
10	Glucosamine	17632888,0	3,74	64,03
11	Glucosamine	13686978,0	3,89	63,85
	NUCLEOTIDE			
SN	**Annotation**	**Intensity**	**^{1}H (ppm)**	**^{13}C (ppm)**
1	Uridine	699938,9	7,83	144,8
2	Uridine	459598,8	5,89	105,32
3	Uridine	3306161,5	4,14	87,2
4	Uridine	1446599,5	4,35	76,95
5	Uridine	945390,0	5,91	91,6
	OTHER METABOLITES			
SN	**Annotation**	**Intensity**	**^{1}H (ppm)**	**^{13}C (ppm)**
1	Histamine	131163,2	8,65	136,83
2	Histamine	66887,0	7,29	120,46
3	Methyl adenine	10765,9	8,18	154,28
4	Choline	1415391,8	4,05	58,23
5	Choline	10457860,0	3,18	56,87

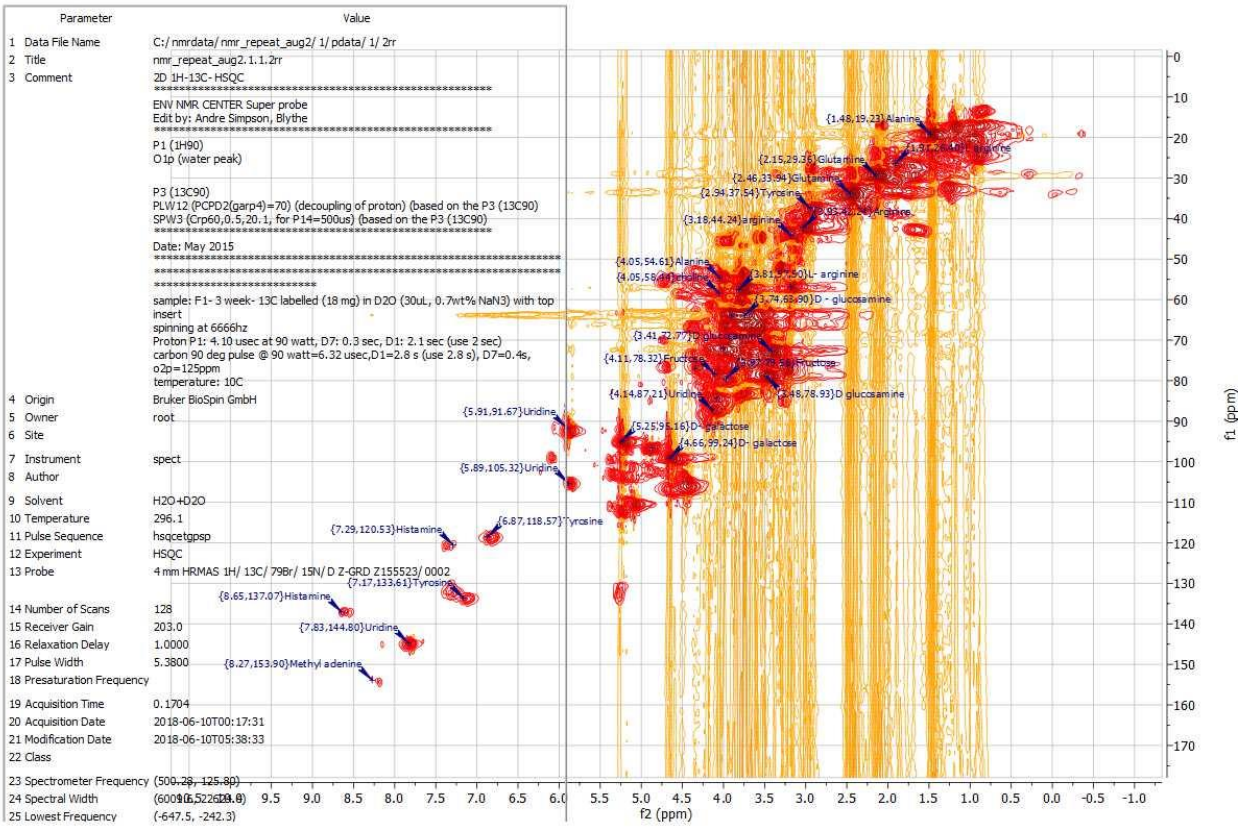

Figure 5.2: Heteronuclear single-quantum coherence (HSQC) spectrum showing color-coded soluble/mobile species as determined by AMIX Bruker Bio reference spectra database.

Table 5.2: Table indicate the area fold changes of annotated constituents calculated as follows (average of treatment-average of controls)/average of controls. Significance of differences were calculated by paired t test. List of metabolites were collected but upon the combined inspection, the metabolites PFOS, PFOA and PFAAs mixture was compared with control, then the metabolites were chosen based on statistical analysis, p< 0.05.

SN	**Control VS 11 PFAAs Mix**				**Control VS PFOA**			**Control VS PFOS**		
		Area fold changes	SD Error	P value	Average fold changes	SD Error	P value	Area fold changes	SD Error	P value
1	Alanine	38.428	30.2	*8.00E-08*	0.052	0.4	0.85	1.377	1.8	0.81
2	Glutamine	10.853	4.4	*2.70E-08*	0.075	0.3	0.89	-0.202	0.2	0.42
3	Glutamine	9.946	3.7	*2.40E-08*	0.070	0.3	0.94	-0.190	0.2	0.44

3.2 Biological significance

Almost 13 metabolites were identified in the current study related to PFAAs treatment on *A. thalaiana* seedling. Some of the metabolites identified here in *Arabidopsis* were observed in some other metabolomic studies (Wheeler et al. 2015) and are further confirmed by HSQC. Glutamine and Alanine were the two significant abundant metabolites in the seedlings treated with PFAAs mixture as compare to control. The HPLC method was further used to confirm the

amino acids that were detected from NMR. By comparing the results obtained by HPLC with NMR, Alanine, Glutamine and Tyrosine were detected by both tools.

Basically, during the germination, the seeds accumulate a large amount of glutamine or asparagine (nitrogen-containing compounds) reported by Tavener et al. (1972); McGill et al. (2017) observed that there is an increase of glutamine in seedlings. HPLC results indicated that, there was less asparagine (fold change by 0.5) as compared with seedlings treated with PFOS (increased by 0.66-fold change) and PFOA (increased by 0.30-fold change) while there were no observed changes of asparagine.

HPLC results indicated that, there was less fold change of asparagine in the seedlings treated with mixture of PFAAs as compared to seedlings treated with PFOS (increased by 0.66-fold change) and PFOA (increased by 0.30-fold change). Thus, glutamine might be involved in the complex mechanisms that alters the TAG metabolism in the seedlings that were treated with the PFAAs contaminates. This was further explained by the high fold changes of phenylalanine by 2.6 in the plants treated with mixture of PFAAs from HPLC. It is known that phenylalanine is primarily deaminated by phenylalanine ammonia-lyase producing an amine group releasing ammonia, which have a toxic effect on the plant. And the mechanism by which plants deal with this amine group is through the amination of glutamate to form glutamine (Peng et al. 2011; Veregin et al. 1986). Likewise, the significant highest fold change of glutamine from CMP- NMR in mixture of PFAAs treated seedlings could be explained by increased nitrogen availability due to phenylalanine deamination and corresponding amination of glutamate, in the process to detoxify the chemical compounds by the plants.

Plants also have the enzymes that play an important role in the metabolism of the chemical contaminants as in animal liver to detoxify the chemical. The process of detoxifying the chemical compounds by the plants is called “green liver” (Sandermann Jr, 1992). And according to Coleman et al. (1997) after uptake of these chemical pollutants, the enzyme related to chemical transformations including phases I, II and III of the contaminants take place in the plants. The phase I involves the reactive groups, resulting hydrolysis and redox-based conversion of pollutants into metabolites. In the phase II metabolites related to glutathione, sugars, or amino acid takes place and at the end the phase III, the metabolites that cannot be transformed further are either stored in vacuoles or incorporated into cell walls (Ohkawa et al. 1999; Dietz and Schnoor, 2001). However, there are not yet evidences that such a

detoxification mechanism operates in plants for PFAAs. Here I observed that PFAAs having a lipophilic property, are taken up by plants and translocated to the plant tissues, especially on roots and leaves. Thus, PFAAs toxicity is related with their accumulation in organs and tissues, which might have caused various adaptive responses in the PFAAs treated seedlings.

Roots need oxygen to produce energy, and sustain root growth; In facts, oxygen is an indispensable substrate for many biochemical reactions in plants, including energy metabolism (respiration). It seems relevant, to this regard, to remind that PFAS are surfactants, and for this property they have been used in industries for decades. In particular, PFAAs are widely used in fire-fighting foams, because they are able to produce a "stable bubble blanket" (Nature, 2019), which prevents oxygen reaching a fire. Thus, here in my study PFAAs might act as a bubble blanket for roots, which is not allowing enough oxygen to reach cells for respiration, acting as a barrier. If there are any changes in oxygen accessibility, then a drastic metabolic rearrangement is observed (van Dongen et al. 2009).

During the plant lifetime, roots are exposed to oxygen concentration which varies from the fully aerobic state (normoxia) to oxygen deficiency (hypoxia) or the total absence of oxygen (anoxia). And under hypoxia or anoxia, which may be caused by eutrophication and organic pollution (Goldberg, 1995; Wu et al. 2002), there is an activation of a series of rapid and profound molecular and metabolic responses to endure the stress (Banti et al. 2013). The huge fold changes of alanine that were observed from CMP-NMR in the seedlings treated with a mixture of 11 different PFAAs could be due to low oxygen availability, consistently with data reported in literature (van Dongen et al. 2009) showing an increase in alanine content in Arabidopsis roots under hypoxia conditions. Plants respond to chemical pollutants with a variety of detoxification pathways as well as adaptive responses to secondary stress effects. The observed increase in the level of metabolites alanine and glutamine following PFAAs exposure suggests that in *A. thaliana* seedlings amino acid metabolism is altered, probably as a consequence of reduced oxygen permeability in roots.

3.3 CMP-NMR on PFAAs contaminated *A. thaliana* seedlings

The NMR spectroscopy has been an effective means for investigating the metabolism of plant at the molecular level. Most of the studies related to plants used plant extracts for the metabolite identification and structural elucidation. Here, CMP-NMR Spectroscopy has

provided a metabolic profiling of the different phases in the PFAAs treated *A. thaliana* seedlings, by using intact samples previously labeled with ^{13}C glucose.

To this regard, CMP-NMR has an advantage since intact seedlings were placed directly in the instrument, thus preventing any possible loss of metabolites due to the extraction process. The use of CMP-NMR to study metabolic alterations in seedlings, could give us an extra dimension to understand the effects of environmental pollutants like PFAAs on plant physiology.

4. Conclusion:

The study illustrated the ability of CMP-NMR based metabolomics as a novel tool to elucidate significant changes in the metabolome of *Arabidopsis thaliana* upon exposure to individual PFAAs (PFOA, PFOS at 10 ppm) and mixture of 11 PFAAs at 11 ppm compared with the control. The plants were forced to feed on the 13C-glucose so that all the metabolites were labeled and the changes induced by PFAAs treatment could be easily detected by CMP-NMR. This study was carried out to test the toxicity of combined PFAAs on plants, and to understand the effects of PFAAs exposure at metabolic level. The identified metabolites (Alanine and Glutamine) which were significantly changed point to metabolic rearrangements which might be due to restricted oxygen availability in roots. This study also demonstrates that the toxicity of a mixture of different PFAAs may differ from the single PFAA, and that a combination of PFAAs, which is also more relevant from an environmental point of view, should be considered in studies aimed at assessing the toxicity of this class of emerging pollutants.

5. References

Banti, V., Giuntoli, B., Gonzali, S., Loreti, E., Magneschi, L., Novi, G., Paparelli, E., Parlanti, S., Pucciariello, C., Santaniello, A., & Perata, P. 2013. Low oxygen response mechanisms in green organisms. *International journal of molecular sciences*. 14(3), 4734-4761. https://doi.org/10.3390/ijms14034734.

Bečanová, J., Melymuk, L., Vojta, Š., Komprdová, K., & Klánová, J. 2016. Screening for perfluoroalkyl acids in consumer products, building materials and wastes. *Chemosphere*. 164, 322-329. https://doi.org/10.1016/j.chemosphere.2016.08.112.

Buck, R. C., Franklin, J., Berger, U., Conder, J. M., Cousins, I. T., De Voogt, P., Astrup Jensen, A., Kannan, K., Mabury, S. A., & van Leeuwen, S. P. 2011. Perfluoroalkyl and polyfluoroalkyl substances in the environment: terminology, classification, and origins. *Integrated environmental assessment and management*. 7(4), 513-541. https://doi.org/10.1002/ieam.258.

Coleman, J., Blake-Kalff, M., & Davies, E. 1997. Detoxification of xenobiotics by plants: chemical modification and vacuolar compartmentation. *Trends in plant science.* 2(4), 144-151. https://doi.org/10.1016/S1360-1385(97)01019-4.

Courtier-Murias D, Farooq H, Masoom H, Botana A, Soong R, Longstaffe JG, Simpson MJ, Maas WE, Fey M, Andrew B, Struppe J, Hutchins H, Krishnamurthy S, Kumar R, Monette M, Stronks HJ, Hume A, Simpson AJ 2012 Comprehensive multiphase NMR spectroscopy: Basic experimental approaches to differentiate phases in heterogeneous samples. *Journal of Magnetic Resonance*. 217, 61–76. https://doi.org/10.1016/j.jmr.2012.02.009.

Cui, L., Zhou, Q. F., Liao, C. Y., Fu, J. J., & Jiang, G. B. 2009. Studies on the toxicological effects of PFOA and PFOS on rats using histological observation and chemical analysis. *Archives of environmental contamination and toxicology*. 56(2), 338. https://doi.org/10.1023/B:MCBI.0000007257.67733.3b.

Dietz, A. C., & Schnoor, J. L. 2001. Advances in phytoremediation. *Environmental health perspectives*. 109, 163-168. https://doi.org/10.1289/ehp.01109s1163.

Ghisi, R., Vamerali, T., & Manzetti, S. 2018. Accumulation of perfluorinated alkyl substances (PFAS) in agricultural plants: A review. *Environmental research*. https://doi.org/10.1016/j.envres.2018.10.023.

Giesy, J. P., & Kannan, K. 2001. Global distribution of perfluorooctane sulfonate in wildlife. *Environmental science & technology*. 35(7), 1339-1342. https://doi.org/10.1021/es001834k.

Hekster, F. M., Laane, R. W., & de Voogt, P. 2003. Environmental and toxicity effects of perfluoroalkylated substances. In *Reviews of Environmental Contamination and Toxicology* (pp. 99-121). Springer, New York, NY. https://doi.org/10.1007/0-387-21731-2_4.

Ji, K., Kim, S., Kho, Y., Sakong, J., Paek, D., & Choi, K. 2012. Major perfluoroalkyl acid (PFAA) concentrations and influence of food consumption among the general population of Daegu, Korea. *Science of the Total Environment*. 438, 42-48. https://doi.org/10.1016/j.scitotenv.2012.08.007.

Jin, Y. H., Liu, W., Sato, I., Nakayama, S. F., Sasaki, K., Saito, N., & Tsuda, S. 2009. PFOS and PFOA in environmental and tap water in China. *Chemosphere*. 77(5), 605-611. https://doi.org/10.1016/j.chemosphere.2009.08.058.

Kamat, C. D., Green, D. E., Curilla, S., Warnke, L., Hamilton, J. W., Sturup, S., Clark, C., & Ihnat, M. A. 2005. Role of HIF signaling on tumorigenesis in response to chronic low-dose arsenic administration. *Toxicological sciences*. 86(2), 248-257. https://doi.org/10.1093/toxsci/kfi190.

Kariuki, M., Nagato, E., Lankadurai, B., Simpson, A., & Simpson, M. 2017. Analysis of sub-lethal toxicity of perfluorooctane sulfonate (PFOS) to Daphnia magna using 1H nuclear magnetic resonance-based metabolomics. *Metabolites.* 7(2), 15. https://doi.org/10.3390/metabo7020015.

Li, F., Zhang, C., Qu, Y., Chen, J., Chen, L., Liu, Y., & Zhou, Q. 2010. Quantitative characterization of short-and long-chain perfluorinated acids in solid matrices in Shanghai, China. *Science of the total environment.* 408(3), 617-623. https://doi.org/10.1016/j.scitotenv.2009.10.032.

Li, M. H. 2009. Toxicity of perfluorooctane sulfonate and perfluorooctanoic acid to plants and aquatic invertebrates. *Environmental Toxicology: An International Journal*. 24(1), 95-101. https://doi.org/10.1002/tox.20396.

Liou, J. C., Szostek, B., DeRito, C. M., & Madsen, E. L. 2010. Investigating the biodegradability of perfluorooctanoic acid. *Chemosphere.* 80(2), 176-183. https://doi.org/10.1016/j.chemosphere.2010.03.009.

Mazzoni, M., Buffo, A., Cappelli, F., Pascariello, S., Polesello, S., Valsecchi, S., Volta, P., & Bettinetti, R. 2019. Perfluoroalkyl acids in fish of Italian deep lakes: Environmental and human risk assessment. *Science of the Total Environment*. 653, 351-358. https://doi.org/10.1016/j.scitotenv.2018.10.274.

Moody, C. A., & Field, J. A. 2000. Perfluorinated surfactants and the environmental implications of their use in fire-fighting foams. *Environmental science & technology*. 34(18), 3864-3870. https://doi.org/10.1021/es991359u. suitable

Ning P, Soong R, Bermel W, Lane D, Simpson MJ, Simpson. A. J. 2018. 13C quantification in heterogeneous multiphase natural samples by CMP-NMR using stepped decoupling. Anal Bioanal Chem 410:7055–7065. https://doi.org/10.1007/s00216-018-1306-1.

OECD (2002) Hazard assessment of perfluorooctanesulfonate (PFOS) and its salts. Unclassified ENV/JM/RD (2002)17/Final. Document No. JT00135607. Organisation for Economic Co-operation and Development, Paris.

Ohkawa, H., Imaishi, H., Shiota, N., Yamada, T., & Inui, H. 1999. Cytochrome P450s and other xenobiotic metabolizing. *Pesticide chemistry and bioscience: The food-environment challenge*. 259.

Peng, P., Peng, F., Bian, J., Xu, F., & Sun, R. 2011. Studies on the starch and hemicelluloses fractionated by graded ethanol precipitation from bamboo Phyllostachys bambusoides f. shouzhu Yi. *Journal of agricultural and food chemistry*. 59(6), 2680-2688. https://doi.org/10.1021/jf1045766.

Sandermann Jr, H. 1992. Plant metabolism of xenobiotics. *Trends in biochemical sciences*. 17(2), 82-84. https://doi.org/10.1016/0968-0004(92)90507-6.

Sanderson, H., Boudreau, T. M., Mabury, S. A., & Solomon, K. R. 2004. Effects of perfluorooctane sulfonate and perfluorooctanoic acid on the zooplanktonic community. *Ecotoxicology and environmental safety*. 58(1), 68-76. https://doi.org/10.1016/j.ecoenv.2003.09.012.

Skinner, H. D., Zhong, X. S., Gao, N., Shi, X., & Jiang, B. H. 2004. Arsenite induces p70S6K1 activation and HIF-1α expression in prostate cancer cells. *Molecular and cellular biochemistry*. 255(1-2), 19-23

Suominen, K., A. Hallikainen, P. Ruokojärvi, R. Airaksinen, J. Koponen, R. Rannikko, and H. Kiviranta. 2011. Occurrence of PCDD/F, PCB, PBDE, PFAS, and organotin compounds in fish meal, fish oil and fish feed. *Chemosphere.* 85(3), 300-306. https://doi.org/10.1016/j.chemosphere.2011.06.010.

Tainted water: the scientists tracing thousands of fluorinated chemicals in our environment. 2019. *Nature International Journal of science.* https://doi.org/10.1038/d41586-019-00441-1.

Tavener, R. J. A., & Laidman, D. L. 1972. The induction of triglyceride metabolism in the germinating wheat grain. *Phytochemistry*. 11(3), 981-987. https://doi.org/10.1016/S0031-9422(00)88442-3.

Van Dongen, J. T., Fröhlich, A., Ramírez-Aguilar, S. J., Schauer, N., Fernie, A. R., Erban, A., Kopka, J., Schauer, N., Fernie, A. R., Erban, A., Kopka, J., Clark, J., Langer, A., & Geigenberger, P. 2008. Transcript and metabolite profiling of the adaptive response to mild decreases in oxygen concentration in the roots of Arabidopsis plants. *Annals of botany*. 103(2), 269-280. https://doi.org/10.1093/aob/mcn126.

Veregin, R. P., Fyfe, C. A., Marchessault, R. H., & Taylor, M. G. 1986. Characterization of the crystalline A and B starch polymorphs and investigation of starch crystallization by high-resolution carbon-13 CP/MAS NMR. *Macromolecules*. 19(4), 1030-1034.

Wheeler HL, Soong R, Courtier-Murias D, Botana A, Fortier-Mcgill B, Maas WE, Fey M, Hutchins H, Krishnamurthy S, Kumar R, Monette M, Stronks HJ, Campbell MM, Simpson A 2015. Comprehensive multiphase NMR: a promising technology to study plants in their native state. Magn Reson Chem 53:735–744. https://doi.org/10.1002/mrc.4230.

Wixon, J. 2001. *Arabidopsis thaliana*. *International Journal of Genomics*. 2(2), 91-98. http://dx.doi.org/10.1002/cfg.75.

Xia, J. 2001. *Protein-Based Surfactants: Synthesis: Physicochemical Properties, and Applications*. CRC Press.

Xiao, F., Simcik, M. F., & Gulliver, J. S. 2013. Mechanisms for removal of perfluorooctane sulfonate (PFOS) and perfluorooctanoate (PFOA) from drinking water by conventional and enhanced coagulation. *Water research*. 47(1), 49-56. https://doi.org/10.1016/j.watres.2012.09.024.

Yang, X., Ye, C., Liu, Y., & Zhao, F. J. 2015. Accumulation and phytotoxicity of perfluorooctanoic acid in the model plant species Arabidopsis thaliana. *Environmental pollution*. 206, 560-566. https://doi.org/10.1016/j.envpol.2015.07.050.

Ye, F., Zushi, Y., & Masunaga, S. 2015. Survey of perfluoroalkyl acids (PFAAs) and their precursors present in Japanese consumer products. *Chemosphere*. 127, 262-268. https://doi.org/10.1016/j.chemosphere.2015.02.026.

Yeung, L. W., De Silva, A. O., Loi, E. I., Marvin, C. H., Taniyasu, S., Yamashita, N., Mabury, S. A., C.G. Muir, D., & Lam, P. K. 2013. Perfluoroalkyl substances and extractable organic fluorine in surface sediments and cores from Lake Ontario. *Environment international*, *59*, 389-397. https://doi.org/10.1016/j.envint.2013.06.026.

Zafeiraki, E., Vassiliadou, I., Costopoulou, D., Leondiadis, L., Schafft, H. A., Hoogenboom, R. L., & van Leeuwen, S. P. 2016. Perfluoroalkylated substances in edible livers of farm animals, including depuration behaviour in young sheep fed with contaminated grass. *Chemosphere*. 156, 280-285. https://doi.org/10.1016/j.chemosphere.2016.05.003.

Zhi, Y., & Liu, J. 2015. Adsorption of perfluoroalkyl acids by carbonaceous adsorbents: Effect of carbon surface chemistry. *Environmental pollution*. 202, 168-176. https://doi.org/10.1016/j.envpol.2015.03.019.

Concluding Remarks

Chemical pollution is one of the most serious pollutions of all the environmental problems and poses a major threat to the health of human beings and the global ecosystem. The World Health Organization has estimated the burden of disease from selected chemicals at 1.6 million lives in 2016, which is likely an underestimate. There are many chemical contaminants, which are extremely dangerous to humans, animals and plants. Among many, here in my study, I chose two man-made chemical pollutants (SDZ and PFAAs) which are widely used by human beings directly and indirectly.

SDZs are a group of synthetic antibacterial agents that contain the sulfonamide group, used in human medicine and are one of the most sold classes of veterinary antimicrobial compounds in EU countries for their low cost and broad-spectrum antibacterial and anti- coccidian activity. It has been proved that plants uptake and accumulate chemical pollutants from contaminated soil and wastewater and there by, introduce them into the food chain. Following which, these compounds affect plant physiological processes such as photosynthesis, respiration and root functionality. Thus, to understand the stress responses, induced and the tolerance and detoxification mechanisms in plants by SDZ, a powerful tool, Proteomics was used to investigate the plant metabolic alterations. SDZ treatment reduced the overall growth, leaf biomass, root length of the model plant *Arabidopsis thaliana*. And proteome analysis indicated that the major proportion of the upregulated proteins were multifunctional stress-responsive proteins.

As PFASs predominantly exist as a mixture, our study gains significance as it addresses their combined effects on plant growth at an environmentally relevant concentration. Therefore, it is important to identify appropriate technologies to remove PFAS from the environment. Phytoremediation being one of the most economical and effective ways to remove contaminants from environment, the potential of *Salix* L. species was addressed. And the trend of uptake and accumulation on plants was dependent on carbon chain length and the functional group of the contaminant. The PFAAs had a species-specific effect on the growth rate and leaf biomass of the plant. Regarding photosynthesis, the gas exchange parameters were affected more than those related to chlorophyll fluorescence. The hydroponic based study done in *Salix* is the novel insights in my study which could be adapted to wetland conditions for future phytoremediation projects targeting PFASs.

It was clear that the contamination of PFAAs was toxic, they are accumulated by plants and could enter into the food chain of human beings in a plant-based diet, especially plants from a contaminated area. Thus, a study was carried out to monitor the effects of PFAAs in the crop plant *Zea mays* as it is one of the most important food crops used worldwide, fast-growing and easy to handle cereal plant. Also, it is a major crop in the Veneto region, which is one of the four major PFAAs contaminated sites in the world. The mixture of 11 PFAAs at a concentration of 100 µg/L each has a significant effect on the growth of maize plants, affecting the uptake of the nutrient solution. It was clear that PFAAs are potentially phytotoxic and could be accumulated by the plant system if they are grown in PFAAs contaminated area. Thus, we could conclude that a cereal crop like maize may contribute to increase human PFAA exposure, with toxic effect for human beings and animals, when grown in hotspot regions, like Veneto region in Italy.

After exploring the plant physiological effects of PFAAs exposure on plants, I further carried out the experiments to identify the metabolites that were altered due to PFAAs treatment. To understand the acclimatization response in plants, *A. thaliana* was chosen as it is easy growing plant and has been sequenced completely and is thus suitable for a metabolomic study. The metabolite fingerprint of the sample was provided by using novel NMR technology called CMP-NMR, an effective tool which was used to compare the PFAAs exposed sample with control. The list of metabolites was obtained, among them, two (Alanine and Glutamine) were abundant in the mixture of 11 PFAAs exposed *A. thaliana* seedlings. This demonstrates that the plants have activated some molecular and metabolic responses to tolerate PFAAs stress. Thus, I could conclude that PFAAs toxicity caused various adaptive responses in the PFAAs treated seedlings.